Title
The Effect of Cicadian Therapies in Models of Neurodegenerative Disease

Permalink
https://escholarship.org/uc/item/9k68356b

Author
Whittaker, Daniel S

Publication Date
2019

Peer reviewed|Thesis/dissertation

UNIVERSITY OF CALIFORNIA

Los Angeles

The Effect of Circadian Therapies

in Models of Neurodegenerative Disease

A dissertation submitted in partial satisfaction of the

requirements for the degree Doctor of Philosophy in

Molecular, Cellular, and Integrative Physiology

by

Daniel Steven Whittaker

2019

ABSTRACT OF THE DISSERTATION

The Effect of Circadian Therapies

in Models of Neurodegenerative Disease

by

Daniel Steven Whittaker

Doctor of Philosophy in Molecular, Cellular, and Integrative Physiology

University of California, Los Angeles, 2019

Professor Christopher S. Colwell, Chair

Huntington's Disease (HD) is an autosomal dominant disorder caused by excessive CAG repeats in the gene encoding the huntingtin protein which leads to progressive neurodegeneration that inflicts cognitive, psychiatric, cardiovascular and motor dysfunction. There is currently no treatment to prevent or delay the course of the disease. Neuronal loss in the striatum is thought to be responsible for the abnormal motor control present in HD patients, though the pathophysiology behind the non-motor symptoms is still unclear. Disturbances in sleep-wake cycles are common among HD patients with reports of delayed sleep onset, frequent bedtime awakenings, and excessive fatigue, and these disruptions are recapitulated in mouse models. Because circadian dysfunction manifests early in the disease in both patients and mouse models, we sought to determine if early interventions that improve circadian rhythmicity could benefit HD symptoms and delay disease progression.

Evidence of altered histaminergic signaling in HD patients suggests that this pathway may contribute to disrupted rhythms in arousal. Utilizing the Q175 mouse model of HD, we demonstrated that nightly treatment with a histamine-3 receptor antagonist/inverse agonist improved several behavioral measures of HD including strengthening activity rhythms, cognitive performance, and mood, as well as reducing inappropriate activity during the normal sleep time. Our findings suggest that drugs targeting the histamine-3 receptor system may be beneficial as cognitive enhancers in the management of HD.

One of the most powerful regulators of the circadian system is the daily feed/fast cycle, and in two separate studies we found that three months of time-restricted feeding (6-hours of feeding in the middle of the active phase followed by 18-hours fasting) improved the sleep/wake cycle, motor symptoms, and autonomic function in both the Q175 and BACHD mouse models.

Finally, we sought to determine whether a ketogenic diet was sufficient to impart motor performance and sleep/wake rhythm benefits in BACHD mice similar to those observed under TRF. We found that the ketogenic diet improves circadian dysfunction as well as motor symptoms in the BACHD mouse model.

Altogether, these studies support the hypothesis that early interventions that improve sleep/wake timing and circadian rhythmicity can ameliorate a range of symptoms of HD and related neurodegenerative disorders.

The dissertation of Daniel Steven Whittaker is approved

Gene D. Block

Cristina A. Ghiani

Fernando Gomez-Pinilla

Elaine Yih-Nien Hsiao

Christopher S. Colwell, Committee Chair

University of California, Los Angeles

2019

Table of Contents

List of Figures

List of Tables

List of Acronyms

a.u.	arbitrary units
AcAc	acetoacetate
ad lib/AL	ad libitum
Ala	alanine
AMPK	5' adenosine monophosphate-activated protein kinase
ATP	adenosine triphosphate
AVP	arginine vasopressin
BBB	blood–brain barrier
BDNF	brain derived neurotrophic factor
BK	large conductance calcium-activated potassium channels
BMAL1	brain and muscle aryl-hydrocarbon receptor nuclear translocator-like 1
CAG	cytosine, adenine, guanine
cAMP	cyclic adenosine monophosphate
CB	challenging beam
CBT	core body temperature
CK1	casein kinase 1
CLOCK	circadian locomotor output cycles kaput
CREB	cyclic adenosine monophosphate response element-binding protein
CRY	cryptochrome
CPT1A	carnitine-palmitoyl transferase 1a
D1	Dopamine Receptor D1
DBP	D site of albumin promoter (Albumin D-Box) binding protein
EEG	electroencephalogram

LC3A	microtubule-associated protein 1 light chain 3
LD	light/dark
LFD	low-fat diet
LUC	Luciferase
lux	measure of light intensity
MCT	medium chain triglyceride
mHTT	mutant Huntingtin protein
mTOR	mammalian Target of Rapamycin protein
mM	millimolar
NN	normal to normal interval
NREM	non-rapid eye movement sleep
OF	open field
P70S6K	Ribosomal protein S6 kinase beta-1
PDK4	pyruvate dehydrogenase kinase 4
PER	period
PER2	Period Circadian Regulator 2
PK2	prokineticin 2
PPARα	peroxisome proliferator activated receptor alpha
REM	rapid eye movement sleep
RI	resident-intruder
RM ANOVA	repeated-measures analysis of variance
ROR	retinoic acid-related orphan receptor
ROS	reactive oxygen species
SCOT	succinyl-CoA: 3-oxoacid CoA transferase

SCN	suprachiasmatic nucleus
SEM	standard error of the mean
SIRT1	sirtuin 1
Sub gland	submandibular gland
TM	T-maze
TMN	tuberomammilary nucleus
TRF	time-restricted feeding
TS	tail suspension
UCP3	uncoupling protein 3
VIP	vasoactive intestinal peptide
VPAC2	vasoactive intestinal peptide receptor 2
WT	wild-type
ZT	zeitgeber time
βOHB	D-β-hydroxybutyrate
μL	microliter

Acknowledgments

There were many people who provided support in immeasurable ways, and I will not, at this moment, thank everyone by name. I am grateful to Vikki Paschetto, who probably sacrificed much more than she ever meant to. Louise Levinson provided the early spark and inspiration. Katie Whittaker provided the support, the respite, the shoulder, the love, and so many other things that mothers do. My mentors and guides on this path have been and are many: Jim Tidball, Christopher Colwell, Cristina Ghiani, Dawn Loh, and many others. There were many who helped with the work and I would be remiss if I did not thank Huei Bin Wang. Yu Tahara always gave excellent feedback after listened to my many hours of intellectual rambling. Finally, I wish to express my deepest thanks to the many student, undergraduate, and graduate researchers who contributed to this work.

DANIEL S. WHITTAKER

EDUCATION

Ph.D. candidate in Molecular, Cellular, and Integrative Physiology, College of Letters and Sciences, University of California, Los Angeles. Research interests: circadian biology, aging, therapeutic interventions that improve health span and quality of life through improving or delaying progression in neurodegenerative conditions and diseases.

Bachelor of Science in Exercise Science and Biosciences, *Summa cum laude,* School of Kinesiology and Nutritional Science, California State University, Los Angeles. June, 2010.

PUBLICATIONS

Whittaker, D.S., Loh, D.H., Wang, H.-B., Tahara, Y., Kuljis, D., Cutler, T., Ghiani, C.A., Shibata, S., Block, G.D., and Colwell, C.S. (2018). Circadian-based treatment strategy effective in the BACHD mouse model of Huntington's disease. J. Biol. Rhythms 33(5), 535–554.

Wang, H.-B., Loh, D.H., **Whittaker, D.S.**, Cutler, T., Howland, D., and Colwell, C.S. (2018). Time-restricted feeding improves circadian dysfunction as well as motor symptoms in the Q175 mouse model of Huntington's disease. ENeuro 5.

Lee, F. Y., Wang, H.-B., Hitchcock, O. N., Loh, D. H., **Whittaker, D. S.**, Kim, Y. S., Aiken, A., Kokikian, C., Dell'Angelica, E. C., Colwell, C. S., … Ghiani, C. A. (2018). Sleep/Wake disruption in a mouse model of BLOC-1 deficiency. Frontiers in neuroscience, 12, 759.

Whittaker, D.S., Wang, H.-B., Loh, D.H., Cachope, R., and Colwell, C.S. (2017). Possible use of a H3R antagonist for the management of nonmotor symptoms in the Q175 mouse model of Huntington's disease. Pharmacol. Res. Perspect. 5, e00344.

Wang, H.-B., **Whittaker, D.S.**, Truong, D., Mulji, A.K., Ghiani, C.A., Loh, D.H., and Colwell, C.S. (2017). Blue light therapy improves circadian dysfunction as well as motor symptoms in two mouse models of Huntington's disease. Neurobiol. Sleep Circadian Rhythms 2, 39–52.

Samengo G, Avik A, Fedor B, **Whittaker D**, Myung KH, Wehling-Henricks M, Tidball JG (2012) Age-related loss of nitric oxide synthase in skeletal muscle causes reductions in calpain S-nitrosylation that increase myofibril degradation and sarcopenia. Aging Cell 11:1036–1045.

ADDITIONAL RESEARCH EXPERIENCE

University of California, Los Angeles. Dr. Melissa Spencer, PI. Investigate immune cell and cytokine origin, expression, and modulation in a model of muscular dystrophy. 4/2013 to 8/2014.

University of California, Los Angeles. Dr. Rachelle Crosbie-Watson, PI. Investigate the role of various proteins in neuromuscular junction stability and morphology in in a model of muscular dystrophy. 1/2013 to 4/2013.

University of California, Los Angeles. Dr. Linda Baum, PI. Study the role of glycosylation in disease. 9/2012 to 1/2013.

University of California, Los Angeles. Dr. James Tidball, PI. Research protein modifications and their roles in the regulation of skeletal muscle wasting and regeneration in a model of muscular dystrophy. 11/2010 to 9/2012.

University of Southern California, Leonard Davis School of Gerontology. Undergraduate Research Assistant. Research Advisor: Dr. Valter Longo. Study novel cancer interventions at the cell and organism level in a mammalian model. 4/2010 to 7/2010.

California State University, Los Angeles, Human Performance Laboratory. Undergraduate Research Assistant. Research Advisor: Dr. Nazareth Khodiguian. Investigate human blood buffering responses to intense training and high altitudes. 2/2008 to 7/2010.

HONORS AND AWARDS

Brain Research Institute Graduate Student Research Grant, $10,000, 2018-2019.
NIH Pre-Doctoral Fellowship, 2012-2013.
UCLA Graduate Fellowship, 2010-2011.
American Veterans Memorial Scholarship, 2011, 2009.
JVS Unites States Marine Corps Service Scholarship, 2007-2011.
Phi Kappa Phi Love of Learning Scholarship, 2011.
Golden Key International Honour Society Scholarship, 2010.
Veterans United Scholarship, 2010.
Ebell Scholarship, 2009-2010.
Dean's List, CSULA, 2007-2010.
CSULA School of Health and Human Services Certificate of Honor, 2009.
UPromise Scholarship, 2008-2009.
Sallie Mae Scholarship, 2008-2009.
CSU Future Scholar Award, 2007.

COLLEGE TEACHING EXPERIENCE

4/19 to 7/19 (GE80) From Test Tube to Community, UCLA, Graduate Student Instructor.
10/18 to 4/19 (GE80) Frontiers in Human Aging - Cluster Course, UCLA, Teaching Fellow.
4/18 to 7/18 (GE80) From Test Tube to Community, UCLA, Graduate Student Instructor.
10/17 to 4/18 (GE80) Frontiers in Human Aging - Cluster Course, UCLA, Teaching Fellow.
4/17 to 7/17 (EEB186) Evolutionary Medicine, UCLA, Teaching Fellow.
9/14 to 6/16 (LS1) Evolution, Ecology, and Biodiversity, UCLA, Teaching Fellow.
7/12 to 9/12 (PhySci136) Exercise and Cardiovascular Function, UCLA, Teaching Associate.
7/11 to 9/12 (PhySci5) Issues in Human Physiology, UCLA, Teaching Associate.
9/10 to 9/12 (LS2) Cells, Tissues, and Organs, UCLA, Teaching Assistant.

MILITARY HONORS

Naval Achievement Medal
Battle Efficiency "E" Award (multiple)
Good Conduct Medal
Sea Service Deployment Ribbon (multiple)
Meritorious Promotion (multiple)
Marine of the Quarter (multiple)
Cold War Recognition Certificate
Honor Man (multiple)
Letter of Commendation (multiple)

Chapter 1: Introduction

Chapter 1: Introduction

Huntington's disease (HD) is characterized by cognitive, psychiatric, cardiovascular, and motor dysfunction resulting from advancing neurodegeneration (Kuljis et al., 2012; Margolis and Ross, 2003). Mortality occurs on average 10 to 20 years after the onset of initial motor symptoms. The underlying pathology in HD is caused by a CAG repeat expansion within the first exon of the Huntingtin *(HTT)* gene. When translated, this produces a polyglutamine repeat and leads to protein misfolding, soluble aggregates, and inclusion bodies detected throughout the body (Ciammola et al., 2006; Saft et al., 2005). Huntingtin (HTT) is expressed throughout the body, with higher levels found in the brain than the peripheral tissues. In particular, HTT expression is found to be higher in brain regions with increased neuronal density, as well as being elevated in neurons versus glial cells (Li et al., 1993; Strong et al., 1993). Similarly, the mutant HTT protein (mHTT) is more abundant in neurons than in glial cells with aggregates demonstrating a comparable distribution (Bradford et al., 2010). In muscle, aggregates are found only in the nucleus of myocytes (Gutekunst et al., 1999). The accretion of mHTT leads to the dysfunction of a wide range of cellular processes as well as loss of many normal functions (Wright et al., 2017). Loss of neurons in the striatum has been well characterized and is considered the hallmark of HD pathology. However, both gray and white matter loss have been well described at different stages of HD progression: pre-symptomatic, early in disease, postmortem (Bartzokis et al., 2007; Bourbon-Teles et al., 2019; Di Paola et al., 2012; Phillips et al., 2016), suggesting that the effects of myelin loss might also be a significant factor in the course of the disease.

HD symptoms manifest at different ages, with an average onset of motor symptoms and diagnosis at 40 years of age. Generally, the longer the CAG repeat, the earlier the age of onset and the greater the severity of the symptoms (Langbehn et al., 2010). Yet, even among

patients with the same CAG repeat length, there is a considerable range in the age of onset and severity of symptoms (Gusella et al., 2014; Wexler et al., 2004). Further, cognitive, affective, and other symptoms may arise up to two decades before the onset of motor symptoms (Paulsen, 2011; Paulsen et al., 2008). Such variability raises the possibility of environmental modifiers influencing the disease and suggests that appropriate and early disease management strategies can increase the health span of these patients. This possibility is important to pursue as there are currently no treatments to prevent or delay the disease course.

Sleep disorders are extremely common in HD patients and have detrimental effects on the daily functioning and quality of life of patients and their caregivers (Aziz et al., 2010a; Cuturic et al., 2009; Goodman et al., 2011; Morton et al., 2005). These disruptions in the timing of sleep often become apparent years before the onset of the motor symptoms. One of the first signs of the disease in HD patients is a phase delay in the nightly rise in melatonin (Kalliolia et al., 2014) and, by the end of life, the central circadian clock (suprachiasmatic nucleus, SCN) shows evidence of degeneration (van Wamelen et al., 2014). In humans, it is extremely difficult to determine if the circadian system is dysfunctional and to explore the underlying mechanisms. In the field of HD research, a number of animal models of HD have been developed, each with strengths and weaknesses (Pouladi et al., 2013). Broadly speaking, mouse models of HD also exhibit a progressive and rapid breakdown of the circadian rest/activity cycle that closely mimics the condition observed in human patients, typified by loss of consolidated sleep, increased wakeful activity during the sleep phase, and more sleep during the active/awake phase (**Table 1**).

The research work in my dissertation uses two mouse models of HD. The first model, the Q175 mouse, is a knock-in model in which the human exon 1 sequence of the huntingtin gene is inserted into the mouse DNA with approximately 190 CAG repeats. Among the

numerous models available, the heterozygous (Het) Q175 offers the advantage of strong construct validity with a single copy of the mutation, genetic precision of the insertion, and control of mutation copy number. The Q175 Het become notably symptomatic around 6 months of age and reach end-stage disease at around 22 months (Menalled et al., 2012).

The second model, the Bacterial artificial chromosome (BAC)-mediated transgenic mouse model (BACHD), is a transgenic mouse expressing the entire human *HTT* gene with 97 mixed CAA–CAG repeats. The BACHD mouse offers the advantage of containing the human gene including all the regulatory elements. BACHD mice have a strong progressive phenotype starting at 2- to 3-months of age (Menalled et al., 2009). Prior studies have demonstrated that these are both strong preclinical models to examine the impact of circadian interventions on the disease trajectory (Kudo et al., 2011a; Loh et al., 2013; Menalled et al., 2009; Pouladi et al., 2013). It is worth noting another well studied model, the R6/2 mouse, which contains N-terminally truncated mutant *Htt* with a CAG repeat expansion (~125 repeats) within exon 1 of the huntingtin gene. The R6/2 model develops HD-like symptoms as early as 6 to 8 weeks of age and suffers rapid decline (Mangiarini et al., 1996). Because circadian dysfunction manifests early in the disease in both patients and mouse models, and based upon the hypothesis that circadian dysfunction interacts with HD pathophysiology and exacerbates HD-related symptoms, we sought to determine if early interventions that improve sleep/wake timing and circadian rhythmicity could benefit HD symptoms and modify the course of the disease. Before describing the interventions, I will provide some brief background on circadian rhythms that is relevant to the dissertation research.

Robust circadian rhythms are important to our health and wellness, with many studies demonstrating that the disturbance of these cycles have broad negative impacts on the body. In mammals, the SCN in the hypothalamus contains the "master" oscillatory network necessary

for coordinating circadian rhythms throughout the body (Astiz et al., 2019; Challet, 2015; Colwell, 2011). The SCN is a bilaterally paired nucleus made up of tightly compacted, small-diameter neurons just lateral to the third ventricle atop the optic chiasm. Anatomical studies generally support the division of the SCN into at least two subdivisions, including a ventral "core" and a dorsal "shell" region. The core neurons are thought to act as an integrator of external input, receiving information from three major pathways: the retinohypothalamic tract, the geniculohypothalamic tract, and projections from the raphe nuclei. Core neurons communicate this environmental information to the rest of the SCN. These sensory processing ventral cells exhibit relatively low amplitude rhythms in clock gene expression. Many of the neurons that receive retinal input within the core SCN express the neuropeptides vasoactive intestinal protein (VIP) or gastrin-releasing peptide (GRP), as well as the neurotransmitter gamma-aminobutyric acid (GABA). In contrast, neurons of the dorsal shell appear to generate the most robust circadian oscillations, at least at the level of gene expression. The neurons in the shell express arginine vasopressin (AVP) or prokineticin 2 (PK2), as well as GABA. The fact that many core projections terminate on shell neurons supports the idea that interplay between these two centers is responsible for the output of circadian information from the SCN. The outputs of the SCN from both core and shell subpopulations largely travel to other hypothalamic regions, including the subparaventricular region and the paraventricular nuclei of the hypothalamus. These hypothalamic relay nuclei send projections throughout the nervous and endocrine systems, providing multiple pathways by which the SCN can convey temporal information to the brain and body (Astiz et al., 2019; Welsh et al., 2010).

Circadian rhythms are driven by cell autonomous molecular feedback loops (Rosbash et al., 2007; Takahashi, 2017). At a molecular level, circadian rhythms are generated by an intracellular transcriptional/translational feedback loop, driving daily oscillations with a period of

approximately 24-hours (hr) in the expression of core clock proteins. Circadian locomotor output cycles kaput (CLOCK) and brain and muscle aryl-hydrocarbon receptor nuclear translocator-like 1 (BMAL1), the positive components of the clock, bind to E-box sequences and drive the expression of the negative elements, period (PER) and cryptochrome (CRY), which can inhibit their own transcription by repressing the CLOCK/BMAL1 heterodimer. Once the levels of PER and CRY are decreased, the new cycle of transcription/translation is started by CLOCK/BMAL1. BMAL1 expression is further regulated through repressed by the circadian nuclear receptor REV-ERBα, and activated by the retinoic acid-related orphan receptor (ROR). Further, post-translational modifications are crucial for regulating the clock. For instance, the serine-threonine kinase casein kinase 1 (CK1) phosphorylates PER and CRY which is vital for modulating circadian cycle length. The expression of other clock-controlled genes and output genes are modulated by the CLOCK/BMAL1 heterodimer, and a substantial fraction of genes in any particular cell or tissue have been found to undergo circadian oscillations (Takahashi, 2017; Zhang et al., 2014). Thus, disruption of circadian timing has profound implications.

These molecular rhythms are not just expressed in the SCN, and work done in the R6/2 mouse model shows that critical circadian rhythms of both core clock and clock-driven genes are abolished *in vivo* in peripheral organs such as the liver (Maywood et al., 2010). This deficiency is accompanied by the arrhythmic expression of the clock genes *CRY1* and D site of albumin promoter (Albumin D-Box) binding protein *(DBP)*, and a phase-advance in the *PER2* cycle. Functionally, this molecular timing system has a major impact on the expression of genes involved in metabolism throughout the body. For example, in peripheral tissues, including muscle, the metabolic genes pyruvate dehydrogenase kinase 4 *(PDK4)* and uncoupling protein 3 *(UCP3)*, are known to be positively regulated by the peroxisome proliferator activated receptor alpha (PPARα) (Dyar et al., 2018), which in turn displays a robust rhythmic expression in many

6

peripheral tissues and modulates BMAL1 expression by directly binding to the *BMAL1* promoter (Canaple et al., 2006). Daily oscillations in the expression of the network of genes involved in mitochondrial lipid metabolism, including *PDK4* and *UCP3*, are associated with oscillations in clock gene expression, with the peak during the rest or fasted phase, and REV-ERB-mediated repression of lipid mobilization and oxidation in anticipation of the active or feeding phase (de Goede et al., 2018a). Glucose levels are also known to exhibit diurnal rhythms. Glucose transporters 1 and 4 (GLUT1,4), responsible for basal blood to cytoplasm transport throughout the body and brain, and insulin-dependent transport primarily into adipose tissue and muscle, respectively, have a peak in expression level at the same time, suggesting increased systemic glucose transport and utilization with same-time diurnal variation (La Fleur et al., 1999). There is still much work to do to understand how transcriptional regulation by the molecular clock interacts with physiological mechanisms. The general assumption is that the temporal pattern of transcription favors adenosine triphosphate (ATP) production and energy utilization during the active phase while allowing remodeling and repair to dominate during rest (de Goede et al., 2018b).

The evidence that the molecular circadian clockwork is disturbed in HD is so far mixed, and more work is required to identify at what stage in disease progression these disruptions occur. For instance, we have previously reported that the circadian rhythms in PER2-driven bioluminescence were altered in the heart but not in the SCN in the BACHD (Whittaker et al., 2018), while deficits in gene expression rhythms have been found in the SCN of the more severely impacted R6/2 model (Morton et al., 2005). There are still large gaps in our understanding of the critical rhythmic outputs impacted by the HD mutation, and thus, we consider this lack of knowledge a major deficiency in the literature as HD-driven alterations in circadian output could be an important clinical symptom of the disease.

HD is a neurodegenerative disease, and the most obvious cause of circadian disruption could be the loss of one or more cell populations in the SCN. HD patients exhibit a loss of SCN neurons by the end of life, with VIP-expressing cells being particularly vulnerable (van Wamelen et al., 2013). In prior work, we examined possible anatomical changes within the SCN of the BACHD mouse at 3-months of age, coinciding with the point when motor symptoms can first be measured. We found that in the BACHD male, but not the female, the SCN was smaller than in wild type (WT) mice. There were no differences in AVP or VIP expression within the SCN with genotype or sex (Kuljis et al., 2016). In the more severely impacted R6/2 mice, the SCN shows decreased expression of VIP and vasoactive intestinal peptide receptor 2 (VPAC2), its receptor (Fahrenkrug et al., 2007). Reductions in VIP would be expected to disrupt the population rhythms in neural activity within and from the SCN as this neuropeptide plays a key role not only in synchronizing SCN cell populations but also its outputs. For instance, VIP projections from the SCN are known to regulate the temporal patterns of activity in several major arousal centers including the orexin expressing cell population in the lateral hypothalamus. Notably, the expression levels of orexin are reduced in HD models (Kotliarova et al., 2005; Petersén et al., 2005; Williams et al., 2011). Thus, in HD mouse models the expression of peptides and neuromodulators is altered in brain regions involved in the neural control of circadian rhythms without a significant loss of hypothalamic neurons.

The circadian system is composed of cell-autonomous clock gene expression rhythms that are synchronized and adaptively phase aligned in tissues throughout the body by both a rhythmic output from the SCN and local or environmental signals (Mohawk et al., 2012). Individual SCN neurons express rhythms in spontaneous firing rate, with higher firing rates observed during the day and lower rates at night (Colwell, 2011; Webb et al., 2009). The BACHD and Q175 mouse models of HD exhibit decreased electrical activity in the SCN during

the day (Kudo et al., 2011a; Kuljis et al., 2018). This decrease in daytime firing in the SCN was

not seen in the R6/2 model (Pallier et al., 2007) although firing rate deficits were seen in the

orexin neurons, an SCN-driven output (Williams et al., 2011). Using electrophysiological

techniques, our laboratory found that SCN neural activity rhythms were lost early in disease

progression and were accompanied by loss of the normal daily variation in resting membrane

potential in the mutant SCN neurons (Kuljis et al., 2018). The low neural activity could be

transiently reversed by direct current injection, thus demonstrating that the neurons have the

capacity to discharge at WT levels. Exploring the potassium currents known to regulate the

electrical activity of SCN neurons, our most striking finding was that these cells in the mutants

exhibited an enhancement in the large-conductance calcium- and voltage-activated potassium

(BK) currents. The expression of the pore-forming subunit, potassium calcium-activated channel

subfamily M alpha 1 (KCNMA1), of the BK channel was higher in the mutant SCN. These

findings show that SCN neurons in the BACHD and Q175 models exhibit early pathophysiology

and that dysregulation of BK current may be responsible. In humans, there is evidence that

mHTT interacts with and impairs the function of a number of transcription factors, in particular

the cyclic adenosine monophosphate (cAMP) response element-binding protein (CREB) (Steffan

et al., 2000; Sugars and Rubinsztein, 2003; Sugars et al., 2004), a known positive regulator of

BK expression (Wang et al., 2009).

     Disorganized circadian timing leads to undesirable effects throughout the body (Colwell,

2015), altering the function of key organ systems including the heart, pancreas, liver, lungs, as

well as the brain. There is evidence that improving the sleep/wake cycle with sleep-inducing

drugs (Kantor et al., 2016; Pallier et al., 2007), stimulants (Cuesta et al., 2012), bright light,

and restricted wheel access (Cuesta et al., 2014) can ameliorate HD symptoms. Collectively,

this prior research supports the hypotheses that circadian dysfunction interacts with HD

pathology leading to the exacerbation of HD-related symptoms and that circadian-based therapies can alter the trajectory of a genetically determined disease. The focus of my dissertation was to determine if circadian based treatments can be usefully applied to treat dysfunction in mouse models of HD.

One of the most significant regulators of the circadian system is the daily feed/fast cycle (Bass and Takahashi, 2010; Tahara and Shibata, 2013). For example, SCN-lesioned animals can still be synchronized to a feeding schedule (Acosta-Galvan et al., 2011; Stephan, 2002; Tahara et al., 2012). Most of the published work has examined the consequences of placing the feeding in the daytime when it is misaligned with normal consumption patterns. However, there have been a few studies that found benefits in scheduling the feeding so that it was aligned with the normal activity cycle. Notably, the Panda lab has shown that healthy mice under time-restricted feeding (TRF) consume equivalent calories from a high fat diet as those with *ad libitum* (*ad lib*) access, display improved motor coordination, and are protected against obesity, hyperinsulinemia, and inflammation (Hatori et al., 2012). The TRF protocol was also beneficial in preventing age-induced cardiovascular dysfunction in *Drosophila* (Gill et al., 2015; Melkani and Panda, 2017). In the HD-N171-82Q mouse model, caloric restriction improved motor performance and survival while reducing cell death (Duan et al., 2003). Prior work in the R6/2 mouse model showed that daytime scheduled feeding can restore HD-driven circadian gene expression in the liver (Maywood et al., 2010). Thus, TRF may represent a circadian-based therapy with the potential to alter the course of a genetic, neurodegenerative disease.

The mechanisms through which TRF conveys benefits may result from a switch in bioenergetic pathways, specific responses to the timing and duration of feeding and fasting, and modulation of circadian rhythm timing and strength. Further, through food-anticipatory activity and reward behavior, TRF may strengthen and synchronize aspects of the circadian

system (Angeles-Castellanos et al., 2010; Astiz et al., 2019; Carneiro and Araujo, 2009; Colwell, 2015), resulting in improved circadian alignment and enhanced signaling. These effects have relevance for HD pathology and symptoms, since normal HTT is found throughout the body and possesses many functional roles. These include trafficking of mitochondria (Reddy and Shirendeb, 2012), autophagosomes (Martin et al., 2015; Ochaba et al., 2014), and brain-derived neurotrophic factor (BDNF) as well as its receptors (Gauthier et al., 2004; Liot et al., 2013). Furthermore, HTT has anti-apoptotic properties (Rigamonti et al., 2000), and interacts with a number of transcriptional repressors and activators (Cattaneo et al., 2005). Importantly, HTT also promotes the production of BDNF (Zuccato et al., 2010).

One mechanism through which TRF may convey benefits is by shifting the body into a state of elevated ketone body production and increasing serum ketone bodies, termed ketogenesis or ketosis. Manipulating the diet to achieve a state of heightened ketone body production has been used to treat epilepsy for nearly a century (Bailey et al., 2005). However, inducing ketosis as a therapy may come under criticism due to the association of ketone bodies with the pathologic state of ketoacidosis associated with Type-I diabetes. However, TRF, as well as ketogenic diets and application of exogenous ketone bodies, produces mild states of ketosis, with blood ketone levels rarely as high as 5 mM, whereas ketoacidosis occurs when blood ketones enter a range of 10 to over 25 mM. Further, central nervous system ketoacidosis has not been found to occur with diet (Al-Mudallal et al., 1996).

Increasing the production of ketone bodies by the liver is dependent upon achieving a period during which glycogen stores are being depleted and fatty acids are being mobilized. Biochemically, carnitine-palmitoyl transferase 1a (CPT1A), a rate-limiting enzyme of fatty acid β-oxidation, catalyzes the transfer of long-chain fatty acids from the outer to the inner mitochondrial membrane where they are liberated as acyl-CoA. This β-oxidation results in

acetyl-CoA that can either enter the Krebs or citric acid cycle, or be used by hydroxymethyl-glutaryl CoA synthase 2 (HMGCS2) for the production of ketone bodies such as D-β-hydroxybutyrate (βOHB). HMGCS2 is the fate committing enzyme in ketone body production. Importantly, CPT1A and HMGCS2, are expressed in a circadian regulated manner (Chavan et al., 2016). Once generated, ketone bodies have multiple fates. One fate of ketone bodies is transport to extrahepatic tissues where they are metabolized to generate ATP, with higher efficiency and lower production of reactive oxygen species (ROS) compared to glucose (Anton et al., 2018; Cahill, 2006; Veech et al., 2001). In addition to their role in bioenergetics, ketone bodies have other important roles and signaling functions which include enhancing mitochondrial respiration and attenuating oxidative stress (Milder et al., 2010; Tieu et al., 2003), increasing BDNF expression (Duan et al., 2003), reducing inflammation (Guo et al., 2018; Youm et al., 2015), functioning in epigenetic modification (Ruan and Crawford, 2018; Tognini et al., 2017), and signaling through G protein-coupled receptors (Offermanns and Schwaninger, 2015).

Pathological changes in mitochondrial energy metabolism and ROS production occur in HD (Guedes-Dias et al., 2016; Siddiqui et al., 2012), and inducing ketosis may influence mitochondrial efficiency and decrease oxidative stress (Milder et al., 2010). Not surprisingly, BDNF levels are reduced in human HD patients and in mouse models of HD by as much as 80% compared to healthy controls, while BDNF levels are increased 3- to 4-fold in HD mice under feeding restriction (Duan et al., 2003; Ferrer et al., 2000).

There is strong evidence for impairment in the clearance of mHTT in HD (Krainc, 2010), and reduction in mHTT levels through degradation has been shown to improve HD symptoms (Lee et al., 2015; Walter et al., 2016). Notably, signaling in the mammalian Target of Rapamycin (mTOR) molecule has been found to be altered in human TRF trials with 6-hr feed,

18-hr fast cycles (Jamshed et al., 2019), and this has important implications for cycles of repair and autophagy as well as mHTT proteolysis and clearance (Camberos-Luna et al., 2016). This is further highlighted by observations of alterations in cycling levels of markers of autophagy in mice, with an accompanying 20% reduction in mHTT, as well as an increase in mesenchymal stem and progenitor cells in mice and humans (Brandhorst et al., 2015; Ehrnhoefer et al., 2018). These effects may be mediated by the switch to ketosis or the timing and duration of feeding and fasting, which can impact mTOR, proteolysis, and glymphatic clearance.

Abnormal activation of microglia, the resident immune cells in the brain, occurs in HD patients (Sapp et al., 2001) and both macrophages and microglia express mHTT, which affects their function (Crotti et al., 2014). Once activated, microglia release inflammatory factors that are toxic to neurons and oligodendrocytes. Activated microglia have been found in the striatum, cerebral cortex, globus pallidus, and white matter of the brain from very early stages of the disease. Additionally, elevation of the pro-inflammatory cytokines TNF-α, IL-6 and IL-1β have been reported in both HD patients and mouse models (Björkqvist et al., 2008; Träger et al., 2015). Through induction of ketosis and significant elevation of the ketone body βOHB, TRF may result in neuroprotection and reduction in inflammation (Guo et al., 2018; Offermanns and Schwaninger, 2015; Youm et al., 2015).

As describe above, disturbances in the timing of the sleep/wake cycle are a well-established symptom of HD that is also commonly present in other neurodegenerative diseases. These behavioral symptoms raise questions about the possible involvement of the circadian system. Using mouse models (**Table 1**), we have demonstrated behavioral and physiological circadian disruptions early in disease progression. Notably, these findings do not preclude the involvement of other structures involved in HD, such as the basal ganglia, in eliciting a disrupted circadian output. The dysfunction found in the circadian system of multiple HD

models does, however, raise the question of whether it is possible to ameliorate such symptoms and, in the end, to "treat" HD and other neurodegenerative diseases using environmental manipulations designed to improve circadian rhythms and enhance the sleep/wake cycle (Morton, 2013; Schroeder and Colwell, 2013). My dissertation work consisted of four studies all designed to determine whether core principles of circadian medicine could be used to reduce the symptoms in mouse models of HD.

In HD patients, there is evidence that histaminergic signaling is disrupted and could contribute to abnormal rhythms in arousal (Shan et al., 2012; van Wamelen et al., 2011). Histamine (HA) is a neuromodulator whose levels vary with a daily rhythm, with peak release during the active cycle and lower levels during sleep. Histamine-3 receptors (H3R) are widely expressed in brain regions involved in cognitive processes and their activation promotes wakefulness (Lin et al., 2011; Parks et al., 2014). Thus, in my first study (Whittaker et al., 2017), we sought to test the hypothesis that daily chronic treatment with a H3R antagonist would improve the non-motor symptoms early in the disease progression in the Q175 model. Homozygous (Hom) and Het Q175 mice received daily treatment in the early night (Zeitgeber Time (ZT) 13) with a H3R antagonist/inverse agonist (GSK189254) for one month. We evaluated the effect of the drug compared to vehicle controls on acute locomotor activity as well as on daily rhythms in activity and sleep behavior. In addition, we examined the impact of the treatment regime on the HD model's performance in open field, T-maze, and tail suspension tests. Finally, as controls, we examined the impact of this treatment on motor performance and resident-intruder aggression.

Because the daily feed/fast cycle is such a powerful regulator of the circadian system, in my second study (Wang et al., 2018), we sought to test the hypothesis that TRF (6-hr of feeding in the middle of the active phase followed by 18-hr fast) could improve the sleep/wake

cycle in the Q175 line. We examined the impact of imposing a regimen composed of 6-hr feeding aligned to the middle (ZT 15-21) of the period when mice are normally active (ZT 12-24) followed by 18-hr of fasting. The treatment was applied to Q175 Hets starting when the mutants were 6 months of age and ending when they were 9 months of age. We selected this age range because this is when the Het Q175 start to show disrupted sleep/wake cycles and when motor symptoms are just beginning. Besides looking at the impact of TRF on rhythms in sleep and activity, we also measured the impact on motor symptoms, which are hallmark features of HD. Since HD patients experience an array of cardiovascular phenotypes, we used a telemetry system to test the hypothesis that TRF improves rhythms in core body temperature, heart rate, and heart rate variability driven by the autonomic nervous system. Finally, we determined whether TRF would alter the HD-driven transcriptional changes measured in the striatum and cortex of the Q175 line.

In my third study (Whittaker et al., 2018), we sought to test the hypothesis that TRF (6-hr feeding aligned to the middle of the active phase and 18-hr fasting) could improve the sleep/wake cycle in the BACHD line. We also evaluated the impact of the treatment on motor performance and autonomic function, and used a BACHD line expressing a PER2::LUCIFERASE (LUC) fusion protein as a bioluminescent circadian reporter to look at the impact of TRF on the amplitude and phase of clock gene expression.

In my final study (Whittaker et al., in preparation), using the BACHD line, we sought to determine whether ketosis without TRF was sufficient to impart similar benefits to TRF in the treatment of HD. First, to test that TRF evokes a rhythm in ketone bodies and that the rhythmic increase in ketones persists for the full 3-months of treatment, the serum levels of ketones were measured across the 24-hr cycle in WT and mutant mice. Finally, we tested the hypothesis that a ketogenic diet could mimic the ketone rhythm observed under TRF and that the induction

of ketosis without TRF was sufficient to impart motor performance and sleep/wake rhythm benefits similar to those observed under TRF.

Recent studies have raised the possibility that neuronal loss is accompanied by myelin breakdown in the striatum (both caudate and putamen) and in the corpus callosum early in the HD process (Bartzokis et al., 2007; Bourbon-Teles et al., 2019; Colwell and Ghiani, 2019). Using the BACHD mouse model, we have found evidence of axonal and myelin loss early in disease progression (3-months of age). In ongoing experiments, we are evaluating the impact of 3-months of TRF on axonal and myelin loss, as well as on other markers of central pathology in HD.

Table 1-1: Summary of circadian phenotypes from mouse models of Huntington's disease.

Phenotype	Models	Citations
Low amplitude activity rhythms	R6/2, BACHD, Q175, HD rats, HD sheep	(Balci et al., 2013; Bode et al., 2009; Kudo et al., 2011a; Kuljis et al., 2016; Loh et al., 2013; Morton et al., 2005, 2014; Oakeshott et al., 2011)
Hypoactivity during active phase	BACHD, Q175,	(Kudo et al., 2011a; Kuljis et al., 2016; Loh et al., 2013; Morton et al., 2005)
Hyperactivity during rest phase	BACHD, Q175	(Kudo et al., 2011a; Kuljis et al., 2016; Loh et al., 2013)
Increase in cycle to cycle variation	BACHD, Q175	(Kudo et al., 2011a; Kuljis et al., 2016; Loh et al., 2013)
Disrupted rhythms in sleep, sleep fragmentation	R6/2, R6/1, Q175	(Fisher et al., 2013, 2016; Kantor et al., 2013; Lebreton et al., 2015; Loh et al., 2013)
Low amplitude rhythms in autonomic driven rhythms in heart rate, core body temperature.	R6/1, R6/2, BACHD, Q175	(Cutler et al., 2017; Kiriazis et al., 2012; Kudo et al., 2011b; Mielcarek, 2015; Schroeder et al., 2016)
Disrupted rhythms in hormones	R6/2	(Dufour and McBride, 2016; Rudenko et al., 2019)
Loss of melanopsin expressing retinal ganglia cells that carry light information to the central circadian clock (SCN)	R6/2, N171-82Q	(Lin et al., 2019; Ouk et al., 2016)
Disrupted rhythms in electrical activity in the SCN	BACHD, Q175	(Kuljis et al., 2018, 2016)
Disrupted gene expression rhythms in central clock	R6/2	(Morton et al., 2005)
Disrupted gene expression rhythms outside SCN	R6/2	(Maywood et al., 2010; Morton et al., 2005)
Pathology in central clock	R6/2, BACHD	(Fahrenkrug et al., 2007; Kuljis et al., 2016)

Chapter 2: Possible use of a histamine-3 receptor antagonist for the management of nonmotor

symptoms in the Q175 mouse model of Huntington's disease

ORIGINAL ARTICLE

Possible use of a H3R antagonist for the management of nonmotor symptoms in the Q175 mouse model of Huntington's disease

Daniel S. Whittaker[1] (ID), Huei-Bin Wang[1], Dawn H. Loh[1], Roger Cachope[2] & Christopher S. Colwell[1] (ID)

[1]Department of Psychiatry & Biobehavioral Sciences, University of California, Los Angeles, California 90095-1751
[2]CHDI Foundation, 6080 Center Drive, Suite 100, Los Angeles, California 90045

Abstract

Huntington's disease (HD) is an autosomal dominant, neurodegenerative disorder characterized by motor as well as nonmotor symptoms for which there is currently no cure. The Q175 mouse model of HD recapitulates many of the symptoms identified in HD patients including disruptions of the sleep/wake cycle. In this study, we sought to determine if the daily administration of the histamine-3 receptor (H3R) antagonist/inverse agonist 6-[(3-cyclobutyl-2,3,4,5-tetra-hydro-1H-3-benzazepin-7-yl)oxy]-N-methyl-3-pyridinecarboxamide hydrochloride (GSK189254) would improve nonmotor symptoms in the Q175 line. This class of drugs acts on autoreceptors found at histaminergic synapses and results in increased levels of histamine (HA). HA is a neuromodulator whose levels vary with a daily rhythm with peak release during the active cycle and relatively lower levels during sleep. H3Rs are widely expressed in brain regions involved in cognitive processes and activation of these receptors promotes wakefulness. We administered GSK189254 nightly to homozygote and heterozygote Q175 mice for 4 weeks and confirmed that the plasma levels of the drug were elevated to a therapeutic range. We demonstrate that daily treatment with GSK189254 improved several behavioral measures in the Q175 mice including strengthening activity rhythms, cognitive performance and mood as measured by the tail suspension test. The treatment also reduced inappropriate activity during the normal sleep time. The drug treatment did not alter motor performance and coordination as measured by the challenging beam test. Our findings suggest that drugs targeting the H3R system may show benefits as cognitive enhancers in the management of HD.

Abbreviations

CB, challenging beam; GSK189254, 6-[(3-cyclobutyl-2,3,4,5-tetrahydro-1H-3-benza-zepin-7-yl)oxy]-N-methyl-3-pyridinecarboxamide; H3R, histamine-3 receptor; HA, histamine; HD, Huntington's disease; KO, knockout; LD, light/dark; OF, open field; RI, resident-intruder; SCN, suprachiasmatic nucleus; TMN, tuberomammilary nucleus; TM, T-maze; TS, tail suspension; ZT, zeitgeber time.

Introduction

Huntington's disease patients suffer from a progressive neurodegenerative process that inflicts cognitive, psychiatric, and motor dysfunction (Margolis and Ross 2003; Kuljis et al. 2012a). HD is caused by a CAG repeat expansion within the first exon of the *huntingtin* (*Htt*) gene which produces a polyglutamine repeat that leads to protein misfolding, soluble aggregates, and inclusion bodies detected throughout the body (Saft et al. 2005; Ciammola et al. 2006). The normal function of the protein (HTT) remains unknown; however, the mutated form

leads to dysfunction of a large range of cellular processes including cytoskeletal organization, protein folding, metabolism, and transcriptional activities (reviewed by Saudou and Humbert 2016). HD symptoms start at a range of ages, with an average onset at 40 years of age. Generally, the longer the CAG repeat, the earlier the age of onset and the greater the severity of the symptoms (Duyao et al. 1993; Langbehn et al. 2010). Still, even among patients with the same CAG repeat length, there is considerable range in the onset of symptoms (around a decade) and their severity (Wexler 2004; Gusella et al. 2014). This variability raises the possibility that optimal disease management can increase the health span of the HD patients.

Histaminergic neurons originate in the tuberomammillary nucleus (TMN) which is in the hypothalamus and broadly releases HA throughout the central nervous system. The release is controlled with a diurnal rhythm with high neural activity in the TMN and subsequent HA release peaking during the organism's active cycle (night time in mice). The postsynaptic effect is largely excitatory and thus HA is considered one of the main transmitters that control arousal (Haas and Panula 2003). One of the major HA outflows targets the central clock, the suprachiasmatic nucleus or SCN (Watanabe et al. 1984), and HA is a potent regulator of the circadian system (e.g., Cote and Harrington 1993; Eaton et al. 1995; Meyer et al. 1998; Jacobs et al. 2000; Parmentier et al. 2002; Abe et al. 2004; Kim et al. 2015). Commonly prescribed wake-promoting compounds, such as methamphetamine-related drugs or modafinil, require a functional dopaminergic system (Wisor et al. 2001). Since dopaminergic pathways are compromised in HD, H3Rs are a promising target to treat hypersomnia and H3R antagonists promote wakefulness (Lin et al. 2011). In HD patients, there is evidence that histaminergic signaling is disrupted and could contribute to disrupted rhythms in arousal in HD patients (van Wamelen et al. 2011; Shan et al. 2012). Disruptions in the sleep/wake cycle are an early part of HD symptoms seen in both patients and mouse models (e.g., Morton et al. 2005). On the basis of this literature, we hypothesized that the nightly treatment with a H3R antagonist would not only acutely increase arousal but also adjust the phase of the underlying circadian system to improve rhythmic behaviors.

Among the mouse models of HD, the heterozygote (Het) Q175 offers advantages of single copy of the mutation, genetic precision of the insertion and control of mutation copy number (Pouladi et al. 2013). These features make the Het Q175 line perhaps the most clinically relevant of the mouse lines. Prior work with this model has demonstrated that the Q175 line exhibits age-dependent disruptions in motor performance (Heikkinen et al.

2012; Menalled et al. 2012) as well as circadian behavior (Loh et al. 2013) when compared with wild-type controls. In this study, we sought to test the hypothesis that the daily chronic treatment with a H3R antagonist would improve the nonmotor symptoms early in the disease progression of the Q175 model. Homozygote (Hom) and Het Q175 mice received daily treatment in the early night (zeitgeber time [ZT] 13) of GSK189254 for 1 month. We evaluated the effect of the drug compared to vehicle controls on acute locomotor activity as well as on daily rhythms in activity and sleep behavior. In addition, we examined the impact of the treatment regime on the HD model's performance in open field, T-maze, and tail suspension tests. Finally, as controls, we examined the impact of the treatment on motor performance and resident-intruder aggression.

Materials and Methods

All experimental protocols used in this study were approved by the University of California, Los Angeles (UCLA) Animal Research Committee. Every effort was made to minimize pain and discomfort. Experiments followed the UCLA Division of Laboratory Animal Medicine recommendations for animal use and welfare, as well as National Institutes of Health guidelines.

Animals

A line of mice with a spontaneous expansion of the CAG repeats, the Q175 mutation (Menalled et al. 2012), was obtained from the CHDI colony of Q175 mice at the Jackson Laboratories (Bar Harbor, Maine). We obtained cohorts of male 9–month-old Q175 Het mice with CAG repeats averaging 191 ± 4, and male 4-month-old Q175 Hom mice with CAG repeats averaging 183 ± 9. Mice were housed in standard mouse cages inside custom cabinets in a light-tight setting allowing continuous sleep behavior recording. All mice were held in a light/dark (LD) cycle of 12 h of light followed by 12 h of dark (LD 12:12) with an average 350 lux white LED light (HitLights LED, Baton Rouge, LA) during light periods. Under LD 12:12 conditions, the time of lights-on defines ZT 0, whereas the time of lights-off is defined as ZT 12. All animals received rodent chow and water ad libitum.

Drug treatment

GSK189254 has a reported oral half-life of 2.5 hrs and is highly brain penetrant. Two hrs after dosing by oral gavage, 1.0 and 3.0 mg/kg are reported to result in serum levels of 115 and 239 ng/mL and 80 ± 9 and $90 \pm 2\%$ receptor occupancy, respectively (Medhurst et al. 2007;

Wilson et al. 2013). While prior work has used oral gavage to deliver the drug, we found that this drug delivery method disrupted activity rhythms in C57 mice (data not shown). Therefore, in this study, we placed the vehicle or drug into condensed milk. GSK189254 was provided in lyophilized form by the CHDI Foundation. The vial was maintained in an airtight bag inside a light-tight box in a 4°C fridge. The drug compound was prepared weekly for administration by grinding the measured antagonist into a fine powder using mortar and pestle, then bringing into suspension by slowly adding 100 μL of 0.5% methylcellulose in saline and mixing for five min. This was then mixed incrementally into 10 g condensed milk (NESTLÉ, Wilkes-Barre, PA) for 10 min followed by 15 min of sonication. Amounts of GSK189254 used depended on the final drug concentration needed in order to generate 0.3, 1.0, or 3.0 mg/kg dosing. Following sonication, final compound formulations were immediately aliquoted into prelabeled 1.5 mL tubes, wrapped with parafilm, boxed, and stored in a 4°C fridge until used. Vehicle treatment was similarly prepared with 100 μL 0.5% methylcellulose in saline and 10 g condensed milk.

The compound was administered daily at ZT 13. Aliquots were sonicated for 10 min, with the condensed milk level held below the sonicator water level. Mouse weights were consulted to determine the amount of compound to administer to each mouse. 10 mg of compound or vehicle for every gram of body weight was weighed into preweighed dishes, one per mouse, using a microbalance. Under dim red light (3-5 lux), the dishes were placed in the corresponding cages and collected 20 min later. Each preweighed dish was re-weighed and differences were recorded to ensure all compound or vehicle was consumed.

As an initial control experiment to ensure that our drug administration method was successful, mice of each genotype were randomly placed into one of the four treatment groups: vehicle, and 0.3, 1.0, or 3.0 mg/kg GSK189254. After drug was administered for 4 weeks, serum was collected 1 h posttreatment. Blood was collected (about 0.7–0.9 mL per animal) via cheek puncture into microvette EDTA tubes (Sarstedt, Nümbrecht, Germany). Tubes were gently inverted a few times and placed immediately on wet ice. Within 1 h following collection, samples were centrifuged at 660 g for 15 min at 4°C. Using a new pipet per sample, the supernatant was collected (0.1–0.25 mL) into prelabeled Eppendorf tubes (Fisher Scientific, Hampton, NH). Tube lids were covered with parafilm and immediately stored at −80°C until shipment. Multiple samples of each formulation prepared were also collected and stored. Measurements of GSK189254 were made with liquid chromatography-mass spectrometry by Discovery - Charles River (Essex, UK).

Vehicle controls were not detectable. We subsequently used 3.0 mg/kg for the remainder of the study. Body weights were recorded weekly.

Experimental design

Initially mice were habituated to the LD cycle and housing conditions, we then measured diurnal rhythms in activity and sleep over a 2-week period from Hom and Het Q175 mice. The performance of the mice on open field, T-maze, tail suspension, challenging beam, and resident-intruder tests was assessed in the early night (ZT 14-17) under dim red light (3-5 lux) under these baseline conditions. Next, the mice were randomly divided into two groups with one group treated with GSK189254 and one group receiving the vehicle control. During the treatment period, mice were given access to a small dish with vehicle or vehicle + drug placed in their cage for 20 min at ZT 13. After 2 weeks of treatment, rhythms in activity and sleep were measured. After 4 weeks of treatment, behavioral tests were repeated while the mice were still receiving vehicle or drug. Again, all tests were performed under dim red light (3-5 lux) in the middle of the night: during ZT 14-17 to coincide with peak drug activity. This design allowed us to both compare the behavioral measures from the drug- and vehicle-treated groups at the end of treatment but also to examine the performance of the same animals before and after treatment. All nonautomated behavioral measurements were carried out by two independent observers who were masked as to the experimental condition and the results averaged.

The sample size of 10 mice per group was determined by both our empirical experience with locomotor activity measures in the Q175 mice and a statistical analysis (SigmaPlot, v13) that assumed a power of 0.8 and an alpha of 0.05. For the liquid chromatography-mass spectrometry measurements of GSK189254, one of the Het Q175 samples was corrupted during collection or shipment and was excluded from the analysis. In addition, a recording error was made during the T-maze tests with one of the vehicle-treated Het Q175 mice so that the sample size was 9 rather than 10 mice.

Video measurement of immobility-defined sleep

Immobility-defined sleep was determined as described previously (Loh et al. 2013). Mice were housed in see-through plastic cages containing bedding, but without the addition of nesting material. Video capture of a side-on view of each cage was obtained, and was not obstructed by the top mounted food bin or water bottle. Cages were under constant infrared LED lighting. Video

was captured using infrared surveillance cameras (DTV Electronics, Inc., San Leandro, CA) equipped with IR850 infrared filters (Neewer Technology Ltd., Guangdong, China) and connected to video-capture cards (Adlink Technology Inc., Irvine, CA). ANY-maze software (Stoelting Co., Wood Dale, IL) was used to track the animals. Immobility detection was set to 95% of the area of the animal immobile for 40 sec, as was previously determined to have 99% correlation with simultaneous EEG/EMG defined sleep (Pack et al. 2007; Fisher et al. 2012). We recorded video continuously, except when administering treatments, performing testing, and changing cages. For each time period analyzed, we used five consecutive days in the period for sleep analysis and three consecutive days for analysis of bouts. Immobility-defined sleep was determined in 1-min bins and total sleep was determined by summing immobility durations. A sleep bout was defined as a duration of continuous immobility (maximum gap: 1 min; threshold: 3 counts/min), and the number of bouts and the average duration of bouts were determined for both day and night using ClockLab software (Actimetrics, Wilmette, IL). An average waveform of hourly sleep over 5 days was produced per genotype and per age and treatment group for the purpose of graphical display.

Cage activity recording

Locomotor activity recording was performed using passive IR sensors (Honeywell International, Inc., Morris Plains, NJ) and recorded with a data acquisition system obtained from Mini Mitter Co. (Bend, OR). Data were analyzed using the El Temps (A. Diez-Noguera, Barcelona, Spain) and ClockLab programs. We recorded continuously, except when performing behavior testing, and changing cages on alternate Mondays. For each time period analyzed, cage activity was recorded in 3-min bins, and 10 days of data was averaged for analysis. The data were analyzed in El Temps to determine the period and rhythmic strength (Kudo et al. 2011; Loh et al. 2013). Major activity duration (alpha, α) was determined in El Temps by the duration of continuous activity over the threshold of the mean using an averaged waveform. Onset variability was determined by calculating the daily variation in onset over 10 days of activity using the Clocklab program. Acute activity in response to treatment was also assessed by obtaining activity in El Temps for one, two, and three hrs post administration and calculating the fraction of total daily activity represented in each respective hour and for the 3-h period. For acute activity, the last day of untreated acclimation was compared to the first day of administration following habituation.

Open field test

The OF test was used to assess anxiety-like behavior (Prut and Belzung 2003; Bailey and Crawley 2009; Southwell et al. 2009) as well as exploratory behavior and spontaneous locomotor activity (Rothe et al. 2015). Animals were individually placed in a plastic arena with opaque walls (47 cm wide $\times$ 40 cm long $\times$ 30 cm tall). The experimenter moved out of the testing area after placement of animals. OF activity was recorded for 10 min by a ceiling-mounted infrared equipped 800TVL dome video camera (101 AudioVideo Inc., Sunnyvale, CA). The tests were performed under dim red light (3-5 lux). ANY-maze software was used to code the videos. Anxiety-like behavior was scored for time spent in the center versus the peripheral zone of the testing arena. The central 25% of the arena was designated as the center zone. To assess exploratory behavior and spontaneous locomotor activity, speed and total distance travelled over 10 min were scored using ANY-maze software.

Tail suspension test

The TS test was employed to develop an index of behavioral despair based upon the duration of immobility, where longer durations of immobility imply a greater degree of behavioral despair (Cryan et al. 2005; Juszczak et al. 2006). The method used was similar to that described previously (Can et al. 2011). Briefly, tape is applied to the tails of mice and they are suspended 15 cm below a bar and in front of a white background for six min. The tests were video recorded during the early night under dim red light (3-5 lux) and manually scored post hoc for their mobility time by two independent investigators. Mobility time is subtracted from total time to generate immobility time.

T-maze test

The TM test was performed to assess cognitive ability (Deacon and Rawlins 2006) in the mice. The TM (UCLA Psychology Department shop, Los Angeles, CA) was mounted on a tripod and consists of two arms perpendicular to one another forming the T-maze. Each arm of the TM is 290 mm and the "T" junction is 80 mm $\times$ 80 mm. All walls of the TM are 145 mm tall and opaque. No habituation to the maze is used, as it is the novelty of the maze that drives the spontaneous alternation exploratory behavior. Mice were tested in their active phase and were not food-deprived prior to testing. Dim red lighting (3-5 lux) was used and placed directly over the center of the "T" to avoid shadows on the starting arm. Prior to the testing, mice were acclimated to the

testing room. At the start of each test, a well-handled mouse is placed at the base of the TM on the starting platform and the experimenter steps straight back away from the maze. The mouse chooses an arm at the "T" junction and is blocked in the arm once all four feet enter the arm. The mouse is retained for 20–30 sec in the arm before starting the next trial. Each mouse undergoes 10 trials. Scoring is performed by recording the choice each trial.

Challenging beam test

The CB test for motor performance and coordination was performed as previously described (Fleming et al. 2004, 2013; Loh et al. 2013). Briefly, animals were trained to walk across an elevated beam (Plastic Zone Inc., Tarzana, CA) ending in their home cage. The beam consists of progressively narrowing 253 mm lengths, with widths of 33 mm, 24 mm, 18 mm, and 6 mm. Training and testing were conducted during the early night under dim red lighting (3-5 lux). Training was conducted for two consecutive days with five beam crossings per mouse each day. On the third day, when testing was conducted, raised 19-gauge mesh wire grids (Ace Hardware, Oak Brook, IL) with 10 mm × 10 mm spacing were overlaid onto the beams. Mice were video recorded from the side as they crossed the gridded beams. Videos were scored post hoc by two independent investigators for the number of step errors made per beam. Errors were counted when the mouse was facing and moving forward. A step was considered an error when any foot passed below the grid and more than half-way to the beam. Counting began when the mouse had all paws on the grid and made its first step forward. Counting ended when the mouse stepped with either forelimb off the end of the final beam grid. Scores were averaged for each beam segment for the five trials per mouse.

Resident-intruder test

The resident-intruder test was performed as described (Koolhaas et al. 2013) to assess the aggression in untreated mice at baseline and in response to the treatment. The "resident" mice (Q175) were acclimated in their home cage for five min before the tests began. Unfamiliar C57 WT mice with lighter body weights were selected as the "intruder" mice. The test started when the intruder mouse was introduced to the resident's cage and preceded for five min. The tests were video recorded during the early night under dim red light (3-5 lux) and manually scored post hoc for aggressive behaviors by two independent investigators. Exploration time before first attack, total time of attacks, and the duration of the

longest attack were recorded. The scores from the two scorers were averaged per mouse.

Statistical analysis

Statistical analysis was performed using SigmaPlot (v. 13). Datasets were examined for normality (Shapiro–Wilk test) and equal variance (Brown–Forsythe test). The values from the groups were analyzed using a two-way or one-way analysis of variance (ANOVA). Pairwise multiple comparison procedures were made using the Holm–Sidak method. In the cases where the normality or equal variance assumptions were not met, a Kruskal–Wallis one-way ANOVA on ranks were used. Finally, paired t-tests were used to determine if the drug treatment altered the performance of the mice before and after treatment. Statistical significance was defined by $P < 0.05$ in all analyses.

Results

Oral administration of 3.0 mg/kg was an effective dose of GSK189254

In our first experiment, we sought to determine what concentration of GSK189254 would be sufficient to increase serum levels of the drug to biologically meaningful levels. Hom and Het Q175 mice ($n = 10$ per group) were randomly placed into one of the four groups: vehicle, and 0.3, 1.0, 3.0 mg/kg GSK189254. After drug or vehicle was administered for 4 weeks, serum was collected between ZT 14-15 and levels of GSK189254 determined by liquid chromatography-mass spectrometry. The resulting measurements were analyzed with a two-way ANOVA with dose and genotype as factors. There was a significant effect of dose ($F = 87.846$, $P < 0.001$) with 3.0 mg/kg moving the serum levels well above our target of 100 ng/mL (Fig. 1). Interestingly, at both the 1.0 and 3.0 mg/kg dose, the serum levels were lower ($P < 0.05$) in the Het Q175 than in the Hom Q175 (Fig. 1). Since the effective concentration varied between the genotypes, we analyzed the findings from the two genotypes separately for the remainder of the study.

Chronic GSK189254 produced short-term increases in activity without altering the total activity over 24 h.

The acute impact of the oral administration of GSK189254 (3.0 mg/kg) was assessed by monitoring the amount of total cage activity measured by IR sensor in Hom and Het Q175 at one, two, and three hrs after treatment (Fig. 2; two-way repeated measures ANOVA with time and treatment as factors). Compared to vehicle-treated controls, drug treatment significantly increased ($F = 15.485, P < 0.001$) cage activity of the Hom Q175 and a multiple comparison procedure indicated that increase
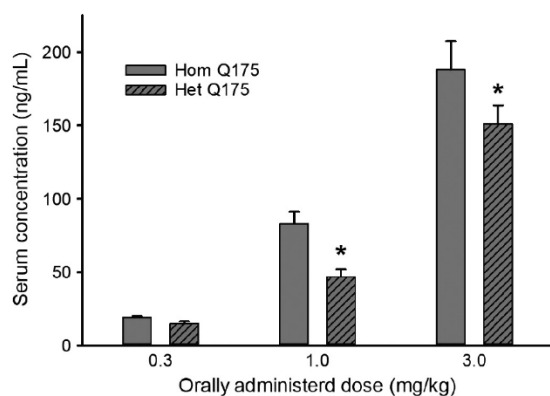
Figure 1. NOTE y-axis label "S" in serum (top of letter is smudged/ blurred) Serum was collected 1 h after oral administration of drug in condensed milk. Measurements made with liquid chromatography-mass spectrometry by Discovery - Charles River (Essex, UK). Vehicle controls were not detectable. The data were analyzed with a two-way ANOVA with dose and genotype as factors. Values are mean $\pm$ SEM in this and remainder of the figures. Asterisk represents significant genotypic differences ($P < 0.05$). The serum concentrations for the 1.0 and 3.0 mg/kg treatments were significantly ($P < 0.05$) higher than those measured after the 0.3 mg/kg treatment.

was seen ($P < 0.05$) at each of the time points following treatment. In contrast, compared to vehicle-treated controls, drug treatment did not alter the activity of the Het Q175 ($F = 4.075$, $P = 0.06$). A comparison of the same animals at the same ZT on the last day of baseline untreated acclimation and on the first day of administration after habituation (Fig. 2; Paired *t*-test) indicated that the drug treatment increased activity in both the Hom ($t = -2.984$, $P = 0.015$) and Het ($t = -2.854$; $P = 0.021$) Q175 when measured 1 h after treatment. Most Hom Q175 (8/10) and all the Het Q175 (9/9) mice exhibited increased activity levels as measured 1 h after treatment when compared with baseline. As measured over the full 24-h cycle, the treatment did not significantly alter activity levels in either the Hom ($F = 1.533$, $P = 0.223$) or Het ($F = 1.838$, $P = 0.158$) Q175. There was a trend toward lower overall activity in both the Hom (baseline: 157 ± 18 au/h; vehicle: 156 ± 13 au/h; drug: 130 ± 8 au/h) and Het (baseline: 174 ± 18 au/h; vehicle: 169 ± 18 au/h; drug: 133 ± 11 au/h) Q175. For this and other behavioral measures, the WT data are shown in Table 1 for comparison. Overall, the drug produced an acute increase in activity that lasted over three hrs in the Hom Q175 line.

Chronic GSK189254 strengthened daily activity rhythms

Next, we examined the impact of the drug on activity rhythms of the Q175 mice recorded over 10 days.

Compared to vehicle-treated mice, administration of GSK189254 improved several measures of the daily rhythm in locomotor activity in Hom and Het Q175 (Fig. 3; one-way ANOVA). In the Hom Q175, the drug treatment increased the power ($F = 3.576$, $P = 0.023$) and reduced the variability in the onset of the nightly activity bout ($H = 14.475$, $P = 0.002$). In the Het Q175, the drug treatment increased the power ($F = 4.663$, $P = 0.007$) as well as reduced the variability in the onset of the nightly activity bout ($F = 5.233$, $P = 0.004$) and inappropriate daytime activity ($F = 8.917$, $P < 0.001$). A comparison of the same animals before and after treatment (paired *t*-test) indicated that the drug treatment also significantly improved power and precision of the activity rhythms of both genotypes and the % activity in the light in the Het Q175 (data not shown). Thus, GSK189254 treatment improved activity rhythms in both Het and Hom Q175 lines.

Chronic GSK189254 altered the daily pattern of sleep behavior

We also examined the impact of the drug on rhythms in sleep behavior measured over 1-week periods with video recording in combination with an automated mouse tracking analysis software system (Li et al. 2015; Wang et al. 2017). In both Hom and Het Q175, the treatment with GSK189254 produced an acute decrease in sleep which lasted for several hrs (Fig. 4, top panels). A 2-way ANOVA was used to analyze the 1-h bins and found significant effects of treatment (Hom: $F = 9.176$, $P = 0.003$; Het: $F = 7.302$, $P = 0.007$) and time (Hom: $F = 42.402$, $P < 0.001$; Het: $F = 51.890$, $P < 0.001$). However, the treatment did not alter the total amount of sleep (Fig. 4, middle panels) or the number of sleep bouts (Fig. 4, bottom panels) in the day or night in either of the mutant lines. A comparison of the same animals before and after treatment (paired *t*-test) indicated that the drug treatment produced significant increases in the duration ($t = -2.742$, $P = 0.023$) and decreased the number of sleep bouts ($t = 3.425$, $P = 0.007$) in the Het Q175 in the day (data not shown). The rest of the values were not significantly different. Thus, GSK189254 treatment produced changes in the temporal pattern of sleep behavior but did not cause sleep deprivation in either the Hom or Het Q175 lines.

Chronic GSK189254 improved performance on OF and TM tests without increasing anxiety-like behavior

We examined the impact of the drug on two commonly used tests that are both dependent upon activity

24
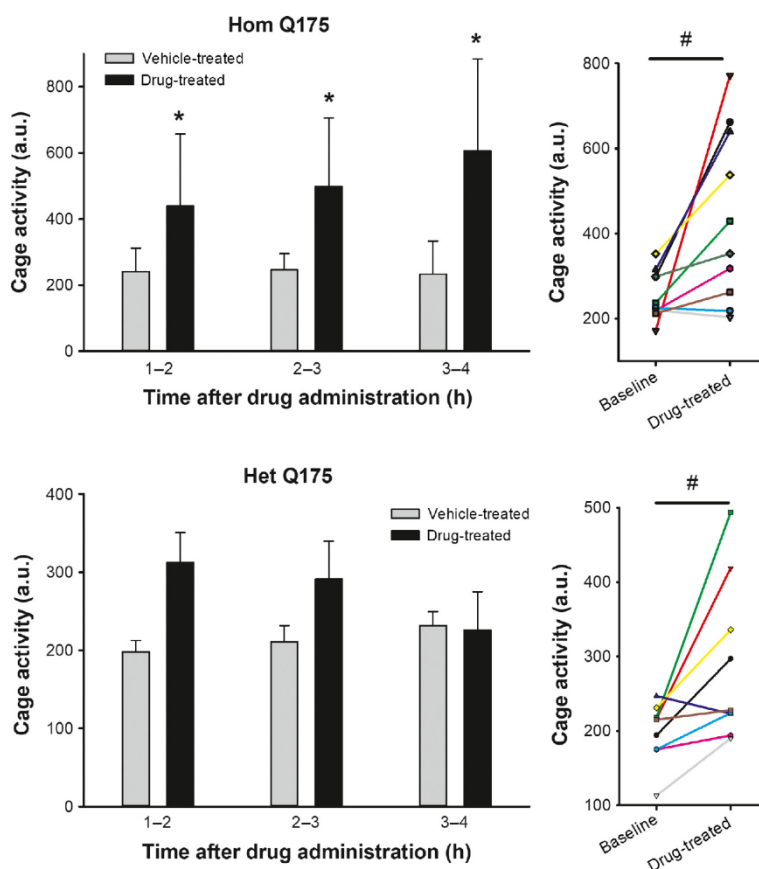
Figure 2. Hom Q175 (top of letter "H" and numbers smudged/blurred) and y-axis "C" in cage activity (Hom bar graph) also same. The acute oral administration of GSK189254 (3.0 mg/kg) significantly increased total cage activity measured by an IR sensor in Hom (top) and Het (bottom) Q175. Left panels illustrate the activity for the 3 h following treatment. After 4 h, activity was no longer elevated compared to vehicle controls in either genotype. Two-way ANOVA was used to analyze the activity levels with time and treatment as factors. Asterisks represent significant differences due to drug treatment compared to vehicle-treated controls ($P < 0.05$). Right panels show the values from individual animals at the same ZT on the last day of untreated acclimation compared to the first day of administration 1 h after treatment. Paired *t*-test found significant ($P < 0.05$) impact of drug treatment on the animal's activity levels shown by a # symbol. Most, but not all, mice exhibited a significant increase in activity as a result of drug treatment.

measures. Administration of GSK189254 improved exploratory behavior as measured in the OF test (Fig. 5). Compared to vehicle-treated controls, drug treatment significantly increased both the distance ($F = 7.279$, $P = 0.001$) and speed of movement ($F = 6.240$, $P = 0.002$) in the Hom Q175. A comparison of the same animals before and after treatment (paired *t*-test) indicated that the drug treatment also significantly improved distance ($t = -4.532$, $P = 0.001$) and speed ($t = -4.485$, $P = 0.001$) of the Hom Q175. The drug treatment did not change the amount of time the mice spent in the center of the OF arena (baseline: $9 \pm 1\%$; vehicle: $14 \pm 2\%$; drug: $13 \pm 2\%$; $F = 3.001$, $P = 0.067$).

The drug-treatment had a less robust impact on the OF behavior in the Het Q175. The GSK189254 treatment did not significantly increase posttreatment values for distance ($H = 5.707$, $P = 0.127$) and speed of movement ($H = 7.169$, $P = 0.057$). A comparison of the same animals before and after treatment (paired *t*-test) indicated that the drug treatment did significantly improved distance ($t = -2.542$, $P = 0.032$) and speed ($t = -2.335$; $P = 0.044$) in the Het Q175 (Fig. 5). The treatment did not alter the amount of time the mice spent in the center of the OF arena (baseline: $17 \pm 2\%$; vehicle: $16 \pm 2\%$; drug: $17 \pm 3\%$; $H = 0.018$; $P = 0.991$).

In the TM test, the benefits of the drug were seen in the Het Q175 (Fig. 6). Compared to vehicle-treated controls, drug treatment significantly increased spontaneous alternations in the Het ($H = 9.612$, $P = 0.022$) but not in the Hom Q175 ($F = 1.224$, $P = 0.310$). A comparison of

Table 1. Selected behavioral values for WT control mice. While not part of the same study, the WT data were obtained using the same equipment and protocols as those used with the Q175 mice. The Het Q175 mice were tested at 9 months, whereas the Hom Q175 at 6 months of age.

Task	WT (6 months)	WT (9 months)
Activity (au/h)	218 ± 28	275 ± 32
Power (%V)	39 ± 3	30 ± 1
Activity in light (%)	20 ± 1	20 ± 1
Onset variability (min)	11 ± 1	26 ± 2
Sleep in day (min)	474 ± 10	534 ± 12
Sleep in night (min)	167 ± 14	174 ± 14
Sleep bouts in day (#)	23 ± 1	26 ± 2
Sleep bouts in night (#)	30 ± 4	44 ± 3
OF distance (m)	43 ± 2	40 ± 2
OF speed (m/s)	0.07 ± 0.001	0.07 ± 0.001
OF center time (%)	14 ± 1	21 ± 1
TM spontaneous alternation (#)	5.3 ± 0.6	5.6 ± 0.5
RI aggressive interactions	20%	12%
CB errors (#)	4.4 ± 0.5	5.5 ± 0.3

the same animals before and after treatment (paired t-test) also indicated that the drug treatment produced significant increases in the alternations in the Het ($t = -2.753$, $P = 0.022$) but not the Hom ($t = -2.123$, $P = 0.0629$) Q175 (Fig. 6). The results from the OF and TM tests indicate that the GSK189254 boosted performance on the tests without an increase in anxiety-like behavior in the mutant lines.

Chronic GSK189254 reduced behavioral despair

The TS test is a commonly used measure of affect in mice, with time that the mouse is immobile as an indicator of behavioral despair. Compared to vehicle controls, chronic administration of GSK189254 significantly decreased the immobile time in the Hom ($H = 13.381$, $P = 0.006$) but not the Het ($F = 0.680$, $P = 0.570$) Q175 mice. A comparison of the same animals before and after treatment (paired t-test) also indicated that the drug treatment produced significant decreases in immobility in the Hom ($t = 3.555$, $P = 0.006$) but not the Het ($t = 1.638$, $P = 0.136$) Q175 (Fig. 7).

To evaluate whether the H3R antagonist might increase aggressive behavior, we used RI test in which a stranger mouse is introduced into the home cage of a Q175 mouse. In the Hom Q175, half of the drug-treated mice (5 of 10) exhibited some type of aggression against the stranger mouse in the test period (5 min), whereas none of the vehicle-treated mice (0 of 10) exhibited aggressive behavior. In the Het Q175, none of the drug treated (0 of

10) nor any of the vehicle controls (0 out 9) exhibited any evidence of aggression during this same test.

Chronic GSK189254 did not alter motor performance

Finally, we examined the impact of drug treatment on the CB test. Compared to vehicle controls, chronic administration of GSK189254 did not alter the number of errors made by either Hom (baseline: $3.8 ± 0.4$; vehicle: $4.3 ± 0.6$; drug: $4.4 ± 0.4$; $F = 0.067$, $P = 0.935$) or Het (baseline: $3.9 ± 0.4$; vehicle: $4.1 ± 0.7$; drug: $3.8 ± 0.4$; $F = 0.101$, $P = 0.904$) Q175. Similarly, there was no difference in the time (sec) that the mouse took to cross the beam in Hom (baseline: $14.8 ± 1.0$; vehicle: $13.7 ± 0.5$; drug: $15.6 ± 0.7$; $F = 1.438$, $P = 0.255$) or Het (baseline: $16.0 ± 1.0$; vehicle: $18.2 ± 1.6$; drug: $16.9 ± 1.5$; $F = 0.754$, $P = 0.480$). Thus, treatment with GSK189254 did not alter the performance on the CB test.

Discussion

In this study, we sought to determine if the daily administration of the H3R antagonist/inverse agonist GSK189254 would improve nonmotor symptoms in the Q175 mouse model of HD. We administered the GSK189254 compound nightly to Hom and Het Q175 mice for 4 weeks starting at ages before the onset of motor symptoms and confirmed that the plasma levels of the drug were elevated to a therapeutic range. We demonstrate that daily treatment with GSK189254 improved the daily activity rhythm with increases in the strength of the rhythm as measured by power of the periodogram and decreases in cycle-to-cycle variability in activity onset. GSK189254 treatment also produced short-term changes in sleep behavior but did not cause an overall change in the amount of sleep as measured over the 24-h cycle. GSK189254 treatment improved performance of the HD mutant mice on exploratory behavior, cognitive performance and mood without increasing anxiety-like behavior. The drug treatment did not alter motor performance and coordination as measured by the challenging beam test. Our findings suggest that drugs targeting the H3R system may benefit somnolence and vigilance in the management of HD.

A potential role for H3R antagonists in promoting wakefulness is supported by a number of previous studies. Centrally, HA is produced by TMN neurons and is thought to play a critical role in daily rhythms in arousal (Brown et al. 2001; Haas and Panula 2003; Lin et al. 2011) with peak release during the active cycle and relatively lower levels during sleep (Mochizuki et al. 1992; Prast et al. 1992). Like other monoamine

Figure 3. Chronic administration of GSK189254 improved some aspects of the daily rhythm in cage locomotor activity in Hom and Het Q175. Top panels show representative examples of cage locomotor activity at baseline and during drug treatment. Drug treatment improved some of the key measurements of activity rhythms in Hom (middle panels) and Het (bottom panels) Q175. One-way ANOVA was used to analyze the group values. Asterisks represent significant differences due to drug treatment compared to vehicle-treated controls ($P < 0.05$).

neurotransmitters, HA has a specialized class of autoreceptors (the H3R) that serve as a synaptic negative feedback system. Activation of H3R results in the inhibition of HA synthesis (Gomez-Ramirez et al. 2002) and release from histaminergic neurons (Arrang et al. 1983). Because

the H3R are constitutively activated (Morisset et al. 2000; Takahashi et al. 2003), pharmacological agents that block H3Rs increase the release of HA. H3R are widely expressed in the mammalian brain, particularly in areas involved in cognitive processes and arousal, such as the

Figure 4. Chronic administration of GSK189254 alters the temporal pattern of sleep behavior in Q175 mice. Video recording in combination with automated mouse tracking analysis software was used to measure immobility-defined sleep. Top panels show running averages (1-h window) of immobility-defined sleep in Hom Q175 (left) and Het Q175 (right) before and during drug treatment. The time of daily drug administration is shown by the dashed line. When examined by day and night (12-h bins), the drug treatment did not alter sleep duration (middle panels) or sleep fragmentation (bottom panels). One-way ANOVA was used to analyze the group values but none of these values were significantly different.

cerebral cortex, hippocampus, basal ganglia, and hypothalamus (Martinez-Mir et al. 1990; Pollard et al. 1993; Pillot et al. 2002). In cultured cortical neurons, activation of H3R results in the phosphorylation of the Akt/GSK-3 beta

pathway (Mariottini et al. 2009). Prior work indicates that H3R antagonists and inverse agonists promote wakefulness via increased HA release stimulating postsynaptic Histamine-1 receptors (Lin et al. 1990; Barbier et al.
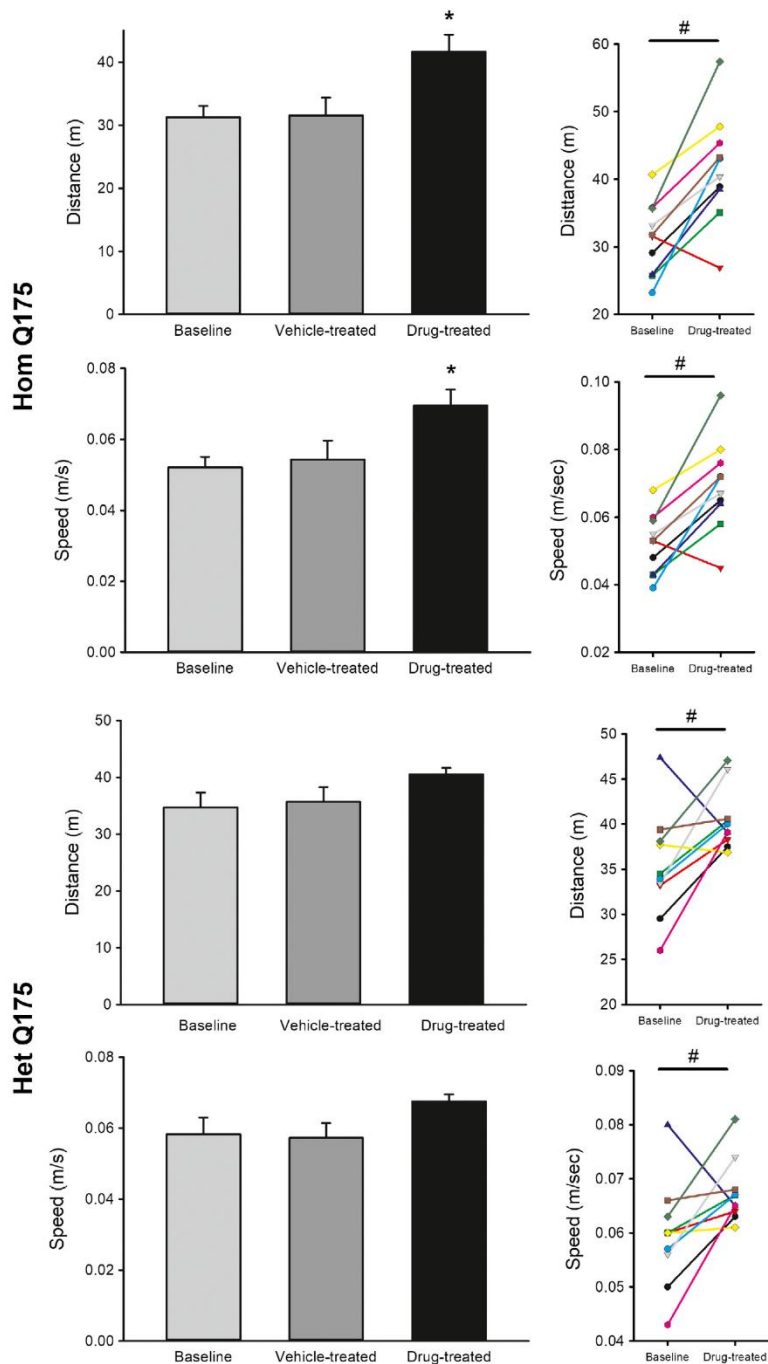
Figure 5. Chronic administration of GSK189254 improved exploratory behavior as measured by the open field test in Hom and Het Q175 mice. One-way ANOVA was used to analyze the group values. Asterisks represent significant differences due to drug treatment compared to vehicle-treated controls ($P < 0.05$). Paired *t*-test found significant ($P < 0.05$) impact of drug treatment on the animal's activity levels before and after treatment, shown by a # symbol. Most, but not all, mice exhibited a significant increase in exploratory activity as a result of drug treatment.
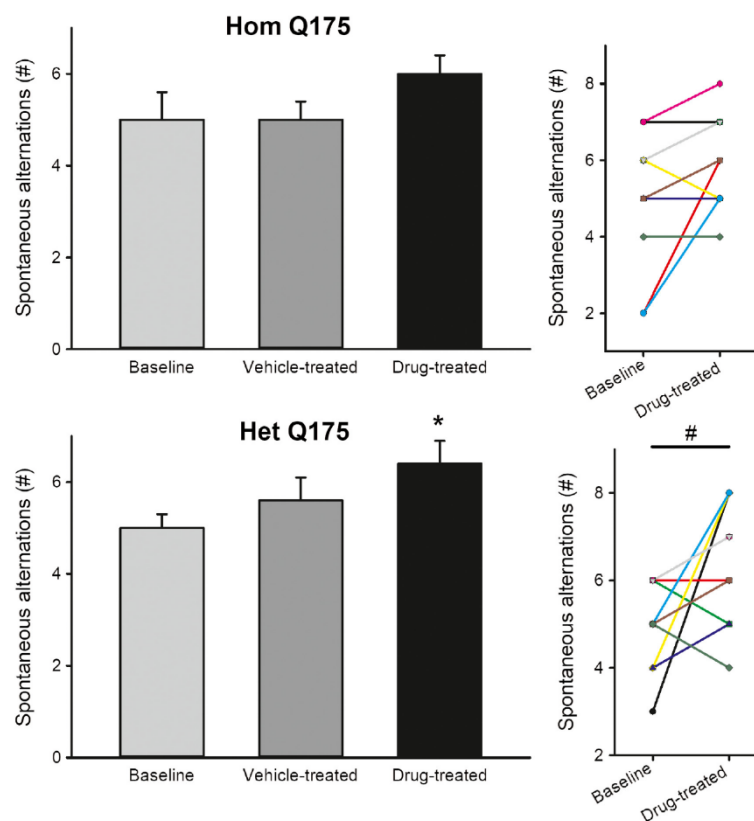
Figure 6. Chronic administration of GSK189254 improved cognitive performance as measured by the T-maze in the Het Q175 mice. One-way ANOVA was used to analyze the group values. Asterisks represent significant differences due to drug treatment compared to vehicle-treated controls ($P < 0.05$). A paired *t*-test was used to compare the values from the same animals before and after treatment. Significance ($P < 0.05$) shown by a # symbol.

2004; Fox et al. 2005; Bonaventure et al. 2007). The drug used in this study (GSK189254) is a potent H3R antagonist (human H3R Ki = 0.2 nmol/L) which increased wakefulness, and improved performance of rats on a number of tests including passive avoidance, water maze, and object recognition at the same dose as used in this study (3.0 mg/kg) (Medhurst et al. 2007; Griebel et al. 2012). It is important to consider that besides increasing HA itself, GSK189254 increased acetylcholine, norepinephrine, and dopamine as measured by microdialysis (Medhurst et al. 2007). In rats, perfusion of the TMN with GSK189254 increased histamine release from the TMN and cortex, but not from the striatum or nucleus accumbens (Giannoni et al. 2010). Broadly speaking, H3R antagonists and inverse agonists have been found to promote wakefulness in a wide range of studies (review in Passani et al. 2004; Lin et al. 2011).

In this study, we administered the H3R antagonist nightly when HA levels would normally be rising. For reasons that could be due to differences in absorption or clearance, the drug levels in the serum were higher in the Hom Q175 than in the Het Q175. Behaviorally, the drug application also increased activity up to four hrs for the Hom Q175 and for at least 1 h for the Het Q175. Regardless, mice of both genotypes exhibited a strengthened activity rhythm with improved precision in activity onset. Additionally, the temporal pattern of sleep behavior was altered with reduced sleep immediately after drug treatment, yet the treatment did not alter the total amount of sleep within a daily cycle. Our observation that daily administration of the H3R antagonist improves the activity rhythm fits a significant body of evidence which indicates that HA is also a potent regulator of the circadian time-keeping system in mammals. The mammalian circadian clock (SCN) receives a dense histaminergic input from the TMN (Watanabe et al. 1984) and expresses HA receptors (Michelsen et al. 2005; Kim et al. 2015) including the *Hrh3* gene (Allen Brain Atlas, Hrh3, exp.

30
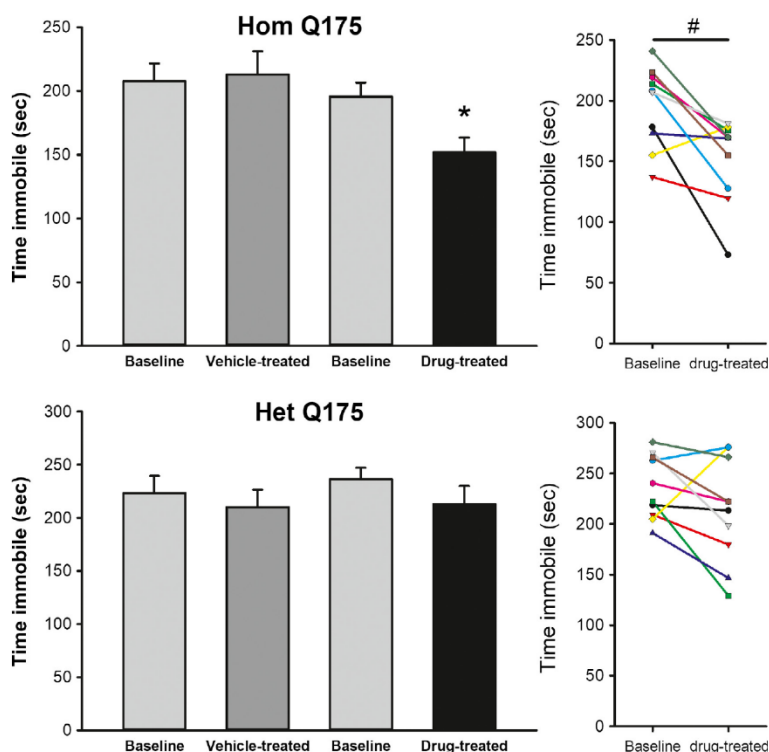
Figure 7. Chronic administration of GSK189254 improved affect as measured by the tail suspension test in Hom Q175 mice. One-way ANOVA was used to analyze the group values. Asterisks represent significant differences due to drug treatment compared to vehicle-treated controls ($P < 0.05$). A paired *t*-test was used to compare the immobility values from the same animals before and after treatment. Significance ($P < 0.05$) shown by a # symbol.

73636034, probe RP_050825_02_B04 – coronal). A recent study also found that *Hrh3* expression varies rhythmically in the SCN with peak levels found in the late day (Pembroke et al. 2015). There is strong evidence that HA can phase-shift the circadian neural activity rhythms in rodent SCN slices (Cote and Harrington 1993; Meyer et al. 1998; Biello 2009; Kim et al. 2015). Inhibition of HA synthesis disrupts the circadian rhythms of locomotor activity, sleep, and corticosterone release (Itowi et al. 1989, 1990, 1991) and histamine-1 receptor knockout (KO) mice exhibit disruption of the circadian rhythms with decreased activity during the active phase (Inoue et al. 1996; Barbier and Bradbury 2007). More recent work has found that the H3R KO exhibits substantially reduced locomotor activity rhythms (Rozov et al. 2015) without a change in the peak/trough expression of core clock genes (Gondard et al. 2013; Rozov et al. 2015). Thus, there is good reason to expect that the daily application of GSK189254 would alter the phase of the underlying circadian rhythm as well as influence the circadian control of locomotor activity.

Selective H3R antagonists have been shown to improve performance in a diverse range of rodent cognition paradigms, including object recognition, olfactory recognition, water maze, radial maze, and passive avoidance, with most pronounced effects being observed in models where a cognitive deficit is present such as in aged animals (Hancock and Fox 2004; Witkin and Nelson 2004; Medhurst et al. 2007). Our data suggest that these benefits can be extended to at least the Q175 HD models. We found modest but significant benefits to performance of the HD model on exploratory behavior in the open field, T-maze, and tail suspension tests. As measured by the amount of time that the mice spent in the center vs. periphery of the open field, anxiety-like behavior was also unchanged. The only potential negative indication was that the Hom Q175 did show an increase in aggressive behavior which should be explored in future work.

H3R are strongly expressed in the cortico-striatal circuits controlling motor behavior (Martinez-Mir et al. 1990; Pollard et al. 1993). In vitro autoradiography of [³H]GSK189254 found strong binding in the rat cortex

and striatum; however, treatment with 3.0 mg/kg GSK189254 did not induce Fos expression in the striatum although it did increase Fos in cortical regions (Medhurst et al. 2007). As measured by number of errors and time required for passage of the mice in the challenging beam test, there were no changes in motor performance in the drug-treated group. The H3R antagonists are known to increase vigilance so improvement might be found with more demanding motor tasks.

H3R antagonists have entered clinical trials for Parkinson's disease and Alzheimer's disease (Lin et al. 2011). A recent search through the NIH clinical trials data base (Clinicaltrials.gov, March 2017) found several clinical trials for histamine H3R antagonists either ongoing or planned. At present, modafinil is widely used as a wake-promoting agent (e.g., Bastuji and Jouvet 1988; Dell'Osso et al. 2014). Modafinil improves waking, but the narcoleptic episodes persist. At least one study has shown that modafinil amplifies the wake-promoting and antinarcoleptic effects of the H3R antagonist pitolisant, suggesting a synergy that could be clinically useful (Lin et al. 2008). Such a simultaneous use of two wake-promoting agents seemed to be well tolerated by the animals because no clear signs of CNS overexcitation or hyperactivity were noted. GSK189254 suppresses narcoleptic episodes in orexin KO mice and repeated dosing (like that used in this study) reinforced the benefits (Guo et al. 2009). Based on the preclinical data obtained in this study, H3R antagonists like GSK189254 would be a reasonable candidate as a cognitive enhancer for HD patients. In addition, a broad range of neurological and psychiatric disorders exhibit disruption in the sleep/wake cycle. These disruptions are likely to have several negative consequences for the patients. Based on our findings, the H3R antagonists/ inverse agonists could also provide benefits as agents that strengthen the activity/rest cycle.

Acknowledgements

Author Contributions

Participated in research design: Whittaker, Wang, Loh, Cachope, Colwell; Conducted experiments: Whittaker, Wang; Performed data analysis: Whittaker, Wang, Loh, Colwell; Contributed to writing of the manuscript: Whittaker, Colwell.

Disclosures

None declared.

References

Abe H, Honma S, Ohtsu H, Honma K (2004). Circadian rhythms in behavior and clock gene expressions in the brain of mice lacking histidine decarboxylase. Mol Brain Res 124: 178–187.

Arrang JM, Garbarg M, Schwartz JC (1983). Auto-inhibition of brain histamine release mediated by a novel class (H3) of histamine receptor. Nature 302: 832–837.

Bailey KR, Crawley JN (2009). Anxiety-related behaviors in mice. in JJ Buccafusco, ed. Methods of behavior analysis in neuroscience, 2nd ed. Frontiers in Neuroscience. CRC Press/ Taylor & Francis, Boca Raton, FL. Available at: http://www.ncbi.nlm.nih.gov/books/NBK5221/

Barbier AJ, Bradbury MJ (2007). Histaminergic control of sleep-wake cycles: recent therapeutic advances for sleep and wake disorders. CNS Neurol Disord Drug Targets 6: 31–43.

Barbier AJ, Berridge C, Dugovic C, Laposky AD, Wilson SJ, Boggs J, et al. (2004). Acute wake-promoting actions of JNJ-5207852, a novel, diamine-based H3 antagonist. Br J Pharmacol 143: 649–661.

Bastuji H, Jouvet M (1988). Successful treatment of idiopathic hypersomnia and narcolepsy with modafinil. Prog Neuropsychopharmacol Biol Psychiatry 12: 695–700.

Biello SM (2009). Circadian clock resetting in the mouse changes with age. Age 31: 293–303.

Bonaventure P, Letavic M, Dugovic C, Wilson S, Aluisio L, Pudiak C, et al. (2007). Histamine H3 receptor antagonists: from target identification to drug leads. Biochem Pharmacol 73: 1084–1096.

Brown RE, Stevens DR, Haas HL (2001). The physiology of brain histamine. Prog Neurobiol 63: 637–672.

Can A, Dao DT, Terrillion CE, Piantadosi SC, Bhat S, Gould TD (2011). The tail suspension test. J Vis Exp 59: e3769.

Ciammola A, Sassone J, Alberti L, Meola G, Mancinelli E, Russo MA, et al. (2006). Increased apoptosis, Huntingtin inclusions and altered differentiation in muscle cell cultures from Huntington's disease subjects. Cell Death Differ 13: 2068–2078.

Cote NK, Harrington ME (1993). Histamine phase shifts the circadian clock in a manner similar to light. Brain Res 613: 149–151.

Cryan JF, Mombereau C, Vassout A (2005). The tail suspension test as a model for assessing antidepressant activity:

review of pharmacological and genetic studies in mice. Neurosci Biobehav Rev 29: 571–625.

Deacon RMJ, Rawlins JNP (2006). T-maze alternation in the rodent. Nat Protoc 1: 7–12.

Dell'Osso B, Dobrea C, Cremaschi L, Arici C, Altamura AC (2014). Wake-promoting pharmacotherapy for psychiatric disorders. Curr Psychiatry Rep 16: 524.

Duyao M, Ambrose C, Myers R, Novelletto A, Persichetti F, Frontali M, et al. (1993). Trinucleotide repeat length instability and age of onset in Huntington's disease. Nat Genet 4: 387–392.

Eaton SJ, Cote NK, Harrington ME (1995). Histamine synthesis inhibition reduces light-induced phase shifts of circadian rhythms. Brain Res 695: 227–230.

Fisher SP, Godinho SIH, Pothecary CA, Hankins MW, Foster RG, Peirson SN (2012). Rapid assessment of sleep/wake behaviour in mice. J Biol Rhythms 27: 48–58.

Fleming SM, Salcedo J, Fernagut P-O, Rockenstein E, Masliah E, Levine MS, et al. (2004). Early and progressive sensorimotor anomalies in mice overexpressing wild-type human α-synuclein. J Neurosci 24: 9434–9440.

Fleming SM, Ekhator OR, Ghisays V (2013). Assessment of sensorimotor function in mouse models of Parkinson's disease. J Vis Exp 76: 50303. https://doi.org/10.3791/50303

Fox GB, Esbenshade TA, Pan JB, Radek RJ, Krueger KM, Yao BB, et al. (2005). Pharmacological properties of ABT-239 [4-(2-{2-[(2R)-2-Methylpyrrolidinyl]ethyl}-benzofuran-5-yl) benzonitrile]: II. Neurophysiological characterization and broad preclinical efficacy in cognition and schizophrenia of a potent and selective histamine H3 receptor antagonist. J Pharmacol Exp Ther 313: 176–190.

Giannoni P, Medhurst AD, Passani MB, Giovannini MG, Ballini C, Corte LD, et al. (2010). Regional differential effects of the novel histamine H3 receptor antagonist 6-[(3-cyclobutyl-2,3,4,5-tetrahydro-1H-3-benzazepin-7-yl)oxy]-N-methyl-3-pyridinecarboxamide hydrochloride (GSK189254) on histamine release in the central nervous system of freely moving rats. J Pharmacol Exp Ther J332: 164–172.

Gomez-Ramirez J, Ortiz J, Blanco I (2002). Presynaptic H3 autoreceptors modulate histamine synthesis through cAMP pathway. Mol Pharmacol 61: 239–245.

Gondard E, Anaclet C, Akaoka H, Guo R-X, Zhang M, Buda C, et al. (2013). Enhanced histaminergic neurotransmission and sleep-wake alterations, a study in histamine H3-receptor knock-out mice. Neuropsychopharmacology 38: 1015–1031.

Griebel G, Decobert M, Jacquet A, Beeské S (2012). Awakening properties of newly discovered highly selective H3 receptor antagonists in rats. Behavioural Brain Res 232: 416–420.

Guo RX, Anaclet C, Roberts JC, Parmentier R, Zhang M, Guidon G, et al. (2009). Differential effects of acute and repeat dosing with the H3 antagonist GSK189254 on the sleep-wake cycle and narcoleptic episodes in Ox-/- mice. Br J Pharmacol 157: 104–117.

Gusella JF, MacDonald ME, Lee J-M (2014). Genetic modifiers of Huntington's disease. Mov Disord 29: 1359–1365.

Haas H, Panula P (2003). The role of histamine and the tuberomamillary nucleus in the nervous system. Nat Rev Neurosci 4: 121–130.

Hancock AA, Fox GB (2004). Perspectives on cognitive domains, H3 receptor ligands and neurological disease. Expert Opin Investig Drugs 13: 1237–1248.

Heikkinen T, Lehtimäki K, Vartiainen N, Puolivǎli J, Hendricks SJ, Glaser JR, et al. (2012). Characterization of neurophysiological and behavioral changes, MRI brain volumetry and 1H MRS in Q175 knock-in mouse model of Huntington's disease. PLoS ONE 7: e50717.

Inoue I, Yanai K, Kitamura D, Taniuchi I, Kobayashi T, Niimura K, et al. (1996). Impaired locomotor activity and exploratory behavior in mice lacking histamine H1 receptors. Proc Natl Acad Sci USA 93: 13316–13320.

Itowi N, Yamatodani A, Cacabelos R, Goto M, Wada H (1989). Effect of histamine depletion on circadian variation of corticotropin and corticosterone in rats. Neuroendocrinology 50: 187–192.

Itowi N, Yamatodani A, Nagai K, Nakagawa H, Wada H (1990). Effects of histamine and alpha-fluoromethylhistidine injections on circadian phase of free-running rhythms. Physiol Behav 47: 549–554.

Itowi N, Yamatodani A, Kiyono S, Hiraiwa ML, Wada H (1991). Effect of histamine depletion on the circadian amplitude of the sleep-wakefulness cycle. Physiol Behav 49: 643–646.

Jacobs EH, Yamatodani A, Timmerman H (2000). Is histamine the final neurotransmitter in the entrainment of circadian rhythms in mammals? Trends Pharmacol Sci 21: 293–298.

Juszczak GR, Sliwa AT, Wolak P, Tymosiak-Zielinska A, Lisowski P, Swiergiel AH (2006). The usage of video analysis system for detection of immobility in the tail suspension test in mice. Pharmacol Biochem Behav 85: 332–338.

Kim YS, Kim YB, Kim WB, Yoon BE, Shen FY, Lee SW, et al. (2015). Histamine resets the circadian clock in the suprachiasmatic nucleus through the H1R-Ca(v)1.3-RyR pathway in the mouse. Eur J Neurosci 42: 2467–2477.

Koolhaas JM, Coppens CM, de Boer SF, Buwalda B, Meerlo P, Timmermans PJA (2013). The resident-intruder paradigm: a standardized test for aggression, violence and social stress. J Vis Exp 77: e4367.

Kudo T, Schroeder A, Loh DH, Kuljis D, Jordan MC, Roos KP, et al. (2011). Dysfunctions in circadian behavior and physiology in mouse models of Huntington's disease. Exp Neurol 228: 80–90.

Kuljis D, Schroeder AM, Kudo T, Loh DH, Willison DL, Colwell CS (2012). Sleep and circadian dysfunction in neurodegenerative disorders: insights from a mouse model of Huntington's disease. Minerva Pneumol 51: 93–106.

Langbehn DR, Hayden MR, Paulsen JS (2010). CAG-repeat length and the age of onset in Huntington disease (HD): a review and validation study of statistical approaches. Am J Med Genet 153B: 397–408.

Li Q, Loh DH, Kudo T, Truong D, Derakhshesh M, Kaswan ZM, et al. (2015). Circadian rhythm disruption in a mouse model of Rett syndrome. Neurobiol Dis 77: 155–164.

Lin JS, Sakai K, Vanni-Mercier G, Arrang JM, Garbarg M, Schwartz JC, et al. (1990). Involvement of histaminergic neurons in arousal mechanisms demonstrated with H3-receptor ligands in the cat. Brain Res 523: 325–330.

Lin JS, Dauvilliers Y, Arnulf I, Bastuji H, Anaclet C, Parmentier R, et al. (2008). An inverse agonist of the histamine H(3) receptor improves wakefulness in narcolepsy: studies in orexin (-/-) mice and patients. Neurobiol Dis 30: 74–83.

Lin JS, Sergeeva OA, Haas HL (2011). Histamine H3 receptors and sleep-wake regulation. J Pharmacol Exp Ther 336: 17–23.

Loh DH, Kudo T, Truong D, Wu Y, Colwell CS (2013). The Q175 mouse model of Huntington's disease shows gene dosage- and age-related decline in circadian rhythms of activity and sleep. PLoS ONE 8: e69993.

Margolis RL, Ross CA (2003). Diagnosis of Huntington disease. Clin Chem 49: 1726–1732.

Mariottini C, Scartabelli T, Bongers G, Arrigucci S, Nosi D, Leurs R, et al. (2009). Activation of the histaminergic H3 receptor induces phosphorylation of the Akt/GSK-3 beta pathway in cultured cortical neurons and protects against neurotoxic insults. J Neurochem 110: 1469–1478.

Martinez-Mir MI, Pollard H, Moreau J, Arrang JM, Ruat M, Traiffort E, et al. (1990). Three histamine receptors (H1, H2 and H3) visualized in the brain of human and non-human primates. Brain Res 526: 322–327.

Medhurst AD, Atkins AR, Beresford IJ, Brackenborough K, Briggs MA, Calver AR, et al. (2007). GSK189254, a novel H3 receptor antagonist that binds to histamine H3 receptors in Alzheimer's disease brain and improves cognitive performance in preclinical models. J Pharmacol Exp Ther 321: 1032–1045.

Menalled LB, Kudwa AE, Miller S, Fitzpatrick J, Watson-Johnson J, Keating N, et al. (2012). Comprehensive behavioral and molecular characterization of a new knock-in mouse model of Huntington's disease: zQ175. PLoS ONE 7: e49838.

Meyer JL, Hall AC, Harrington ME (1998). Histamine phase shifts the hamster circadian pacemaker via an NMDA dependent mechanism. J Biol Rhythms 13: 288–295.

Michelsen KA, Lozada A, Kaslin J, Karlstedt K, Kukko-Lukjanov TK, Holopainen I, et al. (2005). Histamine-immunoreactive neurons in the mouse and rat suprachiasmatic nucleus. Eur J Neurosci 22: 1997–2004.

Mochizuki T, Yamatodani A, Okakura K, Horii A, Inagaki N, Wada H (1992). Circadian rhythm of histamine release from the hypothalamus of freely moving rats. Physiol Behav 51: 391–394.

Morisset S, Rouleau A, Ligneau X, Gbahou F, Tardivel-Lacombe J, Stark H, et al. (2000). High constitutive activity of native H3 receptors regulates histamine neurons in brain. Nature 408: 860–864.

Morton AJ, Wood NI, Hastings MH, Hurelbrink C, Barker RA, Maywood ES (2005). Disintegration of the sleep-wake cycle and circadian timing in Huntington's disease. J Neurosci 25: 157–163.

Pack AI, Galante RJ, Maislin G, Cater J, Metaxas D, Lu S, et al. (2007). Novel method for high-throughput phenotyping of sleep in mice. Physiol Genomics 28: 232–238.

Parmentier R, Ohtsu H, Djebbara-Hannas Z, Valatx JL, Watanabe T, Lin JS (2002). Anatomical, physiological, and pharmacological characteristics of histidine decarboxylase knock-out mice: evidence for the role of brain histamine in behavioral and sleep-wake control. J Neurosci 22: 7695–7711.

Passani MB, Lin JS, Hancock A, Crochet S, Blandina P (2004). The histamine H3 receptor as a novel therapeutic target for cognitive and sleep disorders. Trends Pharmacol Sci 25: 618–625.

Pembroke WG, Babbs A, Davies KE, Ponting CP, Oliver PL (2015). Temporal transcriptomics suggest that twin-peaking genes reset the clock. Elife 4: e10518.

Pillot C, Heron A, Cochois V, Tardivel-Lacombe J, Ligneau X, Schwartz JC, et al. (2002). A detailed mapping of the histamine H(3) receptor and its gene transcripts in rat brain. Neuroscience 114: 173–193.

Pollard H, Moreau J, Arrang J-M, Schwartz J-C (1993). A detailed autoradiographic mapping of histamine H3 receptors in rat brain areas. Neuroscience 52: 169–189.

Pouladi MA, Morton AJ, Hayden MR (2013). Choosing an animal model for the study of Huntington's disease. Nat Rev Neurosci 14: 708–721.

Prast H, Dietl H, Philippu A (1992). Pulsatile release of histamine in the hypothalamus of conscious rats. J Auton Nerv Syst 39: 105–110.

Prut L, Belzung C (2003). The open field as a paradigm to measure the effects of drugs on anxiety-like behaviors: a review. Eur J Pharmacol 463: 3–33.

Rothe T, Deliano M, Wójtowicz AM, Dvorzhak A, Harnack D, Paul S, et al. (2015). Pathological gamma oscillations, impaired dopamine release, synapse loss and reduced dynamic

range of unitary glutamatergic synaptic transmission in the striatum of hypokinetic Q175 Huntington mice. Neuroscience 311: 519–538.

Rozov SV, Porkka-Heiskanen T, Panula P (2015). On the role of histamine receptors in the regulation of circadian rhythms. PLoS ONE 10: e0144694.

Saft C, Zange J, Andrich J, Müller K, Lindenberg K, Landwehrmeyer B, et al. (2005). Mitochondrial impairment in patients and asymptomatic mutation carriers of Huntington's disease. Mov Disord 20: 674–679.

Saudou F, Humbert S (2016). The biology of Huntingtin. Neuron 89: 910–926.

Shan L, Hofman MA, van Wamelen DJ, Van Someren EJW, Bao A-M, Swaab D (2012). Diurnal fluctuation in histidine decarboxylase expression, the rate limiting enzyme for histamine production, and its disorder in neurodegenerative diseases. Sleep 35: 713–715.

Southwell AL, Ko J, Patterson PH (2009). Intrabody gene therapy ameliorates motor, cognitive and neuropathological symptoms in multiple mouse models of Huntington's disease. J Neurosci 29: 13589–13602.

Takahashi K, Tokita S, Kotani H (2003). Generation and characterization of highly constitutive active histamine H3 receptors. J Pharmacol Exp Ther 307: 213–218.

van Wamelen DJ, Shan L, Aziz NA, Anink JJ, Bao A-M, Roos RAC, et al. (2011). Functional increase of brain histaminergic signaling in Huntington's Disease. Brain Pathol 21: 419–427.

Wang H-B, Whittaker DS, Truong D, Mulji AK, Ghiani CA, Loh DH, et al. (2017). Blue light therapy improves circadian dysfunction as well as motor symptoms in two mouse models of Huntington's disease. Neurobiol Sleep Circadian Rhythms 2: 39–52.

Watanabe T, Taguchi Y, Shiosaka S, Tanaka J, Kubota H, Terano Y, et al. (1984). Distribution of the histaminergic neuron system in the central nervous-system of rats - a fluorescent immunohistochemical analysis with histidine-decarboxylase as a marker. Brain Res 295: 13–25.

Wexler NS and The U.S.–Venezuela Collaborative Research Project (2004). Venezuelan kindreds reveal that genetic and environmental factors modulate Huntington's disease age of onset. Proc Natl Acad Sci USA 101: 3498–3503.

Wilson DM, Apps J, Bailey N, Bamford MJ, Beresford IJ, Brackenborough K, et al. (2013). Identification of clinical candidates from the benzazepine class of histamine H3 receptor antagonists. Bioorg Med Chem Lett 23: 6890–6896.

Wisor JP, Nishino S, Sora I, Uhl GH, Mignot E, Edgar DM (2001). Dopaminergic role in stimulant-induced wakefulness. J Neurosci 21: 1787–1794.

Witkin JM, Nelson DL (2004). Selective histamine H3 receptor antagonists for treatment of cognitive deficiencies and other disorders of the central nervous system. Pharmacol Ther 103: 1–20.

Chapter 3: Time-restricted feeding improves circadian dysfunction as well as motor symptoms

in the Q175 mouse model of Huntington's disease

Disorders of the Nervous System

Time-Restricted Feeding Improves Circadian Dysfunction as well as Motor Symptoms in the Q175 Mouse Model of Huntington's Disease

Huei-Bin Wang,[1,*] Dawn H. Loh,[1,*] Daniel S. Whittaker,[1] Tamara Cutler,[1] David Howland,[2] and Christopher S. Colwell[1]

[1]Department of Psychiatry and Biobehavioral Sciences, University of California - Los Angeles, Los Angeles, CA 90024-1759 and [2]CHDI Foundation, Princeton, NJ 08540

Visual Abstract
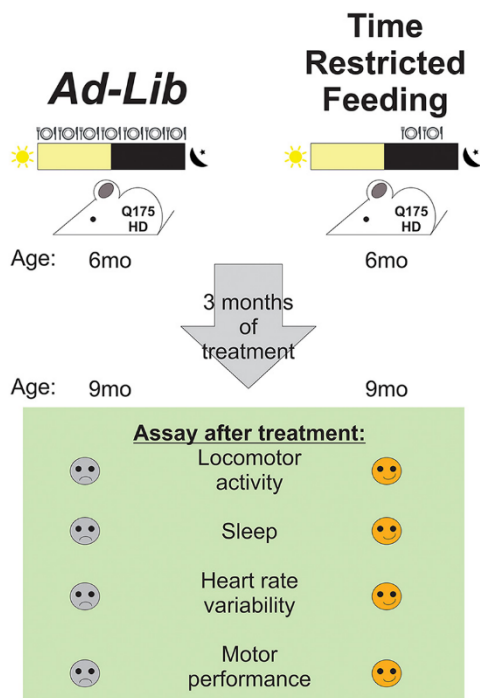
Huntington's disease (HD) patients suffer from a progressive neurodegeneration that results in cognitive, psychiatric, cardiovascular, and motor dysfunction. Disturbances in sleep/wake cycles are common among HD patients with reports of delayed sleep onset, frequent bedtime awakenings, and fatigue during the day. The heterozygous Q175 mouse model of HD has been shown to phenocopy many HD core symptoms including circadian dysfunctions. Because circadian dysfunction manifests early in the disease in both patients and mouse models, we sought to determine if early intervention that improve circadian rhythmicity can benefit HD and delay disease progression. We determined the effects of time-restricted feeding (TRF) on the Q175 mouse model. At six months of age, the animals were divided into two groups: ad libitum (ad lib) and TRF. The TRF-treated Q175 mice were exposed to a 6-h feeding/18-h fasting regimen that was designed to be aligned with the middle of the time when mice are normally active. After three months of treatment (when mice reached the early disease stage), the TRF-treated Q175 mice showed improvements in their locomotor activity rhythm and sleep awakening time. Furthermore, we found improved heart rate variability (HRV), suggesting that their autonomic nervous system dysfunction was improved. Importantly, treated Q175 mice exhibited improved motor performance compared to untreated Q175 controls, and the motor improvements were correlated with improved circadian output. Finally, we found that the expression of several HD-relevant markers was restored to WT levels in the striatum of the treated mice using NanoString gene expression assays.

Significance Statement

Huntington's disease (HD) is a genetically caused disease with no known cure. Lifestyle changes that not only improve the quality of life but also delay disease progression for HD patients are greatly needed. In this study, we found that time-restricted feeding (TRF) improves activity/rest rhythms in the Q175 mouse model of HD. This treatment also improved motor performance and heart rate variability (HRV) in the HD mice. Finally, TRF altered the expression of HD relevant markers in the striatum. Our study demonstrates the therapeutic potential of circadian-based treatment strategies in a preclinical model of HD.

Introduction

Huntington's disease (HD) is caused by an expanded CAG repeat within the first exon of the Huntingtin (*Htt*) gene. The mutated HTT protein leads to dysfunction of a large range of cellular processes, including cytoskeletal organization, metabolism, and transcriptional activities (Bourne et al., 2006; Grimbergen et al., 2008; Fisher et al., 2014). As result, HD patients suffer from progressive neurodegeneration that inflicts cognitive, psychiatric, cardiovascular, and motor dysfunction. The genetic components greatly determine the age of symptom onset and the severity. Generally, the longer the CAG repeat, the earlier the age of onset and the greater the severity of the symptoms (Langbehn et al., 2010). Still, even among patients with the same CAG repeat length, large variabilities in the onset of symptoms (around a decade) and their severity have been reported (Gusella et al., 2014). In addition, studies have shown that environmental factors also affect the disease progression (Wexler et al., 2004). Those reports raise the possibility of environmental modifiers to the disease and suggest that lifestyle changes can increase the health span of the patients. This possibility is important to pursue as there are no known cures for HD.

Disturbances in the timing of sleep, typified by frequent bedtime awakenings, prolonged latency to fall asleep, and more naps during the awake phase, are extremely common in HD and often become apparent years before the onset of classic motor symptoms (Cuturic et al., 2009; Aziz et al., 2010a; Goodman et al., 2011). Similarly, mouse models of HD also exhibit a disrupted circadian rest/activity cycle that mimics the symptoms observed in human patients (Morton et al., 2005; Kudo et al., 2011; Loh et al., 2013). This body of work supports the hypothesis that circadian dysfunctions may interact with HD pathology and exacerbate the symptoms. To test this hypothesis, we have been using the Q175 knock-in model of HD. In previous work (Loh et al., 2013), we have characterized the impact of age (3, 6, 9, and 12 months) and gene dosage (Het and Hom) on the degradation of circadian

rhythms in locomotor activity and other HD core symptoms. Recently, a detailed RNA-seq analysis of striatum, cortex, and liver of the Q175 line has been published (Langfelder et al., 2016); therefore, we have a good understanding of the transcriptional changes that occur with age in this model. Finally, recent work has carefully characterized age-related changes in the electroencephalogram (EEG) in both Hom and Het Q175 (Fisher et al., 2016). This wealth of data makes the Het Q175 an ideal preclinical model to examine the impact of circadian interventions on disease trajectory.

The central circadian clock responsible for the generation of daily rhythms is localized in the suprachiasmatic nucleus (SCN) in the hypothalamus. While lighting conditions are a critical environmental input to this timing system, a body of recent work has lead us to appreciate that the feed/fast cycle is also a powerful regulators of the circadian system (Hamaguchi et al., 2015). While progressive, age-related SCN dysfunction has been reported in HD mouse models (Bartlett et al., 2016), a time-restricted feeding (TRF) regimen promises therapeutic potential and can benefit even SCN-lesioned mice (Hara et al., 2001; Mulder et al., 2014). For example, mice under TRF consume equivalent calories from a high-fat diet as those with ad libitum (ad lib) access yet are protected against obesity, hyperinsulinemia, and inflammation and have improved motor coordination (Hatori et al., 2012). In the present study, we examined the impact of imposing a 6-h feeding/18-h fasting regimen that was aligned to the middle [zeitgeber time (ZT) 15-21] of the period when mice normally active (ZT 12-24). The treatment was applied to Q175 Hets starting when the mutants were six months of age and ending when they were nine months. We selected this age range because the Het Q175 start to show disrupted sleep/wake cycles and motor symptoms are just beginning.

Materials and Methods

The work presented in this study followed all guidelines and regulations of the UCLA Division of Animal Medicine that are consistent with the Animal Welfare Policy Statements and the recommendations of the Panel on Euthanasia of the American Veterinary Medical Association.

Animals

The Q175 mice used in this study were males on the C57BL6/J background. They arose from a spontaneous expansion of the CAG repeat in the CAG140 transgenic knock-in line (Menalled et al., 2012). The mice were heterozygous (Het) for the Q175 allele with an average of 189 ± 3 CAG repeats. Mutant mice were obtained from The Jackson Laboratory from a colony managed by the CHDI Foundation. The animals were singly housed within light-tight chambers with independently controlled lighting conditions: 12 h of light followed by 12 h of dark (12/12 h LD). The chambers were in the same animal housing facility with controlled temperature and humidity, and each chamber held eight cages of mice, grouped together by feeding treatment. All animals received cotton nestlets,

and water was made available at all times. To confirm the effect of timed feeding on daily rhythms and motor performance, we also examined WT mice at nine months of age.

TRF

Mice were first entrained to a 12/12 h LD cycle for a minimum of two weeks before any treatment. Experimental animals were randomly assigned to one of two feeding conditions: food available ad lib and food available for 6 h during the middle of the active phase during ZT 15-21. By definition, ZT 12 referrers to when the lights go off when the mice are in an LD cycle. Experimental mice were singly housed in cages with a custom made programmable food hopper that could temporally control access to food (Diet Teklad 7013: fat, 18 kcal%; caloric density, 3.13 kcal/g) and prevent food consumption during restricted times. These cages were also equipped with an infrared (IR) motion detector to give us the ability to measure cage activity. The mice were held in these conditions for a total of three months (from six to nine months of age).

Monitoring of cage locomotor activity

Experimental mice were singly housed in cages with the food hopper as well as IR motion sensors. The locomotor activity recorded as previously described (Wang et al., 2017). Mice were entrained to a 12/12 h LD cycle for a minimum of two weeks before data collection. Locomotor activity data were recorded using Mini Mitter data loggers in 3-min bins, and 10 d of data were averaged for analysis. We used the 10 d of activity data collected just before the motor performance tests during the final two weeks of the TRF schedule. The data were analyzed to determine the period and rhythmic strength as previously described (Loh et al., 2013; Wang et al., 2017). The periodogram analysis uses a χ^2 test with a threshold of 0.001 significance, from which the amplitude of the periodicities is determined at the circadian harmonic to obtain the rhythm power. The amount of cage activity over a 24-h period was averaged over 10 d and reported here as the arbitrary units (a.u.)/h. The number of activity bouts and the average length of bouts were determined using Clocklab (Actimetrics), where each bout was counted when activity bouts were separated by a gap of 21 min (maximum gap: 21 min; threshold: 3 counts/min). The onset variability was determined using Clocklab by drawing the best-fit line over the 10 d, and averaging the differences between activity onset and best-fit regression of each day.

Monitoring of immobility-defined sleep behavior

Immobility-defined sleep was determined as described previously (Loh et al., 2013; Wang et al., 2017). Mice were housed in see-through plastic cages containing bedding (without the addition of nesting material) and the food hopper. A side-on view of each cage was obtained, with minimal occlusion by the food bin or water bottle, both of which were top-mounted. Cages were side-lit using IR-LED lights. Video capture was accomplished using surveillance cameras with visible light filters (Gadspot Inc) connected to a video-capture card (Adlink Technology

Inc) on a Dell Optiplex computer system. ANY-maze software (Stoelting Co) was used to track the animals.

Immobility was detected when 95% of the area of the animal stayed immobile for >40 s, as was previously determined to have 99% correlation with simultaneous EEG/EMG-defined sleep (Pack et al., 2007; Fisher et al., 2012). Continuous tracking of the mice was performed for a minimum of five sleep-wake cycles, with randomized visits (one to two times per day) by the experimenter to confirm mouse health and video recording. The 3rd and 4th sleep-wake cycles were averaged for further analysis. Immobility-defined sleep data were exported in 1 min bins, and total sleep time was determined by summing the immobility durations in the rest phase (ZT 0-12) or active phase (ZT 12-24). An average wave form of hourly immobile-sleep over the two sleep-wake cycles was produced during the final week of TRF. Variability of awake time was determined using Clocklab to draw the best-fit line over the sleep cycles, and the differences between sleep offset and best-fit regression of each sleep cycle were averaged.

Rotarod test. Accelerating version

The rotarod apparatus (Ugo Basile) is commonly used to measure motor coordination and balance. This apparatus is, in essence, a small circular treadmill. It consists of an axle or rod thick enough for a mouse to rest over the top of it when it is not in motion and a flat platform a short distance below the rod. The rod is covered with smooth rubber to provide traction while preventing the mice from clinging to the rod. In this study, mice were placed on top of the rubber covered rod. When the mice moved at the pace set by the rotation rate of the rod, they would stay on top of it. When mice no longer move at the selected pace they dropped a short distance to the platform below. The time a mouse remained on the rod, before dropping to the platform was called the latency to fall. Following a 15-min habituation to the testing room, mice were placed on the slowly rotating rod. The rod gradually accelerated from 5 rpm to 38 rpm over the course of the trial. The length of time the mouse stays on the rod was recorded. A two-day protocol for the accelerating rotarod tests was used. On the first day, the mice were trained on the rotarod over five trials. The maximum length of each trial was 600 s, and mice were allowed to rest for a minimum of 60 s between trials. On the second day, mice were tested on the rotarod and the latency to fall from the rotarod was recorded from five trials. Mice were again allowed to rest for a minimum of 60 s between trials. Data from each mouse were analyzed after averaging the times from all five trials. The apparatus was cleaned with 70% alcohol and allowed to dry completely between trials. A dim red-light (2 lux) was used for illumination during active phase testing (night).

Challenging beam test

The challenging beam test is a modified version of the beam traversal test first described by Goldberg and colleagues (Goldberg et al., 2003), and was used to characterize the motor deficits of Q175 mutant mice in previous studies (Loh et al., 2013, Wang et al., 2017). The beam narrows in four intervals from 33 mm > 24 mm > 18 mm >

6 mm, with each segment spanning 253 mm in length. Apparatus and methods used are similar to those described by Fleming and colleagues (Fleming et al., 2013). The home cage of each mouse is put on the end of the beam as the motivating factor. In this study, animals were trained on the beam for five consecutive trials on two consecutive days. During each trial, each mouse was placed on the widest end of the beam and allowed to cross with minimal handling by the experimenter. On the testing day, a metal grid (10 × 10-mm spacing, formed using 19-gauge wire) was overlaid on the beam. This overlaid grid increased the difficulty of the beam traversal task and provided a visual reference for foot slips made while crossing the grid. Each mouse was subjected to five consecutive trials, which were recorded by a camcorder under dim red-light conditions (2 lux), supplemented with IR lighting for video recording. The videos were scored *post hoc* by two independent observers for the number of missteps (errors) made by each mouse. The observers were masked as to the treatment group of the mice that they were scoring. An error was scored when any foot dipped below the grid. The number of errors was averaged across the five trials per mouse to give the final reported values. The apparatus was cleaned with 70% alcohol and allowed to dry completely between trials. A dim red-light (2 lux) was used for illumination during active phase testing (night).

Automatic outputs. Core body temperature (CBT), heart rate (HR), and HR variability (HRV)

For the telemetry measurements, methods employed were similar to those previously described (Schroeder et al., 2016; Cutler et al., 2017). Two groups (ad lib and TRF) of Het Q175 mice ($n = 7$/group) were surgically implanted with a wireless radio-frequency transmitter (ETA-F20, Data Sciences International). Mice were singly housed in cages with the food hopper. Cages were placed atop telemetry receivers (Data Sciences International) in a light and temperature-controlled chamber. Standard rodent chow was provided for both groups. Data collection began two weeks after surgery. HR was extrapolated from ECG waveforms using the RR interval.

Data collection and analysis were performed as described previously (Cutler et al., 2017). Data were extracted in 20-s intervals then filtered to remove extreme noise. Remaining valid data segments were averaged into 1-h bins across the 24-h cycle. Mean normal to normal intervals (NN, in ms) and SD of all NN intervals (SDNN, in ms) were calculated for the time domain analysis.

NanoString analysis of gene expression

Tissue collection and data analysis were performed as described previously (Wang et al., 2017). Four weeks after the final behavioral tests were performed, the Q175 mutants were anesthetized with isoflurane before dissection of the striatum at ZT 15. The brain tissue samples were flash frozen and stored at −80°C before NanoString analysis. The NanoString analysis was performed by LabCorp using a custom CodeSet designed to interrogate 100 transcripts previously implicated in transcriptional changes in the striatum of Q175 mice (Langfelder et al., 2016). The

signal intensity of individual genes was normalized by adjusting to internal positive standards within each sample. Eight housekeeping genes were included in the CodeSet: *Gins1, Myh15, Pank2, Poc1b, Pum2, Slc25a15, Ssrp1, and Utp3*. The expression levels for each probe within a sample were scaled using the geometric mean of the eight housekeeping genes for each sample. Each mouse was an individual sample as tissue did not need to be pooled. The fold change of signal intensity was derived by comparing the normalized means between the ad lib group and the TRF group.

Pathway analysis

To study the HD-changed gene expression data in the context of biological networks, the gene expression data of TRF-treated Q175 and untreated Q175 control samples were analyzed with the Ingenuity Pathway Analysis (IPA) system (Ingenuity Systems). Datasets containing gene identifiers and corresponding expression values were uploaded in the application. Each gene identifier was mapped to its corresponding gene object in Ingenuity Pathways Knowledge. A cutoff of corrected p value (i.e., q value $= 0.005$) was set to identify genes whose expression was significantly different as a result of the treatment. These genes were overlaid onto a global molecular network developed from information contained in the Ingenuity Pathways Knowledge Base. Functional analysis using the IPA program identified the biological functions that were most significant to the dataset (uncorrected Fisher's exact test $p < 0.05$).

Statistical analysis

We were interested in determining if TRF can delay the progression of symptoms in the Q175 mouse model; Therefore, treated Q175 mice (TRF group) were compared to age-matched untreated Q175 mice (ad lib group) in all experiments. The sample size per group was determined by both our empirical experience with the variability in the prior measures in the Q175 mice (Loh et al., 2013) and a power analysis (SigmaPlot, SYSTAT Software) that assumed a power of 0.8 and an α of 0.05. For the behavioral measures, the analysis was done by two observes masked as to the experimental condition and their values averaged. To assess the impact of TRF after three months, we applied a t test for the analysis. To determine the impact of the treatment on temporal activity, sleep, CBT, HR, and HRV waveforms, we used a two-way repeated measures ANOVA (two-way RM ANOVA) with treatment and time as factors. To determine the impact of the treatment on errors made in each beam of the challenging beam test, we used a two-way ANOVA with treatment and beam # as factors. F values are reported as F (degrees of freedom between groups, degrees of freedom within groups). Pairwise multiple comparison procedures were made using the Holm–Sidak method. Correlations between circadian parameters and motor performance were examined by applying Pearson correlation analysis. Statistical analysis was performed using SigmaPlot. The dataset was examined for normality (Shapiro–Wilk test) and equal variance (Brown–Forsythe test). The power of the statistical tests is reported in Table 1. Between-group differences were de-

Table 1. List of distribution, statistical test, and power for each dataset analyzed in this study

Letter	Data structure	Type of test	Power
a food consumption	Normal distribution	*t* test	0.052
b body weight	Normal distribution	*t* test	0.050
c power	Normal distribution	*t* test	0.956
d onset	Normal distribution	*t* test	0.536
e cage activity	Normal distribution	*t* test	0.843
f bout #	Normal distribution	*t* test	0.605
g waveform	Normal distribution	Two-way ANOVA	Time 1.000
			Treatment 0.843
h bout duration	Normal distribution	*t* test	0.729
i bout #	Normal distribution	*t* test	0.413
j sleep waveform	Normal distribution	Two-way ANOVA	Time 1.000
			Treatment 0.179
K sleep duration	Normal distribution	*t* test	0.050
l bout #	Normal distribution	*t* test	0.328
m bout duration	Normal distribution	*t* test	0.895
n wake time onset	Normal distribution	*t* test	0.944
o cycle to cycle	Normal distribution	*t* test	0.440
p daytime activity	Normal distribution	*t* test	0.884
q activity waveform	Normal distribution	Two-way ANOVA	Time 1.000
			Treatment 0.997
r average CBT	Normal distribution	*t* test	0.529
s CBT waveform	Normal distribution	Two-way ANOVA	Time 1.000
			Treatment 0.729
t HR average	Normal distribution	*t* test	0.382
u HR amplitude	Normal distribution	*t* test	0.560
v HR waveform	Normal distribution	Two-way ANOVA	Time 1.000
			Treatment 0.895
w average HVR	Normal distribution	*t* test	0.632
x HRV waveform	Normal distribution	Two-way ANOVA	Time 1.000
			Treatment 1.000
y rotarod	Normal distribution	*t* test	0.911
z beam errors	Normal distribution	*t* test	0.989
aa error by beam	Normal distribution	Two-way ANOVA	beam 1.000
			Treatment 1.000

The first column lists the superscript lowercase letter referring to statistical test in the Results section. The second column is the structure of the data (normal distribution or non-normal). Each of the datasets was examined for normality (Shapiro–Wilk test) and equal variance (Brown–Forsythe test). The third column lists the statistical test. The fourth column gives the observed power value of the statistical test calculated from the actual data.

termined significant if $p < 0.05$. All values are reported as group mean ± SEM.

Results

By using the programmable food hopper, we could temporally control access to food (ZT 15-21) and prevent food consumption for the rest of the daily cycle. During this 6-h interval, the mice would eat as much as they wanted and the amount of food consumed daily did not vary between the Het Q175 groups (ad lib: 2.8 ± 0.4 g; TRF: 2.8 ± 0.2 g, $t_{(14)} = -0.13$, $p = 0.900$, *t* test[a]). At the time when we performed the recordings and motor assays, the body weights were not different in Q175 mice under TRF compared to age-matched controls (ad lib: 23.9 ± 0.4 g; TRF: 24.5 ± 0.4 g, $t_{(14)} = -1.03$, $p = 0.320$, *t* test[b]).

TRF increased the amplitude of diurnal rhythms in Het Q175 line

At early disease stage (nine months of age), the TRF-treated group showed greatly improved circadian locomotor activity rhythms (Fig. 1*A–D*), evidenced by the stronger rhythmic power (ad lib: 32.1 ± 2.2; TRF: 43.4 ±

2.9, $t_{(14)} = -3.12$, $p = 0.008$, *t* test[c]) and lower activity onset variability (ad lib: 27.3 ± 4.6 min; TRF: 15.8 ± 2.4 min, $t_{(14)} = 2.2$, $p = 0.045$, *t* test[d]) than the control group. The amount of cage activity was also increased under the TRF regimen (ad lib: 75.3 ± 5.9 a.u./h; TRF: 160.7 ± 21.1 a.u./h, $t_{(14)} = 42$, $p = 0.005$, *t* test[e]). These increases in rhythm power and activity amount coincided with a decreased total number of activity bouts (ad lib: 10.8 ± 0.9; TRF: 7.9 ± 0.6, $t_{(14)} = 2.6$, $p = 0.021$, *t* test[f]). A temporal activity wave form indicated more robust activity levels in the TRF-treated group at night when the mice should be active (Fig. 1*E*). A two-way RM ANOVA[g] revealed a significant effect of time ($F_{(23,382)} = 70.07$, $p < 0.001$), treatment ($F_{(1,14)} = 10.82$, $p = 0.005$), and a significant interaction between the two factors ($F = 8.24$, $P < 0.001$). A further examination of activity bouts at night (ZT 12-24) revealed that the TRF group had longer bout lengths (ad lib: 60.6 ± 17.5 min; TRF: 128.8 ± 27.8 min, $t_{(14)} = 48$, $p = 0.038$, *t* test[h]) without a significant increase in the number (ad lib: 7.6 ± 0.6; TRF: 5.4 ± 0.9, $t_{(14)} = 2.15$, $p = 0.05$, *t* test[i]), suggesting that the robust amplitude of diurnal rhythms in the TRF group was due to the consol-
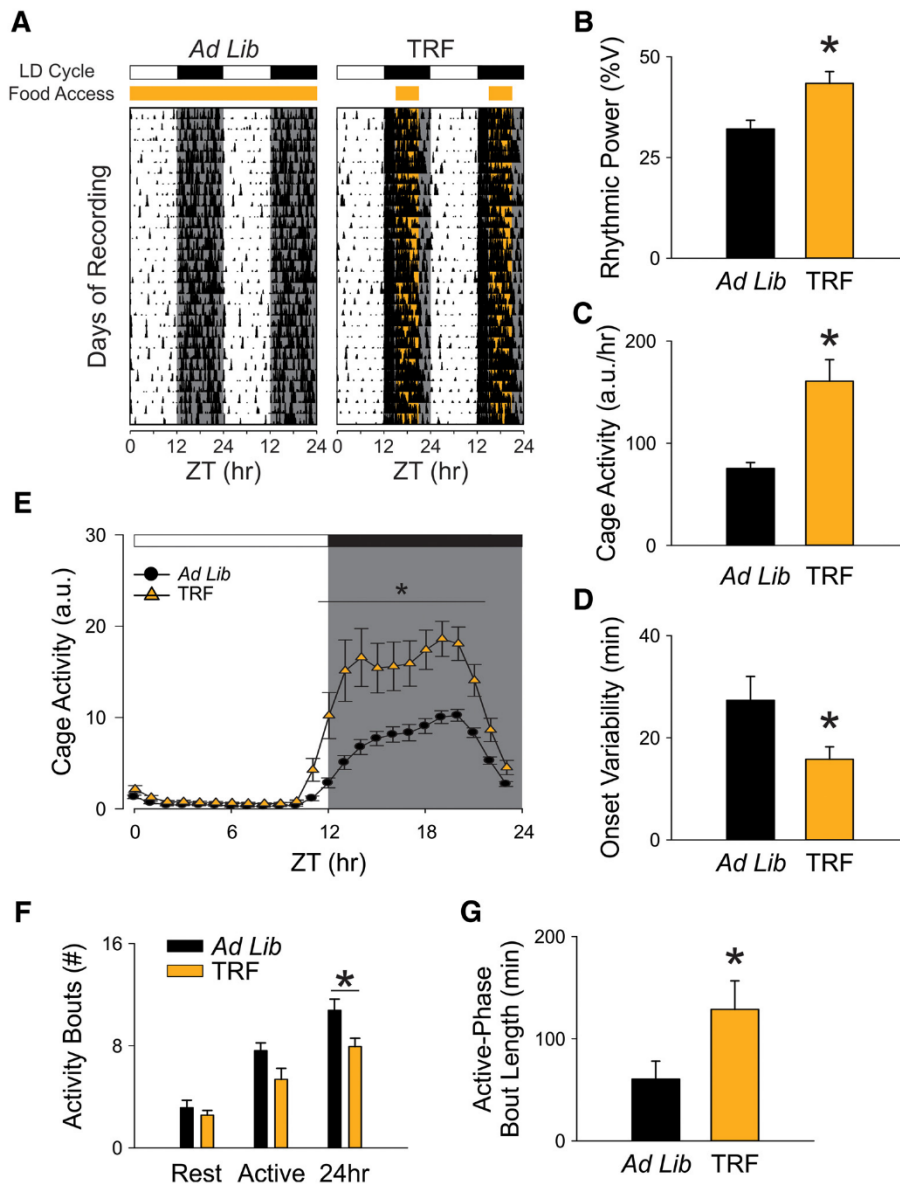
41

Figure 1. Locomotor activity rhythms were improved by the TRF regimen. ***A***, Examples of cage activity rhythms recorded from Q175 mutants under control (left) and TRF (right) conditions. The activity levels in the actograms were normalized to the same scale (85% of the maximum of the most active individual). Each row represents two consecutive days, and the second day is repeated at the beginning of the next row. The orange bar on the top of actograms indicates the time when food hopper is opened. ***B***, The strength of the activity rhythm is indicated by the power (%V) of the χ^2 periodogram analysis. ***C***, The averaged level of cage activity. ***D***, The averaged variation in onset from the best-fit regression line. ***E***, Average waveforms from 10 d of cage activity (1-h window) are shown and SEs across animals are indicated. ***F***, The number of activity bouts (separated by a gap of 21 mins or more) during rest phase (ZT 0-12), active phase (ZT 12-24), and 24 h are reported as the level of fragmentation of the circadian activity cycle. Black bars represent Q175 mutants under ad lib condition, and orange bars represent Q175 mutants under timed feeding condition. ***G***, The average length of activity bouts during their active phase. The white/black bar on the top of actograms (***A***) and waveforms (***E***) indicates the 12/12 h LD cycle. The temporal activity wave form was analyzed using a two-way RM ANOVA with time and treatment as factors. Other comparisons between Q175 cohorts were made using a *t* test. Asterisks represent significant differences due to TRF regimen compared to ad lib controls ($p < 0.05$); $n = 8$/group.

idated and high amount of locomotor activity during the active phase (Fig. 1*F*,*G*). Under TRF, the activity parameters in the Q175 mice were no longer significantly different from WT (Tables 1, 2). These findings demonstrate that TRF treatment significantly improved the activity rhythms of the HD mutant mice.

Table 2. Comparisons of age-matched WT under ad lib conditions to Q175 mice under ad lib or TRF regimen (*n* = 8/group)

	WT ad lib	WT ad lib vs Q175 ad lib		WT ad lib vs Q175 TRF	
Locomotor activity rhythm	AVG ± SEM	Difference	*p* value	Difference	*p* value
Rhythmic power (V%)	>32.59 ± 2.12	3.93	0.234	−10.82	**0.009**
Cage activity (a.u/h)	152.47 ± 19.08	75.67	**0.002**[U]	−8.23	0.7
Onset variability (min)	23.20 ± 2.84	−4.13	0.461	7.41	0.068
Bouts/d	8.44 ± 0.39	−2.34	**0.007**	0.50	0.517
Average bout length (rest-phase)	166.82 ± 22.33	106.20	**0.002**	38.01	0.305
Sleep behavior rhythm					
Daily sleep	665.42 ± 16.28	−57.12	0.081	−20.89	0.534
Bouts/d	8.44 ± 0.79	0.25	0.779	−0.88	0.443
Average bout length (night)	85.54 ± 21.52	−74.83	0.075	20.03	0.721
Awake time (ZT)	12.03 ± 0.1	−0.60	**0.002**[U]	0.10	0.329
Awake deviation time I (min)	13.62 ± 3.26	−24.07	**0.004**	−5.70	0.382
Motor performance					
Latency to fall (s)	320.65 ± 24.37	64.65	0.119	−99.4	**0.028**
Crossing errors (#)	3.09 ± 0.21	−4.35	**<0.001**	−1.88	**0.002**[U]

The results of *t* tests are reported if data passed normality tests. DF = 14. For parameters that did not pass normality tests, the Mann–Whitney rank-sum test was run and the *U* statistic reported; *p* < 0.05 was considered significant. In this and subsequent tables significant differences are shown in bold.

TRF shifted the timing but not the total amount of sleep behavior in the Het Q175 mice
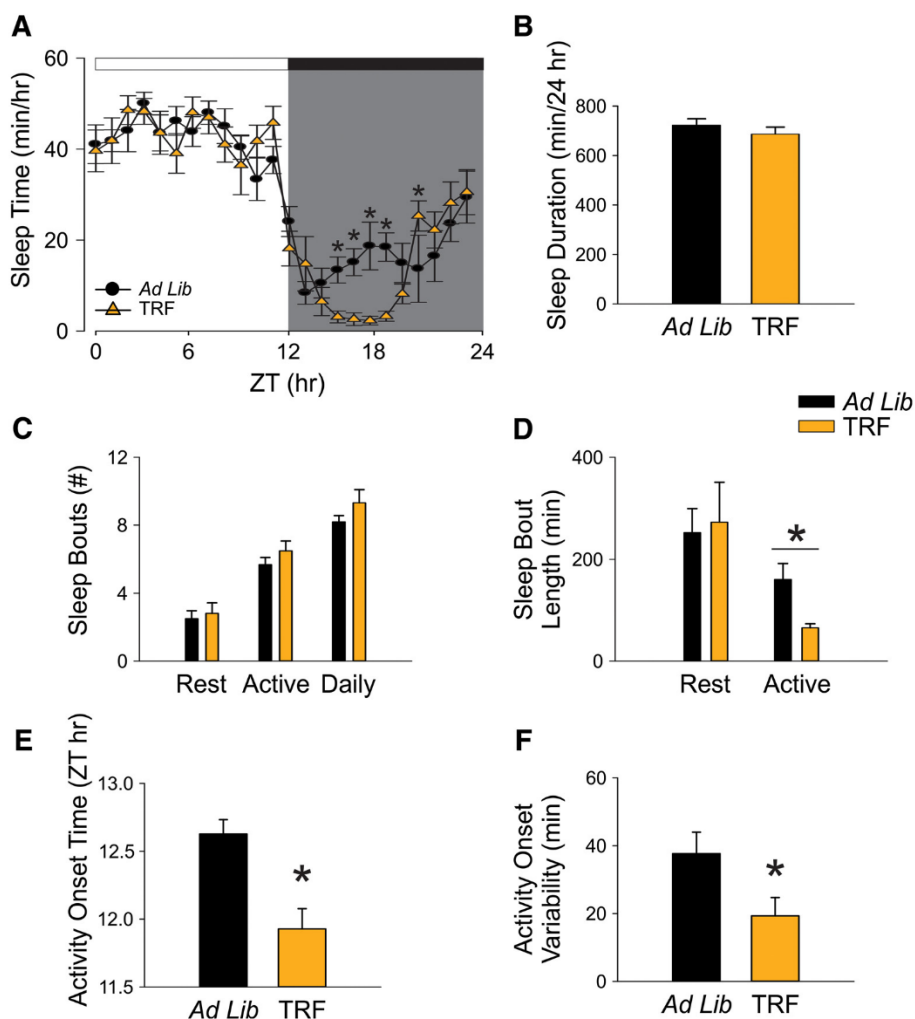
The immobility-defined sleep behavior was measured using video recording in combination with automated mouse tracking analysis software. During the 6 h when food was available at night, the TRF-treated Q175 mice slept less than untreated Q175 controls (Fig. 2*A*). A two-way RM ANOVA[j] was used to analyze the temporal pattern of sleep (1-h bins) of each group. The analysis revealed significant effect of time ($F_{(23,382)} = 36.575$, $p < 0.001$) and significant interaction between time and treatment ($F_{(23)} = 2.23$, $p = 0.002$), but the effect of treatment did not reach a significant level ($F_{(1,14)} = 2.033$, $p = 0.155$). No significant changes were detected in the total amount of sleep time over a 24-h cycle (ad lib: 722.5 ± 25.6 min; TRF: 686.3 ± 28.4 min, $t = 0.95$, $p = 0.36$, *t* test[k]; Fig. 2*B*). No significant difference was found in the total number of sleep bouts over a 24-h cycle (ad lib: 8.2 ± 0.4; TRF: 9.3 ± 0.8, $t_{(14)} = 58$, $p = 0.33$, *t* test[l]). The sleep bouts at night were significantly shorter in the TRF group than the control group (ad lib: 160.4 ± 31.6; TRF: 65.5 ± 7.9, $t_{(14)} = 93$, $p = 0.007$, *t* test[m]), suggesting that TRF group had shorter naps than the control group in their active phase (Fig. 2*C,D*).

The TRF treatment advanced the phase when the Q175 mice transitioned from sleep to awake states (ad lib: ZT 12.6 ± 0.2 h; TRF: ZT 11.9 ± 0.1 h, $t_{(14)} = 3.84$, $p = 0.002$, *t* test[n]; Fig. 2*E*). The TRF group also exhibited a more precise awakening time than the Q175 control mutants (ad lib: 37.7 ± 6.3 min; TRF: 19.3 ± 5.4 min, $t_{(14)} = 2.21$, $p = 0.044$, *t* test[o]; Fig. 2*F*). Under TRF, the beginning of activity and the cycle-to-cycle variability in sleep behavior in the Q175 mice were no longer significantly different from WT (Tables 2, 3). Overall, these findings demonstrate that the TRF regimen improved sleep behavior in Q175 mice.

TRF improved autonomic outputs in the Het Q175 mice

It has been shown that dysfunction in the circadian regulation of autonomic outputs can be detected early in disease progression in the Q175 mice (Cutler et al., 2017). In the present study, we measured the impact of TRF on activity, CBT, HR, and HRV measured simultaneously in freely moving Q175 mice (Fig. 3). The TRF Q175 mice exhibited higher levels in activity, CBT, and HR at some phases of the daily cycle (Fig. 3*A–C*). TRF also reduced the inappropriate activity during the daytime (ZT 0-12) when mice are normally less active (ad lib: 618.6 ± 96.6 a.u.; TRF: 308.4 ± 33.9 a.u., $t_{(12)} = 3.03$, $p = 0.010$, *t* test[p]). A two-way RM ANOVA[q] was applied on the activity wave form and significant effects of time ($F_{(23,334)} = 21.86$, $p < 0.001$), treatment ($F_{(1,12)} = 23.81$, $p < 0.001$) and interaction ($F_{(23)} = 3.68$, $p < 0.001$) were detected. In addition, the daily 24-h averaged CBT was not significantly different between the two groups (ad lib: 37.1 ± 0.1°C.; TRF: 36.7 ± 0.3°C, $t_{(12)} = 3.03$, $p = 0.17$, *t* test[r]). The TRF-treated group showed a lower CBT at the dark/light transition (ZT 23-2; Fig. 3*B*). A two-way RM ANOVA[s] confirmed significant effects of time ($F_{(23,334)} = 28.64$, $p < 0.001$) and treatment ($F_{(1,12)} = 7.65$, $p = 0.006$) without an interaction between the two factors ($F_{(23)} = 1.05$, $p = 0.398$). Despite no difference in the daily 24-h averaged HR (ad lib: 405.9 ± 8.0 bpm; TRF: 424.1 ± 10.2, $t = −1.4$, $p = 0.190$, *t* test[t]), the amplitude of the rhythm (max/min ratio) was improved by the TRF regimen (ad lib: 1.5 ± 0.02 bpm; TRF: 1.6 ± 0.03 bpm, $t = −2.18$, $p = 0.049$, *t* test[u]; Fig. 3*E*). The TRF group exhibited higher HR (ZT 13-17) when the food was available. As measured by two-way ANOVA[v], significant effects of time ($F_{(23,334)} = 10.21$, $p < 0.001$) and treatment ($F_{(1,12)} = 11.39$, $p < 0.001$) were detected. But no interaction between the two factors ($F_{(23)} = 1.52$, $p = 0.06$) was detected. Finally, the TRF-treated group exhibited higher levels in HRV in the rest phase as well as the beginning of active phase than the Q175 control group (Fig. 3*D*). The TRF-treated Q175 mice had significantly higher 24-h averaged HRV than the control Q175 mice (ad lib: 13.7 ± 0.8 msec.; TRF: 17.0 ± 1.0 msec, $t_{(12)} = −2.5$, $p = 0.028$, *t* test[w]). A two-way RM ANOVA[x] confirmed significant effect of time ($F_{(23,334)} = 8.23$, $p < 0.001$) and treatment ($F_{(1,12)} = 39.6$, $p < 0.001$) without a significant interaction ($F_{(23)} = 1.33$, $p = 0.140$).

Figure 2. TRF prevented disease-caused awakening time without altering the amount of sleep behavior. Video recording in combination with automated mouse tracking analysis software was used to measure immobility-defined sleep. **A**, Running averages (1-h window) of immobility-defined sleep in Q175 mutants with ad lib (black) and timed feeding (orange) are plotted. The white/black bar on the top of wave form indicates the 12/12 h LD cycle. **B–F**, Quantification of the immobility-defined sleep rhythms. The temporal sleep wave form was analyzed using a two-way RM ANOVA with time and treatment as factors. Other comparisons between Q175 cohorts were made using a t test. Asterisks represent significant differences due to TRF regimen compared to ad lib controls ($p <$ 0.05); $n = 8$/group.

Overall, the TRF regimen improved the daily rhythms in physiologic, autonomically-driven outputs.

TRF improved motor performance in the Het Q175 mice

One of the defining symptoms of HD is the incidence of movement disorders in early-stage patients and we hypothesized that TRF may improve the motor symptoms. To test this hypothesis, we assessed motor performance using two tests that have been shown to detect motor coordination deficits in Q175 mice: the accelerating rotarod (Fig. 4A) and challenging beam tests (Fig. 4B). The Q175 mice on TRF had a longer latency to fall compared to age-matched Q175 ad lib-fed mutants (ad lib: 256 ± 30.4 min; TRF: 420.1 ± 32.2 min, $t_{(14)} = -3.7$, $p = 0.002$,

t test[y]). In addition, the treated Q175 mice made significantly fewer errors compared to control Q175 mice (ad lib: 7.4 ± 0.5; TRF: 4.9 ± 0.5, $t_{(14)} = 3.23$, $p = 0.006$, t test[z]). Breaking down the errors made by beam width, the two-way ANOVA[aa] revealed a significant effect of treatment ($F_{(1,14)} = 15.22$, $p < 0.001$), effect of beam width ($F_{(3,62)} = 26.17$, $p < 0.001$), and interaction between the two factors ($F_{(3)} = 3.924$, $p = 0.013$). *Post hoc* analysis indicates that the main difference between treated and control Q175 mice were the errors in the narrowest beam (ad lib: 3.4 ± 0.5; TRF: 1.8 ± 0.2, t = 4.84, $p < 0.001$, t test).

The TRF-treated Q175 mice which showed the most improved circadian output also had better performance in the two motor tests (Fig. 4C). In a XYZ grid composed of key activity rhythms parameters and performance of mo-

Table 3. Comparisons of age-matched WT under ad lib to regimen (*n* = 8/group)

	WT TRF	WT TRF vs WT ad lib	
Locomotor activity rhythm	AVG ± SEM	Difference	*p* value
Rhythmic power (V%)	57.03 ± 3.15	24.44	**<0.001**
Cage activity (a.u/h)	269.96 ± 20.24	117.49	**<0.001**
Onset variability (min)	31.54 ± 2.49	8.34	**0.028**[U]
Bouts/d	6.8 ± 0.38	−1.64	**0.009**
Average bout length (rest-phase)	202.55 ± 25.87	35.74	0.313
Sleep behavior rhythm			
Daily sleep	646.25 ± 31.61	−19.17	0.598
Bouts/d	9.5 ± 0.61	1.06	0.279
Average bout length (night)	60.06 ± 12.8	−25.47	0.326
Awake time (ZT)	11.90 ± 0.16	−0.12	0.095
Awake deviation time I (min)	19.57 ± 6.04	5.94	0.42
Motor performance			
Latency to fall (sec)	457.08 ± 22.12	136.43	**<0.001**
Crossing errors (#)	3.28 ± 0.31	0.19	0.6
Body weight (g)	29.02 ± 0.87	−0.76	0.343

Find the values of ad lib in Table 2. The results of *t* tests are reported if data passed normality tests. DF = 14. For parameters that did not pass normality tests, the Mann–Whitney rank-sum test was run and the *U* statistic reported; *p* < 0.05 was considered significant.

tor tests, there were two distinctive clusters which indicated that the mice with improved locomotor activity rhythm performed better in both motor tests. The correlation analysis indicated that the rhythmic power tended to be positively correlated with the amount of time staying on the accelerating rotarod (coefficient = 0.54, *p* = 0.17) and was negatively correlated with numbers of errors made crossing the narrowest beam (coefficient = −0.52, *p* = 0.04) in the TRF group. This correlation was not detected in the Q175 control group (coefficient = 0.16 and 0.13, respectively). Similarly, the TRF-treated group showed a negative correlation between their cage activity level and beam crossing errors (coefficient = −0.51, *p* = 0.01). This correlation was, again, not detected in the Q175 control group (coefficient = −0.06). These data indicate that the TRF-driven improvement in activity rhythms is correlated with the reduction in beam crossing errors.

Expression of multiple HD markers in striatum were altered by TRF

Striatum is one of the key brain structures of the cortical-basal ganglia circuit controlling motor function, and it has been shown to be particularly vulnerable in HD. Previous work has identified HD-driven changes in transcription in the striatum of the Q175 mouse (Langfelder et al., 2016). Using NanoString technology, we examined the impact of TRF on changes in gene expression of HD markers in the striatum of the Q175 mice as previously described (Wang et al., 2017). The expression patterns were compared to Q175 ad lib controls (Table 4). The TRF regimen altered expression of immediate early genes such as *Arc*, *Erg1,2,4*, and *Fos*, as well as receptors for neurotransmitters such as acetylcholine, histamine, 5HT, tachykinin, and dynorphin (Fig. 5A). The IPA analysis tool was applied to the total dataset (Table 5) to identify corresponding enriched pathways and biofunctions (Table 6). The top canonical pathways identified included (in descending order of significance): G protein-coupled receptor (GPCR) signaling, cAMP-mediated signaling, and glutamate receptor signaling. The top upstream regulators included BDNF,

CREB1, and HTT. Hence, the TRF treatment significantly altered the patterns of expression of genes linked to HD and modulated multiple transcriptional pathways.

Discussion

A range of circadian deficits in the mouse models of HD have been reported, detailing the impact on rhythms in behavior and physiology (Bourne et al., 2006; Ciammola et al., 2006; Grimbergen et al., 2008; Cuturic et al., 2009; Kuljis et al., 2012; Fisher et al., 2016). The findings suggest that the most common sleep-related clinical complaints of HD patients (i.e., difficulty falling asleep, frequent awakenings during sleep, and difficulty staying awake during the active cycle) are due, at least in part, to the disease-induced dysfunction in the circadian system. These findings raise the possibility of treating HD symptoms by improving the regularity/robustness of circadian rhythms in activity and rest (Wang et al., 2017; Whittaker et al., 2017).

In the present study, the Het Q175 mice were allowed access to their food (standard chow, 6 h) nightly for three months starting at an age before the onset of motor symptoms. We confirmed that the animals consumed similar amounts of food and the body weights were not significantly decreased by this feeding regimen. We demonstrate that the nightly TRF regimen improved the daily activity rhythm with increases in the rhythmic strength as measured by power of the periodogram and decreases in cycle-to-cycle variability in activity onset. Prior work in WT mice did not find an impact of TRF on locomotor activity patterns (Hatori et al., 2012). While we are not sure of the difference, we did evaluate older mice (six months) who may be already exhibiting some age-related decline in locomotor activity rhythms. The TRF treatment also advanced the time that the mice ended their sleep phase without changes in total amount of sleep per cycle. Critically, the TRF regimen also improved performance of the HD mutant mice on two different motor tests.

The beneficial impact of TRF on motor performance could be dependent on or independent from the improvements in circadian output. We examined this issue by
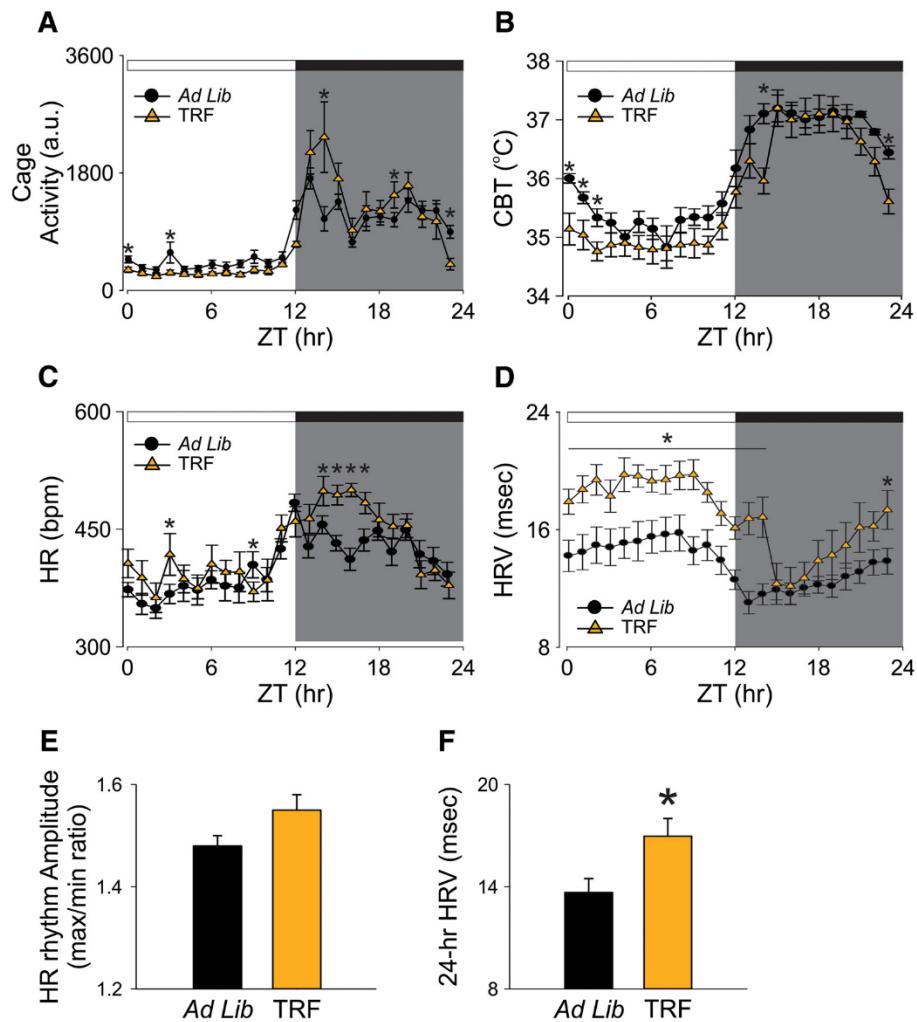
Figure 3. Autonomic output rhythms were improved by the TRF regimen. The autonomic outputs from ad lib (black circles) and TRF (orange triangles) Q175 mice were recorded simultaneously using telemetry device. *A–D*, Hourly running averages of activity (*A*), CBT (*B*), HR (*C*), and HRV from both groups are plotted (*D*). *E*, The HR rhythm amplitude, determined by the ratio of max and min of the day, in control and TRF-treated Q175 mice. *F*, The 24-h averaged HRV in control and TRF-treated Q175 mice. The temporal waveforms of autonomic outputs were analyzed using a two-way RM ANOVA with time and treatment as factors. Other comparisons between Q175 cohorts were made using a *t* test. Asterisks represent significant differences due to TRF regimen compared to ad lib controls ($p < 0.05$); $n = 7$/group.

taking advantage of the animal-to-animal variation in the impact of the treatment on circadian and motor function. Using our most sensitive motor assay (i.e., challenge beam test), we found that the improved circadian behavior was correlated with improved motor function in the TRF group (coefficient = −0.52, $P = 0.04$). This finding leads us to conclude that improved circadian timing underlies the improved motor function in the treated mice. Furthermore, a variety of different approaches aiming to boost circadian output have now been found to improve motor functions in different HD mouse models. There is evidence that improving the sleep/wake cycle with sleep-inducing drugs (Pallier et al., 2007; Kantor et al., 2016), stimulants (Cuesta et al., 2012; Whittaker et al., 2017), bright light and restricted wheel access (Cuesta et al.,

2014), and blue light (Wang et al., 2017) can treat HD symptoms. This body of work supports our general hypothesis that TRF improves circadian robustness and acts via this mechanism to delay disease symptoms in HD.

Our data clearly demonstrate that the benefits of TRF extend to physiologic measures such as HRV. Cardiovascular events are a major cause of early death in the HD population (Lanska et al., 1988; Sørensen and Fenger 1992) and the dysfunctional autonomic nervous system may be linked to the increased cardiovascular susceptibility. HRV measures the variation in the beat-to-beat (R-R) interval. It reflects the dynamic balance of sympathetic and parasympathetic control of heart function, and displays a robust circadian rhythm. A prior study demon-
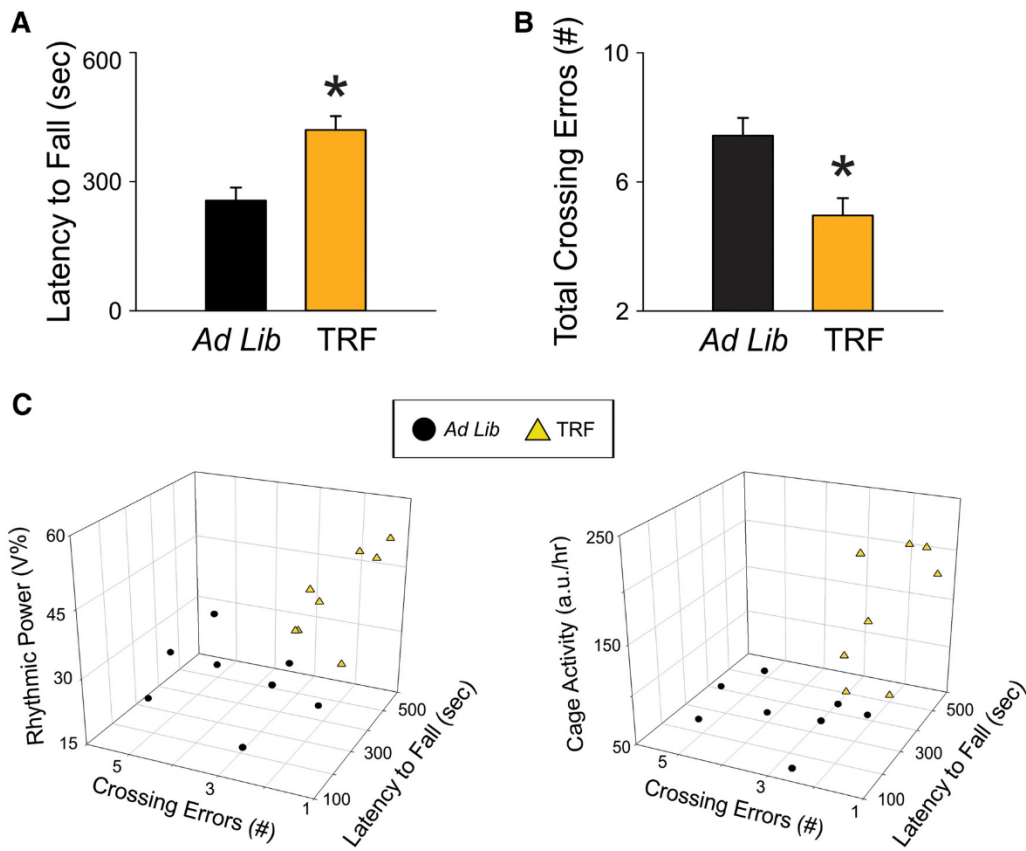
Figure 4. TRF improved motor performance in the Q175 HD model. **A**, The accelerating rotarod test revealed that the TRF treatment improved motor performance by showing longer latency to fall. **B**, The challenging beam motor test indicated that the TRF treatment improved performance (fewer errors) by making fewer errors when the mice crossed the balanced beam. **C**, The circadian parameters and the performance in the two motor tests of individual mouse in ad lib group (black circles) and TRF group (orange triangles) are plotted in a 3D-XYZ grid. In this XYZ grid, there are two distinctive clusters, suggesting that the mouse with stronger circadian rhythms performed better in both motor tests. Comparisons between Q175 cohorts were made using a t test. Asterisks represent significant differences due to TRF regimen compared to ad lib controls ($p < 0.05$). The correlations between circadian parameters and motor performance are described in the text; $n = 8$/group.

strated that the Q175 mice exhibit a loss of circadian control in HRV day/night differences, as well as an overall decrease in HRV over a 24-h period when compared to WT controls (Cutler et al., 2017). It is worthwhile to note that a similar decrease in HRV has also been reported in HD patients beginning during the presymptomatic stage of disease progression (Andrich et al., 2002; Aziz et al., 2010b). Reduced HRV is generally considered an indica-

Table 4. Top 5 HD markers in the striatum of Q175 altered by the TRF treatment

	Comparison	Q175 vs WT			Ad lib vs TRF	
	Age	2 months	6 months o	10 months	9 months	
Gene Symbol	Full name	Log2 fold change			Log2 fold change	p value
Striatum						
Fos	FBJ osteosarcoma oncogene	ns	↓	ns	↑	0.0004
Htr2a∗	5-Hydroxytryptamine (serotonin) receptor 2A	ns	ns	ns	↑	0.0005
Hrh3	Histamine receptor H3	ns	↓	↓	↑	0.0009
Chrm4	Cholinergic receptor, muscarinic 4	↓	↓	↓	↑	0.0012
Tacr1	Tachykinin receptor 1	ns	↓	↓	↑	0.0020

P value of the *t* test comparison with Q175 housed under ad lib is shown. Asterisk indicates HD markers changed in both the striatum and cortex. Transcripts increased by the treatment (Log2 fold change) are shown in green (↑) and those decreased by the treatment in red (↓). Transcripts without significant change ($p > 0.05$) are shown in gray (ns); 24% gene expressions in the striatum and 7% gene expressions in the cortex are altered by the TRF treatment. Among altered genes in striatum, >50% genes (13/24) that are shown downregulated in Q175 controls (comparison with age-matched WT controls (Lengfelder et al., 2016) are upregulated by TRF.

47
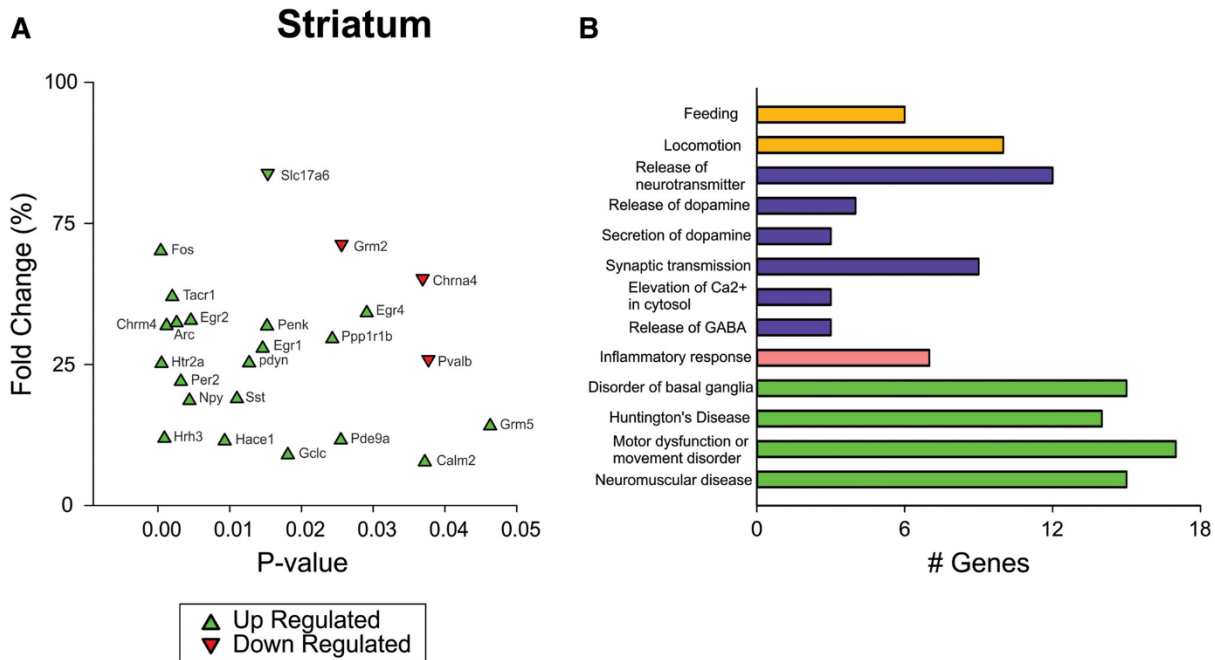
Figure 5. Altered expression level of multiple HD markers in the striatum of the Q175 HD model. ***A***, Differentially expressed genes in the striatum observed between TRF group and ad lib group using NanoString (find all gene expression data in Table 6). The same Q175 mice that underwent activity/sleep monitoring and behavioral tests were allowed to recover for four weeks from manipulations before tissue collection. The signal intensity of individual genes was normalized by adjusting to internal positive standards within each sample (see Materials and Methods). ***B***, Enriched functional clustering in the striatum using the IPA analysis tool (based on data in Table 6; uncorrected Fisher's exact test p value < 0.05). The clusters of interest with statistical significance are picked and enriched biofunctions in those picked clusters are shown (in descending order of significance). The picked clusters include Behavior (p = 2.72E-17, color orange), Cell-to-cell signaling and interaction (p = 1.02E-17, color blue), inflammatory response (p = 2.87E-04, color pink), and neurologic disease (p = 8.74E-14, color green).

tion of poor cardiovascular health and a predictor for cardiovascular disease and mortality (Thayer et al., 2010). To our knowledge, this is the first study showing that a TRF regimen can improve HRV in a disease model.

Prior work in *Drosophila* has also demonstrated the benefits of TRF in ameliorating age-related cardiovascular decline (Melkani and Panda, 2017). In this model, TRF downregulates expression of gene involved in mitochondrial electron transport while increasing expression of a cytoplasmic chaperonin (Gill et al., 2015). This study also found that mutations in circadian clock genes prevented the benefits of TRF. TRF improved the amplitude of the day/night rhythms in many circadian-regulated transcripts. In mice, genetic disruption of the circadian clock results in a variety of cardiovascular deficits (Paschos and FitzGerald, 2010; Young, 2016). Together, this work suggests that TRF can work in concert with the photic regulation of the circadian system to boast the amplitude and perhaps the phasing of the molecular clock-work.

Lifestyle interventions have been suggested to be preventative and therapeutic for diseases associated with aging, such as type-2 diabetes, cardiovascular disease and increasingly neurodegenerative disorders. For example, caloric restriction (CR) has consistently been found to prolong life span and protect against a variety of pathologic conditions (Heilbronn and Ravussin 2003; Fontana

Table 5. Top 10 canonical pathways and upregulators identified using IPA analysis in striatum of Q175 under TRF regimen

Ingenuity canonical pathways	−log (p value)
G protein-coupled receptor signaling	7.65
cAMP-mediated signaling	6.73
Glutamate receptor signaling	6.08
Neuropathic pain signaling in dorsal horn neurons	5.02
Gαi signaling	4.94
Synaptic long-term potentiation	3.38
Gαq signaling	3.03
iNOS signaling	2.88
CREB signaling in neurons	2.87
Serotonin receptor signaling	2.77
Upstream regulator	−log (p value)
BDNF	13.41
CREB1	12.27
Cocaine	11.87
CNTF	11.14
HTT	10.82
TET1	10.40
GDNF	9.74
ADCYAP1R1	9.72
Dalfampridine	8.95
Haloperidol	8.90

Table 6. Full dataset of expression of HD markers in the striatum of Q175 that are tested by using NanoString technology. Bold text indicates significant difference between ad lib and TRF feeding protocols

Gene symbol	−Log (p value)	Log 2 Fold Change
Aco2	0.51	−0.09
Aif1	0.58	0.13
Apba2bp	0.60	−0.37
Arc	**2.58**	0.11
Bdnf	0.54	−0.56
Bhlhb2	0.16	−0.12
C1qc	0.17	0.14
C3	0.49	0.05
C4a	0.60	0.08
calb1	0.39	0.11
Calm1	0.74	0.03
Calm2	**1.43**	−0.16
Calm3	0.06	−0.09
Cdkn1c	0.04	−0.21
Chat	0.55	0.07
Chga	0.54	−0.01
Chrm1	0.33	−0.13
Chrm4	**2.92**	0.17
Chrna4	**1.43**	−0.15
Chrnb2	0.62	0.07
Cnr1	1.02	0.04
Cth	0.28	0.09
Dnajb5	0.13	−0.04
Drd1a	1.06	0.21
Drd2	1.00	0.25
Egr1	**1.84**	0.13
Egr2	**2.34**	0.24
Egr3	0.86	0.08
Egr4	**1.54**	0.21
F8a	1.24	−0.01
Fos	**3.39**	0.23
Fth1	0.34	0.03
Gabra1	0.43	−0.02
Gabrd	0.05	0.11
Gclc	**1.74**	0.15
Gclm	0.07	−0.08
Gfap	1.03	0.03
Grm2	**1.59**	−0.47
Grm5	**1.33**	0.01
Hace1	**2.03**	−0.03
Hmox1	0.86	0.20
Hrh3	**3.04**	0.31
Htr1a	0.03	−0.36
Htr1b	1.22	0.27
Htr2a	**3.32**	0.15
Htt	0.50	−0.10
Il12b	0.73	0.04
Il6	0.41	−0.16
Kcnip2	1.05	0.10
Lonp1	0.67	0.05
Nfe2l2	0.01	−0.05
Ngf	0.75	−0.26
Nos1	0.96	0.02
Nos3	0.09	0.10
Npy	**2.35**	−0.02
Nqo1	0.90	0.03
Ntrk1	1.18	0.13
Ntrk2	1.12	−0.09
Pde10a	0.97	0.20
Pde9a	**1.59**	0.02
		(Continued)

Table 6. Continued

Gene symbol	−Log (p value)	Log 2 Fold Change
pdyn	**1.89**	0.22
Penk	**1.82**	0.26
Penk1	**1.80**	0.23
Per2	**2.50**	−0.01
Ppargc1a	0.08	0.05
Ppp1r1b	**1.61**	0.19
Ptpn5	0.76	0.09
Pvalb	**1.42**	0.02
Rgs4	0.09	0.00
Rrs1	0.88	0.16
Ryr1	0.15	−0.14
Sap25	0.72	0.03
Slc17a6	**1.81**	−0.15
Slc17a7	0.10	−0.70
Slc1a2	0.12	−0.09
Slc6a3	0.78	0.16
Slco6b1	0.61	0.41
Snap25	0.12	−0.08
Sod1	1.01	0.01
Sod2	0.00	0.05
Sst	**1.96**	0.17
Tac1	1.09	0.15
Tacr1	**2.71**	0.33
Tfeb	0.98	0.03
Tmsb10	0.05	0.24
Vgf	0.69	0.08
hHTT polypro	0.01	−0.12
mHTT polypro	0.15	−0.01

et al., 2004). Conceptually, the TRF regimen used in the present study is quite distinct from CR. While CR focuses on overall, dramatic reduction in energy intake, TRF emphasizes the temporal pattern of fasting without a reduction in overall energy intake. Mechanistically, TRF may activate the same beneficial biochemical pathways as CR (Mattson et al., 2014; Longo and Panda 2016) but would likely be easier to implement in a patient population (Scheen, 2008; Marder et al., 2009). In humans, the time of food availability would be during the day when food is normally consumed while the fast would be extended past the normal night. Prior studies have demonstrated the benefits of an 8:16 feed/fast cycle in improving the metabolic state and motor coordination of mice without altering caloric intake or nutrient composition (Hatori et al., 2012; Chaix et al., 2014). In the HD-N171-82Q mouse model, CR improves motor performance and survival while reducing cell death (Duan et al., 2003). Prior work in the R6/2 HD model has shown that TRF can restore HD-driven disruption in circadian gene expression in the liver (Maywood et al., 2010) and improve locomotor activity as well as exploratory behavior in the open field without increasing life span (Skillings et al., 2014). Together, these data suggest that feeding schedules could play a role in the treatment of HD and could lead to the development of new treatment options for neurodegenerative disorders.

The mechanisms underlying the beneficial effects of the TRF regimen on Q175 mouse model are uncertain and likely mediated by multiple pathways. Our data indicate that the TRF treatment changes the transcriptional envi-

49

ronment in a brain region intimately involved in HD, i.e., the striatum. We used the NanoString technology with the IPA platform to analyze the transcriptional changes evoked by TRF. We found that >50% of genes (13/24) that had been shown downregulated in Q175 controls in a prior study (comparison with age-matched WT controls (Langfelder et al., 2016) were upregulated by this treatment (Table 4), suggesting our circadian manipulation may exert beneficial effects through these pathways (Table 5). For example, striatal histamine receptor H3 (*Hrh3*) may connect improved circadian rhythms to improved motor functions. *Hrh3*, a GPCR, is strongly expressed in the cortico-striatal circuits controlling motor behavior (Pollard et al., 1993). Prior work found a significant reduction in Hrh3 radioligand binding in tissue of HD patients (Goodchild et al., 1999) suggesting a central role of the histaminergic system in this basal ganglia disorder. Histamine is a well-known regulator of the sleep-wake cycle (Lin et al., 2011; Gondard et al., 2013) and specifically, H3R modulates striatal neurons through its regulation of glutamate (Ellender et al., 2011), GABA (Garcia et al., 1997; Ellender et al., 2011), and dopamine (Schlicker et al., 1993; González-Sepúlveda et al., 2013) release. In a recent study, we found that daily treatment with an H3R inverse agonist improved several behavioral measures in the Q175 mice including activity and sleep rhythms, exploratory behavior, mood (Whittaker et al., 2017). GPCR signaling and glutamate receptor signaling are the top three pathways identified in the IPA analysis as being regulated by TRF. Unfortunately, the feeding schedule did not reduce the levels of mutant *Htt* (Table 6). Nevertheless, identifying treatments that improve the standard of living for HD patients remains an important goal. Future work will need to specifically evaluate the role of the histaminergic system in mediating the benefits of TRF for the sleep-wake cycles as well as motor performance.

Conclusion

Imposed feeding cycles have the capacity to synchronize or increase the amplitude of circadian oscillations throughout the body. Disturbances in the sleep/wake cycle are by now a well-established symptom of neurodegenerative diseases, and here we show that we can treat the HD symptoms by controlling the timing of food availability. The results presented in our preclinical study suggest that a TRF regimen could be a useful management tool for neurodegenerative disease patients. More generally, the present study adds to a growing body of evidence that improvements in "circadian hygiene" through attention to regularity in environmental signaling, including timed feeding, leads to improvements in health outcomes for a wide range of human diseases including neurodegenerative disorders.

References

Andrich J, Schmitz T, Saft C, Postert T, Kraus P, Epplen JT, Przuntek H, Agelink MW (2002) Autonomic nervous system function in Huntington's disease. J Neurol Neurosurg Psychiatry 72:726–731. Medline [TQ1]

Aziz NA, Anguelova GV, Marinus J, Lammers GJ, Roos RA (2010a) Sleep and circadian rhythm alterations correlate with depression and cognitive impairment in Huntington's disease. Parkinsonism Relat. Disord 16:345–350.

Aziz NA, Anguelova GV, Marinus J, Van Dijk JG, Roos RAC (2010b) Autonomic symptoms in patients and pre-manifest mutation carriers of Huntington's disease. Eur J Neurol 17:1068–1074. CrossRef Medline

Bartlett DM, Cruickshank TM, Hannan AJ, Eastwood PR, Lazar AS, Ziman MR (2016) Neuroendocrine and neurotrophic signaling in Huntington's disease: implications for pathogenic mechanisms and treatment strategies. Neurosci Biobehav Rev 71:444–454. CrossRef Medline

Bourne C, Clayton C, Murch A, Grant J (2006) Cognitive impairment and behavioural difficulties in patients with Huntington's disease. Nurs Stand 20:41–44. CrossRef Medline

Chaix A, Zarrinpar A, Miu P, Panda S (2014) Time-restricted feeding is a preventative and therapeutic intervention against diverse nutritional challenges. Cell Metab 20:991–1005. CrossRef Medline

Ciammola A, Sassone J, Alberti L, Meola G, Mancinelli E, Russo MA, Squitieri F, Silani V (2006) Increased apoptosis, huntingtin inclusions and altered differentiation in muscle cell cultures from Huntington's disease subjects. Cell Death Differ 13:2068–2078. CrossRef Medline

Cuesta M, Aungier J, Morton AJ (2012) The methamphetamine-sensitive circadian oscillator is dysfunctional in a transgenic mouse model of Huntington's disease. Neurobiol Dis 45:145–155. CrossRef

Cuesta M, Aungier J, Morton AJ (2014) Behavioral therapy reverses circadian deficits in a transgenic mouse model of Huntington's disease. Neurobiol Dis 63:85–91. CrossRef

Cutler TS, Park S, Loh DH, Jordan MC, Yokota T, Roos KP, Ghiani CA, Colwell CS (2017) Neurocardiovascular deficits in the Q175 mouse model of Huntington's disease. Physiol Rep 5:e13289. CrossRef

Cuturic M, Abramson RK, Vallini D, Frank EM, Shamsnia M (2009) Sleep patterns in patients with Huntington's disease and their unaffected first-degree relatives: a brief report. Behav Sleep Med 7:245–254. CrossRef

Duan W, Guo Z, Jiang H, Ware M, Li X, Mattson M (2003) Dietary restriction normalizes glucose metabolism and BDNF levels, slows disease progression, and increases survival in huntingtin mutant mice. Proc Natl Acad Sci USA 100:2911–2916. CrossRef

Ellender TJ, Huerta-Ocampo I, Deisseroth K, Capogna M, Bolam JP (2011) Differential modulation of excitatory and inhibitory striatal synaptic transmission by histamine. J Neurosci 31:15340–15351. CrossRef

Fisher CA, Sewell K, Brown A, Churchyard A (2014) Aggression in Huntington's disease: a systematic review of rates of aggression and treatment methods. J Huntingtons Dis 3:319–332. CrossRef Medline

Fisher SP, Godinho SIH, Pothecary CA, Hankins MW, Foster RG, Peirson SN (2012) Rapid assessment of sleep-wake behavior in mice. J Biol Rhythms 27:48–58. CrossRef Medline

Fisher SP, Schwartz MD, Wurts-Black S, Thomas AM, Chen T-M, Miller MA, Palmerston JB, Kilduff TS, Morairty SR (2016) Quantitative electroencephalographic analysis provides an early-stage indicator of disease onset and progression in the zQ175 knock-in mouse model of Huntington's disease. Sleep 39:379–391. CrossRef

Fleming SM, Ekhator OR, Ghisays V (2013) Assessment of sensorimotor function in mouse models of Parkinson's disease. J Vis Exp 50303

Fontana L, Meyer TE, Klein S, Holloszy JO (2004) Long-term calorie restriction is highly effective in reducing the risk for atherosclerosis in humans. Proc Natl Acad Sci USA 101:6659–6663. CrossRef Medline

Garcia M, Floran B, Arias-Montaño JA, Young JM, Aceves J (1997) Histamine H3 receptor activation selectively inhibits dopamine D1 receptor-dependent [3H]GABA release from depolarization-stimulated slices of rat substantia nigra pars reticulata. Neuroscience 80:241–249. CrossRef

Gill S, Le HD, Melkani GC, Panda S (2015) Time-restricted feeding attenuates age-related cardiac decline in *Drosophila*. Science 347: 1265–1269. CrossRef Medline

Goldberg MS, Fleming SM, Palacino JJ, Cepeda C, Lam HA, Bhatnagar A, Meloni EG, Wu N, Ackerson LC, Klapstein GJ, Gajendiran M, Roth BL, Chesselet M-F, Maidment NT, Levine MS, Shen J (2003) Parkin-deficient mice exhibit nigrostriatal deficits but not loss of dopaminergic neurons. J Biol Chem 278:43628–43635. CrossRef

Gondard E, Anaclet C, Akaoka H, Guo R-X, Zhang M, Buda C, Franco P, Kotani H, Lin J-S (2013) Enhanced histaminergic neurotransmission and sleep-wake alterations, a study in histamine H3-receptor knock-out mice. Neuropsychopharmacology 38:1015–1031. CrossRef

González-Sepúlveda M, Rosell S, Hoffmann HM, Castillo-Ruiz MdM, Mignon V, Moreno-Delgado D, Vignes M, Díaz J, Sabriá J, Ortiz J (2013) Cellular distribution of the histamine H3 receptor in the basal ganglia: functional modulation of dopamine and glutamate neurotransmission. Basal Ganglia 3:109–121. CrossRef

Goodchild RE, Court JA, Hobson I, Piggott MA, Perry RH, Ince P, Jaros E, Perry EK (1999) Distribution of histamine H3-receptor binding in the normal human basal ganglia: comparison with Huntington's and Parkinson's disease cases. Eur J Neurosci 11:449–456. CrossRef

Goodman AOG, Rogers L, Pilsworth S, McAllister CJ, Shneerson JM, Morton AJ, Barker RA (2011) Asymptomatic sleep abnormalities are a common early feature in patients with Huntington's disease. Curr Neurol Neurosci Rep 11:211–217. CrossRef

Grimbergen YAM, Knol MJ, Bloem BR, Kremer BPH, Roos RAC, Munneke M (2008) Falls and gait disturbances in Huntington's disease. Mov Disord 23:970–976. CrossRef Medline

Gusella JF, MacDonald ME, Lee J-M (2014) Genetic modifiers of Huntington's disease. Mov Disord 29:1359–1365. CrossRef Medline

Hamaguchi Y, Tahara Y, Hitosugi M, Shibata S (2015) Impairment of circadian rhythms in peripheral clocks by constant light is partially reversed by scheduled feeding or exercise. J Biol Rhythms 30: 533–542. CrossRef Medline

Hara R, Wan K, Wakamatsu H, Aida R, Moriya T, Akiyama M, Shibata S (2001) Restricted feeding entrains liver clock without participation of the suprachiasmatic nucleus. Genes Cells 6:269–278. CrossRef

Hatori M, Vollmers C, Zarrinpar A, DiTacchio L, Bushong EA, Gill S, Leblanc M, Chaix A, Joens M, Fitzpatrick James AJ, Ellisman Mark H, Panda S (2012) Time-restricted feeding without reducing caloric intake prevents metabolic diseases in mice fed a high-fat diet. Cell Metab 15:848–860. CrossRef

Heilbronn LK, Ravussin E (2003) Calorie restriction and aging: review of the literature and implications for studies in humans. Am J Clin Nutr 78:361–369. Medline

Kantor S, Varga J, Morton AJ (2016) A single dose of hypnotic corrects sleep and EEG abnormalities in symptomatic Huntington's disease mice. Neuropharmacology 105:298–307. CrossRef Medline

Kudo T, Schroeder A, Loh DH, Kuljis D, Jordan MC, Roos KP, Colwell CS (2011) Dysfunctions in circadian behavior and physiology in mouse models of Huntington's disease. Exp Neurol 228:80–90. CrossRef Medline

Kuljis D, Schroeder AM, Kudo T, Loh DH, Willison DL, Colwell CS (2012) Sleep and circadian dysfunction in neurodegenerative disorders: insights from a mouse model of Huntington's disease. Minerva Pneumol 51:93–106.

Langbehn DR, Hayden M, Paulsen JS; PREDICT-HD Investigators of the Huntington Study Group (2010) CAG-repeat length and the age of onset in Huntington disease (HD): a review and validation study of statistical approaches. Am J Med Genet B Neuropsychiatr Genet 153B:397–408. CrossRef

Langfelder P, Cantle JP, Chatzopoulou D, Wang N, Gao F, Al-Ramahi I, Lu X-H, Ramos EM, El-Zein K, Zhao Y, Deverasetty S, Tebbe A, Schaab C, Lavery DJ, Howland D, Kwak S, Botas J, Aaronson JS, Rosinski J, Coppola G, et al. (2016) Integrated genomics and proteomics define huntingtin CAG length-dependent networks in mice. Nat Neurosci 19:623–633. CrossRef

Lanska DJ, Lanska M, Lavine L, Schoenberg BS (1988) Conditions associated with huntington's disease at death: a case-control study. Arch Neurol 45:878–880. Medline

Lin J-S, Sergeeva OA, Haas HL (2011) Histamine H3 receptors and sleep-wake regulation. J Pharmacol Exp Ther 336:17–23. CrossRef

Loh DH, Kudo T, Truong D, Wu Y, Colwell CS (2013) The Q175 mouse model of Huntington's disease shows gene dosage- and age-related decline in circadian rhythms of activity and sleep. PLoS One 8:e69993. CrossRef Medline

Longo VD, Panda S (2016) Fasting, circadian rhythms, and time-restricted feeding in healthy lifespan. Cell Metab 23:1048–1059. CrossRef Medline

Marder K, Zhao H, Eberly S, Tanner CM, Oakes D, Shoulson I; Huntington Study Group (2009) Dietary intake in adults at risk for Huntington disease: analysis of PHAROS research participants. Neurology 73:385–392. CrossRef

Mattson MP, Allison DB, Fontana L, Harvie M, Longo VD, Malaisse WJ, Mosley M, Notterpek L, Ravussin E, Scheer FAJL, Seyfried TN, Varady KA, Panda S (2014) Meal frequency and timing in health and disease. Proc Natl Acad Sci USA 111:16647–16653. CrossRef

Maywood ES, Fraenkel E, McAllister CJ, Wood N, Reddy AB, Hastings MH, Morton AJ. Disruption of peripheral circadian timekeeping in a mouse model of Huntington's disease and its restoration by temporally scheduled feeding. J Neurosci. 2010 Jul 28; 30(30): 10199–10204. CrossRef

Melkani GC, Panda S (2017) Time-restricted feeding for prevention and treatment of cardiometabolic disorders. J Physiol 595:3691–3700. CrossRef Medline

Menalled LB, Kudwa AE, Miller S, Fitzpatrick J, Watson-Johnson J, Keating N, Ruiz M, Mushlin R, Alosio W, McConnell K, Connor D, Murphy C, Oakeshott S, Kwan M, Beltran J, Ghavami A, Brunner D, Park LC, Ramboz S, Howland D (2012) Comprehensive behavioral and molecular characterization of a new knock-in mouse model of Huntington's disease: zQ175. PLoS One 7:e49838. CrossRef

Morton AJ, Wood NI, Hastings MH, Hurelbrink C, Barker RA, Maywood ES (2005) Disintegration of the sleep-wake cycle and circadian timing in Huntington's disease. J Neurosci 25:157–163. CrossRef Medline

Mulder CK, Papantoniou C, Gerkema MP, Van Der Zee EA (2014) Neither the SCN nor the adrenals are required for circadian time-place learning in mice. Chronobiol Int 31:1075–1092. CrossRef Medline

Pack AI, Galante RJ, Maislin G, Cater J, Metaxas D, Lu S, Zhang L, Smith RV, Kay T, Lian J, Svenson K, Peters LL (2007) Novel method for high-throughput phenotyping of sleep in mice. Physiol Genomics 28:232–238. CrossRef

Pallier PN, Maywood ES, Zheng Z, Chesham JE, Inyushkin AN, Dyball R, Hastings MH, Morton AJ (2007) Pharmacological imposition of sleep slows cognitive decline and reverses dysregulation of circadian gene expression in a transgenic mouse model of Huntington's disease. J Neurosci 27:7869–7878. CrossRef

Paschos GK, FitzGerald GA (2010) Circadian clocks and vascular function. Circ Res 106:833–841. CrossRef Medline

Pollard H, Moreau J, Arrang JM, Schwartz JC (1993) A detailed autoradiographic mapping of histamine H3 receptors in rat brain areas. Neurosci 52:169–189. CrossRef

Scheen AJ (2008) The future of obesity: new drugs versus lifestyle interventions. Expert Opin Invest Drugs 17:263–267. CrossRef

Schlicker E, Fink K, Detzner M, Göthert M (1993) Histamine inhibits dopamine release in the mouse striatum via presynaptic H3 receptors. J Neural Transm Gen Sect 93:1–10. CrossRef

Schroeder AM, Wang HB, Park S, Jordan MC, Gao F, Coppola G, Fishbein MC, Roos KP, Ghiani CA, Colwell CS (2016) Cardiac dysfunction in the BACHD mouse model of Huntington's disease. PLoS One 11:e0147269. CrossRef Medline

Skillings EA, Wood NI, Morton AJ (2014) Beneficial effects of environmental enrichment and food entrainment in the R6/2 mouse model of Huntington's disease. Brain Behav 4:675–686. CrossRef Medline

Sørensen SA, Fenger K (1992) Causes of death in patients with Huntington's disease and in unaffected first degree relatives. J Med Genet 29:911–914. Medline

Thayer JF, Yamamoto SS, Brosschot JF (2010) The relationship of autonomic imbalance, heart rate variability and cardiovascular disease risk factors. Int J Cardiol 141:122–131. CrossRef

Young ME (2016) Temporal partitioning of cardiac metabolism by the cardiomyocyte circadian clock. Exp Physiol 101:1035–1039. CrossRef Medline

Wang H-B, Whittaker DS, Truong D, Mulji AK, Ghiani CA, Loh DH, Colwell CS (2017) Blue light therapy improves circadian dysfunction as well as motor symptoms in two mouse models of Huntington's disease. Neurobiol Sleep Circadian Rhythms 2:39–52. CrossRef

Wexler NS, Lorimer J, Porter J, Gomez F, Moskowitz C, Shackell E, Marder K, Penchaszadeh G, Roberts SA, Gayan J, Brocklebank D, Cherny SS, Cardon LR, Gray J, Dlouhy SR, Wiktorski S, Hodes ME, Conneally PM, Penney JB, Gusella J, et al. (2004) Venezuelan kindreds reveal that genetic and environmental factors modulate Huntington's disease age of onset. Proc Natl Acad Sci USA 101: 3498–3503.

Whittaker DS, Wang HB, Loh DH, Cachope R, Colwell CS (2017) Possible use of a H3R antagonist for the management of non-motor symptoms in the Q175 mouse model of Huntington's disease. Pharmacol Res Perspect 5. CrossRef

Chapter 4: Circadian-based treatment strategy effective in the BACHD mouse model of

Huntington's disease

Circadian-based Treatment Strategy Effective in the BACHD Mouse Model of Huntington's Disease

Daniel S. Whittaker,*,[1] (iD) Dawn H. Loh,*,[1] Huei-Bin Wang,* Yu Tahara,* Dika Kuljis,*
Tamara Cutler,* Cristina A. Ghiani,[†] (iD) Shigenobu Shibata,[‡] Gene D. Block,*
and Christopher S. Colwell*,[2] (iD)

*Department of Psychiatry and Biobehavioral Sciences, University of California, Los Angeles, Los Angeles,
California, USA, [†]Department of Pathology & Laboratory Medicine, University of California, Los Angeles,
California, USA, and [‡]Waseda Institute for Advanced Study, Waseda University, Shinjuku-ku, Tokyo, Japan

Abstract Huntington's disease (HD) patients suffer from progressive neurodegeneration that results in cognitive, psychiatric, cardiovascular, and motor dysfunction. Disturbances in sleep-wake cycles are common among HD patients with reports of delayed sleep onset, frequent bedtime awakenings, and excessive fatigue. The BACHD mouse model exhibits many HD core symptoms including circadian dysfunction. Because circadian dysfunction manifests early in the disease in both patients and mouse models, we sought to determine if early interventions that improve circadian rhythmicity could benefit HD symptoms and delay disease progression. We evaluated the effects of time-restricted feeding (TRF) on the BACHD mouse model. At 3 months of age, the animals were divided into 2 groups: ad lib and TRF. The TRF-treated BACHD mice were exposed to a 6-h feeding/18-h fasting regimen that was designed to be aligned with the middle (ZT 15-21) of the period when mice are normally active (ZT 12-24). Following 3 months of treatment (when mice reached the early disease stage), the TRF-treated BACHD mice showed improvements in their locomotor activity and sleep behavioral rhythms. Furthermore, we found improved heart rate variability, suggesting that their autonomic nervous system dysfunction was improved. On a molecular level, TRF altered the phase but not the amplitude of the PER2::LUC rhythms measured in vivo and in vitro. Importantly, treated BACHD mice exhibited improved motor performance compared with untreated BACHD controls, and the motor improvements were correlated with improved circadian output. It is worth emphasizing that HD is a genetically caused disease with no known cure. Lifestyle changes that not only improve the quality of life but also delay disease progression for HD patients are greatly needed. Our study demonstrates the therapeutic potential of circadian-based treatment strategies in a preclinical model of HD.

Keywords time-restricted feeding, feed/fast cycle, circadian rhythms, Huntington's disease, BACHD

---

1. These authors contributed equally to this work.
2. To whom all correspondence should be addressed: Christopher S. Colwell, Department of Psychiatry and Biobehavioral Sciences, University of California, Los Angeles, 760 Westwood Plaza, Los Angeles, CA 90024, USA; e-mail: ccolwell@mednet.ucla.edu.

Huntington's disease (HD) patients suffer from progressive neurodegeneration that inflicts cognitive, psychiatric, cardiovascular, and motor dysfunction (Margolis and Ross, 2003; Kuljis et al., 2012). HD is caused by a CAG repeat expansion within the first exon of the Huntingtin (Htt) gene, and when translated, it produces a polyglutamine repeat that leads to protein misfolding, soluble aggregates, and inclusion bodies detected throughout the body (Saft et al., 2005; Ciammola et al., 2006). The mutated HTT protein triggers dysfunction of a large range of cellular processes, including glucose, cholesterol, and lipid metabolic pathways. HD symptoms appear at different ages, with an average onset at 40 years of age. Generally, the longer the CAG repeat, the earlier the age of onset and the greater the severity of the symptoms (Langbehn et al., 2010). Yet, even among patients with the same CAG repeat length, there is a considerable range in the time of onset and severity of symptoms (Wexler et al., 2004; Gusella et al., 2014). Such variability raises the possibility of environmental modifiers influencing the disease and suggests that appropriate disease management strategies can increase the health span of the patients. This possibility is important to pursue, as there are no known cures for HD.

Sleep disorders are extremely common in HD patients and have detrimental effects on the daily functioning and quality of life of patients and their caregivers (Morton et al., 2005; Cuturic et al., 2009; Aziz et al., 2010; Goodman et al., 2011). Disruptions in the timing of sleep are common in HD patients and often become apparent years before the onset of the motor symptoms. One of the first signs of the disease in HD patients is a phase delay in the nightly rise in melatonin (Kalliolia et al., 2014), and by the end of life, the central circadian clock (suprachiasmatic nucleus [SCN]) shows evidence of degeneration (van Wamelen et al., 2014). Mouse models of HD also exhibit a progressive and rapid breakdown of the circadian rest/activity cycle that closely mimics the condition observed in human patients, typified by loss of consolidated sleep, increased wakeful activity during the light (rest) phase, and more sleep during the dark (active) phase (Morton et al., 2005; Kudo et al., 2011; Loh et al., 2013; Kuljis et al., 2016). Disorganized circadian timing leads to undesirable effects throughout the body (Colwell, 2015), altering the function of key organ systems including heart, pancreas, liver, lungs, as well as the brain. Collectively, this prior research supports the hypothesis that circadian dysfunction interacts with HD pathology, leading to the exacerbation of HD-related symptoms. If this hypothesis is correct, we would anticipate a retardation of HD progression by employing treatments that improve the sleep-wake cycle.

To test this hypothesis, we have been using the BACHD knock-in mouse model of HD. While there are several good mouse models of HD, the BACHD offers the advantage of containing the human mutation (Gray et al., 2008; Wang et al., 2014). We have characterized the impact of age (3, 6, 9, and 12 months old) on the diurnal and circadian rhythms in wheel-running behavior, core body temperature (CBT), and heart rate (HR; Kudo et al., 2011) and have also documented clear dysfunction in the daily rhythms in autonomic regulation of cardiac output (Schroeder et al., 2011; Schroeder et al., 2016). SCN neurons are spontaneously active and generate action potentials with peak firing rates during the day (Colwell, 2011). We have previously shown that BACHD SCN neurons show significantly reduced daytime spontaneous firing rates (Kudo et al., 2011; Kuljis et al., 2016) demonstrating that, early in the disease, these mice have deficits in the central circadian clock. Decreased daytime electrical activity in the SCN would weaken both neural and hormonal outputs. These observations suggest that a pathological weakening of the electrical output from the SCN is responsible for the circadian behavioral phenotypes observed in the BACHD. This wealth of data makes the BACHD an ideal preclinical model to examine the impact of circadian interventions on disease trajectory.

One of the most powerful regulators of the circadian system is the daily feed/fast cycle (Bass and Takahashi, 2010; Tahara and Shibata, 2013). For example, SCN-lesioned animals can still be synchronized to a feeding schedule (Stephan, 2002; Acosta-Galvan et al., 2011; Tahara et al., 2012). Most of the published work has examined the consequences of placing the feeding in the light (rest) phase when it is misaligned with normal consumption patterns. However, there have been a few studies that found benefits in scheduling the feeding so that it is aligned with the normal active phase. Most notably, the Panda lab has shown that mice under time-restricted feeding (TRF) consume equivalent calories from a high-fat diet as those with ad libitum (ad lib) access and yet are protected against obesity, hyperinsulinemia, and inflammation and have improved motor coordination (Hatori et al., 2012). The TRF protocol was also beneficial in preventing age-induced cardiovascular dysfunction in *Drosophila* (Gill et al., 2015; Melkani and Panda, 2017). We felt that this protocol could be usefully applied to the BACHD model to determine whether the scheduled feeding provides benefits to a preclinical neurodegenerative disease model with a focus on the sleep-wake, motor, and cardiovascular phenotypes.

MATERIALS AND METHODS

The work presented in this study followed all guidelines and regulations of the University of California, Los Angeles, Division of Animal Medicine, which are consistent with the Animal Welfare Policy Statements and the recommendations of the Panel on Euthanasia of the American Veterinary Medical Association.

Animals

The BACHD mouse model that we used in this study expresses the full-length human mutant Htt gene encoding 97 glutamine repeats under the control of endogenous regulatory machinery (BACHD; Gray et al., 2008). Female BACHD dams backcrossed on a C57BL/6J background (minimum 12 generations) were bred with C57BL/6J (wild-type [WT]) males from the Jackson Laboratory (Bar Harbor, ME) in our own breeding facility to obtain male and female offspring, either WT or heterozygous for the BACHD transgene. Data were also collected from WT mice from this colony. Only male mice were used in this study as there is a sex difference in the circadian and motor phenotypes (Kuljis et al., 2016). Genotyping was performed at 15 days of age by tail snips, and after weaning, littermates were group housed until otherwise noted. All animals were housed in sound-proof, humidity-controlled chambers with controlled lighting conditions, using a 12-h light, 12-h dark cycle (12:12 LD, intensity 300 lux) for at least 2 weeks prior to experimentation. For all experiments, a light meter (BK Precision, Yorba Linda, CA) was used to measure light intensity (lux). The chambers were in the same animal housing facility with controlled temperature and humidity, and each chamber held 8 cages of mice, grouped together by feeding treatment. All animals received cotton nestlets, and water was made available at all times. To confirm the effect of timed feeding on daily rhythms and motor performance, we also examined WT mice at 6 months of age.

This study used a total of 86 C57 mice divided into 5 cohorts. The first group of BACHD (5) and WT (5) mice were used to examine the amount of food consumed and body weight under the scheduled feeding protocol. This pilot was used just to demonstrate the feasibility of the protocol, and the results are presented as a supplemental figure. The second cohort of BACHD (16) and WT (16) mice were used for the measurements of behavior (sleep, activity, motor performance). The third cohort of BACHD (16) were used for telemetry measurements. Two mice did not recover well from the surgery and were euthanized shortly after surgery. The fourth cohort of BACHD

(14) and WT (14) mice were used for in vivo and in vitro measurements of bioluminescence. For these experiments, the BACHD were crossed into the PER2::LUC line.

TRF

Mice were first entrained to a 12:12 h LD cycle for a minimum of 2 weeks prior to any treatment. Experimental animals were then exposed to one of two feeding conditions: food available ad libitum (ad lib) or food available for 6 h during the middle of the active phase during zeitgeber time (ZT) 15-21. By definition, ZT 12 is the time when the lights go off when the mice are in an LD cycle. Experimental mice were singly housed in cages with a custom-made programmable food hopper that could temporally control access to food (standard chow) and prevent food consumption during restricted times. Mice are coprophagic, and the mice were not moved to new cages between their daily feeding and fasting cycles. It is likely that the mice consumed their own feces during the fast interval. These cages were also equipped with an infrared (IR) motion detector to give us the ability to measure cage activity. The mice were held in these conditions for a total of 3 months (from 3 mo to 6 mo of age).

Automated Episodic Food Intake Monitoring

Mouse episodic food intake was performed using the BioDAQ intake monitoring system (Research Diets, Inc., New Brunswick, NJ). WT and BACHD mice ($n = 5$) were housed and habituated in normal cages for 2 weeks. All mice were transferred to BioDAQ monitoring cages, and 2 weeks of episodic food intake under ad lib was automatically collected and recorded (Supplementary Fig. S1). Mice were then returned to normal cages, where treated mice were acclimated to TRF. When daily TRF food consumption values were consistent, after 2 weeks, all mice were again transferred to BioDAQ monitoring cages. To the extent possible, the conditions were kept identical to our normal housing conditions. Two weeks of episodic food intake under TRF or ad lib was automatically collected and recorded. Data were analyzed using the BioDAQ DataViewer software (Research Diets, Inc.). Data from 14 days were averaged into 1-h and 12-h bins across a 24-h cycle for analysis.

Monitoring of Cage Locomotor Activity

Experimental mice were singly housed in cages with the food hopper as well as IR motion sensors. The locomotor activity was recorded as previously

described (Wang et al., 2017). Mice were entrained to a 12:12 h LD cycle for a minimum of 2 weeks prior to data collection. Locomotor activity data were recorded using Mini Mitter (Bend, OR) data loggers in 3-min bins, and 10 days of data were averaged for analysis. We used the 10 days of activity data collected just prior to the motor performance tests during the final 2 weeks of the TRF schedule. The data were analyzed to determine the period and rhythmic strength as previously described (Loh et al., 2013; Wang et al., 2017). The periodogram analysis uses a χ^2 test with a threshold of 0.001 significance, from which the amplitude of the periodicities is determined at the circadian harmonic to obtain the rhythm power. The amount of cage activity over a 24-h period was averaged over 10 days and reported here as the arbitrary units (a.u.)/h. The number of activity bouts and the average length of bouts were determined using Clocklab (Actimetrics, Wilmette, IL), in which each bout was counted when activity bouts were separated by a gap of 21 min (maximum gap: 21 min; threshold: 3 counts/min). The onset variability was determined using Clocklab by drawing the best-fit line over the 10 days and averaging the differences between activity onset and best-fit regression of each day.

Monitoring of Immobility-defined Sleep Behavior

Immobility-defined sleep was determined as described previously (Loh et al., 2013; Wang et al., 2017). Mice were housed in see-through plastic cages containing bedding (without the addition of nesting material) and the food hopper. A side-on view of each cage was obtained, with minimal occlusion by the food bin or water bottle, both of which were top mounted. Cages were top lit using IR/light-emitting diode lights. Video capture was accomplished using surveillance cameras with visible light filters (Gadspot Inc., City of Industry, CA) connected to a video-capture card (Adlink Technology Inc., Irvine, CA) on a Dell Optiplex computer system. ANY-maze software (Stoelting Co., Wood Dale, IL) was used for automated tracking of mouse immobility.

Immobility was registered when 95% of the area of the animal stayed immobile for more than 40 sec, as was previously determined to have 99% correlation with simultaneous EEG/electromyography defined sleep (Pack et al., 2007; Fisher et al., 2012). Continuous tracking of the mice was performed for a minimum of 5 sleep-wake cycles, with randomized visits (1-2 times/day) by the experimenter to confirm mouse health and video recording. The third and fourth sleep-wake cycles were averaged for further analysis. Immobility-defined sleep data were exported in 1-min bins, and total sleep time was determined by summing the immobility durations in the rest phase (ZT 0-12) or active phase (ZT 12-24). An average waveform of hourly immobile sleep over the 2 sleep-wake cycles was produced during the final week of TRF. Variability of sleep onset and awake time was determined using Clocklab to draw the best-fit line over the sleep cycles, and the differences between sleep offset and best-fit regression of each sleep cycle were averaged.

Autonomic Outputs: CBT, HR, and Heart Rate Variability (HRV)

For the telemetry measurements, methods employed were similar to those previously described (Schroeder et al., 2016; Cutler et al., 2017). Two groups (ad lib and TRF) of BACHD mice ($n = 7$/group) were surgically implanted with a wireless radiofrequency transmitter (ETA-F20, Data Sciences International, St. Paul, MN). Mice were singly housed in cages with the food hopper. Cages were placed atop telemetry receivers (Data Sciences International) in a light- and temperature-controlled chamber. Standard rodent chow was provided for both groups. Data collection began 2 weeks postsurgery. HR was extrapolated from electrocardiogram waveforms using the RR interval. After the baseline recordings, the sensors were turned off to conserve battery life and turned on again for the final 2 weeks of measurements. The final measurements were made when the mice were between 5 and 6 months of age.

Data collection and analysis were performed as described previously (Cutler et al., 2017). Data were extracted in 20-sec intervals and then filtered to remove extreme noise. Remaining valid data segments were averaged into 1-h bins across the 24-h cycle. Mean normal to normal intervals (NN; in msec) and standard deviation of all NN intervals (in msec) were calculated for the time domain analysis.

In Vivo Bioluminescence

In vivo monitoring was performed as previously described (Tahara et al., 2012) with an in vivo kinetic imaging system (IVIS Kinetics; Caliper Life Sciences, Hopkinton, MA). BACHD PER2::LUC male mice (6-7 months) were subjected to ad lib or TRF for 2 weeks prior to sampling. The mice were anesthetized with isoflurane (Zoetis, Kalamazoo, MI) using a gas anesthesia system (XGI-8; Caliper Life Sciences). While the mice were under anesthesia, they were subcutaneously injected with d-luciferin potassium salt (Promega Corporation, Madison, WI) in the back near the neck at a dosage of 15 mg/kg (30 mg/10 mL or 0.05 mL/10 g body weight). Images with a 1-min

exposure time were captured 8 min after the luciferin injection in the dorsal-up position for the kidney and 10 min after the injection in the ventral-up position for the liver and submandibular gland (Sub gland). For each time point, the bioluminescence image was merged with a gray-scale image. To investigate the circadian oscillations of PER2::LUC in the peripheral tissues, images were obtained 6 times per day at 4-h intervals. The average photon/sec value of the data of each day was designated as 100%, and the bioluminescence rhythms of the individual organs of the day were expressed as a percentage. The peak phase and amplitude of the normalized data were determined with the single cosinor procedure (acro.exe; designed by Dr. Refinetti). Data with p values less than 0.05 were considered rhythmic oscillations, and the graphs of the amplitudes and peak phases contained only rhythmic data.

In Vitro Bioluminescence

In vitro measurements of bioluminescence were performed as previously described (Loh et al., 2011; Loh et al., 2013). BACHD PER2::LUC male mice (6-9 months) were subjected to ad lib or TRF for 2 weeks prior to sampling. Mice were sacrificed after anesthesia (isoflurane) between ZT 10 and 11, and 1- to 2-mm^3 explants were immediately dissected in ice-cold Hanks' balanced salt solution (HBSS; Sigma, St. Louis, MO) supplemented with 4.5 mM NaHCO$_3$, 10 mM HEPES, and 100 U/mL penicillin-streptomycin. Brains were incubated in ice-cold slice solution (in mM: 26 NaHCO$_3$, 1.25 NaH$_2$PO$_4$, 10 glucose, 125 NaCl, 3 KCl, 5 MgCl$_2$, 1 CaCl$_2$) aerated with 95% O$_2$/5% CO$_2$ for 5 min, and 300-μm coronal sections were collected using a vibratome and further microdissected in HBSS under a 10× dissecting microscope. The SCN was cut away from the rest of the section using 2 cuts with a surgical scalpel (No. 21 blade, Fisher Scientific, Waltham, MA). All explants were individually transferred to Millicell membranes (0.4 μm, PICMORG50; Millipore, Bedford, MA) resting on 1.2 mL of recording media: 1X DMEM (Sigma); 1X B27 supplement (Gibco, Waltham, MA); 4.5 mM NaHCO$_3$, 10 mM HEPES, 40 mM Glutamax (Gibco), 4.5 mg/mL D-glucose, 25 U/mL penicillin, 25 U/mL streptomycin, 0.1 mM sodium salt monohydrate luciferin (Biosynth, Staad, Switzerland) in a 35-mm dish sealed with autoclaved vacuum grease (Dow Corning, Midland, MI). SCN, heart, and liver explants were inserted into the Lumicycle photometer (Actimetrics), incubated at 37 °C, and bioluminescence was continuously monitored for 7 consecutive days. Raw bioluminescence values were normalized by baseline subtraction (24-h running average) and smoothed with 2-h windows to prepare the representative

bioluminescence traces. The phase and amplitude of each explant were determined as previously described (Loh et al., 2011). Period was determined using the sine-wave fit function in Lumicycle Analysis (Actimetrics).

Rotarod Test: Accelerating Version

The rotarod apparatus (Ugo Basile, Varese, Italy) is commonly used to measure motor coordination and balance. This apparatus is, in essence, a small circular treadmill. It consists of an axle or rod thick enough for a mouse to stand on when it is not in motion and a flat platform a short distance below the rod. The rod is covered with smooth rubber to provide traction while preventing the mice from clinging to the rod. In this study, mice were placed on top of the rubber-covered rod. When the mice moved at the pace set by the rotation rate of the rod, they would stay on top of it. When mice no longer moved at the selected pace, they dropped a short distance to the platform below. The time a mouse remains on the rod before dropping to the platform is called the latency to fall. Following a 15-min habituation to the testing room, mice were placed on the slowly rotating rod. The rod gradually accelerated from 5 rpm to 38 rpm over the course of the trial. The length of time the mouse stayed on the rod was recorded. A 2-day protocol for the accelerating rotarod tests was used. On the first day, the mice were trained on the rotarod over 5 trials. The maximum length of each trial was 600 sec, and mice were allowed to rest for a minimum of 60 sec between trials. On the second day, mice were tested on the rotarod, and the latency to fall from the rotarod was recorded from 5 trials. Mice were again allowed to rest for a minimum of 60 sec between trials. Data from each mouse were analyzed after averaging the times from all 5 trials. The apparatus was cleaned with 70% alcohol and allowed to dry completely between trials. A dim red light (2 lux) was used for illumination during active (dark) phase testing.

Challenging Beam Test

The challenging beam test is a modified version of the beam traversal test described by Goldberg and colleagues (Goldberg et al., 2003; Fleming et al., 2013), and was used to characterize the motor deficits of BACHD mutant mice in previous studies (Kudo et al., 2011; Wang et al., 2017). The beam narrows in 4 intervals from 33 mm > 24 mm > 18 mm > 6 mm, with each segment spanning 253 mm in length. The home cage of each mouse is put on the end of the beam as the motivating factor. In this study, animals

were trained on the beam for 5 consecutive trials on 2 consecutive days. During each trial, each mouse was placed on the widest end of the beam and allowed to cross with minimal handling by the experimenter. On the testing day, a metal grid (10 $\times$ 10 mm spacing, formed using 19-gauge wire) was overlaid on the beam. This overlaid grid increased the difficulty of the beam traversal task and provided a visual reference for foot slips made while crossing the grid. Each mouse was subjected to 5 consecutive trials conducted during their active (dark) phase. Trials were recorded by a camcorder under dim red-light conditions (2 lux), supplemented with infrared lighting for video recording. The videos were scored post hoc by 2 independent observers for the number of missteps (errors) made by each mouse. The observers were masked as to the treatment group of the mice that they were scoring. An error was scored when any foot dipped below the grid. The number of errors was averaged across the 5 trials per mouse to give the final reported values. The apparatus was cleaned with 70% alcohol and allowed to dry completely between trials.

Statistical Analysis

We were interested in determining if TRF can improve the symptoms in the BACHD mouse model; therefore, treated BACHD mice (TRF group) were compared with age-matched untreated BACHD mice (ad lib group) in all experiments. The sample size per group was determined by both our empirical experience with the variability in the prior measures in the BACHD mice and a power analysis (SigmaPlot, SYSTAT Software, San Jose, CA) that assumed a power of 0.8 and an alpha of 0.05. To assess the impact of TRF after 3 months, we applied a t test for the analysis. To determine the impact of the treatment on temporal activity, sleep, CBT, HR, and HRV waveforms, we used a 2-way repeated-measures analysis of variance (RM ANOVA) with treatment and time as factors. To determine the impact of the treatment on errors made in each beam of the challenging beam test, we used a 2-way ANOVA with treatment and beam as factors. Pairwise multiple-comparison procedures were made using the Holm-Sidak method. Correlations between circadian parameters and motor performance were examined by applying Pearson correlation analysis. Statistical analysis was performed using SigmaPlot. Data were examined for normality (Shapiro-Wilk test) and equal variance (Brown-Forsythe test). Between-group differences were determined significant if $p < 0.05$. All values are reported as group mean $\pm$ standard error of the mean. For each of the tests, we report the t- or F-values as well as the degrees of freedom.

RESULTS

In these experiments, we used a TRF protocol consisting of a scheduled 6-h feeding/18-h fast, with the feeding between ZT 15 and 21 aligned to the middle of the active phase when mice normally eat. During this 6-h interval, the mice could eat without any restrictions, and the total amount of food consumed daily did not vary between the BACHD groups (ad lib: 3.6 $\pm$ 0.3 g; TRF: 3.3 $\pm$ 0.1 g, $t = 1.110$, $p = 0.179$, t test). The body weights at the end of the study were not different in BACHD mice under TRF (28.7 $\pm$ 0.7 g) compared with age-matched ad lib–fed mutants (28.2 $\pm$ 4.1 g, $U = 21.5$, $p = 0.279$, rank-sum test). The treatment was applied starting when the mutants begin to exhibit disrupted activity rhythms and motor symptoms (3 months) and ended at 6 months (Kudo et al., 2011).

TRF Improved Activity and Sleep Behavioral Rhythms in the BACHD Line

TRF noticeably improved the temporal pattern of cage activity (Fig. 1; Table 1). Compared with ad lib BACHD of the same age (6 months), the BACHD mice on TRF exhibited increased power of the rhythm, $t(14) = 6.891$, $p < 0.001$ (t test); percentage of activity in the active (dark) phase, $t(14) = 4.457$, $p < 0.001$ (t test); and precision in onset, $U(14) = 1.000$, $p < 0.001$ (rank-sum test). Overall activity per hour was not altered by the treatment, $t(14) = 1.679$, $p = 0.115$ (t test), compared with the ad lib–fed mutants. A 2-way RM ANOVA of the activity waveforms revealed a significant effect of time, $F(23) = 53.811$, $p < 0.001$, and treatment, $F(1) = 16.239$, $p < 0.001$, and a significant interaction between the 2 factors ($F = 2.788$, $p < 0.001$). A comparison of the same animals before (3 months) and after (6 months) treatment indicated that the TRF also significantly improved power, $t(7) = -4.622$, $p = 0.002$ (paired t test), and the percentage activity in the light, $t(7) = -6.318$, $p < 0.001$ (paired t test), in the BACHD, whereas activity levels and precision were not altered pre- and posttreatment.

The temporal distribution of sleep behavior was altered by TRF. During their rest (light) phase, the treated mice spent more time sleeping, $t(14) = 3.322$, $p = 0.005$ (t test), as well as exhibiting fewer sleep bouts, $t(14) = 3.812$, $p = 0.001$ (t test), compared with untreated BACHD mice (Fig. 2; Table 1). In contrast, during the active (dark) phase, there were no differences in the amount of sleep, $U(14) = 24$, $p = 0.442$ (rank-sum test), or in the number of sleep bouts, $t(14) = 1.758$, $p = 0.101$. Finally, TRF decreased variability and phase advanced the time of sleep onset. A 2-way RM ANOVA revealed a significant effect of time,
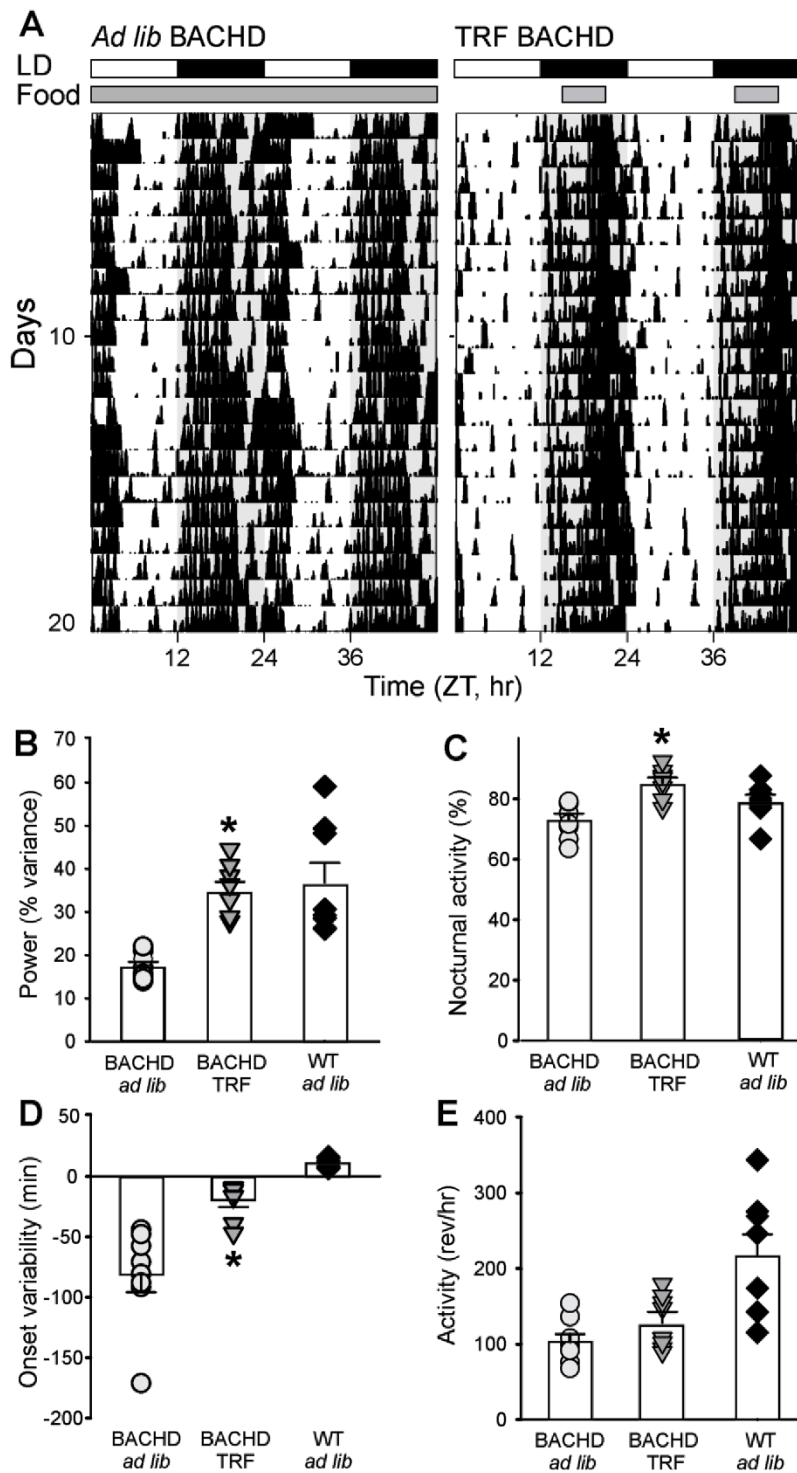
Figure 1.   Locomotor activity rhythms were improved by the TRF regimen. (A) Examples of cage activity rhythms recorded from BACHD mutant mice under *ad lib* (left) and TRF (right) conditions. The activity levels in the actograms were normalized to the same scale (85% of the maximum of the most active individual). Each row represents two consecutive days, and the second day is repeated at the beginning of the next row. The white/black bars on the top of the actograms and the white/grey shading in the actograms

Figure 1. (continued)

indicate the lighting condition. The grey bar at the top of the actogram indicates food availability under *ad lib* conditions, and the grey bar at the top of TRF actogram indicates the time when food hopper is opened. (B) The strength of the activity rhythm is indicated by the power (% variance) of the X^2 periodogram analysis. (C) The % of total activity that occurred in the dark (active) phase. (D) The averaged onset variability was calculated from the best-fit regression line. (E) Average hourly activity levels from 10 days of cage activity. For this and other figures, the vertical bar plots show group means and SEM. The symbols show the values from individual animals in each group (BACHD *ad lib*, circles; BACHD TRF, triangles, WT *ad lib*, diamonds). Comparisons between BACHD cohorts were made using a *t*-test. Asterisks represent significant differences due to TRF regimen compared to the BACHD ad lib controls ($p < 0.05$; n = 8 per group).

Table 1.   Rhythms in locomotor activity and sleep behavior in BACHD mice were improved by TRF.

	BACHD	BACHD + TRF	WT	WT + TRF	Genotype	Treatment
Locomotor activity rhythms						
Rhythmic power (% variance)	17.46 ± 1.1	34.8 ± 2.3	37.2 ± 4.9	61.8 ± 2.7	*F* = 64.068; *p* < 0.001	*F* = 57.937; *p* < 0.001
Cage activity (a.u./h)	103.0 ± 11.1	130.3 ± 12.5	217.8 ± 29.5	354.6 ± 36.1	*F* = 53.201; *p* < 0.001	*F* = 12.451; *p* = 0.001
Activity in night (%)	67.0 ± 1.2	85.3 ± 1.9	79.0 ± 2.0	91.6 ± 1.1	*F* = 56.809; *p* < 0.001	*F* = 125.991; *p* < 0.001
Onset variability (min)	81.5 ± 15.3	20.2 ± 5.5	11.0 ± 1.6	21.1 ± 5.7	*F* = 68.719; *p* < 0.001	*F* = 19.517; *p* < 0.001
Sleep behavior rhythms						
Daily sleep (min)	647.2 ± 30.08	652.8 ± 17.8	641.7 ± 16.8	669.5 ± 12.9	*F* = 0.085; *p* = 0.773	*F* = 0.753; *p* = 0.393
Sleep in day (min)	443.7 ± 15.0	515.3 ± 13.8	473.9 ± 10.6	449.1 ± 5.1	*F* = 2.639; *p* = 0.115	*F* = 4.453; *p* = 0.044
Sleep in night (min)	203.5 ± 40.1	141.3 ± 9.2	167.8 ± 15.2	143.5 ± 6.3	*F* = 0.636; *p* = 0.432	*F* = 4.242; *p* = 0.049
Bouts in day (No.)	3.8 ± 0.4	1.8 ± 0.2	3.5 ± 0.3	3.4 ± 0.4	*F* = 1.118; *p* = 0.299	*F* = 14.492; *p* < 0.001
Bouts in night (No.)	8.1 ± 0.7	6.5 ± 0.6	7.5 ± 0.6	7.4 ± 0.5	*F* = 0.067; *p* = 0.797	*F* = 1.966; *p* = 0.172
Wake time (ZT)	12.7 ± 0.3	12.4 ± 0.2	10.5 ± 0.1	11.3 ± 0.4	*F* = 38.590; *p* < 0.001	*F* = 0.991; *p* = 0.328

Comparisons of age-matched wild-type (WT) and BACHD mice under ad lib or time-restricted feeding (TRF) regimen (*n* = 8/group). Values are shown as averages ± SEM. Data were analyzed with a 2-way analysis of variance using genotype and treatment as factors. The Holm-Sidak test for multiple comparisons was used when appropriate. *p* values <0.05 were considered significant and are shown in bold.

$F_{(23)} = 41.656$, $p < 0.001$, and treatment, $F_{(1)} = 13.986$, $p = 0.001$, and a significant interaction between the 2 factors ($F = 2.771$, $p < 0.001$). Significant differences between the genotypes were found in both the rest (light) phase (ZT 0, 3, 4) and dark phase (ZT 12, 20, 23). A comparison of the same animals before and after treatment indicated that TRF produced significant increases in the duration of sleep, $t_{(7)} = -3.212$, $p = 0.015$ (paired *t* test) and decreased the number of sleep bouts, $t_{(7)} = 13.133$, $p < 0.001$ (paired *t* test) in the BACHD in the light phase. During the dark phase, TRF did not alter either the duration, $t_{(7)} = 0.934$, $p = 0.381$ (paired *t* test), or number of bouts, $t_{(7)} = 0.789$, $p = 0.456$ (paired *t* test). In summary, daily rhythms in both activity and sleep behavior were significantly improved in the BACHD mice by the TRF protocol.

TRF Improved Autonomic Outputs in the BACHD Mice

It has been shown that dysfunction in the circadian regulation of autonomic outputs can be detected early in disease progression in the BACHD mice (Kudo et al., 2011; Schroeder et al 2016). In the present study, we measured the impact of TRF on daily rhythms in HR, HRV, and CBT measured simultaneously in freely moving BACHD mice under ad lib and TRF (Fig. 3A-C). TRF-treated BACHD exhibited higher light (rest) phase HRV than the ad lib–fed BACHD group. (ad lib: 10.0 ± 0.6 msec; TRF: 12.7 ± 0.7 msec, $t_{[6]} = 2.672$, $p = 0.032$, *t* test) as well as increased amplitude of the HRV rhythm (ad lib: 2.7 ± 0.1 msec; TRF: 5.9 ± 0.8 msec, $t = 3.270$, $p = 0.005$, *t* test). A 2-way ANOVA on the waveform confirmed a significant effect of time, $F_{(23)} = 7.471$, $p < 0.001$, and treatment, $F_{(1)} = 53.362$, $p < 0.001$, and an interaction ($F = 6.478$, $p < 0.001$). TRF-treated BACHD also exhibited increased amplitude (max-min) of the HR rhythm (ad lib: 95.0 ± 12.4 bpm; TRF: 196 ± 20.0 bpm, $t = 8.081$, $P = 0.0002$, *t* test). A 2-way RM ANOVA run on the waveform (1-h bins) confirmed significant effects of time, $F_{(23)} = 28.223$, $p < 0.001$, and treatment, $F_{(1)} = 95.153$, $p < 0.001$, and an interaction between the 2 factors ($F = 6.768$, $p < 0.001$). Finally, the daily 24-h averaged CBT was not significantly different between the 2 groups (ad lib: 36.4 ± 0.2 °C; TRF: 36.7 ± 0.1 °C; $U = 5$, $p = 0.486$, rank-sum test), nor did the TRF drive a change in amplitude (ad lib: 2.45 ± 0.15; TRF: 2.75 ± 0.15; $t = 1.386$, $p = 0.215$, *t* test). A 2-way RM ANOVA did find

61
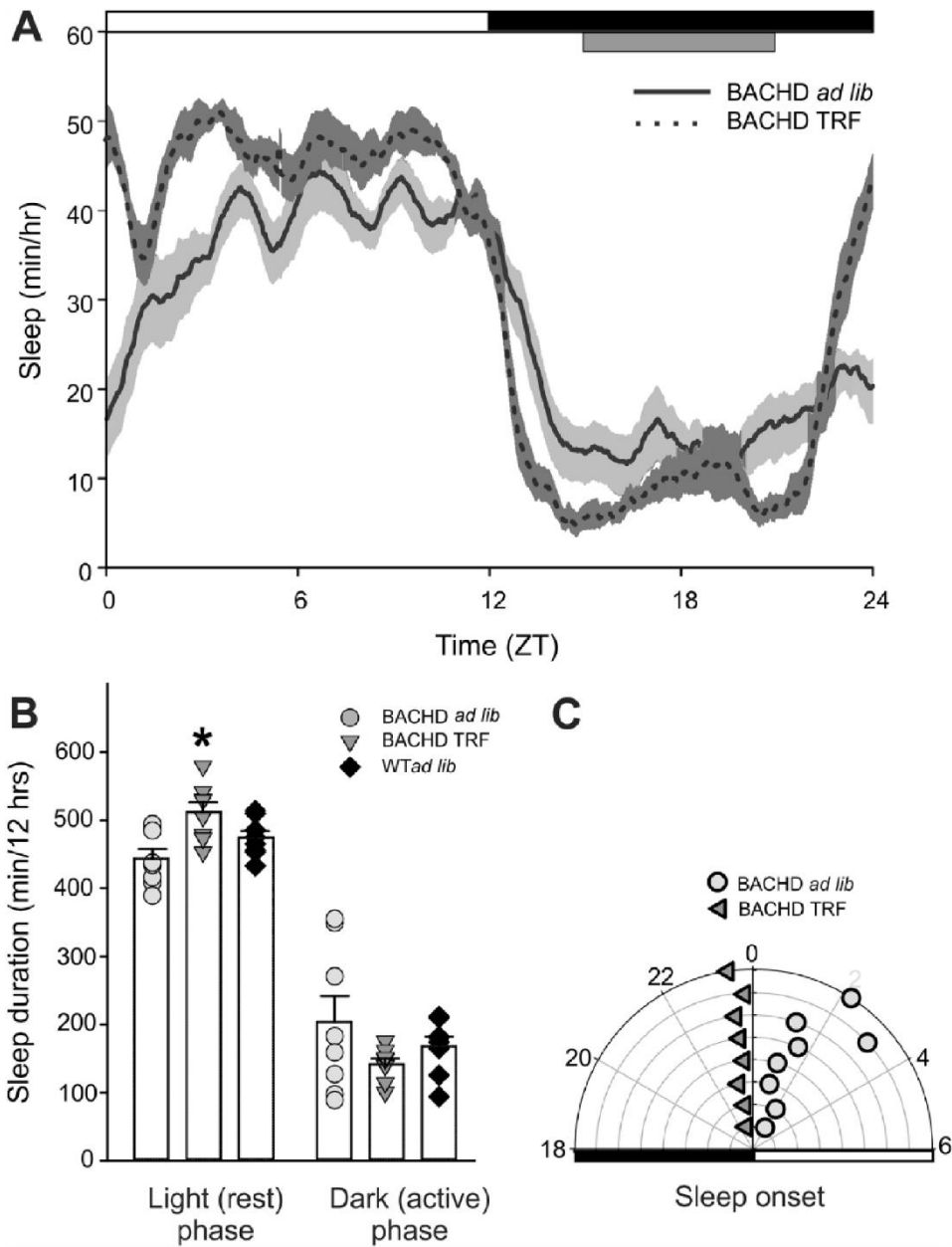
Figure 2. Sleep behavior was altered by the TRF protocol. Video recording in combination with automated mouse tracking analysis software was used to measure immobility-defined sleep (n = 8 per group). **(A)** Running averages of immobility-defined sleep in BACHD mutants with *ad lib* (solid line) and timed feeding (dotted line) are plotted. The white/black bar on the top of the waveforms indicates the 12:12 hr LD cycle. The grey bar on the top of waveforms indicates the time when food hopper is opened for TRF. **(B)** Quantification of the immobility-defined sleep in the light (rest) phase and dark (active) phase. Comparisons between BACHD cohorts were made using a *t*-test. Asterisks represent significant differences due to TRF regimen compared to *ad lib* controls ($p < 0.05$; n = 8 per group). **(C)** Radial plot showing the time of sleep onset for the *ad lib* feed group (circles) and the TRF group (triangles). The numbers show the phases (ZT) with ZT 0 showing the time of light-onset. TRF reduced the variability when the mutant mice initiated sleep.

overall significant effects of time, $F(23) = 36.0.29$, $p < 0.001$, and treatment, $F(1) = 21.321$, $p < 0.001$, without an interaction between the 2 factors ($F = 0.648$, $p = 0.887$). Overall, the TRF regimen improved the daily rhythms in physiological, autonomically driven outputs with the most robust effect on HRV.

62
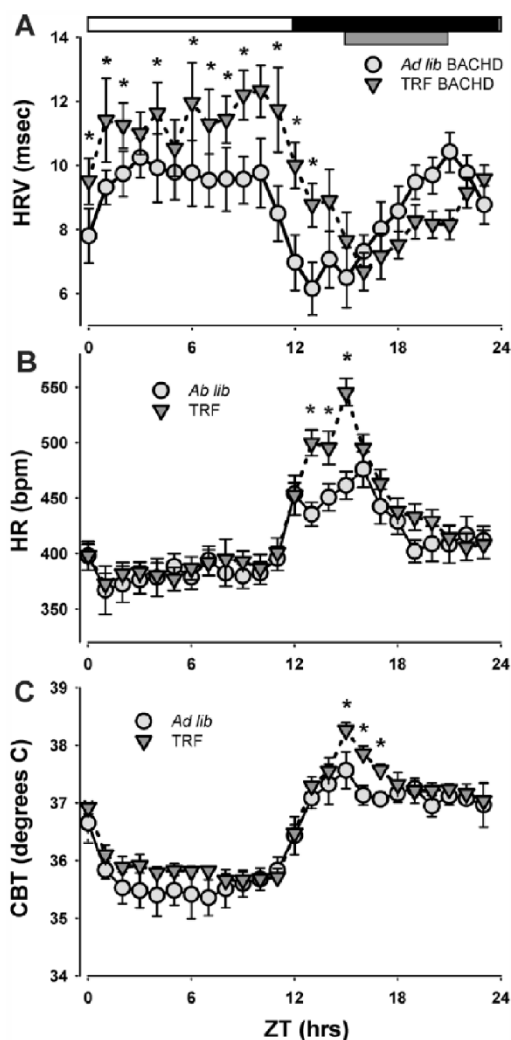
Figure 3. Autonomic output rhythms from BACHD mice were improved by the TRF regimen. (A, B, C) The autonomic outputs from *ad lib* (light grey circles) and TRF (dark grey triangles) BACHD mice were recorded simultaneously using a telemetry device. Hourly running averages of (A) heart rate variability (HRV), (B) heart rate (HR) and (C) core body temperature (CBT) from both groups are plotted. The temporal waveforms of autonomic outputs were analyzed using a 2-way RM ANOVA with time and treatment as factors. Asterisks represent significant differences due to TRF regimen compared to ad lib controls ($p < 0.05$, n = 7 per group).

TRF Shifted the Phase of PER2::LUC Rhythms in the BACHD Mice

Next, we used in vivo imaging of BACHD and WT PER2::LUC mice to examine the impact of the mutation on clock gene expression rhythms in 3 peripheral organs. These rhythms were measured at 6 months of age, and we observed robust daily rhythms in the liver, submandibular gland, and kidneys (Fig. 4A). We found no genotypic differences in the amplitude, phase, or goodness of fit for the rhythms measured in these 3 structures (Table 2). Next, the mice were placed on the TRF for 2 weeks

(Fig. 4B). As analyzed by paired t test, the phase of the peak in the rhythm in the liver ($t = 13.402$, $p = 0.000179$), kidney ($t = 12.996$, $p = 0.000202$), and submandibular gland ($t = 7.292$, $p = 0.00188$) were all phase shifted (Fig. 4E). In contrast, TRF had no measurable impact on the amplitude of the rhythms (liver: $t = 0.263$, $p = 0.805$; kidney: $t = 0.0261$, $p = 0.980$; submandibular gland: $t = 0.234$, $p = 0.827$; Fig. 4F). 2-way ANOVA with genotype and treatment as factors found significant effects of both factors for the liver and kidney (Table 2).

The in vivo imaging does not allow us to measure bioluminescence rhythms from all structures, so we
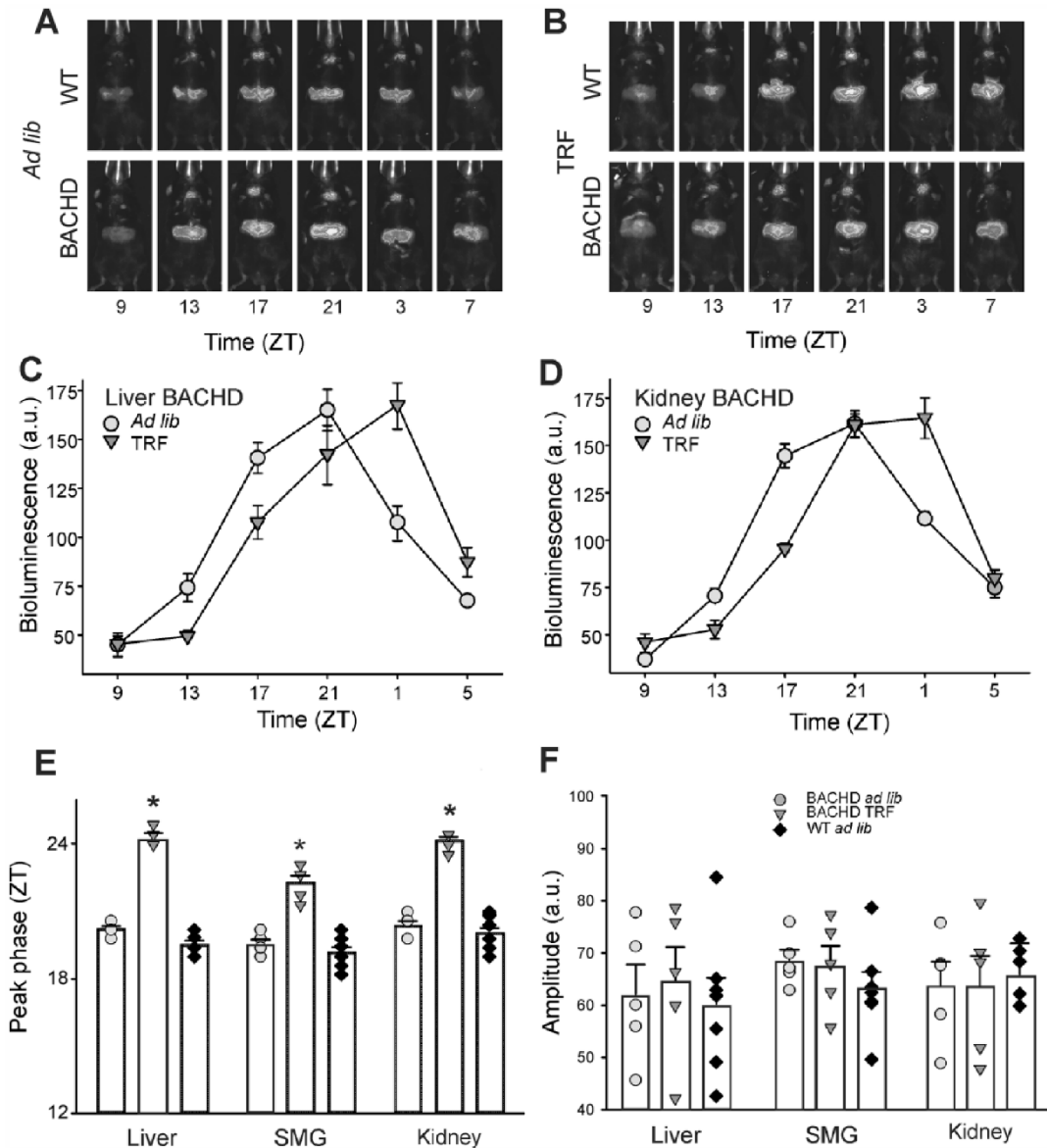
Figure 4. TRF alters the peak phase, but not the amplitude, of the PER2::LUC rhythms measured in peripheral organs *in vivo*. Representative examples of *in vivo* imaging performed to measure bioluminescence from the liver and submandibular gland under (A) *ad lib* and (B) TRF conditions. Average bioluminescent measurements at each time point (mean ± SEM) are shown for the (C) liver and (D) kidney. (E) The peak phase of the rhythm was shifted by the TRF protocol. (F) The amplitude of the rhythms was not altered. Circles are used to indicate data from the *ad lib* controls while triangles represent data from the TRF group. The vertical bar plots show group means and SEM. The symbols show the values from individual animals in each group (BACHD *ad lib*, circles; BACHD TRF, triangles, WT *ad lib*, diamonds). Asterisks represent significant differences due to TRF regimen compared to BACHD *ad lib* controls (paired *t*-tests, $p < 0.05$, n = 5 BACHD and n = 7 BACHD).

turned to in vitro measurements of PER2::LUC in the SCN, liver, and heart. Again, we observed robust daily rhythms from all 3 regions and found no genotypic differences in the amplitude, phase, or goodness of fit for the rhythms measured in these 3 structures (Table 3). The amplitude of the rhythm

measured from the SCN was reduced in the BACHD, but this effect was not significant. We found no significant impact of TRF on the amplitude or phase of the rhythms measured in the SCN. The peak and amplitude of the PER2::LUC rhythm in the heart were altered by TRF. Overall, our data indicated that

Table 2.   TRF alters the peak phase but not the amplitude of the PER2::LUC rhythms measured in peripheral organs in the intact animal.

	BACHD	BACHD + TRF	WT	WT + TRF	Genotype	Treatment
Liver						
Amplitude	62.1 ± 5.7	68.6 ± 5.1	60.2 ± 4.2	63.6 ± 4.2	$F = 0.538; p = 0.472$	$F = 1.098; p = 0.307$
Phase	20.2 ± 0.2	24.4 ± 0.2	19.5 ± 0.2	23.7 ± 0.2	$F = 7.822; p = 0.011$	$F = 289.973; p < 0.001$
Goodness of fit	0.07 ± 0.04	0.03 ± 0.01	0.03 ± 0.01	0.03 ± 0.01		
Kidney						
Amplitude	63.7 ± 4.6	63.5 ± 5.9	65.9 ± 5.9	75.7 ± 4.7	$F = 1.714; p = 0.205$	$F = 0.750; p = 0.397$
Phase	20.4 ± 0.2	24.2 ± 0.2	20.1 ± 0.2	23.2 ± 0.2	$F = 4.957; p = 0.038$	$F = 230.711; p < 0.001$
Goodness of fit	0.02 ± 0.01	0.02 ± 0.01	0.01 ± 0.01	0.01 ± 0.01		
Submandibular gland						
Amplitude	68.4 ± 3.7	67.5 ± 3.7	63.1 ± 3.3	70.6 ± 3.2	$F = 0.102; p = 0.752$	$F = 0.887; p = 0.358$
Phase	19.6 ± 0.2	22.3 ± 0.3	19.2 ± 0.3	21.9 ± 0.3	$F = 1.672; p = 0.211$	$F = 93.507; p < 0.001$
Goodness of fit	0.01 ± 0.01	0.02 ± 0.01	0.02 ± 0.01	0.02 ± 0.01		

In vivo imaging was performed to measure rhythms in bioluminescence from the liver, kidney, and submandibular gland. Comparisons of age-matched wild-type (WT) and BACHD mice under ad lib or time-restricted feeding (TRF) regimen (n = 5-7/group). Data were analyzed with a 2-way analysis of variance using genotype and treatment as factors. The Holm-Sidak test for multiple comparisons was used when appropriate. p values <0.05 were considered significant and are shown in bold.

Table 3.   TRF alters some aspects of the PER2::LUC rhythms measured in culture in a tissue-specific manner.

	BACHD	BACHD + TRF	WT	WT + TRF	Genotype	Treatment
SCN						
Amplitude	41.5 ± 12.9	42.4 ± 2.4	55.3 ± 18.3	35.9 ± 2.2	$F = 0.404; p = 0.533$	$F = 3.037; p = 0.098$
Phase	13.7 ± 0.7	13.9 ± 0.2	13.7 ± 0.7	13.7 ± 0.2	$F = 0.426; p = 0.521$	$F = 0.617; p = 0.441$
Period	24.0 ± 0.5	24.7 ± 0.1	24.1 ± 0.5	24.6 ± 0.1	$F = 0.008; p = 0.926$	$F = 2.462; p = 0.132$
Liver						
Amplitude	18.6 ± 3.6	30.5 ± 12.4	21.2 ± 9.6	15.7 ± 2.7	$F = 0.570; p = 0.458$	$F = 0.213; p = 0.649$
Phase	16.7 ± 0.9	18.5 ± 0.3	18.9 ± 0.3	18.6 ± 0.2	$F = 3.331; p = 0.082$	$F = 1.204; p = 0.285$
Period	23.6 ± 0.5	22.4 ± 0.3	23.8 ± 0.3	22.5 ± 0.3	$F = 0.184; p = 0.674$	$F = 7.425; p = 0.016$
Heart						
Amplitude	15.9 ± 3.7	28.1 ± 3.2	11.9 ± 3.1	24.9 ± 3.6	$F = 1.045; p = 0.320$	$F = 12.605; p = 0.002$
Phase	16.5 ± 0.5	18.7 ± 0.3	16.1 ± 1.0	18.3 ± 0.6	$F = 0.356; p = 0.557$	$F = 9.670; p = 0.005$
Period	23.1 ± 0.3	23.4 ± 0.2	22.8 ± 0.4	24.1 ± 0.2	$F = 0.076; p = 0.785$	$F = 10.359; p = 0.005$

In vitro imaging was performed to measure rhythms in bioluminescence from the suprachiasmatic nucleus (SCN), liver, and heart. Comparisons of age-matched wild-type (WT) and BACHD mice under ad lib or time-restricted feeding (TRF) regimen (n = 5-7/group). Data were analyzed with a 2-way analysis of variance using genotype and treatment as factors. The Holm-Sidak test for multiple comparisons was used when appropriate. p values <0.05 were considered significant and are shown in bold.

the BACHD still had robust PER2:LUC rhythms and TRF modified the phase of these rhythms.

TRF Improved Motor Function in the BACHD Mice

The defining symptoms of HD are centered on motor dysfunction; thus, we hypothesized that TRF would also improve motor performance in the BACHD model. Motor performance in the BACHD was assessed using 2 well-defined tests: the accelerating rotarod and the challenging beam tests (Fig. 5A-C; Table 4). BACHD mice on TRF exhibited a longer latency to fall, $t(14) = 3.557$, $p = 0.003$ (t test) off the rotarod and made significantly fewer errors, $t(14) = 3.139$, $p = 0.007$ (t test), on the challenging beam

compared with ad lib–fed mutants. We also analyzed the number of errors on each beam. A 2-way ANOVA found overall significant effects of beam, $F(3) = 54.499$, $p < 0.001$, and treatment, $F(1) = 32.910$, $p < 0.001$, without an interaction between the 2 factors ($F = 2.191$, $p = 0.099$). Multiple-comparison procedures (Holm-Sidak method) found significant reduction in errors in all but the easiest beam (Fig. 5C). Finally, we found that the power of the rhythms of the individual mice under TRF was negatively correlated with their errors in the challenging beam (Pearson correlation: -0.722, $p = 0.043$) and positively correlated with the latency on the rotarod (Pearson correlation: 0.743, $p = 0.035$). In contrast, untreated mutant mice exhibited no correlation between power and errors (Pearson correlation: -0.040, $p = 0.925$) or
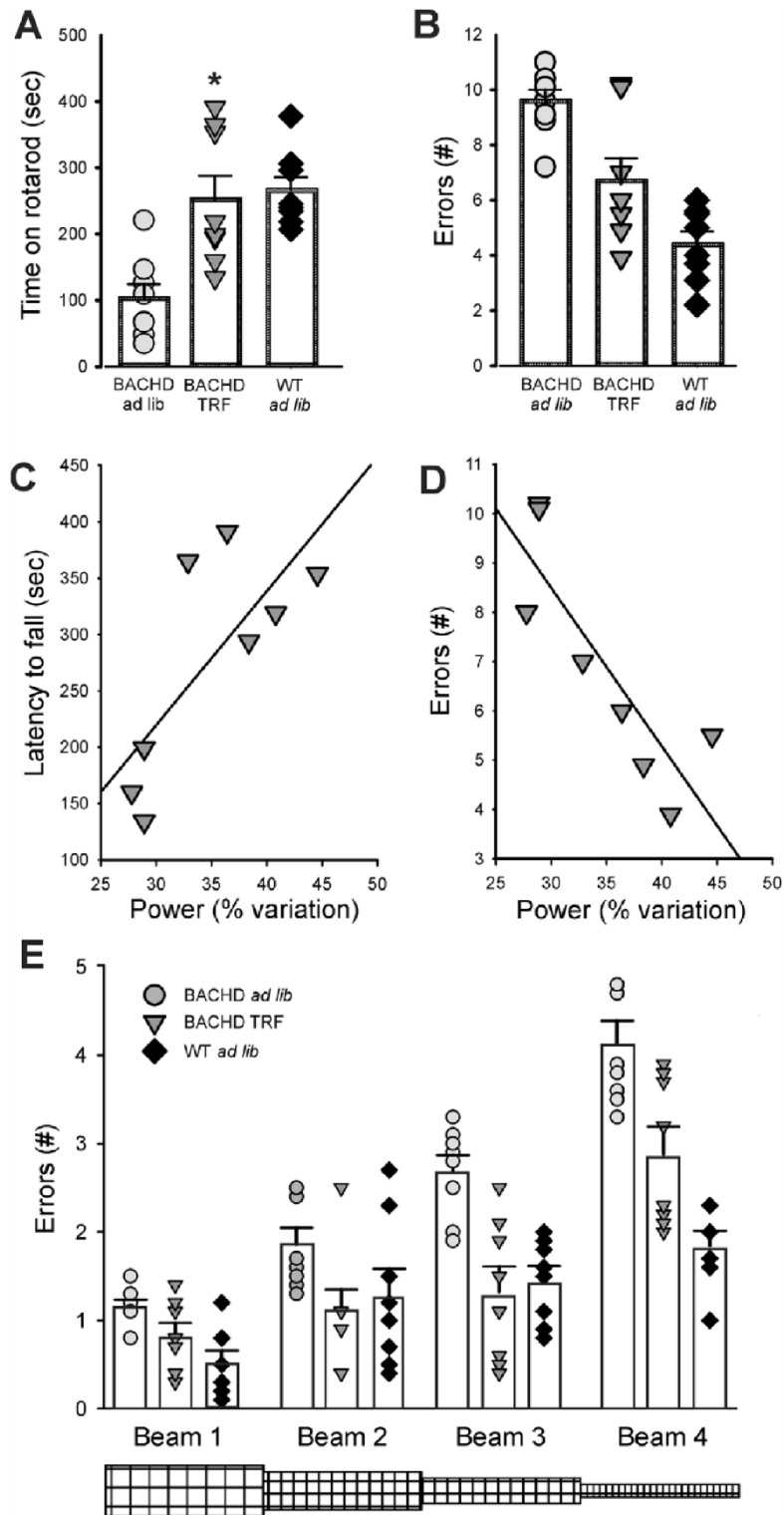
65

Figure 5. TRF improved motor performance in the BACHD model. **(A)** The accelerating rotarod test revealed that the TRF treatment improved motor performance by showing longer latency to fall. Comparisons between the BACHD cohorts were made using a *t*-test. **(B)**

(continued)

66

Figure 5. (continued)

The challenging beam motor test indicated that the TRF treatment improved performance signified by mice making fewer errors when crossing the beam. Asterisks represent significant differences due to TRF regimen compared to *ad lib* controls (paired *t*-tests, $p < 0.05$, n = 8 per group). (C, D) Correlations between the power of the rhythms and motor performance were evaluated using Pearson correlations. Power of the individual mice under TRF was negatively correlated with their errors in the challenging beam (Pearson Correlation: -0.722, p = 0.043) and positively correlated with the latency on the rotarod (Pearson Correlation: 0.743, p = 0.035). (E) Analysis of the performance of the BACHD mice on each beam of the challenging beam indicated that the TRF improved performance on the three more difficult of the four beams. Comparisons between BACHD cohorts were made using a 2-way ANOVA with beam and treatment as factors. Asterisks represent significant differences due to TRF regimen compared to BACHD *ad lib* controls ($p < 0.05$, n = 8 per group).

Table 4.   TRF improved motor performance in the BACHD model.

	BACHD	BACHD + TRF	WT	WT + TRF	Genotype	Treatment
Latency to fall (sec)	102.6 ± 23.3	277.0 ± 37.5	265.8 ± 21.6	280.6 ± 28.7	$F = 13.181; p = 0.001$	$F = 9.660; p = 0.004$
Crossing errors (No.)	9.6 ± 0.4	7.0 ± 0.9	4.4 ± 0.5	3.5 ± 0.4	$F = 56.636; p < 0.001$	$F = 11.355; p = 0.002$

Comparisons of age-matched wild-type (WT) and BACHD mice under ad lib or time-restricted feeding (TRF) regimen ($n = 8$/group). The "latency to fall" was measured from the rotarod test while the errors were measured from the challenging beam. Data were analyzed with a 2-way analysis of variance using genotype and treatment as factors. The Holm-Sidak test for multiple comparisons was used when appropriate. *p* values <0.05 were considered significant and are shown in bold.

latency (Pearson correlation: 0.456, $p = 0.256$). A comparison of the same mutant animals before (3 months) and after (6 months) treatment indicated that there was no decline in performance in latency on rotarod, $t(7) = -0.283$, $p = 0.785$ (paired t test), or in errors in challenge beam, $t(7) = -1.268$, $p = 0.245$ (paired t test). Thus, the BACHD mice exhibited no age-related decline in motor performance while they were on the treatment schedule. Overall, a key finding of this study is that 2 distinct measures of motor performance (challenging beam and rotarod) in the BACHD model were improved by TRF.

DISCUSSION

The present study demonstrates that TRF can ameliorate a range of symptoms relative to HD and related neurodegenerative disorders. Using the BACHD mouse model of HD, we demonstrate that TRF boosts the amplitude and reduces variability in activity rhythms. The temporal patterning of both sleep behavior and sleep fragmentation were improved by the scheduled feeding. Physiologically, TRF increased the HRV during the sleep time and altered the diurnal rhythm in HR but had minimal impact on CBT. On a molecular level, the BACHD still exhibited robust peripheral PER2:LUC rhythms and TRF modified the phase, but not the amplitude, of the rhythms. Finally, a key finding of this study is that 2 distinct measures of motor performance (challenging beam and rotarod) in the BACHD model were improved by TRF. Thus, the scheduled feeding protocol successfully improved several behavioral

and physiological parameters that have been shown to be compromised in HD.

There is a substantial body of literature demonstrating that rats and mice display food anticipatory behavior (FAA) characterized by increased arousal and activity immediately prior to the time of scheduled feeding (Mistlberger, 1994; Stephan, 2002). The FAA does not depend on an intact SCN (Krieger et al., 1977; Phillips and Mikulka, 1979; Angeles-Castellanos et al., 2010), and thus, we reasoned that feeding schedules could be particularly useful when a disease process compromises the functioning of the central clock. In the present study, the BACHD mice were allowed access to their food (standard chow, 6 h) nightly for 3 months starting at an age coinciding with the onset of motor symptoms. We provided the food between ZT 15 and 21 to maximize activity in the beginning of the night. We confirmed that the animals consumed similar amounts of food and the body weights were not significantly decreased by this feeding regimen. We demonstrate that the nightly TRF regimen improved the daily activity rhythm with enhancement in the rhythmic strength as measured by power of the periodogram and a decrement in the cycle-to-cycle variability in activity onset (Fig. 1). The amount of inappropriate activity during the light (rest) phase was also reduced. The power, precision, and percentage of activity during the dark (active) phase were improved approaching WT levels. However, the overall activity levels were not different between the treated and untreated BACHD groups, and both cohorts exhibited significantly lower activity compared with WT (Table 1). Prior work using scheduled feeding protocols also improved locomotor activity rhythms in the Q175

(Wang et al., 2018) and R6/2 (Skillings et al., 2014) mouse models of HD. These improvements in the locomotor activity rhythms under TRF could be driven by the nightly acute effects of FAA with its still unknown anatomical loci or through an enhancement of SCN-driven outputs.

The benefits of the TRF protocol were not limited to this transient arousal prior to feeding in the dark phase. In this work, we used a video analysis of sleep behavior that allows us to measure the temporal patterning of sleep as well as sleep fragmentation but does not allow identification of sleep stages. Both the amount of sleep during the light phase and the precision of sleep onset were improved while the fragmentation of light phase sleep was reduced by TRF (Fig. 2; Table 1). To our knowledge, this is the first demonstration that TRF can improve sleep parameters in mice, although earlier work has shown that feeding mice during their normal rest phase can disrupt sleep patterns (Szentirmai et al., 2010). There has been a report in *Drosophila* that TRF can improve sleep behavior (Gill et al., 2015). Variability in sleep onset has been associated with decreased academic performance and reduced white matter in humans (Telzer et al., 2015; Fuligni et al., 2018); thus, improvements in precision of sleep onset are an important target for therapeutic interventions. These improvements to sleep behavior occurred during the light phase (ZT 0-12) several hours after the feeding time (ZT 15-21) and could not be due to acute increase in arousal due to FAA mechanisms alone. Prior work with the R6/2 (Kantor et al., 2013; Fisher et al., 2013) and Q175 (Fisher et al., 2016) mouse HD models has provided evidence of dysfunction in EEG-defined sleep, including increases in sleep fragmentation as well as characteristic changes in the EEG spectral profiles. The total amount of non–rapid eye movement (NREM) and rapid eye movement (REM) sleep over 24 h as well as homeostatic responses to sleep loss were not affected by the mutation (Fisher et al., 2016). In the R6/2 model, these HD-evoked changes in the EEG responded to treatment with either a serotonin uptake inhibitor (paroxetine; Kantor et al., 2017) or a hypnotic (zolpidem; Kantor et al., 2016). The circuits responsible for REM and NREM sleep are centered in the basal forebrain, lateral hypothalamus, and brainstem (Weber and Dan, 2016; Saper and Fuller, 2017; Scammell et al., 2017). Pathology in these regions could contribute to the sleep fragmentation seen in HD. In addition, given the well-established dysfunction in the basal ganglia circuits in HD patients and animal models, deficits in these circuits could be the site of action for some of the sleep deficits. There is a variety of evidence indicating that dopamine signaling within the striatum and the external globus pallidus (GPe) plays an important role in suppressing movements during sleep, and dysfunction in these pathways has been implicated in restless leg syndrome (e.g., Jones and Cavanna, 2013; Guo et al., 2017) and REM sleep disorder (e.g., Arnulf, 2012; Rolinski et al., 2016). Neurons in the GPe exhibit alterations in GABA-mediated synaptic transmission in the R6/1 HD mouse model (Du et al., 2016), and deep-brain stimulation of this same region promotes sleep (Qiu et al., 2016a, 2016b). Dopamine is a rhythmically regulated neurotransmitter (e.g., Mendoza and Challet, 2014), and the impact of feeding schedules on activity appears to be mediated by D1 receptors in the striatum (Gallardo et al., 2014). Therefore, we speculate that TRF modulation of dopamine levels could underlie the improvements that we observed in sleep behavior in the present study. Given the body of prior work that suggests a critical role for sleep in motor learning (e.g., Walker et al., 2002; Backhaus et al., 2015), the improvements in sleep that we observed could drive improvements in motor performance.

The data in this study indicate that TRF can affect autonomically driven parameters, with the most striking impact on HRV (Fig. 3). HRV measures the variation in the beat-to-beat (R-R) interval and reflects the dynamic balance of sympathetic and parasympathetic control of heart function. Reduced HRV is generally considered an indication of poor cardiovascular health and a predictor for cardiovascular disease and mortality (e.g., Kemp et al., 2017). Prior work demonstrated that the BACHD mice exhibit a loss of circadian control in HRV day/night differences as well as an overall decrease in HRV over a 24-h period when compared with WT controls (Schroeder et al., 2016). We have now shown that TRF increases HRV in both the Q175 (Wang et al., 2018) and the BACHD models (present study). Importantly, reduced HRV has also been reported in HD patients beginning during the presymptomatic stage of disease progression (Andrich et al., 2002; Aziz et al., 2010; Bellosta Diago et al., 2017), and cardiovascular events are a major cause of early death in the HD population (Lanska et al., 1988; Sørensen and Fenger 1992). In *Drosophila*, TRF reduces age-related decline in cardiovascular function through a mechanism that is dependent on circadian clock genes (Melkani and Panda, 2017). Together, this work suggests that TRF can reduce cardiovascular dysfunction, and at least in *Drosophila*, feeding schedules can boost the amplitude and perhaps the phasing of the molecular clockwork.

The BACHD mouse model shows alterations in the temporal patterning of neural activity recorded in the SCN (Kudo et al., 2011; Kuljis et al., 2016). The weakening of the electrical output of the SCN would be expected to affect the phase of peripheral molecular clocks that are driven by the SCN. For example, in

aging mice, there are parallel reductions in SCN neural activity (Nakamura et al., 2011; Farajnia et al., 2012) and shifts in the phase of at least some extra-SCN molecular clockwork (Nakamura et al., 2011; Sellix et al., 2012; Nakamura et al., 2015; Tahara et al., 2017). In the R6/2 model of HD, circadian rhythms of PER2 bioluminescence were normal in the SCN but phase advanced in the liver (Maywood et al., 2010). Prior work examining PER2 rhythms in the liver found that TRF (8/16 feed/fast cycle) increased the amplitude (Hatori et al., 2012) but not the phase (Hirao et al., 2010) of the gene expression rhythms in WT mice. Based on these data, we anticipated that we would see phase shifts in the peripheral oscillations as measured by PER2::LUC, whereas the SCN rhythm in clock gene expression would not show genotypic differences (Kudo et al., 2011). Unexpectedly, we did not see any evidence for genotypic differences between the clock gene expression in WT and BACHD mice (Fig. 4; Table 3). The TRF protocol shifted the phase of the rhythm in the heart but not in the SCN. This shift in phase fits with a variety of prior work showing that feeding schedules can shift the phase of clock gene expression rhythms throughout the body, including in limbic structures involved in motivation and reward (Angeles-Castellanos et al., 2007; Waddington Lamont et al., 2007) as well as in the striatum (Akiyama et al., 2004). The amplitude of the rhythms in PER2 expression in the heart, but not the liver, was increased by treatment. One of the limitations of these experiments is that we relied exclusively on the PER2::LUC reporter and perhaps other clock genes could have shown the anticipated increase in amplitude driven by TRF.

HD is defined as a movement disorder, as the most striking and debilitating symptoms of this disease include motor deficits and loss of neurons in the striatum. Critically, the TRF regimen dramatically improved performance of the HD mutant mice on 2 different motor tests (Fig. 5). The beneficial impact of TRF on motor performance could be dependent on or independent from the improvements in circadian output. We examined this issue by taking advantage of the animal-to-animal variation in the impact of the treatment on circadian and motor function. Using our most sensitive motor assay (i.e., challenging beam test), we found that the improved circadian behavior was negatively correlated with number of errors in the TRF group (coefficient = −0.722, p = 0.043). This finding leads us to suggest that improved circadian timing underlies the improved motor function in the treated mice. Prior work has shown that scheduled feeding can improve motor function in the Q175 (Wang et al., 2018) and exploratory behavior in the open field (Skillings et al., 2014) in the R6/2 HD models. Furthermore, mice challenged with a

high-fat diet or other nutritional perturbations perform significantly better on the rotarod under TRF (Hatori et al., 2012; Chaix et al., 2014). Varieties of different approaches aiming to boost circadian output improve motor functions in different HD mouse models. There is evidence that improving the sleep-wake cycle with sleep-inducing drugs (Pallier et al., 2007; Kantor et al., 2016), stimulants (Cuesta et al., 2012; Whittaker et al., 2017), bright light and restricted wheel access (Cuesta et al., 2014), enhanced blue light (Wang et al., 2017), and scheduled feeding (Wang et al., 2018) can improve HD symptoms. This body of work supports the general hypothesis (Morton, 2013; Schroeder and Colwell, 2013; van Wamelen et al., 2015; Longo and Panda 2016) that circadian-based therapies can alter the trajectory of a genetically determined disease.

CONFLICT OF INTEREST STATEMENT

The authors declared no potential conflicts of interest with respect to the research, authorship, and/or publication of this article.

NOTE

Supplemental material is available for this article online.

ORCID ID

D. S. Whittaker [iD] https://orcid.org/0000-0002-4293-5192

C. A. Ghiani [iD] https://orcid.org/0000-0002-9867-6185

C. S. Colwell [iD] https://orcid.org/0000-0002-1059-184X

REFERENCES

Acosta-Galvan G, Yi CX, van der Vliet J, Jhamandas JH, Panula P, Angeles-Castellanos M, Del Carmen Basualdo M, Escobar C, and Buijs RM (2011) Interaction between hypothalamic dorsomedial nucleus and the suprachiasmatic nucleus determines intensity of food anticipatory behavior. Proc Natl Acad Sci U S A 108(14): 5813-5818.

Akiyama M, Yuasa T, Hayasaka N, Horikawa K, Sakurai T, and Shibata S (2004) Reduced food anticipatory activity in genetically orexin (hypocretin) neuron-ablated mice. Eur J Neurosci 20(11):3054-3062.

Andrich J, Schmitz T, Saft C, Postert T, Kraus P, Epplen JT, Przuntek H, and Agelink MW (2002) Autonomic

nervous system function in Huntington's disease. J Neurol Neurosurg Psychiatry 72(6):726-731.

Angeles-Castellanos M, Mendoza J, and Escobar C (2007) Restricted feeding schedules phase shift daily rhythms of c-Fos and protein Per1 immunoreactivity in corticolimbic regions in rats. Neuroscience 144(1):344-355.

Angeles-Castellanos M, Salgado-Delgado R, Rodriguez K, Buijs RM, and Escobar C (2010) The suprachiasmatic nucleus participates in food entrainment: a lesion study. Neuroscience 165(4):1115-1126.

Arnulf I (2012) REM sleep behavior disorder: motor manifestations and pathophysiology. Mov Disord 27(6): 677-689.

Aziz NA, Anguelova GV, Marinus J, van Dijk JG, and Roos RAC (2010) Autonomic symptoms in patients and pre-manifest mutation carriers of Huntington's disease. Eur J Neurol 17:1068-1074.

Backhaus W, Kempe S, and Hummel FC (2015) The effect of sleep on motor learning in the aging and stroke population—a systematic review. Restor Neurol Neurosci 34(1):153-156.

Bass J and Takahashi JS (2010) Circadian integration of metabolism and energetics. Science 330(6009): 1349-1354.

Bellosta Diago E, Pérez Pérez J, Santos Lasaosa S, Viloria Alebesque A, Martínez Horta S, Kulisevsky J, and López Del Val J (2017) Circadian rhythm and autonomic dysfunction in presymptomatic and early Huntington's disease. Parkinsonism Relat Disord 44:95-100.

Chaix A, Zarrinpar A, Miu P, and Panda S (2014) Time-restricted feeding is a preventative and therapeutic intervention against diverse nutritional challenges. Cell Metab 20:991-1005.

Ciammola A, Sassone J, Alberti L, Meola G, Mancinelli E, Russo MA, Squitieri F, and Silani V (2006) Increased apoptosis, Huntingtin inclusions and altered differentiation in muscle cell cultures from Huntington's disease subjects. Cell Death Differ 13(12):2068-2078.

Colwell CS (2011) Linking neural activity and molecular oscillations in the SCN. Nat Rev Neurosci 12:553-569.

Colwell CS (2015) Circadian Medicine. Hoboken (NJ): Wiley.

Cuesta M, Aungier J, and Morton AJ (2012) The methamphetamine-sensitive circadian oscillator is dysfunctional in a transgenic mouse model of Huntington's disease. Neurobiol Dis 45(1):145-155.

Cuesta M, Aungier J, and Morton AJ (2014) Behavioral therapy reverses circadian deficits in a transgenic mouse model of Huntington's disease. Neurobiol Dis 63:85-91.

Cutler TS, Park S, Loh DH, Jordan MC, Yokota T, Roos KP, Ghiani CA, and Colwell CS (2017) Neurocardiovascular deficits in the Q175 mouse model of Huntington's disease. Physiol Rep 5(11):e13289.

Cuturic M, Abramson RK, Vallini D, Frank EM, and Shamsnia M (2009) Sleep patterns in patients with

Huntington's disease and their unaffected first-degree relatives: a brief report. Behav Sleep Med 7(4): 245-254.

Du Z, Chazalon M, Bestaven E, Leste-Lasserre T, Baufreton J, Cazalets JR, Cho YH, and Garret M (2016) Early GABAergic transmission defects in the external globus pallidus and rest/activity rhythm alteration in a mouse model of Huntington's disease. Neuroscience 329: 363-379.

Farajnia S, Michel S, Deboer T, vanderLeest HT, Houben T, Rohling JH, Ramkisoensing A, Yasenkov R, and Meijer JH (2012) Evidence for neuronal desynchrony in the aged suprachiasmatic nucleus clock. J Neurosci 32(17):5891-5899.

Fisher SP, Black SW, Schwartz MD, Wilk AJ, Chen TM, Lincoln WU, Liu HW, Kilduff TS, and Morairty SR (2013) Longitudinal analysis of the electroencephalogram and sleep phenotype in the R6/2 mouse model of Huntington's disease. Brain 136(pt 7):2159-2172.

Fisher SP, Godinho SIH, Pothecary CA, Hankins MW, Foster RG, and Peirson SN (2012) Rapid assessment of sleep/wake behaviour in mice. J Biol Rhythms 27: 48-58.

Fisher SP, Schwartz MD, Wurts-Black S, Thomas AM, Chen TM, Miller MA, Palmerston JB, Kilduff TS, and Morairty SR (2016) Quantitative electroencephalographic analysis provides an early-stage indicator of disease onset and progression in the zQ175 knock-in mouse model of Huntington's disease. Sleep 39(2):379-391.

Fleming SM, Ekhator OR, Ghisays V (2013) Assessment of sensorimotor function in mouse models of Parkinson's disease. J Vis Exp JoVE:50303.

Fuligni AJ, Arruda EH, Krull JL, and Gonzales NA (2018) Adolescent sleep duration, variability, and peak levels of achievement and mental health. Child Dev 89(2): e18-e28.

Gallardo CM, Darvas M, Oviatt M, Chang CH, Michalik M, Huddy TF, Meyer EE, Shuster SA, Aguayo A, Hill EM, et al. (2014) Dopamine receptor 1 neurons in the dorsal striatum regulate food anticipatory circadian activity rhythms in mice. eLife 3:e03781.

Gill S, Le HD, Melkani GC, and Panda S (2015) Time-restricted feeding attenuates age-related cardiac decline in Drosophila. Science 347(6227):1265-1269.

Goldberg MS, Fleming SM, Palacino JJ, Cepeda C, Lam HA, Bhatnagar A, Meloni EG, Wu N, Ackerson LC, Klapstein GJ, et al. (2003) Parkin-deficient mice exhibit nigrostriatal deficits but not loss of dopaminergic neurons. J Biol Chem 278:43628-43635.

Goodman AO, Rogers L, Pilsworth S, McAllister CJ, Shneerson JM, Morton AJ, and Barker RA (2011) Asymptomatic sleep abnormalities are a common early feature in patients with Huntington's disease. Curr Neurol Neurosci Rep 11(2):211-217.

Gray M, Shirasaki DI, Cepeda C, Andre VM, Wilburn B, Lu XH, Tao J, Yamazaki I, Li SH, Sun YE, et al. (2008)

Full-length human mutant huntingtin with a stable polyglutamine repeat can elicit progressive and selective neuropathogenesis in BACHD mice. J Neurosci 28:6182-6195.

Guo CN, Yang WJ, Zhan SQ, Yang XF, Chen MC, Fuller PM, and Lu J (2017) Targeted disruption of supraspinal motor circuitry reveals a distributed network underlying restless legs syndrome (RLS)-like movements in the rat. Sci Rep 7(1):9905.

Gusella JF, MacDonald ME, and Lee JM (2014) Genetic modifiers of Huntington's disease. Mov Disord 29: 1359-1365.

Hatori M, Vollmers C, Zarrinpar A, DiTacchio L, Bushong EA, Gill S, Leblanc M, Chaix A, Joens M, Fitzpatrick JA, et al. (2012) Time-restricted feeding without reducing caloric intake prevents metabolic diseases in mice fed a high-fat diet. Cell Metab 15(6):848-860.

Hirao A, Nagahama H, Tsuboi T, Hirao M, Tahara Y, and Shibata S (2010) Combination of starvation interval and food volume determines the phase of liver circadian rhythm in Per2::Luc knock-in mice under two meals per day feeding. Am J Physiol Gastrointest Liver Physiol 299(5):G1045-G1053.

Jones R and Cavanna AE (2013) The neurobiology and treatment of restless legs syndrome. Behav Neurol 26(4):283-292.

Kalliolia E, Silajdžić E, Nambron R, Hill NR, Doshi A, Frost C, Watt H, Hindmarsh P, Björkqvist M, and Warner TT (2014) Plasma melatonin is reduced in Huntington's disease. Mov Disord 29(12):1511-1515.

Kantor S, Szabo L, Varga J, Cuesta M, and Morton AJ (2013) Progressive sleep and electroencephalogram changes in mice carrying the Huntington's disease mutation. Brain 136(pt 7):2147-2158.

Kantor S, Varga J, Kulkarni S, and Morton AJ (2017) Chronic paroxetine treatment prevents the emergence of abnormal electroencephalogram oscillations in Huntington's disease mice. Neurotherapeutics 14(4): 1120-1133.

Kantor S, Varga J, and Morton AJ (2016) A single dose of hypnotic corrects sleep and EEG abnormalities in symptomatic Huntington's disease mice. Neuropharmacology 105:298-307.

Kemp AH, Koenig J, and Thayer JF (2017) From psychological moments to mortality: a multidisciplinary synthesis on heart rate variability spanning the continuum of time. Neurosci Biobehav Rev 2017;83:547-567.

Krieger DT, Hauser H, and Krey LC (1977) Suprachiasmatic nuclear lesions do not abolish food-shifted circadian adrenal and temperature rhythmicity. Science 197: 398-399.

Kudo T, Schroeder A, Loh DH, Kuljis D, Jordan MC, Roos KP, and Colwell CS (2011) Dysfunctions in circadian behavior and physiology in mouse models of Huntington's disease. Exp Neurol 228:80-90.

Kuljis DA, Gad L, Loh DH, MacDowell Kaswan Z, Hitchcock ON, Ghiani CA, and Colwell CS (2016) Sex differences in circadian dysfunction in the BACHD mouse model of Huntington's disease. PLoS One 11:e0147583.

Kuljis D, Schroeder AM, Kudo T, Loh DH, Willison DL, and Colwell CS (2012) Sleep and circadian dysfunction in neurodegenerative disorders: insights from a mouse model of Huntington's disease. Minerva Pneumol 51:93-106.

Langbehn DR, Hayden M, Paulsen JS, and the PREDICT-HD Investigators of the Huntington Study Group (2010) CAG-repeat length and the age of onset in Huntington disease (HD): a review and validation study of statistical approaches. Am J Med Genet B Neuropsychiatr Genet 153B:397-408.

Lanska DJ, Lanska MJ, Lavine L, and Schoenberg BS (1988) Conditions associated with Huntington's disease at death: a case-control study. Arch Neurol 45(8):878-880.

Loh DH, Dragich JM, Kudo T, Schroeder AM, Nakamura TJ, Waschek JA, Block GD, and Colwell CS (2011) Effects of vasoactive intestinal peptide genotype on circadian gene expression in the suprachiasmatic nucleus and peripheral organs. J Biol Rhythms 26:200-209.

Loh DH, Kudo T, Truong D, Wu Y, and Colwell CS (2013) The BACHD mouse model of Huntington's disease shows gene dosage- and age-related decline in circadian rhythms of activity and sleep. PLoS One 8(7):e69993.

Longo VD and Panda S (2016) Fasting, circadian rhythms, and time-restricted feeding in healthy lifespan. Cell Metab 23(6):1048-1059.

Margolis RL and Ross CA (2003) Diagnosis of Huntington disease. Clin Chem 49:1726-1732.

Maywood ES, Fraenkel E, McAllister CJ, Wood N, Reddy AB, Hastings MH, and Morton AJ (2010). Disruption of peripheral circadian timekeeping in a mouse model of Huntington's disease and its restoration by temporally scheduled feeding. J Neurosci 30:10199-10204.

Melkani GC and Panda S (2017) Time-restricted feeding for prevention and treatment of cardiometabolic disorders. J Physiol 595(12):3691-3700.

Mendoza J and Challet E (2014) Circadian insights into dopamine mechanisms. Neuroscience 282:230-242.

Mistlberger RE (1994) Circadian food anticipatory activity: formal models and physiological mechanisms. Neurosci Biobehav Rev 18:171-195.

Morton AJ (2013) Circadian and sleep disorder in Huntington's disease. Exp Neurol 243:34-44.

Morton AJ, Wood NI, Hastings MH, Hurelbrink C, Barker RA, and Maywood ES (2005) Disintegration of the sleep-wake cycle and circadian timing in Huntington's disease. J Neurosci 25(1):157-163.

Nakamura TJ, Nakamura W, Tokuda IT, Ishikawa T, Kudo T, Colwell CS, and Block GD (2015) Age-related

changes in the circadian system unmasked by constant conditions. eNeuro 2(4):ENEURO.0064-15.2015.

Nakamura TJ, Nakamura W, Yamazaki S, Kudo T, Cutler T, Colwell CS, and Block GD (2011) Age-related decline in circadian output. J Neurosci 31(28):10201-10205.

Pack AI, Galante RJ, Maislin G, Cater J, Metaxas D, Lu S, Zhang L, Von Smith R, Kay T, Lian J, et al. (2007) Novel method for high-throughput phenotyping of sleep in mice. Physiol Genomics 28(2):232-238.

Pallier PN, Maywood ES, Zheng Z, Chesham JE, Inyushkin AN, Dyball R, Hastings MH, and Morton AJ (2007) Pharmacological imposition of sleep slows cognitive decline and reverses dysregulation of circadian gene expression in a transgenic mouse model of Huntington's disease. J Neurosci 27:7869-7878.

Phillips JL and Mikulka PJ (1979) The effects of restricted food access upon locomotor activity in rats with suprachiasmatic nucleus lesions. Physiol Behav 23: 257-262.

Qiu MH, Chen MC, Wu J, Nelson D, and Lu J (2016a) Deep brain stimulation in the globus pallidus externa promotes sleep. Neuroscience 322:115-120.

Qiu MH, Yao QL, Vetrivelan R, Chen MC, and Lu J (2016b) Nigrostriatal dopamine acting on globus pallidus regulates sleep. Cereb Cortex 26(4):1430-1439.

Rolinski M, Griffanti L, Piccini P, Roussakis AA, Szewczyk-Krolikowski K, Menke RA, Quinnell T, Zaiwalla Z, Klein JC, Mackay CE, et al. (2016) Basal ganglia dysfunction in idiopathic REM sleep behaviour disorder parallels that in early Parkinson's disease. Brain 139(pt 8):2224-2234.

Saft C, Zange J, Andrich J, Müller K, Lindenberg K, Landwehrmeyer B, Vorgerd M, Kraus PH, Przuntek H, and Schöls L (2005) Mitochondrial impairment in patients and asymptomatic mutation carriers of Huntington's disease. Mov Disord 20(6):674-679.

Saper CB and Fuller PM (2017) Wake-sleep circuitry: an overview. Curr Opin Neurobiol 44:186-192.

Scammell TE, Arrigoni E, and Lipton JO (2017) Neural circuitry of wakefulness and sleep. Neuron 93:747-765.

Schroeder AM and Colwell CS (2013) How to fix a broken clock. Trends Pharmacol Sci 34(11):605-619.

Schroeder AM, Loh DH, Jordan MC, Roos KP, and Colwell CS (2011) Baroreceptor reflex dysfunction in the BACHD mouse model of Huntington's disease. PLoS Currents 3:RRN1266.

Schroeder AM, Wang HB, Park S, Jordan MC, Gao F, Coppola G, Fishbein MC, Roos KP, Ghiani CA, and Colwell CS (2016) Cardiac dysfunction in the BACHD mouse model of Huntington's disease. PLoS One 11:e0147269.

Sellix MT, Evans JA, Leise TL, Castanon-Cervantes O, Hill DD, DeLisser P, Block GD, Menaker M, and Davidson AJ (2012) Aging differentially affects the re-entrainment response of central and peripheral circadian oscillators. J Neurosci 32(46):16193-16202.

Skillings EA, Wood NI, and Morton AJ (2014) Beneficial effects of environmental enrichment and food entrainment in the R6/2 mouse model of Huntington's disease. Brain Behav 4(5):675-686.

Sørensen SA and Fenger K (1992) Causes of death in patients with Huntington's disease and in unaffected first degree relatives. J Med Genet 12:911-914.

Stephan FK (2002) The "other" circadian system: food as a zeitgeber. J Biol Rhythms 17:284-292.

Szentirmai E, Kapás L, Sun Y, Smith RG, and Krueger JM (2010) Restricted feeding-induced sleep, activity, and body temperature changes in normal and preproghrelin-deficient mice. Am J Physiol Regul Integr Comp Physiol 298(2):R467-R477.

Tahara Y, Kuroda H, Saito K, Nakajima Y, Kubo Y, Ohnishi N, Seo Y, Otsuka M, Fuse Y, Ohura Y, et al. (2012) In vivo monitoring of peripheral circadian clocks in the mouse. Curr Biol 22(11):1029-1034.

Tahara Y and Shibata S (2013) Chronobiology and nutrition. Neuroscience 253:78-88.

Tahara Y, Takatsu Y, Shiraishi T, Kikuchi Y, Yamazaki M, Motohashi H, Muto A, Sasaki H, Haraguchi A, Kuriki D, et al. (2017) Age-related circadian disorganization caused by sympathetic dysfunction in peripheral clock regulation. NPJ Aging Mech Dis 3:16030.

Telzer EH, Goldenberg D, Fuligni AJ, Lieberman MD, and Gálvan A (2015) Sleep variability in adolescence is associated with altered brain development. Dev Cogn Neurosci 14:16-22.

van Wamelen DJ, Aziz NA, Roos RA, and Swaab DF (2014) Hypothalamic alterations in Huntington's disease patients: comparison with genetic rodent models. J Neuroendocrinol 26(11):761-775.

van Wamelen DJ, Roos RA, and Aziz NA (2015) Therapeutic strategies for circadian rhythm and sleep disturbances in Huntington disease. Neurodegener Dis Manag 5(6):549-559.

Waddington Lamont E, Harbour VL, Barry-Shaw J, Renteria Diaz L, Robinson B, Stewart J, and Amir S (2007) Restricted access to food, but not sucrose, saccharine, or salt, synchronizes the expression of Period2 protein in the limbic forebrain. Neuroscience 144(2): 402-411.

Walker MP, Brakefield T, Morgan A, Hobson JA, and Stickgold R (2002) Practice with sleep makes perfect: sleep-dependent motor skill learning. Neuron 35(1): 205-211.

Wang HB, Loh DH, Whittaker DS, Cutler T, Howland D, and Colwell CS (2018) Time-restricted feeding improves circadian dysfunction as well as motor symptoms in the Q175 mouse model of Huntington's disease. eNeuro 5(1).ENEURO.0431-17.2017.

Wang HB, Whittaker DS, Truong D, Mulji AK, Ghiani CA, Loh DH, and Colwell CS (2017) Blue light therapy improves circadian dysfunction as well as motor

symptoms in two mouse models of Huntington's disease. Neurobiol Sleep Circad Rhythms 2:39-52.

Wang N, Gray M, Lu X-H, Cantle JP, Holley SM, Greiner E, Gu X, Shirasaki D, Cepeda C, Li Y, et al. (2014) Neuronal targets for reducing mutant huntingtin expression to ameliorate disease in a mouse model of Huntington's disease. Nat Med 20:536-541.

Weber F and Dan Y (2016) Circuit-based interrogation of sleep control. Nature 538(7623):51-59.

Wexler NS, Lorimer J, Porter J, Gomez F, Moskowitz C, Shackell E, Marder K, Penchaszadeh G, Roberts SA, Gayan J, et al. (2004) Venezuelan kindreds reveal that genetic and environmental factors modulate Huntington's disease age of onset. Proc Natl Acad Sci U S A 101:3498-3503.

Whittaker DS, Wang HB, Loh DH, Cachope R, and Colwell CS (2017) Possible use of a H3R antagonist for the management of nonmotor symptoms in the Q175 mouse model of Huntington's disease. Pharmacol Res Perspect 5(5).
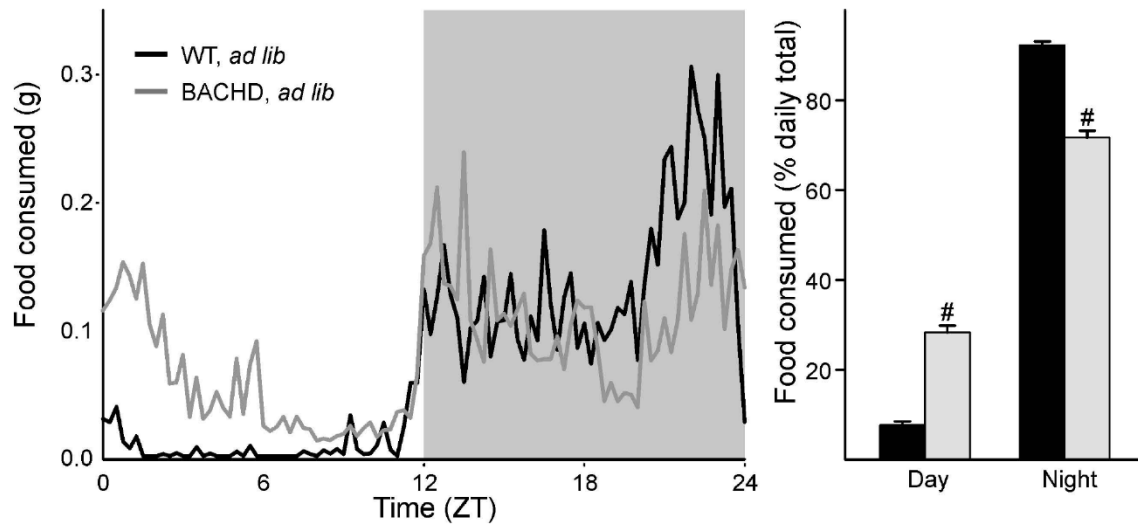
Supplemental Fig. 1: The temporal pattern of eating is altered in BACHD compared to WT controls (n = 5 per group). (Left) BACHD mice (grey) at 3 months of age show altered rhythms of food consumption compared to WT controls (black). (Right) The BACHD mice take significantly more food in the light (rest) phase than the WT controls.

Chapter 5: A ketogenic diet improves circadian dysfunction as well as motor symptoms in the

BACHD mouse model of Huntington's disease

Chapter 5: A ketogenic diet improves circadian dysfunction as well as motor symptoms in the BACHD mouse model of Huntington's disease

Introduction

Huntington's disease is a progressive neurodegenerative disease that imposes motor dysfunction accompanied by cognitive, psychiatric, and cardiovascular disturbance (Kuljis et al., 2012; Margolis and Ross, 2003). HD is caused by a CAG trinucleotide repeat expansion within exon 1 of the Huntingtin *(HTT)* gene in excess of 35 CAG repeats. The CAG repeats are translated into abnormally long glutamine segments in the mutant Huntingtin protein (mHTT), leading to protein misfolding, soluble aggregates, and inclusion bodies detected throughout the body (Ciammola et al., 2006; Saft et al., 2005). The Huntingtin (HTT) protein is expressed throughout the body, with higher levels found in the brain than in the periphery. Further, brain regions with increased neuronal density are found to have higher HTT, with HTT expression being elevated in neurons versus glial cells (Li et al., 1993; Strong et al., 1993). Correspondingly, the mHTT protein is also more abundant in neurons than in glial cells with a similar distribution of aggregates (Bradford et al., 2010). While the loss of neurons in the striatum has been well characterized and is considered the hallmark of HD pathology, both gray and white matter loss have been well reported at different stages of HD progression (Bartzokis et al., 2007; Bourbon-Teles et al., 2019; Di Paola et al., 2012; Phillips et al., 2016), suggesting that the effects of myelin loss might be a significant factor in the disease course.

The mHTT protein triggers dysfunction or loss in a wide range of cellular processes (Wright et al., 2017). Generally, the longer the CAG repeat, the greater the severity of the symptoms and the earlier the age of onset (Langbehn et al., 2010), with an average age of onset of motor symptoms and subsequent diagnosis around 40. Typically, mortality occurs 10 to 20 years after the onset of initial motor symptoms, however, even among patients with the

same CAG repeat length, there is a significant range in the age of onset and severity of symptoms (Gusella et al., 2014; Wexler et al., 2004). Further, cognitive, affective, and other symptoms may arise up to two decades before the onset of motor symptoms (Paulsen, 2011; Paulsen et al., 2008). This variability supports the possibility that environmental modifiers can influence the disease, which suggests that appropriate and early disease management strategies can increase the health span and improve the quality of life of these patients. Therefore, it is vital to pursue this possibility as there are currently no treatments to prevent or delay the course of the disease.

Sleep disorders are prevalent among HD patients and disruptions in sleep have detrimental effects on activities of daily living and the quality of life of patients and their caregivers (Morton et al., 2005; Cuturic et al., 2009; Aziz et al., 2010; Goodman et al., 2011). Mouse models of HD recapitulate the progressive and rapid breakdown of the circadian rest/activity cycle observed in human patients, which is typified by loss of consolidated sleep, increased wakeful activity during the rest (light) phase, and more sleep during the active (dark) phase (Morton et al., 2005; Kudo et al., 2011; Loh et al., 2013; Kuljis et al., 2016).

Vigorous circadian rhythms are important to health and wellbeing, and disrupted circadian timing can lead to undesirable consequences throughout the body (Colwell, 2015), altering the function of key organ systems including the heart, pancreas, liver, lungs, as well as the brain. There is evidence that improving the sleep/wake cycle with sleep-inducing drugs (Kantor et al., 2016; Pallier et al., 2007), stimulants (Cuesta et al., 2012; Whittaker et al., 2017), blue light therapy (Wang et al., 2017), bright light, and restricted wheel access (Cuesta et al., 2014) can ameliorate HD symptoms. Collectively, this body of research supports the hypotheses that circadian dysfunction interacts with HD pathology leading to the exacerbation

of HD-related symptoms and that circadian-based therapies can alter the trajectory of a genetically determined disease.

One of the most significant regulators of the circadian system is the daily feed/fast cycle (Bass and Takahashi, 2010; Tahara and Shibata, 2013). Notably, SCN-lesioned animals can still be synchronized to a feeding schedule (Acosta-Galvan et al., 2011; Stephan, 2002; Tahara et al., 2012). Much of the published work investigating the consequences of TRF have done so by placing feeding during the rest phase when it is misaligned with normal feeding behaviors. However, a number of studies have investigated the effects of scheduling feeding aligned with normal activity and feeding behaviors. Notably, the Panda lab reported that healthy mice under a high-fat-diet TRF regimen consume equivalent calories as those with unrestricted or *ad lib* access, and that they display improved motor coordination and are protected against obesity, hyperinsulinemia, and inflammation (Hatori et al., 2012). In *Drosophila*, a TRF protocol was also beneficial in preventing age-induced cardiovascular dysfunction (Gill et al., 2015; Melkani and Panda, 2017). In HD-N171-82Q mice, feeding restriction increased BDNF levels 3- to 4-fold, improved motor performance and survival, and reduced cell death (Duan et al., 2003). Prior work in the R6/2 mouse model showed that daytime scheduled feeding can restore circadian rhythmicity, and reverse HD-driven impairment in the expression of circadian output genes in the liver (Maywood et al., 2010). We recently published results demonstrating that TRF (6-hr feeding aligned to the middle of the active phase and 18-hr fasting) could improve the sleep/wake cycle, motor performance, and autonomic function in the BACHD and Q175 lines (Wang et al., 2018; Whittaker et al., 2018).

In recent human TRF trials utilizing 6-hr feed, 18-hr fast cycles, the diurnal pattern in cortisol and the expression of several circadian clock genes were altered, as were markers of autophagy, including pre-feeding increases in ketone bodies, the stress response and aging

gene sirtuin 1 *(SIRT1)*, and the autophagy gene microtubule-associated protein 1 light chain 3

(LC3A), and post feeding increases in mTOR and BDNF (Jamshed et al., 2019). This has

important implications for improving circadian rhythms, cycles of repair and autophagy, as well

as mHTT proteolysis and clearance (Camberos-Luna et al., 2016). This is further highlighted by

studies with treatments that promoted alterations in cycling levels of markers of autophagy,

with an accompanying 20% reduction in mHTT, as well as increases in mesenchymal stem and

progenitor cells in mice and humans (Brandhorst et al., 2015; Ehrnhoefer et al., 2018).

Reductions in the levels of mHTT by improved/stimulated autophagy/degradation have been

shown to ameliorate HD symptoms (Lee et al., 2015; Walter et al., 2016).

The mechanisms through which TRF conveys benefits have not been fully elucidated and

may result from a switch in bioenergetic pathways, specific responses to the timing and

duration of feeding and fasting, modulation of circadian rhythm timing and strength, and

through food-anticipatory activity and reward behavior (Angeles-Castellanos et al., 2010; Astiz

et al., 2019; Carneiro and Araujo, 2009; Colwell, 2015).

One mechanism through which TRF may convey benefits is by shifting the body into a

state of elevated ketone body production and increasing serum ketone bodies, called

ketogenesis or ketosis. Increasing the production of ketone bodies by the liver is dependent

upon achieving a period during which glycogen stores are being depleted, such as during

starvation, fasting, and very low-carb, high-fat feeding. During these states, ketone bodies are

generated at higher levels, regulated by the rate limiting enzymes CPT1A and HMGCS2, gating

beta-oxidation and ketone body production respectively, which are both regulated in a circadian

manner (Chavan et al., 2016).

During ketogenesis, fat metabolism in the liver generates the ketone bodies βOHB,

AcAc, and acetone which accumulate in the blood stream and result in ketosis. Acetone is

volatile and readily excreted in the breath. Ketone bodies are transported in the bloodstream to extrahepatic tissues where they have multiple fates (Achanta and Rae, 2017; Branco et al., 2016; Newman and Verdin, 2014). βOHB and AcAc readily enter tissues and cross the blood–brain barrier (BBB) through monocarboxylic transporters, which have also been identified in neurons and glia (Halestrap and Wilson, 2012; Pierre et al., 2000). One fate of ketone bodies is to be converted to acetyl CoA in mitochondria and enter the Krebs cycle at the level of citrate, bypassing glycolysis to generate ATP. Notably, this happens with higher efficiency and lower production of ROS compared to glucose (Anton et al., 2018; Cahill, 2006; Veech et al., 2001). While most of the βOHB that is used as an energy source in the brain is synthesized by the liver, ketone bodies also undergo synthesis and release by astrocytes (Guzmán and Blázquez, 2004; Le Foll and Levin, 2016).

In addition to their role in bioenergetics, ketone bodies have other important roles and signaling functions which include enhancing mitochondrial respiration and attenuating oxidative stress (Milder et al., 2010; Tieu et al., 2003), increasing BDNF expression (Duan et al., 2003; Ferrer et al., 2000), reducing inflammation (Guo et al., 2018; Youm et al., 2015), functioning in epigenetic modification (Ruan and Crawford, 2018), and signaling through G protein-coupled receptors (Offermanns and Schwaninger, 2015).

All the above potential benefits have relevance for HD pathology and symptoms. For instance, due to the loss of functional HTT, BDNF levels are reduced in human HD patients and in mouse models of HD by as much as 80% compared to healthy controls (Ferrer et al., 2000; Gauthier et al., 2004) which is likely to have implications for neuronal survival. Additionally, pathological changes in mitochondrial energy metabolism and ROS production occur in HD (Guedes-Dias et al., 2016; Siddiqui et al., 2012). Further, there is strong evidence for impairment in the clearance of mHTT in HD (Krainc, 2010). Finally, abnormally activated

microglia, the resident immune cells in the brain, along with peripheral/invading macrophages are present in HD patients (Sapp et al., 2001). Both immune cell types express mHTT, affecting their function (Crotti et al., 2014). Together, these represent significant therapeutic targets in HD.

Ketogenic approaches have been investigated in the treatment of other neurodegenerative diseases, including Alzheimer's disease (Broom et al., 2019; Newman et al., 2017; Ota et al., 2019; Roberts et al., 2017) and Parkinson's disease (Jabre and Bejjani, 2006; Kashiwaya et al., 2000; Phillips et al., 2018).

In this last study, using the BACHD line we sought to test the hypothesis that ketosis without TRF was sufficient to impart motor performance and sleep/wake rhythm benefits similar to those observed under TRF. To accomplish this, mice were placed on a custom low-carbohydrate, high-fat diet rich in medium chain triglyceride (MCT) oils that are known to be rapidly metabolized in the liver (Brownlow et al., 2013).

Materials and Methods

The work presented in this study followed all guidelines and regulations of the UCLA Division of Animal Medicine that are consistent with the Animal Welfare Policy Statements and the recommendations of the Panel on Euthanasia of the American Veterinary Medical Association.

Animals

The BACHD mouse model that we used in this study expresses the full-length human mutant *HTT* gene encoding 97 glutamine repeats under the control of endogenous regulatory machinery (Gray et al., 2008). Female BACHD dams backcrossed on a C57BL/6J background (minimum 12 generations) were bred with C57BL/6J (WT) males from The Jackson Laboratory (Bar Harbor, Maine) in our own breeding facility to obtain male and female offspring, either WT

or heterozygous for the BACHD transgene. Data were also collected from WT mice from this colony. Only male mice were used in this study as there is a sex difference in the circadian and motor phenotypes (Kuljis et al., 2016). Genotyping was performed at 15 days of age by tail snips, and after weaning, littermates were group housed, until otherwise noted. All animals were housed in soundproof chambers with controlled lighting conditions, using a 12-hr light, 12-hr dark cycle (12:12 LD, intensity 350 lux) for at least two-weeks prior to experimentation. For all experiments, a light meter (BK precision, Yorba Linda, CA) was used to measure light-intensity (lux). The chambers were in the same animal housing facility with controlled temperature and humidity, and each chamber held 8 cages of mice, grouped together by feeding treatment. All animals received cotton nestlets, and water was made available at all times. Except where noted, mice were fed Teklad normal chow diet 7013 (NIH-31 Modified Open Formula Mouse/Rat sterilizable diet; Envigo, Madison, WI).

This study used a total of 60 mice divided into 4 cohorts. The first group of BACHD (20) and WT (20) mice were placed on TRF or *ad lib* feeding and underwent around-the-clock ketone and glucose measurements. The second cohort of BACHD (10) and WT (10) mice were fed a ketogenic diet (KD) *ad lib* and measurements of ketones and behavior (sleep, activity, motor performance) were performed. Brain regions and peripheral tissues were collected from all cohorts for molecular and genetic experiments.

Time-restricted feeding

Mice were first entrained to a 12:12 LD cycle for a minimum of 2 weeks prior to any treatment. Experimental mice were housed in either normal cages or cages with a custom-made programmable food hopper that could temporally control access to food (NIH-31 diet; standard chow) and prevent food consumption during restricted times. Mice are coprophagic and were moved to new cages twice per week, as determined empirically to be the interval that

maintained very clean cages with low fecal count and visibly reduced coprophagic behavior during the fasting period. As mice were not moved to new cages between every daily feeding and fasting cycle, it is still possible that the mice consumed their own feces during the fast interval. The mice were held in these conditions from 3-months of age until collection.

Ketogenic diet

KD treated mice had *ad lib* access to a custom ketogenic diet (see Supplemental figure 1; Teklad custom diet TD.10911.PWD, Envigo, Madison, WI). Food consumption was measured, and food was renewed twice per week. Mice were fed the KD diet from 10 weeks of age.

β-hydroxybutyrate and glucose measurements

Tail vein blood sampling was performed by making a small incision in the tail vein to permit repeat measures (under 3 µL per collection) with minimal pain and stress to the mice. Mice were retrieved from cages, placed on a stable surface and were minimally restrained by the tail at the time of collection. Blood sampling was performed under normal room lighting (350 lux) for testing ZT 0-12 and under dim-red-light conditions (3 lux) for testing ZT 12-24. Blood was tested for βOHB (1.5 µL sample). Glucose (0.6 µL sample) was measured at the same time as βOHB, when measured. Metabolite measurements were made using a commercially available glucose/ketone meter (Precision Xtra Blood Glucose and Ketone Monitoring System, Abbott Laboratories, Chicago, IL). Blood flow was stopped by applying pressure with sterile gauze to achieve hemostasis.

Monitoring of cage locomotor activity

Experimental mice were singly housed in cages with IR motion sensors and analyzed using the El Temps (A. Diez-Nogura, Barcelona, Spain; http://www.el-temps.com/principal.html) and ClockLab (Actimetrics, Wilmette, IL) programs. The locomotor activity was recorded as previously described (Wang et al., 2017). From before 3-months of age, mice were entrained to

a 12:12 LD cycle. Locomotor activity data were recorded using Mini Mitter (Bend, OR) data loggers in 3-min bins, and 7 to 10 days of data were averaged for analysis. We used the days of activity data collected just prior to the motor performance tests when the mice reached 6 months of age. The data were analyzed to determine the period and rhythmic strength as previously described (Loh et al., 2013; Wang et al., 2017). The periodogram analysis uses a $\chi 2$ test with a threshold of 0.001 significance, from which the amplitude of the periodicities is determined at the circadian harmonic to obtain the rhythm power. The amount of cage activity over a 24-hr period was averaged and reported here as the arbitrary units (a.u.)/hr. The number of activity bouts and the average length of bouts were determined using Clocklab, where each bout was counted when activity bouts were separated by a gap of 21 min (maximum gap: 21 min; threshold: 3 counts/min). The onset variability was determined using Clocklab by averaging the daily activity onset values.

Monitoring of immobility-defined sleep behavior

Immobility-defined sleep was determined as described previously (Loh et al., 2013; Wang et al., 2017). Mice were housed in see-through plastic cages containing bedding (without the addition of nesting material). A side-on view of each cage was obtained, with minimal occlusion by the food bin or water bottle, both of which were top-mounted. Cages were top lit using IR LED lights. Video capture was accomplished using surveillance cameras with visible light filters (Gadspot Inc., City of Industry, CA) connected to a video-capture card (Adlink Technology Inc., Irvine, CA) on a custom-built computer system. ANY-maze software (Stoelting Co., Wood Dale, IL) was used for automated tracking of mouse immobility.

Immobility was registered when 95% of the area of the animal stayed immobile for more than 40 sec, as was previously determined to have 99% correlation with simultaneous EEG/EMG defined sleep (Fisher et al., 2012; Pack et al., 2007). Continuous tracking of the mice

was performed for a minimum of 5 sleep-wake cycles, with randomized visits (1-2 times/day) by the experimenter to confirm mouse health and video recording. The 3rd and 4th sleep-wake cycles were averaged for further analysis. Immobility-defined sleep data were exported in 1-min bins, and total sleep time was determined by summing the immobility durations in the rest phase (ZT 0-12) and active phase (ZT 12-24). An average waveform of hourly immobile-sleep over the two sleep-wake cycles was produced per genotype and treatment for graphical display. Variability of sleep onset, sleep offset, and sleep fragmentation was determined using Clocklab.

Grip strength test

Grip strength testing was used to measure neuromuscular function as maximal muscle strength of forelimbs. The grip strength ergometer (Santa Cruz Biotechnology, Santa Cruz, CA) was set up on a flat surface with a mouse grid firmly secured in place. The grid was cleaned with 70% ethanol and allowed to dry before testing each cohort. Peak mode was selected to enable measurement of maximal strength exerted. The sensor is reset to zero before each trial. Well-handled mice were tested in their active phase under dim red light (3 Lux) and acclimated to the testing room for 10 minutes prior to testing. Mice underwent five trials with an inter-trial interval of at least two minutes. For each trial, each mouse was removed from its home cage by gripping the tail between the thumb and the forefinger. The mice are lowered slowly over the grid, and only their forepaws were allowed to grip the grid. Mice are pulled by the tail ensuring the torso remains horizontal until they are no longer able to grip the grid. Mice are then returned to their cages. The maximal grip strength value of each mouse is utilized.

Rotarod test – accelerating version

The rotarod apparatus (Ugo Basile, Varese, Italy) is commonly used to measure motor coordination and balance. This apparatus consists of an axle or rod thick enough for a mouse to stand over the top of when it is not in motion and a flat platform a short distance below the

rod. The rod is covered with smooth rubber to provide traction while preventing the mice from clinging to the rod. In this study, mice were placed on top of the rubber-covered rod. When the mice moved at the pace set by the rotation rate of the rod, they would stay on top of it. When mice no longer moved at the selected pace, they dropped a short distance to the platform below. The time a mouse remains on the rod, before dropping to the platform is the latency to fall. Following a 15-min habituation to the testing room, mice were placed on the slowly rotating rod. The rod gradually accelerates from 5 rpm to 38 rpm over the course of the trial. The length of time the mouse stayed on the rod was recorded. A two-day protocol for the accelerating rotarod tests was used. On the first day, the mice were trained on the rotarod over 5 trials. The maximum length of each trial was 600 sec, and mice were allowed to rest for a minimum of 60 sec between trials. On the second day, mice were tested on the rotarod and the latency to fall from the rotarod was recorded from 5 trials. Mice were again allowed to rest for a minimum of 60 sec between trials. Data from each mouse were analyzed after averaging the times from all 5 trials. The apparatus was cleaned with 70% alcohol and allowed to dry completely between cohorts. A dim-red-light (3 lux) was used for illumination during active (dark) phase testing.

Statistical methods

We were interested in determining if ketones without TRF are sufficient to improve the symptoms in the BACHD mouse model, therefore, BACHD and WT *ad lib* KD-fed mice were compared to BACHD and WT *ad lib* normal chow-fed mice. The sample size per group was determined by both our empirical experience with the variability in the prior measures in the BACHD mice and a power analysis (SigmaPlot, SYSTAT Software, San Jose, CA) that assumed a power of 0.8 and an alpha of 0.05. To assess the impact of the treatments after 3-months, we applied a *t*-test and two-way analysis of variance for the analysis (2-way ANOVA) with genotype

and treatment as factors. To determine the impact of the treatment on temporal activity, sleep, and ketone waveforms, we used a two-way repeated measures analysis of variance (2-way RM ANOVA) with treatment and time as factors. Pairwise Multiple Comparison Procedures were made using the Holm-Sidak method. Correlations between circadian parameters and motor performance were examined by applying Pearson correlation analysis. Statistical analysis was performed using SigmaPlot. Data sets were examined for normality (Shapiro-Wilk test) and equal variance (Brown-Forsythe test). Between-group differences were determined significant if $p < 0.05$. All values are reported as group mean ± standard error of the mean (SEM). For each of the tests, we report the t- or F-values as well as the degrees of freedom.

Results

In these experiments, we examined the effect of KD on BACHD and WT mice. Treated mice were compared to normal chow diet controls. KD treated mice had *ad lib* access to a ketogenic diet from 3-months of age until collection. The body weights at the end of the study were different with the normal chow-fed mice being heavier than the KD-fed mice (not shown). The 2-way ANOVA found no effect of genotype ($F_{(1,31)} = 0.004$, P = 0.949) but an effect of treatment ($F_{(1,31)} = 5.438$, P = 0.027). Tail blood was sampled at 6 time-points throughout the 24-hr cycle and ketones (βOHB) were measured. Both BACHD (n=8) and WT (n=8) exhibited clear rhythms in βOHB under KD-feeding but not under normal chow feeding conditions (**Fig. 5-1**). βOHB levels in the BACHD exhibited significant effects of time ($F_{(5, 107)} = 20.443$, $P < 0.001$) and treatment ($F_{(1, 107)} = 76.599$, $P < 0.001$). Post-hoc analysis by Multiple Comparison Procedures (Holm-Sidak method) indicated significant changes in βOHB levels were observed in BACHD under the KD at most phases (ZT 2, 6, 14, 18, and 22) of the daily cycle. In WT mice, βOHB levels exhibited significant effects of time ($F_{(5, 107)} = 8.833$, $P < 0.001$) and treatment ($F_{(1, 107)} = 16.267$, $P < 0.001$). Post-hoc analysis indicated significant changes in βOHB levels in WT

mice elicited by the KD during the night (ZT 14, 18, 22). Therefore, both genotypes responded to the *ad lib* KD with the BACHD showing elevated βOHB at most phases while the WT mice exhibited elevated βOHB during the night.

KD improved activity rhythms in the BACHD line.

KD noticeably improved the temporal pattern of cage activity (**Fig. 5-2**). Both BACHD and WT (n=8 per group) exhibited clear rhythms in behavior under both the KD and the normal chow diet. Quantitative analysis of the activity rhythms of all 4 groups (2-way ANOVA) found that the power of the rhythms (**Fig. 5-2A**) were significantly altered by both genotype ($F_{(1, 31)}$=5.387, $P = 0.028$) and treatment ($F_{(1, 31)}$=23.503, $P < 0.001$). The average amount of activity (**Fig. 5-2B**) varied with the genotype ($F_{(1,31)}$=6.048, $P = 0.020$) but was not rescued by treatment ($F_{(1,31)}$=0.074, $P = 0.788$). The % of activity in the day (**Fig. 5-2C**) surprisingly did not vary with genotype ($F_{(1,31)}$=2.880, $P = 0.101$) but was improved by treatment ($F_{(1,31)}$=37.388, $P < 0.001$). The variation in onset (**Fig. 5-2D**) was impacted by both genotype ($F_{(1,31)}$=17.962 $P < 0.001$) and treatment ($F_{(1,31)}$=8.232, $P = 0.008$). Overall, the mutants exhibited weaker rhythms than WT, and the KD improved all of the parameters.

KD improved the temporal pattern of sleep behavior in the BACHD line.

The amount of sleep is controlled by homeostatic mechanisms and appears to be largely unaltered by the KD. The total amount of sleep in a 24-hr cycle (**Fig. 5-3A**) was not altered by genotype ($F_{(1, 31)}$= 0.018, $P = 0.895$) or treatment ($F_{(1, 31)}$= 1.276, $P = 0.268$). Similarly, during their active (night) phase (**Fig. 5-3B**), there were no effects of genotype ($F_{(1, 31)}$= 0.218, $P = 0.644$) or treatment ($F_{(1, 31)}$= 0.277, $P = 0.603$). During their rest (day) phase (**Fig. 5-3C**), there were effects of genotype ($F_{(1, 31)}$= 8.841, $P = 0.006$) but no effect of the KD ($F_{(1, 31)}$= 1.524, $P = 0.227$). The untreated mutant mice exhibited less daytime sleep under normal chow feeding and this difference was no longer seen under the KD. Another key measure of sleep

quality is fragmentation or the number of sleeping bouts. The total number of sleep bouts in a 24-hr cycle (**Fig. 5-3D**) was not altered by genotype ($F_{(1, 31)}$= 0.284, P = 0.598) or treatment ($F_{(1, 31)}$= 3.574, P = 0.069). During the day (ZT0-12), the number of sleep bouts was not altered by genotype ($F_{(1, 31)}$= 0.001, P = 1.000) but was reduced by treatment ($F_{(1, 31)}$= 7.724, P = 0.010). There were not any corresponding changes during the night. Finally, the BACHD mice exhibited a phase delayed sleep onset that was corrected by the KD. The phase of sleep onset (**Fig. 5-3E**) was altered by genotype ($F_{(1, 31)}$= 8.516, P = 0.007) but not treatment ($F_{(1, 31)}$= 2.487, P = 0.126). On average, the mutant mice on the normal chow diet started sleep at ZT 1.6 ± 0.4 while the KD started sleeping at 0.2 ± 0.2 or closely aligned with lights-off ($t_{(14)}$ = 2.924. P = 0.011, t-test). In summary, the KD increased daytime sleep and corrected the phase delay in sleep onset seen in the BACHD mice.

KD improved motor function in the BACHD mice.

The defining symptoms of HD are centered on motor dysfunction, thus, we hypothesized that KD would improve motor performance in the BACHD model. Motor performance in the BACHD was assessed using two well-defined tests: the accelerating rotarod and the grip strength tests (**Fig. 5-4A, B**). BACHD mice on the KD exhibited a longer latency to fall (t(14) = 2.924, P = 0.005, t-test) off the rotarod compared to those on the normal chow diet. The performance on the rotarod (**Fig. 5-4A**) was influenced by genotype ($F_{(1, 31)}$ = 63.330, P < 0.001) and treatment ($F_{(1, 31)}$= 8.337, P = 0.007). Conversely, the decrease in grip strength was not improved in the mutants. The grip strength (**Fig. 5-4B**) varied with genotype ($F_{(1, 31)}$ = 6.330, P = 0.015) but there was no effect of treatment ($F_{(1, 31)}$ = 0.249, P = 0.622). Overall, a key finding of this study is that rotarod performance in the BACHD model was improved by KD.

Discussion

The present study demonstrates that a KD can ameliorate a range of symptoms linked to HD and related neurodegenerative disorders. Using the BACHD mouse model of HD, we showed that the KD boosted the amplitude and reduced variability in activity rhythms. The KD also corrected the phase delay in sleep onset seen in the BACHD mice although most sleep parameters were not altered by the diet. Finally, a key finding of this study is that the rotarod performance was improved by the KD. Thus, the KD successfully improved several behavioral and physiological parameters that have been shown to be compromised in HD.

In this study, mice received *ad lib* access to a custom low-carbohydrate, adequate protein, high-fat diet rich in MCT oils that are known to be rapidly metabolized in the liver (Augustin et al., 2018; Brownlow et al., 2013). Under these dietary conditions, mice experience elevated ketone body production and a resulting increase in serum ketone bodies, a state referred to as ketogenesis or ketosis (Liu, 2008; McPherson and McEneny, 2012; Yeh and Zee, 1976). Lipids entering the liver to undergo beta-oxidation are regulated by the rate limiting enzyme CPT1A. Following beta-oxidation, the liver generates ketone bodies through a process regulated by the rate limiting enzyme HMGCS2. Importantly, both enzymes are regulated in a circadian manner (Chavan et al., 2016).

During ketogenesis, the ketone bodies βOHB, AcAc, and acetone are synthesized by the liver from fatty acids. Acetone volatilizes easily and is excreted in the breath. Ketone bodies are transported in the bloodstream to extrahepatic tissues where they have multiple fates (Achanta and Rae, 2017; Branco et al., 2016; Newman and Verdin, 2014). βOHB and AcAc readily enter extrahepatic tissues, including the brain. One fate of the ketone bodies is to be converted to acetyl CoA in mitochondria, after which they enter the Krebs cycle to generate ATP with high efficiency and with low production of ROS (Anton et al., 2018; Cahill, 2006; Veech et al., 2001).

Other important non-bioenergetic roles of Ketone bodies consist of signaling functions which include enhancing mitochondrial respiration and attenuating oxidative stress (Milder et al., 2010; Tieu et al., 2003), increasing BDNF expression (Duan et al., 2003), reducing the activation and release of inflammatory mediators (Guo et al., 2018; Youm et al., 2015), functioning in chromatin remodeling and epigenetic modification (Ruan and Crawford, 2018; Tognini et al., 2017), and signaling through G protein-coupled receptors to induce a neuroprotective phenotype in monocytes and/or macrophages (Offermanns and Schwaninger, 2015).

In this study, we showed that under *ad lib* KD conditions, the levels of βOHB are strongly rhythmic (**Fig. 5-1**). All of the KD treated mice (BACHD, WT) exhibited clear rhythms in ketones, while those under normal chow feeding conditions did not (**Fig. 5-1**). The KD-fed mutants, but not the KD-fed WT, showed higher levels of ketones during the early day, taking longer to resolve βOHB levels below 0.5 mM. Therefore, both genotypes responded to the KD with the BACHD showing elevated ketones at most phases while the WT exhibited elevated ketones during the night. One prior study has also shown that KD induces serum and intestinal βOHB levels to robustly oscillate in a circadian manner, an event coupled to tissue-specific cyclic histone deacetylase (HDAC) activity and histone acetylation (Tognini et al., 2017). This was complemented by another study where KD shifted the phase of *Bdnf* transcript expression in the liver and brain and increased protein levels in the brain (Genzer et al., 2016).

The *ad lib* fed KD noticeably improved the temporal pattern of cage activity (**Fig. 5-2**). This regimen increased the power of the rhythms as well as reduced the inappropriate activity in the day and the variability in onset. Some the benefits were only observed in the mutant mice and not in the WT, including the improvement in power, increase in activity, and reduction in onset variability. Interestingly, the reduction of activity during the rest cycle was seen in both

genotypes. Prior work using scheduled feeding protocols also improved locomotor activity

rhythms in several mouse models of HD, including the R6/2 (Skillings et al., 2014), Q175 (Wang

et al., 2018) and BACHD (Whittaker et al., 2018) lines. These improvements in the locomotor

activity rhythms under TRF could be driven by the nightly increase in ketones observed in the

present study. We could only find one other study that examined the impact of *ad lib* KD-

feeding on locomotor rhythms (Genzer et al., 2015), which reported improvements in nocturnal

activity levels in WT mice.

The amount of sleep is controlled by homeostatic mechanisms and was largely unaltered

by the KD (**Fig. 5-3**). We did see some evidence that the KD improved daytime sleep and

reduced fragmentation during this phase. In addition, a striking improvement in the onset of

sleeping was observed in the mutant mice, which likely has more to do with circadian regulation

than sleep homeostatic mechanisms. Variability in sleep onset has been associated with

decreased academic performance and reduced white matter in humans (Fuligni et al., 2018;

Telzer et al., 2015), thus improvements in precision of sleep onset are an important target for

therapeutic interventions. Prior work with the R6/2 (Fisher et al., 2013; Kantor et al., 2013) and

Q175 (Fisher et al., 2016) mouse models has provided evidence of dysfunction in

electroencephalogram (EEG) defined sleep including increases in sleep fragmentation as well as

characteristic changes in the EEG spectral profiles. Total amount of non-rapid eye movement

(NREM) and rapid eye movement (REM) sleep over 24-hrs as well as homeostatic responses to

sleep loss were not impacted by the mutation (Fisher et al., 2016).

There is a rich literature linking energy metabolism and sleep homeostasis. The ketone

bodies AcAc and βOHB, generated from the breakdown of fatty acids, are major metabolic fuels

for the brain, especially under conditions of low glucose availability. Ketogenesis is modulated

by the activity of PPARα, and treatment with a PPAR activator has been shown to induce a

marked increase in plasma AcAc and βOHB in mice, accompanied by increased slow-wave activity during NREM sleep (Chikahisa et al., 2014). This study also reported that sleep deprivation increased mRNA expression of ketogenic genes such as PPARα and HMGCS2 in the brain and decreased ketolytic enzymes such as succinyl-CoA:3-oxoacid CoA transferase (SCOT).

In humans, there has been a fair amount of work exploring the links between use of the KD and sleep in the context of epilepsy. Many patients exhibit epileptic discharges during sleep and the KD is one of the few non-pharmacological approaches that helps to reduce seizures. Reviews of this work consistently find support for the hypothesis that KD-feeding impacts sleep architecture [e.g. (Jain and Glauser, 2014)], with several reports of KD-feeding improving sleep in epileptic and type 2 diabetes patients (Siegmann et al., 2019). Therefore, there are good reasons to explore the impact of the KD on sleep architecture in the BACHD model.

The BACHD mouse model shows alterations in the temporal patterning of neural activity recorded in the SCN (Kudo et al., 2011a; Kuljis et al., 2016). The weakening of the electrical output of the SCN would be expected to impact the phase of peripheral molecular clocks that are driven by the SCN. In the R6/2 model of HD, circadian rhythms of PER2 bioluminescence were normal in the SCN but phase advanced in the liver (Maywood et al., 2010). One of the weaknesses of this study is that we have not evaluated the impact of the KD on the circadian system in the BACHD. Specifically, we need to determine if the *ad lib* KD improves circadian rhythms measured under constant darkness. In addition, using our BACHD PER2::LUC mice, the impact of KD should be evaluated on circadian rhythms in bioluminescence measured from the SCN and peripheral organs like the liver. In prior work (Whittaker et al., 2018), we did not see any evidence for genotypic differences between the clock gene expression in WT and BACHD mice. Still the TRF protocol shifted the phase of the rhythm in peripheral organs but not in the SCN. We expect similar results with the *ad lib* KD, i.e. the phase of peripheral rhythms but not

the SCN will be altered by the diet. Prior work shows that feeding schedules can shift the phase of the rhythms in clock gene expression throughout the body including in limbic structures involved in motivation and reward (Angeles-Castellanos et al., 2007; Waddington Lamont et al., 2007) as well as in the hypothalamus (Akiyama et al., 2004).

A prior study (Genzer et al., 2015) examined the effect of *ad lib* KD-feeding on locomotor activity, clock gene expression, and average daily levels of 5' adenosine monophosphate-activated protein kinase (AMPK), mTOR, and SIRT1 for two months, compared to a low-fat diet (LFD) in WT mice. The KD resulted in increased basal levels of locomotor activity during the dark and light periods. Additionally, the KD led to a 1.5-fold increase in the levels of blood glucose and insulin. In the brain, the phosphorylated-AMPK/AMPK ratio was 40% higher under KD, whereas in the liver it was not affected. Notably, Phosphorylated-AMPK induces the degradation of PER and CRY proteins, leading to phase advances in the clock. The KD led to 40% and 20% down-regulation of the ratio of phosphorylated-P70S6K/P70S6K, in the brain and liver, respectively. P70S6K is a downstream target of mTOR, which was also decreased. SIRT1 levels were 40% higher in the brain, but 40% lower in the liver of KD-fed mice. Clock genes showed delayed rhythms under the KD. Importantly, in the brain of KD-fed mice, amplitudes of clock genes were down-regulated, whereas a 6-fold up-regulation was found in the liver. It should be noted that mice were fasted 12 or more hours before collection, which was indicated by the elevated ketones in the non-ketogenic LFD fed mice at collection (Genzer et al., 2015) which complicates interpretation of this data. Another important study from the Sassone-Corsi laboratory (Tognini et al., 2017) found that a KD had profound and differential effects on liver and intestine clocks. Specifically, the amplitude of clock-controlled genes and BMAL1 chromatin recruitment were drastically altered by a KD in the liver, but not in the intestine. The KD induced nuclear accumulation of PPARα in both tissues but with a

different circadian phase. Also, gut and liver clocks responded differently to carbohydrate supplementation during KD-feeding. This data indicates that the metabolic state under a KD reduced satiety and, in the liver, reduced anabolism along with increased gluconeogenesis. These changes may well be beneficial to patients with HD as well as those with other neurodegenerative diseases.

HD is defined as a movement disorder, as the most striking and debilitating symptoms include motor deficits. Critically, the KD improved performance of the HD mutant mice on at least one motor test (**Fig. 5-4**). In contrast, the grip strength was not improved by the treatment. In prior work, aged mice on a cyclic, *ad lib* fed KD did not show improvement in motor strength tests (Newman et al., 2017), while those on a defined daily caloric intake from a KD did improve in motor strength tests (Roberts et al., 2017). Further, scheduled feeding has been found to improve motor function in the Q175 (Wang et al., 2018) and BACHD models (Whittaker et al., 2018), as well as the exploratory behavior in the open field (Skillings et al., 2014) in the R6/2 model. Notably, marginal improvement in motor performance has been reported in other mouse disease models treated with a KD (Ari et al., 2014; Brownlow et al., 2013).

Another key symptom of HD is the loss of neurons in the striatum. At the ages we have been working with the BACHD, there is no obvious neuronal loss, although we have evidence that these mutants begin to present signs of axonal degeneration, loss of myelin, and inflammation at early ages (See Chapter 6). We have collected the tissue from the mice used in this study and are determining whether the KD ameliorates some of these histopathological features.

Approaches directed at boosting circadian output have shown efficacy for improving outcomes in different HD mouse models. There is evidence that improving the sleep/wake cycle

95

with sleep-inducing drugs (Kantor et al., 2016; Pallier et al., 2007), stimulants (Cuesta et al., 2012; Whittaker et al., 2017), bright light & restricted wheel access (Cuesta et al., 2014), enhanced blue light (Wang et al., 2017), and scheduled feeding (Wang et al., 2018; Whittaker et al., 2018) can improve HD symptoms. This body of work supports the general hypothesis (Longo and Panda, 2016; Morton, 2013; Schroeder and Colwell, 2013; van Wamelen et al., 2015) that circadian-based therapies can alter the trajectory of a genetically determined disease.
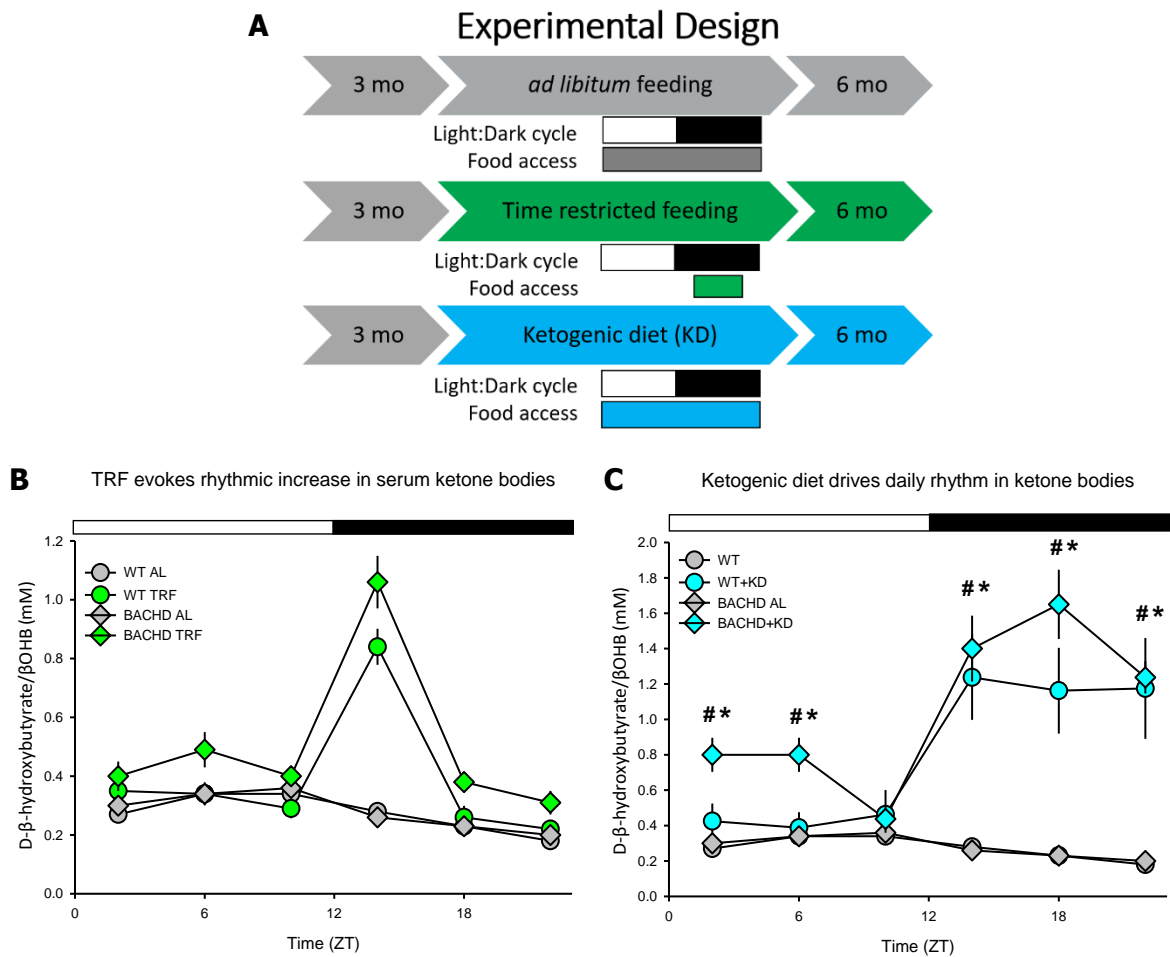
Figure 20: **Figure 5-1: TRF and KD evoke daily rhythms in serum ketones (βOHB).**
(A) Schematic of experimental design. Mice were held in 12:12 LD cycle so the time of lights-on is ZT 0 and the time of lights-off is ZT 12. LD cycle is represented by light-dark bars. **(B)** Tail vein blood was collected at 6 time points for BACHD (diamonds) and WT (circles) mice under ad lib (grey) and TRF (green). Green shading represents the feeding period. **(C)** Tail vein blood was collected at 6 time points for BACHD (diamonds) and WT (circles) mice under ad lib (grey) and KD (blue). The symbols show group mean with SEM plotted. Comparisons between the mice of each genotype were made with two-way ANOVA for repeated measures with time and treatment as factors. Asterisks represent significant differences due to KD compared to the ad lib controls, number signs represent significant differences due to time ($P < 0.05$; $n = 8$ per group).
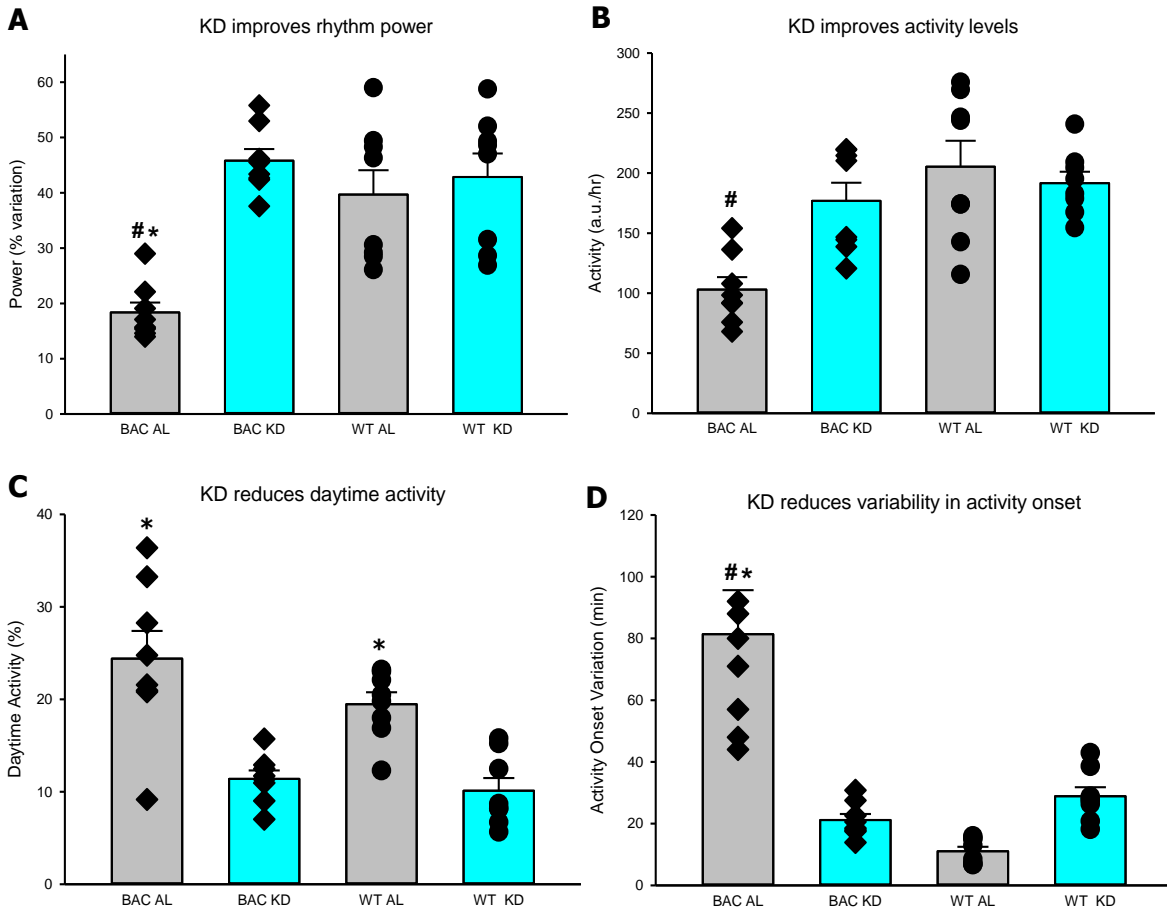
Figure 21: **Figure 5-2: Locomotor activity rhythms were improved by the KD.**
(A) The strength of the activity rhythm is indicated by the power (% variance) of the χ2
periodogram analysis. **(B)** Average hourly activity levels from 7-10 days of cage activity. **(C)**
The % of total activity that occurred in the daytime (rest) phase. **(D)** The averaged onset
variability was calculated from the best-fit regression line. For this and other figures, the vertical
bar plots show group means and SEM while the symbols show the values from individual
animals in each group (BACHD *ad lib*, grey diamonds; BACHD KD, blue diamonds, WT *ad lib*,
grey circles; WT KD, blue circles). Comparisons between cohorts were made using a 2-way
ANOVA with genotype and treatment as factors. Asterisks represent significant differences ($P <$
0.05) by two-way ANOVA due to treatment while number sign represents significant differences
due to genotype.
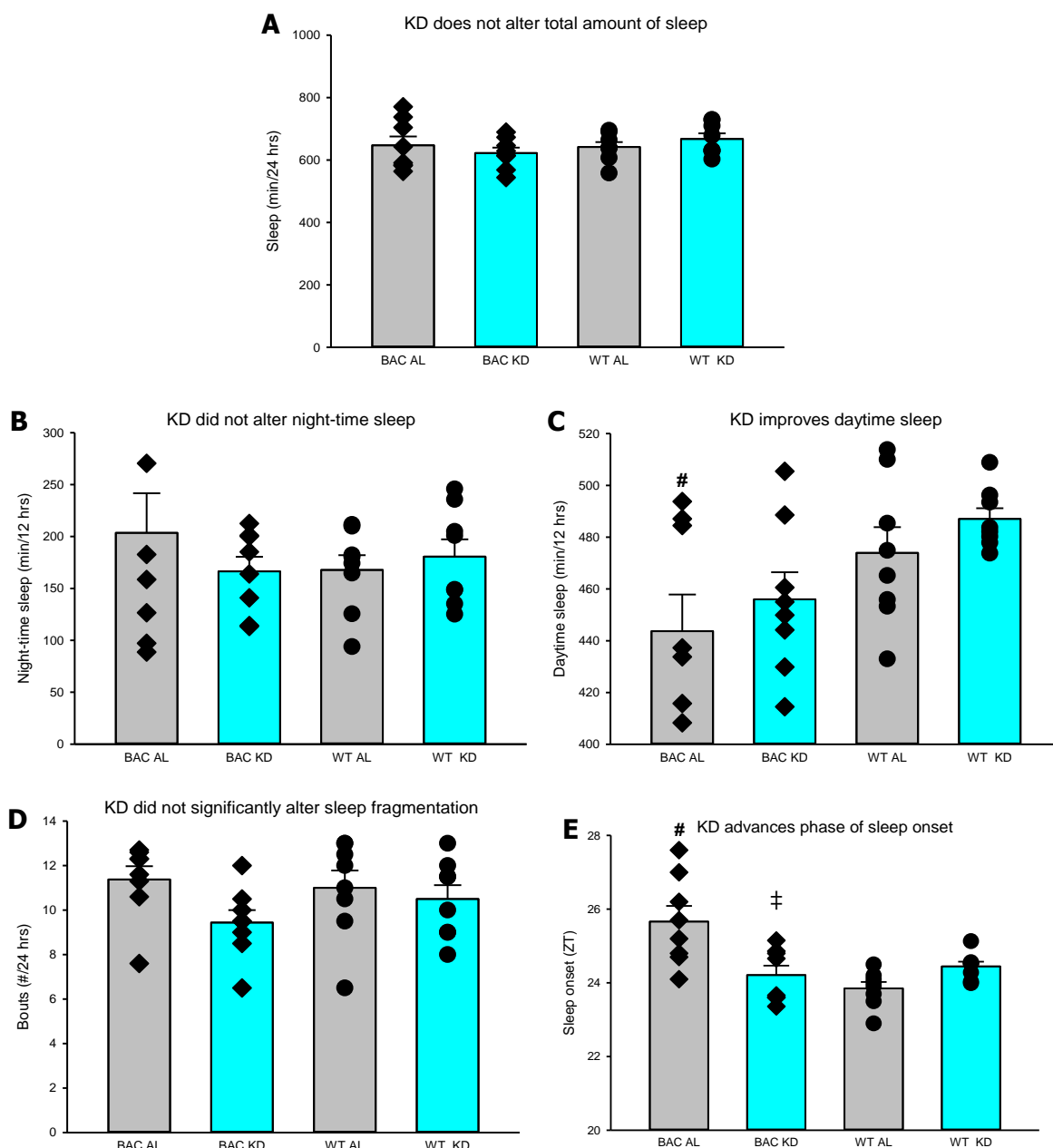
Figure 22: **Figure 5-3: Sleep behavior was altered by the KD.**
Video recording in combination with automated mouse tracking analysis software was used to measure immobility-defined sleep (n = 8 per group). **(A)** Total sleep in the 24-hr cycle while amount of sleep in night **(B)** and day **(C)** are plotted. **(D)** Sleep fragmentation is defined as the number of sleep bouts in the 24-hr cycle. **(E)** the phase (ZT) of sleep onset is shown. Comparisons between cohorts were made using a 2-way ANOVA with genotype and treatment as factors. Asterisks represent significant differences ($P < 0.05$) by two-way ANOVA due to treatment while number sign represents significant differences due to genotype. The double dagger represents significant differences ($P < 0.05$) by t-test.
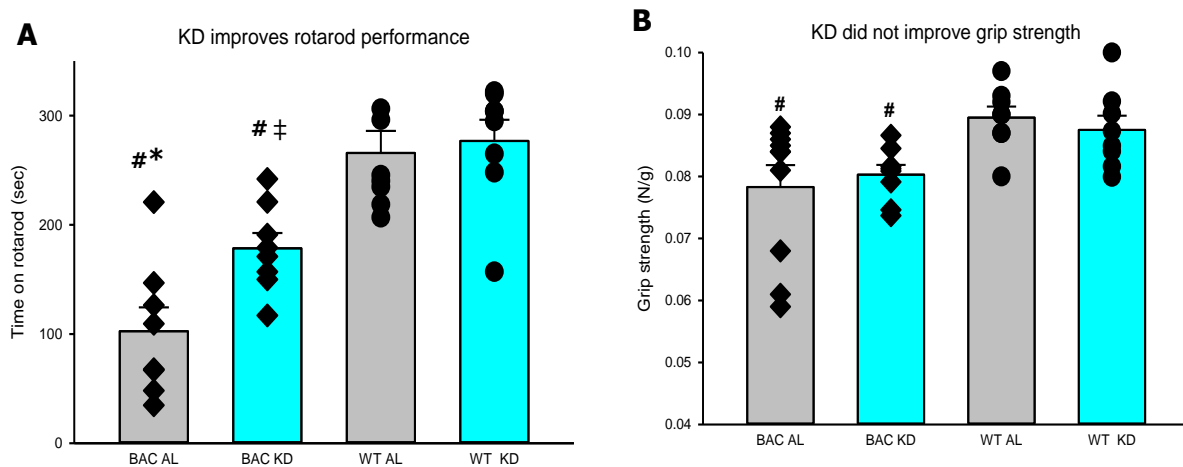
Figure 23: **Figure 5-4: KD improved motor performance in the BACHD model.**
(A) The accelerating rotarod test measures time on the rod until the mice fall. Improvements in motor performance are shown by longer latency to fall. **(B)** Grip strength measurements. Comparisons between cohorts were made using a 2-way ANOVA with genotype and treatment as factors. Asterisks represent significant differences ($P < 0.05$) by two-way ANOVA due to treatment while number sign represents significant differences due to genotype. The double dagger represents significant differences ($P < 0.05$) by t-test.

	NIH-31 (g)	KD (g)
Casein	210	300
L-Cystine	3	2.86
Sucrose	200	0
Maltodextrin	100	0
Corn Starch	369	0
Cellulose (fiber)	40	245.31
Medium Chain Triglycerides	0	270
Flaxseed Oil	21	70
Canola Oil	19	60
Mineral Mix, Ca-P Deficient (79055)	13.4	18.5
Calcium Phosphate, dibasic, CaHPO4	7	8.5
Calcium Carbonate, CaCO3	7.3	10.75
Vitamin Mix, Teklad (40060)	10	14
Ethoxyquin, preservative	0.01	0.08
Total	1000	1000
Protein % by weight	17.9	26.4
Protein % by kcal	23.8	22.4
Carbohydrate % by weight	46.8	0.6
Carbohydrate % by kcal	62.2	0.5
Fat % by weight	4.7	40.3
Fat % by kcal	14	77.1
Kcal/g	3	4.7

Figure 24: **Figure 5-Supplemental figure 1: Comparison of NIH-31 standard chow diet with KD.**
The KD is a custom very-low-carbohydrate, adequate protein, high-fat diet rich in MCT oils. The KD diet was modified from a stock Teklad KD diet from Envigo. The modified KD removed sources of carbohydrates and added MCT oil in order to better generate ketosis. The KD has ~50% more calories per gram compared to NIH-31.

Chapter 6: Conclusions

Chapter 6: Conclusions

In these studies, I sought to test the hypotheses that circadian dysfunction interacts with HD pathology leading to the exacerbation of HD-related symptoms and that circadian-based therapies can alter the trajectory of a genetically determined disease.

In the first study, we sought to determine if the daily administration of the H3R antagonist/inverse agonist GSK189254 would improve nonmotor symptoms in the Q175 mouse model of HD. Several previous studies support a role for H3R in promoting wakefulness and for HA as a potent regulator of the circadian system (Cote and Harrington, 1993; Eaton et al., 1995; Haas and Panula, 2003; Jacobs et al., 2000; Kim et al., 2015; Lin et al., 2011; Parmentier et al., 2002; Watanabe et al., 1984). For three months, starting at ages before the onset of motor symptoms in Hom and Het Q175 mice, we administered GSK189254 nightly at a time when HA levels would normally be rising. We found that this treatment improved daily activity rhythms and produced short-term changes in daily sleep behavior while not altering the overall amount of sleep in a 24-hr cycle. Further, GSK189254 treatment improved exploratory behavior, cognitive performance, and mood without increasing anxiety-like behavior. Our findings suggest that drugs targeting the H3R system may benefit somnolence and arousal in the management of HD.

In the second study, we placed Het Q175 mice on TRF for three months starting at an age before the onset of motor symptoms. We found that the TRF regimen improved the daily activity rhythms and advanced the time that the mice ended their sleep phase without changes in total amount of sleep in each 24-hr cycle. Additionally, the TRF regimen improved motor performance. Markedly, we found that the improved circadian behavior was correlated with improved motor function in the TRF group, suggesting that improved circadian timing underlies the improved motor function in the treated mice. Cardiovascular events are a major cause of

death in the HD population (Lanska et al., 1988; Sørensen and Fenger, 1992), and we found that TRF improved cardiovascular performance, including increased HRV. Notably, decreased HRV, generally considered an indication of poor cardiovascular health and a predictor for cardiovascular disease and mortality (Thayer et al., 2010), has been reported in HD patients beginning during the pre-symptomatic stage of disease progression (Andrich et al., 2002; Aziz et al., 2010b). To our knowledge, this is the first study showing that a TRF regimen can improve HRV in a disease model.

Furthermore, we reported an analysis of the Q175 striatum using NanoString technology in which over 50% of the genes shown to be downregulated in Q175 controls (Langfelder et al., 2016) were upregulated by TRF. We then looked at the top upregulated factors of canonical pathways identified using IPA analysis. Three were neurotrophic factors, including BDNF, which is reduced in human HD patients and in mouse models of HD (Duan et al., 2003; Ferrer et al., 2000). Additionally, we identified CREB1, also reduced in HD patients (Steffan et al., 2000; Sugars and Rubinsztein, 2003; Sugars et al., 2004), as well as a demthylase, tet methylcytosine dioxygenase 1 (TET1), which has been reported to upregulate several neuronal memory-associated genes and impair contextual fear memory (Kaas et al., 2013).

In the third study, we kept BACHD mice on a TRF regimen for three months starting at an age before the onset of motor symptoms. We found that TRF boosted the amplitude and reduced variability in activity rhythms, and that the temporal patterning of both sleep behavior and sleep fragmentation were improved. Physiologically, TRF increased HRV during sleep and increased the amplitude of the HR rhythm. We found that BACHD still exhibit robust peripheral PER2::LUC rhythms and that TRF was sufficient to modify the phase but not the amplitude of the rhythms. Further, motor performance in the BACHD was improved by TRF. As in the Q175, we observed a correlation between improved circadian behavior and improved motor function in

the TRF group, further supporting that improved circadian timing underlies the improvements observed in motor function.

In the final study, we first determined that TRF induced robust rhythms in serum levels of βOHB in both BACHD and WT mice. While this work is still ongoing, the behavioral data has been collected and analyzed. We found that an *ad lib* fed KD evoked robust rhythms in serum levels of βOHB in both genotypes, although daytime levels of ketones were only elevated in the mutants. The KD did not alter total behavioral sleep, night-time sleep or total sleep fragmentation, however it did increase daytime sleep as well as improve the timing of sleep onset in the mutant mice. Additionally, improved activity rhythms, including rhythmic power, average activity levels, as well as reduced inappropriate daytime activity and onset variability were observed. Notably, the KD improved the performance of the mutants on the rotarod but not the grip strength. Finally, we have collected tissue to determine if the KD or TRF alter core pathology in the striatum of the BACHD mice. We have found evidence that the striatum of 3-month-old male BACHD mice, under *ad lib* normal chow feeding conditions, begin to present signs of axonal degeneration and reduction in myelination, accompanied by inflammation and astrogliosis, as suggested by major histocompatibility complex class II (MHCII) and glial fibrillary acid protein (GFAP) expression (**Fig. 6**). Future work will determine if KD or TRF alter these pathological markers.

Taken together, these studies support the use of circadian approaches in delaying progression and improving quality of life of HD patients as well as other neurodegenerative disorders with similar biology. It should be emphasized that these circadian treatments were applied at early symptomatic stages of the disease. In progressive degenerative diseases and especially in genetic diseases such as HD, our data is consistent with recommendations of early genetic testing and use of circadian based therapeutic approaches.

There may be some concerns about using a TRF protocol in HD populations because of the low body weights associated with the disease progression. It has been reported that HD patients with a higher body mass index (BMI) in early-stage HD have a slower progression of disease (Costa de Miranda et al., 2019; Myers et al., 1991). Additionally, increased leptin production has been reported in HD patients which could suppress hunger (Aziz et al., 2010c), and early-stage impairment in energy balance and higher sedentary energy expenditure are also seen in the patients (Gaba et al., 2005; Pratley et al., 2000). This all culminates in progressive weight loss, a well-documented component of pathology in HD patients (Djoussé et al., 2002; Hamilton et al., 2004; Sanberg et al., 1981). However, and most importantly, TRF did not result in weight loss in our studies. Mice under TRF consumed the same volume of food as the *ad lib* fed normal chow mice, and the body weights of TRF fed HD mice remained comparable to WT mice (Wang et al., 2018; Whittaker et al., 2018). Similarly, the KD diet resulted in a small increase in bodyweight in the WT and a small decrease in bodyweight in the BACHD over the three months of the trial (Chap. 5), and neither of these changes was significant. A reduction in food consumption or bodyweight would have introduced confounding variables. However, it has been previously reported in WT mice that TRF with normal chow can reduce fat mass and increase lean mass while not significantly impacting overall body mass when compared to *ad lib* feeding with normal chow (Chaix et al., 2014).

Altogether, these findings support the hypothesis that early interventions that improve sleep/wake timing and circadian rhythmicity will reduce HD symptoms; however, there remain important gaps in our knowledge. Although we have strong evidence of axonal and myelin loss early in the striatum, motor cortex, and corpus collosum in male BACHD mice (unpublished), we have not yet determined whether TRF or the KD alter central aspects of the pathology. Prior work in the R6/2 model found that rhythms in *mPer2* gene expression were globally

106

downregulated throughout the brain and that peak/trough differences were lost. However, PER2::LUC bioluminescence expression in the R6/2 SCN revealed that intrinsic pace-making mechanisms remained intact (Maywood et al., 2010). On the other hand, these mutants were reported to have disrupted circadian function with phase advanced *mPer2* and arrhythmic *Dbp* in the liver, which were restored by TRF. In the same mice, *Pk2* mRNA in the SCN demonstrated progressive reduction in expression, while in WT mice, *Pk2* is high during circadian daytime and low at night. The product of *Pk2* is proposed to suppress daytime activity in nocturnal rodents (Cheng et al., 2002; Prosser et al., 2007). Notably, *Pk2* is a transcriptional target of BMAL1, which was also found to be disrupted in R6/2 mice (Morton et al., 2005). The central impact of TRF or the KD on rhythmic outputs has not yet been examined and is an important gap in our knowledge. Furthermore, we do not know the impact of the BACHD mutation on rhythmic outputs in gene expression and would also like to address whether rhythms in corticosterone and cytokines are altered in serum, and if so, determine if TRF or the KD are able to repristinate them.

The mechanisms through which TRF and the KD convey benefits are uncertain and may be mediated by multiple pathways. Both likely interact with various molecular clocks in the body, including the liver clock, and this may be an important aspect of the benefits. While we showed that TRF can alter the phase of some peripheral rhythms, it is also important to determine if KD can exert similar effects on peripheral rhythms, as well as ascertain whether TRF and KD can alter the phase and amplitude of molecular clock driven outputs. Finally, it must be established whether the KD can exert benefits similar to those elicited by TRF in the improvement of autonomic parameters.

Future directions of our work comprise determining if the BACHD mutation disrupts rhythms in gene expression and if these rhythms are altered by TRF and the KD, thus we

107

collected striatum, cortex, and hypothalamus, as well as peripheral organs and serum, from WT and BACHD mice under TRF and *ad lib* fed normal chow in a 4-hr interval time-course. Based upon TRF data shared with us from the laboratory of Satchin Panda (unpublished), some of the key genes to consider in this follow-up work include a) circadian clock genes *Per2*, *Bmal1*, *Npas2*, *Nrld2*; b) clock controlled genes *Pk2, Avp, Ppara, Ppargcla*; c) transcriptional related genes *Creb1, Fos, Arc, Erg4*; d) metabolism related genes *Ppargc1A, Sirt1, Parp1, Prkaa1, Mtor*; d) autophagy related genes *Bnip3*, *Dram1*; e) HD related genes *Htt, Kcnab1, Homer1a, Bdnf*.

Following on our findings of early signs of axonal and myelin loss in brain regions in 3-month-old male BACHD mice, it is important to examine the impact of TRF or the KD on central aspects of pathology. Using Western blot and immunohistochemistry [as described in (Lee et al., 2018); **Fig. 6; Table 6-1**], we observed clear early signs of axonal and myelin loss in the striatum, as evidenced by increased expression of non-phosphorylated neurofilament (NF)-H (SMI-32), a marker suggestive of axonal degeneration, accompanied by decreased expression of axonal and myelin markers NF-160 and myelin basic protein (MBP), respectively (**Fig. 6-1**). These abnormalities were accompanied by elevated expression of GFAP, an astrocytic marker, and of MHCII, suggesting astroglial activation and a concurrent immune response in the brain parenchyma (**Fig. 6-2**). MHCII was expressed by the astrocytes and other cells in what appear to be blood vessels, possibly implicating immune cells recruited from the periphery. This observation is currently under further investigation to better define these cell types. Bizarrely, we did not observe altered expression of ionized calcium binding adaptor molecule 1 (Iba-1), a microglia marker, or evidence of co-expression of MCHII and Iba-1. These findings are supported by reports of astrocytic dysfunction (Hsiao et al., 2013; Khakh et al., 2017), as well as cerebral vasculature alterations and BBB leakage in HD patients and mouse models of HD (Di Pardo et al., 2017; Drouin-Ouellet et al., 2015; Lim et al., 2017). However, it will be important

to establish what cell types are expressing MHCII and if they are recruited from the periphery at this early stage of disease (Konishi et al., 2017).

Abnormal and deficient neural cell development and adult neurogenesis have been reported in autopsied human HD brains and animal models of HD (HD iPSC Consortium, 2017). We have preliminary evidence of persisting oligodendrocyte progenitors in the male BACHD striatum as shown by nuclear expression of glutathione S-transferase pi (GSTπ; not shown). Although preliminary, this finding is encouraging as TRF may promote maturation of progenitor cells committed to the oligodendrocyte lineage to support early repair and restoration of myelin (Boulanger and Messier, 2014).

In conclusion, we show that early-stage arousal promoting substances such as H3R antagonists, and dietary approaches such as TRF or a KD can ameliorate a range of symptoms of HD and related neurodegenerative disorders. These studies add to a growing body of evidence showing that enhancements in "circadian hygiene" lead to improvements in health outcomes for a wide range of human diseases including neurodegenerative disorders.

Figure 6-1: Western blot and immunohistochemistry in BACHD striatum show axonal and myelin loss early in disease progression.
Increased expression of SMI-32, a marker for axonal degeneration, and decreased levels of myelin marker MBP were observed in 3-month male BACHD brain (upper panels). Higher magnification insets show axonal bundles in the striatum. BACHD striatum also showed decreased axonal marker NF-160 immunoreactivity (lower panels). Western blot analyses showing lower levels of NF-160 (axon) and MBP (myelin) in the BACHD striatum. These results suggest that axonal and myelin loss begin early in disease progression. St=striatum, V=lateral ventricle, CC=corpus callosum
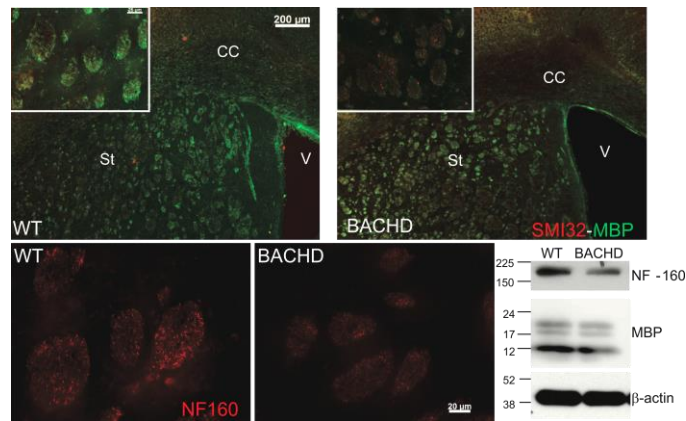
Figure 6-2: **Western blot and immunohistochemistry in BACHD brain suggests astroglial activation and a concurrent immune response in the brain.**
Enhanced expression of the astrocytic marker GFAP in the striatum (upper panels) of 3-month BACHD shown by immunohistochemistry and western blot. In addition, an increase in the expression of the MHCII was observed in the BACHD mice, suggesting a concurrent immune response, due to activated microglia and possibly to immune cells from the periphery.

110
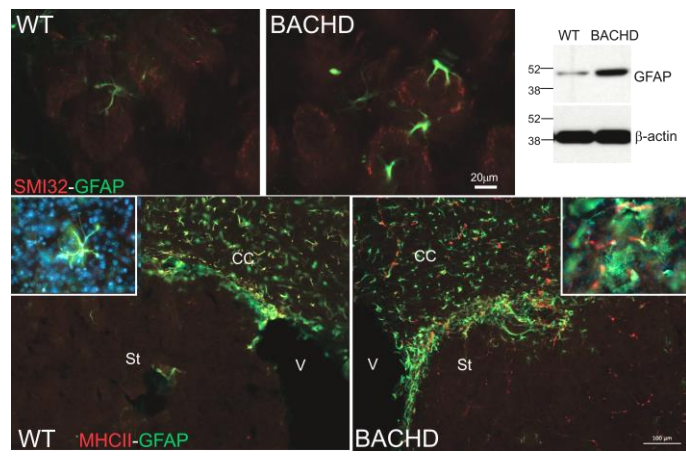
Table 13: Table 6-1: Primary antibodies were used at the following concentrations for immunohistochemistry (IHC) or western blot (WB):

Markers	Cell Type and Target	IHC	WB
SMI32	Dephosphorylated Neurofilament (200kDa)	1:200	
NF160	Neurofilament (160kDa)	1:50	1:200
MBP	Myelin Basic Protein	1:1000	1:10000
GFAP	Astrocyte	1:500	1:5000
MHCII	Monocytes/macrophages	1:400	

Bibliography

Achanta, L.B., and Rae, C.D. (2017). β-Hydroxybutyrate in the Brain: One Molecule, Multiple Mechanisms. Neurochem. Res. *42*, 35–49.

Acosta-Galvan, G., Yi, C.-X., van der Vliet, J., Jhamandas, J.H., Panula, P., Angeles-Castellanos, M., del Carmen Basualdo, M., Escobar, C., and Buijs, R.M. (2011). Interaction between hypothalamic dorsomedial nucleus and the suprachiasmatic nucleus determines intensity of food anticipatory behavior. Proc Natl Acad Sci U S A *108*, 5813–5818.

Akiyama, M., Yuasa, T., Hayasaka, N., Horikawa, K., Sakurai, T., and Shibata, S. (2004). Reduced food anticipatory activity in genetically orexin (hypocretin) neuron-ablated mice. European Journal of Neuroscience *20*, 3054–3062.

Al-Mudallal, A.S., LaManna, J.C., Lust, W.D., and Harik, S.I. (1996). Diet-induced ketosis does not cause cerebral acidosis. Epilepsia *37*, 258–261.

Andrich, J., Schmitz, T., Saft, C., Postert, T., Kraus, P., Epplen, J.T., Przuntek, H., and Agelink, M.W. (2002). Autonomic nervous system function in Huntington's disease. J. Neurol. Neurosurg. Psychiatry *72*, 726–731.

Angeles-Castellanos, M., Mendoza, J., and Escobar, C. (2007). Restricted feeding schedules phase shift daily rhythms of c-Fos and protein Per1 immunoreactivity in corticolimbic regions in rats. Neuroscience *144*, 344–355.

Angeles-Castellanos, M., Salgado-Delgado, R., Rodriguez, K., Buijs, R.M., and Escobar, C. (2010). The suprachiasmatic nucleus participates in food entrainment: a lesion study. Neuroscience *165*, 1115–1126.

Anton, S.D., Moehl, K., Donahoo, W.T., Marosi, K., Lee, S., Mainous, A.G., Leeuwenburgh, C., and Mattson, M.P. (2018). Flipping the Metabolic Switch: Understanding and Applying Health Benefits of Fasting. Obesity (Silver Spring) *26*, 254–268.

Ari, C., Poff, A.M., Held, H.E., Landon, C.S., Goldhagen, C.R., Mavromates, N., and D'Agostino, D.P. (2014). Metabolic Therapy with Deanna Protocol Supplementation Delays Disease Progression and Extends Survival in Amyotrophic Lateral Sclerosis (ALS) Mouse Model. PLoS One *9*.

Astiz, M., Heyde, I., and Oster, H. (2019). Mechanisms of Communication in the Mammalian Circadian Timing System. Int J Mol Sci *20*.

Augustin, K., Khabbush, A., Williams, S., Eaton, S., Orford, M., Cross, J.H., Heales, S.J.R., Walker, M.C., and Williams, R.S.B. (2018). Mechanisms of action for the medium-chain triglyceride ketogenic diet in neurological and metabolic disorders. Lancet Neurol *17*, 84–93.

Aziz, N.A., Anguelova, G.V., Marinus, J., Lammers, G.J., and Roos, R.A.C. (2010a). Sleep and circadian rhythm alterations correlate with depression and cognitive impairment in Huntington's disease. Parkinsonism Relat. Disord. *16*, 345–350.

Aziz, N.A., Anguelova, G.V., Marinus, J., van Dijk, J.G., and Roos, R. a. C. (2010b). Autonomic symptoms in patients and pre-manifest mutation carriers of Huntington's disease. Eur. J. Neurol. *17*, 1068–1074.

Aziz, N.A., Pijl, H., Frölich, M., Graaf, A.W.M. van der, Roelfsema, F., and Roos, R.A.C. (2010c). Leptin secretion rate increases with higher CAG repeat number in Huntington's disease patients. Clinical Endocrinology *73*, 206–211.

Bailey, E.E., Pfeifer, H.H., and Thiele, E.A. (2005). The use of diet in the treatment of epilepsy. Epilepsy Behav *6*, 4–8.

Balci, F., Oakeshott, S., Shamy, J.L., El-Khodor, B.F., Filippov, I., Mushlin, R., Port, R., Connor, D., Paintdakhi, A., Menalled, L., et al. (2013). High-Throughput Automated Phenotyping of Two Genetic Mouse Models of Huntington's Disease. PLoS Curr *5*.

Bartzokis, G., Lu, P.H., Tishler, T.A., Fong, S.M., Oluwadara, B., Finn, J.P., Huang, D., Bordelon, Y., Mintz, J., and Perlman, S. (2007). Myelin breakdown and iron changes in Huntington's disease: pathogenesis and treatment implications. Neurochem. Res. *32*, 1655–1664.

Bass, J., and Takahashi, J.S. (2010). Circadian Integration of Metabolism and Energetics. Science *330*, 1349–1354.

Björkqvist, M., Wild, E.J., Thiele, J., Silvestroni, A., Andre, R., Lahiri, N., Raibon, E., Lee, R.V., Benn, C.L., Soulet, D., et al. (2008). A novel pathogenic pathway of immune activation detectable before clinical onset in Huntington's disease. J Exp Med *205*, 1869–1877.

Bode, F.J., Stephan, M., Wiehager, S., Nguyen, H.P., Björkqvist, M., von Hörsten, S., Bauer, A., and Petersén, A. (2009). Increased numbers of motor activity peaks during light cycle are associated with reductions in adrenergic alpha(2)-receptor levels in a transgenic Huntington's disease rat model. Behav. Brain Res. *205*, 175–182.

Boulanger, J.J., and Messier, C. (2014). From precursors to myelinating oligodendrocytes: Contribution of intrinsic and extrinsic factors to white matter plasticity in the adult brain. Neuroscience *269*, 343–366.

Bourbon-Teles, J., Bells, S., Jones, D.K., Coulthard, E., Rosser, A., and Metzler-Baddeley, C. (2019). Myelin Breakdown in Human Huntington's Disease: Multi-Modal Evidence from Diffusion MRI and Quantitative Magnetization Transfer. Neuroscience *403*, 79–92.

Bradford, J., Shin, J.-Y., Roberts, M., Wang, C.-E., Sheng, G., Li, S., and Li, X.-J. (2010). Mutant Huntingtin in Glial Cells Exacerbates Neurological Symptoms of Huntington Disease Mice. J. Biol. Chem. *285*, 10653–10661.

Branco, A.F., Ferreira, A., Simões, R.F., Magalhães-Novais, S., Zehowski, C., Cope, E., Silva, A.M., Pereira, D., Sardão, V.A., and Cunha-Oliveira, T. (2016). Ketogenic diets: from cancer to mitochondrial diseases and beyond. Eur. J. Clin. Invest. *46*, 285–298.

Brandhorst, S., Choi, I.Y., Wei, M., Cheng, C.W., Sedrakyan, S., Navarrete, G., Dubeau, L., Yap, L.P., Park, R., Vinciguerra, M., et al. (2015). A Periodic Diet that Mimics Fasting Promotes Multi-System Regeneration, Enhanced Cognitive Performance, and Healthspan. Cell Metabolism *22*, 86–99.

Broom, G.M., Shaw, I.C., and Rucklidge, J.J. (2019). The ketogenic diet as a potential treatment and prevention strategy for Alzheimer's disease. Nutrition *60*, 118–121.

Brownlow, M.L., Benner, L., D'Agostino, D., Gordon, M.N., and Morgan, D. (2013). Ketogenic Diet Improves Motor Performance but Not Cognition in Two Mouse Models of Alzheimer's Pathology. PLoS One *8*.

Cahill, G.F. (2006). Fuel Metabolism in Starvation. Annual Review of Nutrition *26*, 1–22.

Camberos-Luna, L., Gerónimo-Olvera, C., Montiel, T., Rincon-Heredia, R., and Massieu, L. (2016). The Ketone Body, β-Hydroxybutyrate Stimulates the Autophagic Flux and Prevents Neuronal Death Induced by Glucose Deprivation in Cortical Cultured Neurons. Neurochem Res *41*, 600–609.

Canaple, L., Rambaud, J., Dkhissi-Benyahya, O., Rayet, B., Tan, N.S., Michalik, L., Delaunay, F., Wahli, W., and Laudet, V. (2006). Reciprocal regulation of brain and muscle Arnt-like protein 1 and peroxisome proliferator-activated receptor alpha defines a novel positive feedback loop in the rodent liver circadian clock. Mol. Endocrinol. *20*, 1715–1727.

Carneiro, B.T.S., and Araujo, J.F. (2009). The food-entrainable oscillator: a network of interconnected brain structures entrained by humoral signals? Chronobiol. Int. *26*, 1273–1289.

Cattaneo, E., Zuccato, C., and Tartari, M. (2005). Normal huntingtin function: an alternative approach to Huntington's disease. Nature Reviews Neuroscience *6*, 919–930.

Chaix, A., Zarrinpar, A., Miu, P., and Panda, S. (2014). Time-Restricted Feeding Is a Preventative and Therapeutic Intervention against Diverse Nutritional Challenges. Cell Metabolism *20*, 991–1005.

Challet, E. (2015). Keeping circadian time with hormones. Diabetes Obes Metab *17*, 76–83.

Chavan, R., Feillet, C., Costa, S.S.F., Delorme, J.E., Okabe, T., Ripperger, J.A., and Albrecht, U. (2016). Liver-derived ketone bodies are necessary for food anticipation. Nat Commun *7*, 10580.

Cheng, M.Y., Bullock, C.M., Li, C., Lee, A.G., Bermak, J.C., Belluzzi, J., Weaver, D.R., Leslie, F.M., and Zhou, Q.-Y. (2002). Prokineticin 2 transmits the behavioural circadian rhythm of the suprachiasmatic nucleus. Nature *417*, 405–410.

Chikahisa, S., Shimizu, N., Shiuchi, T., and Séi, H. (2014). Ketone body metabolism and sleep homeostasis in mice. Neuropharmacology *79*, 399–404.

Ciammola, A., Sassone, J., Alberti, L., Meola, G., Mancinelli, E., Russo, M.A., Squitieri, F., and Silani, V. (2006). Increased apoptosis, Huntingtin inclusions and altered differentiation in muscle cell cultures from Huntington's disease subjects. Cell Death Differ. *13*, 2068–2078.

Colwell, C.S. (2011). Linking neural activity and molecular oscillations in the SCN. Nat Rev Neurosci *12*, 553–569.

Colwell, C.S. (2015). Circadian medicine (Hoboken, New Jersey: John Wiley & Sons Inc).

Colwell, C.S., and Ghiani, C.A. (2019). Potential Circadian Rhythms in Oligodendrocytes? Working Together Through Time. Neurochem. Res.

Costa de Miranda, R., Di Lorenzo, N., Andreoli, A., Romano, L., De Santis, G.L., Gualtieri, P., and De Lorenzo, A. (2019). Body composition and bone mineral density in Huntington's disease. Nutrition *59*, 145–149.

Cote, N.K., and Harrington, M.E. (1993). Histamine phase shifts the circadian clock in a manner similar to light. Brain Res. *613*, 149–151.

Crotti, A., Benner, C., Kerman, B.E., Gosselin, D., Lagier-Tourenne, C., Zuccato, C., Cattaneo, E., Gage, F.H., Cleveland, D.W., and Glass, C.K. (2014). Mutant Huntingtin promotes autonomous microglia activation via myeloid lineage-determining factors. Nat. Neurosci. *17*, 513–521.

Cuesta, M., Aungier, J., and Morton, A.J. (2012). The methamphetamine-sensitive circadian oscillator is dysfunctional in a transgenic mouse model of Huntington's disease. Neurobiol. Dis. *45*, 145–155.

Cuesta, M., Aungier, J., and Morton, A.J. (2014). Behavioral therapy reverses circadian deficits in a transgenic mouse model of Huntington's disease. Neurobiology of Disease *63*, 85–91.

Cutler, T.S., Park, S., Loh, D.H., Jordan, M.C., Yokota, T., Roos, K.P., Ghiani, C.A., and Colwell, C.S. (2017). Neurocardiovascular deficits in the Q175 mouse model of Huntington's disease. Physiol Rep *5*.

Cuturic, M., Abramson, R.K., Vallini, D., Frank, E.M., and Shamsnia, M. (2009). Sleep patterns in patients with Huntington's disease and their unaffected first-degree relatives: a brief report. Behav Sleep Med *7*, 245–254.

Di Paola, M., Luders, E., Cherubini, A., Sanchez-Castaneda, C., Thompson, P.M., Toga, A.W., Caltagirone, C., Orobello, S., Elifani, F., Squitieri, F., et al. (2012). Multimodal MRI analysis of the corpus callosum reveals white matter differences in presymptomatic and early Huntington's disease. Cereb. Cortex *22*, 2858–2866.

Di Pardo, A., Amico, E., Scalabrì, F., Pepe, G., Castaldo, S., Elifani, F., Capocci, L., De Sanctis, C., Comerci, L., Pompeo, F., et al. (2017). Impairment of blood-brain barrier is an early event in R6/2 mouse model of Huntington Disease. Sci Rep *7*.

Djoussé, L., Knowlton, B., Cupples, L.A., Marder, K., Shoulson, I., and Myers, R.H. (2002). Weight loss in early stage of Huntington's disease. Neurology *59*, 1325–1330.

Drouin-Ouellet, J., Sawiak, S.J., Cisbani, G., Lagacé, M., Kuan, W.-L., Saint-Pierre, M., Dury, R.J., Alata, W., St-Amour, I., Mason, S.L., et al. (2015). Cerebrovascular and blood-brain barrier impairments in Huntington's disease: Potential implications for its pathophysiology. Ann. Neurol. *78*, 160–177.

Duan, W., Guo, Z., Jiang, H., Ware, M., Li, X.-J., and Mattson, M.P. (2003). Dietary restriction normalizes glucose metabolism and BDNF levels, slows disease progression, and increases survival in huntingtin mutant mice. Proc Natl Acad Sci U S A *100*, 2911–2916.

Dufour, B.D., and McBride, J.L. (2016). Corticosterone dysregulation exacerbates disease progression in the R6/2 transgenic mouse model of Huntington's disease. Exp. Neurol. *283*, 308–317.

Dyar, K.A., Hubert, M.J., Mir, A.A., Ciciliot, S., Lutter, D., Greulich, F., Quagliarini, F., Kleinert, M., Fischer, K., Eichmann, T.O., et al. (2018). Transcriptional programming of lipid and amino acid metabolism by the skeletal muscle circadian clock. PLOS Biology *16*, e2005886.

Eaton, S.J., Cote, N.K., and Harrington, M.E. (1995). Histamine synthesis inhibition reduces light-induced phase shifts of circadian rhythms. Brain Res. *695*, 227–230.

Ehrnhoefer, D.E., Martin, D.D.O., Schmidt, M.E., Qiu, X., Ladha, S., Caron, N.S., Skotte, N.H., Nguyen, Y.T.N., Vaid, K., Southwell, A.L., et al. (2018). Preventing mutant huntingtin proteolysis and intermittent fasting promote autophagy in models of Huntington disease. Acta Neuropathol Commun *6*.

Fahrenkrug, J., Popovic, N., Georg, B., Brundin, P., and Hannibal, J. (2007). Decreased VIP and VPAC2 receptor expression in the biological clock of the R6/2 Huntington's disease mouse. J. Mol. Neurosci. *31*, 139–148.

Ferrer, I., Goutan, E., Marín, C., Rey, M.J., and Ribalta, T. (2000). Brain-derived neurotrophic factor in Huntington disease. Brain Research *866*, 257–261.

Fisher, S.P., Godinho, S.I.H., Pothecary, C.A., Hankins, M.W., Foster, R.G., and Peirson, S.N. (2012). Rapid assessment of sleep/wake behaviour in mice. J Biol Rhythms *27*, 48–58.

Fisher, S.P., Black, S.W., Schwartz, M.D., Wilk, A.J., Chen, T.-M., Lincoln, W.U., Liu, H.W., Kilduff, T.S., and Morairty, S.R. (2013). Longitudinal analysis of the electroencephalogram and sleep phenotype in the R6/2 mouse model of Huntington's disease. Brain *136*, 2159–2172.

Fisher, S.P., Schwartz, M.D., Wurts-Black, S., Thomas, A.M., Chen, T.-M., Miller, M.A., Palmerston, J.B., Kilduff, T.S., and Morairty, S.R. (2016). Quantitative Electroencephalographic Analysis Provides an Early-Stage Indicator of Disease Onset and Progression in the zQ175 Knock-In Mouse Model of Huntington's Disease. Sleep *39*, 379–391.

Fuligni, A.J., Arruda, E.H., Krull, J.L., and Gonzales, N.A. (2018). Adolescent Sleep Duration, Variability, and Peak Levels of Achievement and Mental Health. Child Dev *89*, e18–e28.

Gaba, A.M., Zhang, K., Marder, K., Moskowitz, C.B., Werner, P., and Boozer, C.N. (2005). Energy balance in early-stage Huntington disease. Am J Clin Nutr *81*, 1335–1341.

Gauthier, L.R., Charrin, B.C., Borrell-Pagès, M., Dompierre, J.P., Rangone, H., Cordelières, F.P., De Mey, J., MacDonald, M.E., Lessmann, V., Humbert, S., et al. (2004). Huntingtin controls neurotrophic support and survival of neurons by enhancing BDNF vesicular transport along microtubules. Cell *118*, 127–138.

Genzer, Y., Dadon, M., Burg, C., Chapnik, N., and Froy, O. (2015). Ketogenic diet delays the phase of circadian rhythms and does not affect AMP-activated protein kinase (AMPK) in mouse liver. Mol. Cell. Endocrinol. *417*, 124–130.

Genzer, Y., Dadon, M., Burg, C., Chapnik, N., and Froy, O. (2016). Effect of dietary fat and the circadian clock on the expression of brain-derived neurotrophic factor (BDNF). Molecular and Cellular Endocrinology *430*, 49–55.

Gill, S., Le, H.D., Melkani, G.C., and Panda, S. (2015). Time-restricted feeding attenuates age-related cardiac decline in Drosophila. Science *347*, 1265–1269.

de Goede, P., Sen, S., Su, Y., Foppen, E., Poirel, V.-J., Challet, E., and Kalsbeek, A. (2018a). An Ultradian Feeding Schedule in Rats Affects Metabolic Gene Expression in Liver, Brown Adipose Tissue and Skeletal Muscle with Only Mild Effects on Circadian Clocks. Int J Mol Sci *19*.

de Goede, P., Wefers, J., Brombacher, E.C., Schrauwen, P., and Kalsbeek, A. (2018b). Circadian rhythms in mitochondrial respiration. J Mol Endocrinol *60*, R115–R130.

Goodman, A.O.G., Rogers, L., Pilsworth, S., McAllister, C.J., Shneerson, J.M., Morton, A.J., and Barker, R.A. (2011). Asymptomatic sleep abnormalities are a common early feature in patients with Huntington's disease. Curr Neurol Neurosci Rep *11*, 211–217.

Gray, M., Shirasaki, D.I., Cepeda, C., André, V.M., Wilburn, B., Lu, X.-H., Tao, J., Yamazaki, I., Li, S.-H., Sun, Y.E., et al. (2008). Full-length human mutant huntingtin with a stable polyglutamine repeat can elicit progressive and selective neuropathogenesis in BACHD mice. J. Neurosci. *28*, 6182–6195.

Guedes-Dias, P., Pinho, B.R., Soares, T.R., de Proença, J., Duchen, M.R., and Oliveira, J.M.A. (2016). Mitochondrial dynamics and quality control in Huntington's disease. Neurobiology of Disease *90*, 51–57.

Guo, M., Wang, X., Zhao, Y., Yang, Q., Ding, H., Dong, Q., Chen, X., and Cui, M. (2018). Ketogenic Diet Improves Brain Ischemic Tolerance and Inhibits NLRP3 Inflammasome Activation by Preventing Drp1-Mediated Mitochondrial Fission and Endoplasmic Reticulum Stress. Frontiers in Molecular Neuroscience *11*.

Gusella, J.F., MacDonald, M.E., and Lee, J.-M. (2014). Genetic modifiers of Huntington's disease. Mov. Disord. *29*, 1359–1365.

Gutekunst, C.A., Li, S.H., Yi, H., Mulroy, J.S., Kuemmerle, S., Jones, R., Rye, D., Ferrante, R.J., Hersch, S.M., and Li, X.J. (1999). Nuclear and neuropil aggregates in Huntington's disease: relationship to neuropathology. J. Neurosci. *19*, 2522–2534.

Guzmán, M., and Blázquez, C. (2004). Ketone body synthesis in the brain: possible neuroprotective effects. Prostaglandins, Leukotrienes and Essential Fatty Acids *70*, 287–292.

Haas, H., and Panula, P. (2003). The role of histamine and the tuberomamillary nucleus in the nervous system. Nat. Rev. Neurosci. *4*, 121–130.

Halestrap, A.P., and Wilson, M.C. (2012). The monocarboxylate transporter family--role and regulation. IUBMB Life *64*, 109–119.

Hamilton, J., Wolfson, T., Peavy, G., Jacobson, M., and Corey-Bloom, J. (2004). Rate and correlates of weight change in Huntington's disease*. J Neurol Neurosurg Psychiatry *75*, 209–212.

Hatori, M., Vollmers, C., Zarrinpar, A., DiTacchio, L., Bushong, E.A., Gill, S., Leblanc, M., Chaix, A., Joens, M., Fitzpatrick, J.A.J., et al. (2012). Time restricted feeding without reducing caloric intake prevents metabolic diseases in mice fed a high fat diet. Cell Metab *15*, 848–860.

HD iPSC Consortium (2017). Developmental alterations in Huntington's disease neural cells and pharmacological rescue in cells and mice. Nat. Neurosci. *20*, 648–660.

Hsiao, H.-Y., Chen, Y.-C., Chen, H.-M., Tu, P.-H., and Chern, Y. (2013). A critical role of astrocyte-mediated nuclear factor-κB-dependent inflammation in Huntington's disease. Hum. Mol. Genet. *22*, 1826–1842.

Jabre, M.G., and Bejjani, B.-P.W. (2006). Treatment of Parkinson disease with diet-induced hyperketonemia: a feasibility study. Neurology *66*, 617; author reply 617.

Jacobs, E.H., Yamatodani, A., and Timmerman, H. (2000). Is histamine the final neurotransmitter in the entrainment of circadian rhythms in mammals? Trends Pharmacol. Sci. *21*, 293–298.

Jain, S.V., and Glauser, T.A. (2014). Effects of epilepsy treatments on sleep architecture and daytime sleepiness: an evidence-based review of objective sleep metrics. Epilepsia *55*, 26–37.

Jamshed, H., Beyl, R.A., Della Manna, D.L., Yang, E.S., Ravussin, E., and Peterson, C.M. (2019). Early Time-Restricted Feeding Improves 24-Hour Glucose Levels and Affects Markers of the Circadian Clock, Aging, and Autophagy in Humans. Nutrients *11*, 1234.

Kaas, G.A., Zhong, C., Eason, D.E., Ross, D.L., Vachhani, R.V., Ming, G.-L., King, J.R., Song, H., and Sweatt, J.D. (2013). TET1 controls CNS 5-methylcytosine hydroxylation, active DNA demethylation, gene transcription, and memory formation. Neuron *79*, 1086–1093.

Kalliolia, E., Silajdžić, E., Nambron, R., Hill, N.R., Doshi, A., Frost, C., Watt, H., Hindmarsh, P., Björkqvist, M., and Warner, T.T. (2014). Plasma melatonin is reduced in Huntington's disease. Mov. Disord. *29*, 1511–1515.

Kantor, S., Szabo, L., Varga, J., Cuesta, M., and Morton, A.J. (2013). Progressive sleep and electroencephalogram changes in mice carrying the Huntington's disease mutation. Brain *136*, 2147–2158.

Kantor, S., Varga, J., and Morton, A.J. (2016). A single dose of hypnotic corrects sleep and EEG abnormalities in symptomatic Huntington's disease mice. Neuropharmacology *105*, 298–307.

Kashiwaya, Y., Takeshima, T., Mori, N., Nakashima, K., Clarke, K., and Veech, R.L. (2000). d-β-Hydroxybutyrate protects neurons in models of Alzheimer's and Parkinson's disease. Proc Natl Acad Sci U S A *97*, 5440–5444.

Khakh, B.S., Beaumont, V., Cachope, R., Munoz-Sanjuan, I., Goldman, S.A., and Grantyn, R. (2017). Unravelling and Exploiting Astrocyte Dysfunction in Huntington's Disease. Trends Neurosci. *40*, 422–437.

Kim, Y.S., Kim, Y.-B., Kim, W.B., Yoon, B.-E., Shen, F.-Y., Lee, S.W., Soong, T.-W., Han, H.-C., Colwell, C.S., Lee, C.J., et al. (2015). Histamine resets the circadian clock in the suprachiasmatic nucleus through the H1R-CaV 1.3-RyR pathway in the mouse. Eur. J. Neurosci. *42*, 2467–2477.

Kiriazis, H., Jennings, N.L., Davern, P., Lambert, G., Su, Y., Pang, T., Du, X., La Greca, L., Head, G.A., Hannan, A.J., et al. (2012). Neurocardiac dysregulation and neurogenic arrhythmias in a transgenic mouse model of Huntington's disease. J. Physiol. (Lond.) *590*, 5845–5860.

Konishi, H., Kobayashi, M., Kunisawa, T., Imai, K., Sayo, A., Malissen, B., Crocker, P.R., Sato, K., and Kiyama, H. (2017). Siglec-H is a microglia-specific marker that discriminates microglia from CNS-associated macrophages and CNS-infiltrating monocytes. Glia *65*, 1–17.

Kotliarova, S., Jana, N.R., Sakamoto, N., Kurosawa, M., Miyazaki, H., Nekooki, M., Doi, H., Machida, Y., Wong, H.K., Suzuki, T., et al. (2005). Decreased expression of hypothalamic neuropeptides in Huntington disease transgenic mice with expanded polyglutamine-EGFP fluorescent aggregates. J. Neurochem. *93*, 641–653.

Krainc, D. (2010). Clearance of Mutant Proteins as a Therapeutic Target in Neurodegenerative Diseases. Arch Neurol *67*, 388–392.

Kudo, T., Schroeder, A., Loh, D.H., Kuljis, D., Jordan, M.C., Roos, K.P., and Colwell, C.S. (2011a). Dysfunctions in circadian behavior and physiology in mouse models of Huntington's disease. Experimental Neurology *228*, 80–90.

Kudo, T., Loh, D.H., Kuljis, D., Constance, C., and Colwell, C.S. (2011b). Fast Delayed Rectifier Potassium Current: Critical for Input and Output of the Circadian System. J. Neurosci. *31*, 2746–2755.

Kuljis, D., Schroeder, A.M., Kudo, T., Loh, D.H., Willison, D.L., and Colwell, C.S. (2012). Sleep and circadian dysfunction in neurodegenerative disorders: insights from a mouse model of Huntington's disease. Minerva Pneumol *51*, 93–106.

Kuljis, D., Kudo, T., Tahara, Y., Ghiani, C.A., and Colwell, C.S. (2018). Pathophysiology in the suprachiasmatic nucleus in mouse models of Huntington's disease: XXXX. Journal of Neuroscience Research *96*, 1862–1875.

Kuljis, D.A., Gad, L., Loh, D.H., MacDowell Kaswan, Z., Hitchcock, O.N., Ghiani, C.A., and Colwell, C.S. (2016). Sex Differences in Circadian Dysfunction in the BACHD Mouse Model of Huntington's Disease. PLoS One *11*.

La Fleur, S.E., Kalsbeek, A., Wortel, J., and Buijs, R.M. (1999). A suprachiasmatic nucleus generated rhythm in basal glucose concentrations. J. Neuroendocrinol. *11*, 643–652.

Langbehn, D.R., Hayden, M., and Paulsen, J.S. (2010). CAG-Repeat Length and the Age of Onset in Huntington Disease (HD): A Review and Validation Study of Statistical Approaches. Am J Med Genet B Neuropsychiatr Genet *153B*, 397–408.

Langfelder, P., Cantle, J.P., Chatzopoulou, D., Wang, N., Gao, F., Al-Ramahi, I., Lu, X.-H., Ramos, E.M., El-Zein, K., Zhao, Y., et al. (2016). Integrated genomics and proteomics define huntingtin CAG length-dependent networks in mice. Nat. Neurosci. *19*, 623–633.

Lanska, D.J., Lanska, M.J., Lavine, L., and Schoenberg, B.S. (1988). Conditions associated with Huntington's disease at death. A case-control study. Arch. Neurol. *45*, 878–880.

Le Foll, C., and Levin, B.E. (2016). Fatty acid-induced astrocyte ketone production and the control of food intake. Am J Physiol Regul Integr Comp Physiol *310*, R1186–R1192.

Lebreton, F., Cayzac, S., Pietropaolo, S., Jeantet, Y., and Cho, Y.H. (2015). Sleep Physiology Alterations Precede Plethoric Phenotypic Changes in R6/1 Huntington's Disease Mice. PLoS ONE *10*, e0126972.

Lee, F.Y., Wang, H.-B., Hitchcock, O.N., Loh, D.H., Whittaker, D.S., Kim, Y.-S., Aiken, A., Kokikian, C., Dell'Angelica, E.C., Colwell, C.S., et al. (2018). Sleep/Wake Disruption in a Mouse Model of BLOC-1 Deficiency. Front. Neurosci. *12*.

Lee, J.H., Tecedor, L., Chen, Y.H., Monteys, A.M., Sowada, M.J., Thompson, L.M., and Davidson, B.L. (2015). Reinstating aberrant mTORC1 activity in Huntington's disease mice improves disease phenotypes. Neuron *85*, 303–315.

Li, S.H., Schilling, G., Young, W.S., Li, X.J., Margolis, R.L., Stine, O.C., Wagster, M.V., Abbott, M.H., Franz, M.L., and Ranen, N.G. (1993). Huntington's disease gene (IT15) is widely expressed in human and rat tissues. Neuron *11*, 985–993.

Lim, R.G., Quan, C., Reyes-Ortiz, A.M., Lutz, S.E., Kedaigle, A.J., Gipson, T.A., Wu, J., Vatine, G.D., Stocksdale, J., Casale, M.S., et al. (2017). Huntington's Disease iPSC-Derived Brain Microvascular Endothelial Cells Reveal WNT-Mediated Angiogenic and Blood-Brain Barrier Deficits. Cell Rep *19*, 1365–1377.

Lin, J.-S., Sergeeva, O.A., and Haas, H.L. (2011). Histamine H3 Receptors and Sleep-Wake Regulation. J Pharmacol Exp Ther *336*, 17–23.

Lin, M.-S., Liao, P.-Y., Chen, H.-M., Chang, C.-P., Chen, S.-K., and Chern, Y. (2019). Degeneration of ipRGCs in Mouse Models of Huntington's Disease Disrupts Non-Image-Forming Behaviors Before Motor Impairment. J. Neurosci. *39*, 1505–1524.

Liot, G., Zala, D., Pla, P., Mottet, G., Piel, M., and Saudou, F. (2013). Mutant Huntingtin alters retrograde transport of TrkB receptors in striatal dendrites. J. Neurosci. *33*, 6298–6309.

Liu, Y.C. (2008). Medium-chain triglyceride (MCT) ketogenic therapy. Epilepsia *49 Suppl 8*, 33–36.

Loh, D.H., Kudo, T., Truong, D., Wu, Y., and Colwell, C.S. (2013). The Q175 Mouse Model of Huntington's Disease Shows Gene Dosage- and Age-Related Decline in Circadian Rhythms of Activity and Sleep. PLoS One *8*.

Longo, V.D., and Panda, S. (2016). Fasting, Circadian Rhythms, and Time-Restricted Feeding in Healthy Lifespan. Cell Metab. *23*, 1048–1059.

Mangiarini, L., Sathasivam, K., Seller, M., Cozens, B., Harper, A., Hetherington, C., Lawton, M., Trottier, Y., Lehrach, H., Davies, S.W., et al. (1996). Exon 1 of the HD gene with an expanded CAG repeat is sufficient to cause a progressive neurological phenotype in transgenic mice. Cell *87*, 493–506.

Margolis, R.L., and Ross, C.A. (2003). Diagnosis of Huntington disease. Clin. Chem. *49*, 1726–1732.

Martin, D.D.O., Ladha, S., Ehrnhoefer, D.E., and Hayden, M.R. (2015). Autophagy in Huntington disease and huntingtin in autophagy. Trends in Neurosciences *38*, 26–35.

Maywood, E.S., Fraenkel, E., McAllister, C.J., Wood, N., Reddy, A.B., Hastings, M.H., and Morton, A.J. (2010). Disruption of Peripheral Circadian Timekeeping in a Mouse Model of Huntington's Disease and Its Restoration by Temporally Scheduled Feeding. J. Neurosci. *30*, 10199–10204.

McPherson, P.A.C., and McEneny, J. (2012). The biochemistry of ketogenesis and its role in weight management, neurological disease and oxidative stress. J. Physiol. Biochem. *68*, 141–151.

Melkani, G.C., and Panda, S. (2017). Time-restricted feeding for prevention and treatment of cardiometabolic disorders. J Physiol *595*, 3691–3700.

Menalled, L., El-Khodor, B.F., Patry, M., Suárez-Fariñas, M., Orenstein, S.J., Zahasky, B., Leahy, C., Wheeler, V., Yang, X.W., MacDonald, M., et al. (2009). Systematic behavioral evaluation of Huntington's disease transgenic and knock-in mouse models. Neurobiology of Disease *35*, 319–336.

Menalled, L.B., Kudwa, A.E., Miller, S., Fitzpatrick, J., Watson-Johnson, J., Keating, N., Ruiz, M., Mushlin, R., Alosio, W., McConnell, K., et al. (2012). Comprehensive Behavioral and Molecular Characterization of a New Knock-In Mouse Model of Huntington's Disease: zQ175. PLoS One *7*.

Mielcarek, M. (2015). Huntington's disease is a multi-system disorder. Rare Diseases *3*, e1058464.

Milder, J.B., Liang, L.-P., and Patel, M. (2010). Acute Oxidative Stress and Systemic Nrf2 Activation by the Ketogenic Diet. Neurobiol Dis *40*, 238–244.

Mohawk, J.A., Green, C.B., and Takahashi, J.S. (2012). Central and peripheral circadian clocks in mammals. Annu Rev Neurosci *35*, 445–462.

Morton, A.J. (2013). Circadian and sleep disorder in Huntington's disease. Exp. Neurol. *243*, 34–44.

Morton, A.J., Wood, N.I., Hastings, M.H., Hurelbrink, C., Barker, R.A., and Maywood, E.S. (2005). Disintegration of the Sleep-Wake Cycle and Circadian Timing in Huntington's Disease. J. Neurosci. *25*, 157–163.

Morton, A.J., Rudiger, S.R., Wood, N.I., Sawiak, S.J., Brown, G.C., Mclaughlan, C.J., Kuchel, T.R., Snell, R.G., Faull, R.L.M., and Bawden, C.S. (2014). Early and progressive circadian abnormalities in Huntington's disease sheep are unmasked by social environment. Hum. Mol. Genet. *23*, 3375–3383.

Myers, R.H., Sax, D.S., Koroshetz, W.J., Mastromauro, C., Cupples, L.A., Kiely, D.K., Pettengill, F.K., and Bird, E.D. (1991). Factors Associated With Slow Progression in Huntington's Disease. Arch Neurol *48*, 800–804.

Newman, J.C., and Verdin, E. (2014). Ketone bodies as signaling metabolites. Trends Endocrinol Metab *25*, 42–52.

Newman, J.C., Covarrubias, A.J., Zhao, M., Yu, X., Gut, P., Ng, C.-P., Huang, Y., Haldar, S., and Verdin, E. (2017). Ketogenic Diet Reduces Midlife Mortality and Improves Memory in Aging Mice. Cell Metab. *26*, 547-557.e8.

Oakeshott, S., Balci, F., Filippov, I., Murphy, C., Port, R., Connor, D., Paintdakhi, A., Lesauter, J., Menalled, L., Ramboz, S., et al. (2011). Circadian Abnormalities in Motor Activity in a BAC Transgenic Mouse Model of Huntington's Disease. PLoS Curr *3*, RRN1225.

Ochaba, J., Lukacsovich, T., Csikos, G., Zheng, S., Margulis, J., Salazar, L., Mao, K., Lau, A.L., Yeung, S.Y., Humbert, S., et al. (2014). Potential function for the Huntingtin protein as a scaffold for selective autophagy. Proc. Natl. Acad. Sci. U.S.A. *111*, 16889–16894.

Offermanns, S., and Schwaninger, M. (2015). Nutritional or pharmacological activation of HCA2 ameliorates neuroinflammation. Trends in Molecular Medicine *21*, 245–255.

Ota, M., Matsuo, J., Ishida, I., Takano, H., Yokoi, Y., Hori, H., Yoshida, S., Ashida, K., Nakamura, K., Takahashi, T., et al. (2019). Effects of a medium-chain triglyceride-based ketogenic formula on cognitive function in patients with mild-to-moderate Alzheimer's disease. Neuroscience Letters *690*, 232–236.

Ouk, K., Hughes, S., Pothecary, C.A., Peirson, S.N., and Morton, A.J. (2016). Attenuated pupillary light responses and downregulation of opsin expression parallel decline in circadian disruption in two different mouse models of Huntington's disease. Hum. Mol. Genet. *25*.

Pack, A.I., Galante, R.J., Maislin, G., Cater, J., Metaxas, D., Lu, S., Zhang, L., Smith, R.V., Kay, T., Lian, J., et al. (2007). Novel method for high-throughput phenotyping of sleep in mice. Physiological Genomics *28*, 232–238.

Pallier, P.N., Maywood, E.S., Zheng, Z., Chesham, J.E., Inyushkin, A.N., Dyball, R., Hastings, M.H., and Morton, A.J. (2007). Pharmacological Imposition of Sleep Slows Cognitive Decline and Reverses Dysregulation of Circadian Gene Expression in a Transgenic Mouse Model of Huntington's Disease. J. Neurosci. *27*, 7869–7878.

Parks, G.S., Olivas, N.D., Ikrar, T., Sanathara, N.M., Wang, L., Wang, Z., Civelli, O., and Xu, X. (2014). Histamine inhibits the melanin-concentrating hormone system: implications for sleep and arousal. J Physiol *592*, 2183–2196.

Parmentier, R., Ohtsu, H., Djebbara-Hannas, Z., Valatx, J.-L., Watanabe, T., and Lin, J.-S. (2002). Anatomical, physiological, and pharmacological characteristics of histidine decarboxylase knock-out mice: evidence for the role of brain histamine in behavioral and sleep-wake control. J. Neurosci. *22*, 7695–7711.

Paulsen, J.S. (2011). Cognitive Impairment in Huntington Disease: Diagnosis and Treatment. Curr Neurol Neurosci Rep *11*, 474–483.

Paulsen, J.S., Langbehn, D.R., Stout, J.C., Aylward, E., Ross, C.A., Nance, M., Guttman, M., Johnson, S., MacDonald, M., Beglinger, L.J., et al. (2008). Detection of Huntington's disease decades before diagnosis: the Predict-HD study. J. Neurol. Neurosurg. Psychiatry *79*, 874–880.

Petersén, Å., Gil, J., Maat-Schieman, M.L.C., Björkqvist, M., Tanila, H., Araújo, I.M., Smith, R., Popovic, N., Wierup, N., Norlén, P., et al. (2005). Orexin loss in Huntington's disease. Hum. Mol. Genet. *14*, 39–47.

Phillips, M.C.L., Murtagh, D.K.J., Gilbertson, L.J., Asztely, F.J.S., and Lynch, C.D.P. (2018). Low-fat versus ketogenic diet in Parkinson's disease: A pilot randomized controlled trial. Movement Disorders *33*, 1306–1314.

Phillips, O.R., Joshi, S.H., Squitieri, F., Sanchez-Castaneda, C., Narr, K., Shattuck, D.W., Caltagirone, C., Sabatini, U., and Di Paola, M. (2016). Major Superficial White Matter Abnormalities in Huntington's Disease. Front Neurosci *10*, 197.

Pierre, K., Pellerin, L., Debernardi, R., Riederer, B.M., and Magistretti, P.J. (2000). Cell-specific localization of monocarboxylate transporters, MCT1 and MCT2, in the adult mouse brain revealed by double immunohistochemical labeling and confocal microscopy. Neuroscience *100*, 617–627.

Pouladi, M.A., Morton, A.J., and Hayden, M.R. (2013). Choosing an animal model for the study of Huntington's disease. Nature Reviews Neuroscience *14*, 708–721.

Pratley, R.E., Salbe, A.D., Ravussin, E., and Caviness, J.N. (2000). Higher sedentary energy expenditure in patients with Huntington's disease. Ann. Neurol. *47*, 64–70.

Prosser, H.M., Bradley, A., Chesham, J.E., Ebling, F.J.P., Hastings, M.H., and Maywood, E.S. (2007). Prokineticin receptor 2 (Prokr2) is essential for the regulation of circadian behavior by the suprachiasmatic nuclei. Proc Natl Acad Sci U S A *104*, 648–653.

Reddy, P.H., and Shirendeb, U.P. (2012). Mutant huntingtin, abnormal mitochondrial dynamics, defective axonal transport of mitochondria, and selective synaptic degeneration in Huntington's disease. Biochim. Biophys. Acta *1822*, 101–110.

Rigamonti, D., Bauer, J.H., De-Fraja, C., Conti, L., Sipione, S., Sciorati, C., Clementi, E., Hackam, A., Hayden, M.R., Li, Y., et al. (2000). Wild-type huntingtin protects from apoptosis upstream of caspase-3. J. Neurosci. *20*, 3705–3713.

Roberts, M.N., Wallace, M.A., Tomilov, A.A., Zhou, Z., Marcotte, G.R., Tran, D., Perez, G., Gutierrez-Casado, E., Koike, S., Knotts, T.A., et al. (2017). A ketogenic diet extends longevity and healthspan in adult mice. Cell Metab *26*, 539-546.e5.

Rosbash, M., Bradley, S., Kadener, S., Li, Y., Luo, W., Menet, J.S., Nagoshi, E., Palm, K., Schoer, R., Shang, Y., et al. (2007). Transcriptional feedback and definition of the circadian pacemaker in Drosophila and animals. Cold Spring Harb. Symp. Quant. Biol. *72*, 75–83.

Ruan, H.-B., and Crawford, P.A. (2018). Ketone bodies as epigenetic modifiers. Curr Opin Clin Nutr Metab Care *21*, 260–266.

Rudenko, O., Springer, C., Skov, L.J., Madsen, A.N., Hasholt, L., Nørremølle, A., and Holst, B. (2019). Ghrelin-mediated improvements in the metabolic phenotype in the R6/2 mouse model of Huntington's disease. J. Neuroendocrinol. *31*, e12699.

Saft, C., Zange, J., Andrich, J., Müller, K., Lindenberg, K., Landwehrmeyer, B., Vorgerd, M., Kraus, P.H., Przuntek, H., and Schöls, L. (2005). Mitochondrial impairment in patients and asymptomatic mutation carriers of Huntington's disease. Mov. Disord. *20*, 674–679.

Sanberg, P.R., Fibiger, H.C., and Mark, R.F. (1981). Body weight and dietary factors in Huntington's disease patients compared with matched controls. Med. J. Aust. *1*, 407–409.

Sapp, E., Kegel, K.B., Aronin, N., Hashikawa, T., Uchiyama, Y., Tohyama, K., Bhide, P.G., Vonsattel, J.P., and DiFiglia, M. (2001). Early and progressive accumulation of reactive microglia in the Huntington disease brain. J. Neuropathol. Exp. Neurol. *60*, 161–172.

Schroeder, A.M., and Colwell, C.S. (2013). How to fix a broken clock. Trends in Pharmacological Sciences *34*, 605–619.

Schroeder, A.M., Wang, H.B., Park, S., Jordan, M.C., Gao, F., Coppola, G., Fishbein, M.C., Roos, K.P., Ghiani, C.A., and Colwell, C.S. (2016). Cardiac Dysfunction in the BACHD Mouse Model of Huntington's Disease. PLoS One *11*.

Shan, L., Hofman, M.A., van Wamelen, D.J., Van Someren, E.J.W., Bao, A.-M., and Swaab Dick, F. (2012). Diurnal fluctuation in histidine decarboxylase expression, the rate limiting enzyme for histamine production, and its disorder in neurodegenerative diseases. Sleep *35*, 713–715.

Siddiqui, A., Rivera-Sánchez, S., Castro, M. del R., Acevedo-Torres, K., Rane, A., Torres-Ramos, C.A., Nicholls, D.G., Andersen, J.K., and Ayala-Torres, S. (2012). Mitochondrial DNA damage is associated with reduced mitochondrial bioenergetics in Huntington's disease. Free Radic. Biol. Med. *53*, 1478–1488.

Siegmann, M.J., Athinarayanan, S.J., Hallberg, S.J., McKenzie, A.L., Bhanpuri, N.H., Campbell, W.W., McCarter, J.P., Phinney, S.D., Volek, J.S., and Van Dort, C.J. (2019). Improvement in patient-reported sleep in type 2 diabetes and prediabetes participants receiving a continuous care intervention with nutritional ketosis. Sleep Med. *55*, 92–99.

Skillings, E.A., Wood, N.I., and Morton, A.J. (2014). Beneficial effects of environmental enrichment and food entrainment in the R6/2 mouse model of Huntington's disease. Brain Behav *4*, 675–686.

Sørensen, S.A., and Fenger, K. (1992). Causes of death in patients with Huntington's disease and in unaffected first degree relatives. J. Med. Genet. *29*, 911–914.

Steffan, J.S., Kazantsev, A., Spasic-Boskovic, O., Greenwald, M., Zhu, Y.Z., Gohler, H., Wanker, E.E., Bates, G.P., Housman, D.E., and Thompson, L.M. (2000). The Huntington's disease protein interacts with p53 and CREB-binding protein and represses transcription. Proc. Natl. Acad. Sci. U.S.A. *97*, 6763–6768.

Stephan, F.K. (2002). The "Other" Circadian System: Food as a Zeitgeber. J Biol Rhythms *17*, 284–292.

Strong, T.V., Tagle, D.A., Valdes, J.M., Elmer, L.W., Boehm, K., Swaroop, M., Kaatz, K.W., Collins, F.S., and Albin, R.L. (1993). Widespread expression of the human and rat Huntington's disease gene in brain and nonneural tissues. Nat. Genet. *5*, 259–265.

Sugars, K.L., and Rubinsztein, D.C. (2003). Transcriptional abnormalities in Huntington disease. Trends Genet. *19*, 233–238.

Sugars, K.L., Brown, R., Cook, L.J., Swartz, J., and Rubinsztein, D.C. (2004). Decreased cAMP response element-mediated transcription: an early event in exon 1 and full-length cell models of Huntington's disease that contributes to polyglutamine pathogenesis. J. Biol. Chem. *279*, 4988–4999.

Tahara, Y., and Shibata, S. (2013). Chronobiology and nutrition. Neuroscience *253*, 78–88.

Tahara, Y., Kuroda, H., Saito, K., Nakajima, Y., Kubo, Y., Ohnishi, N., Seo, Y., Otsuka, M., Fuse, Y., Ohura, Y., et al. (2012). In Vivo Monitoring of Peripheral Circadian Clocks in the Mouse. Current Biology *22*, 1029–1034.

Takahashi, J.S. (2017). Transcriptional architecture of the mammalian circadian clock. Nat. Rev. Genet. *18*, 164–179.

Telzer, E.H., Goldenberg, D., Fuligni, A.J., Lieberman, M.D., and Galvan, A. (2015). Sleep Variability in Adolescence is Associated with Altered Brain Development. Dev Cogn Neurosci *14*, 16–22.

Thayer, J.F., Yamamoto, S.S., and Brosschot, J.F. (2010). The relationship of autonomic imbalance, heart rate variability and cardiovascular disease risk factors. Int. J. Cardiol. *141*, 122–131.

Tieu, K., Perier, C., Caspersen, C., Teismann, P., Wu, D.-C., Yan, S.-D., Naini, A., Vila, M., Jackson-Lewis, V., Ramasamy, R., et al. (2003). D-β-Hydroxybutyrate rescues mitochondrial respiration and mitigates features of Parkinson disease. J Clin Invest *112*, 892–901.

Tognini, P., Murakami, M., Liu, Y., Eckel-Mahan, K.L., Newman, J.C., Verdin, E., Baldi, P., and Sassone-Corsi, P. (2017). Distinct Circadian Signatures in Liver and Gut Clocks Revealed by Ketogenic Diet. Cell Metabolism *26*, 523-538.e5.

Träger, U., Andre, R., Magnusson-Lind, A., Miller, J.R.C., Connolly, C., Weiss, A., Grueninger, S., Silajdžić, E., Smith, D.L., Leavitt, B.R., et al. (2015). Characterisation of immune cell function in fragment and full-length Huntington's disease mouse models. Neurobiology of Disease *73*, 388–398.

Veech, R.L., Chance, B., Kashiwaya, Y., Lardy, H.A., and Cahill, G.F. (2001). Ketone Bodies, Potential Therapeutic Uses. IUBMB Life *51*, 241–247.

Waddington Lamont, E., Harbour, V.L., Barry-Shaw, J., Renteria Diaz, L., Robinson, B., Stewart, J., and Amir, S. (2007). Restricted access to food, but not sucrose, saccharine, or salt, synchronizes the expression of Period2 protein in the limbic forebrain. Neuroscience *144*, 402–411.

Walter, C., Clemens, L.E., Müller, A.J., Fallier-Becker, P., Proikas-Cezanne, T., Riess, O., Metzger, S., and Nguyen, H.P. (2016). Activation of AMPK-induced autophagy ameliorates Huntington disease pathology in vitro. Neuropharmacology *108*, 24–38.

van Wamelen, D.J., Shan, L., Aziz, N.A., Anink, J.J., Bao, A.-M., Roos, R.A.C., and Swaab, D.F. (2011). Functional Increase of Brain Histaminergic Signaling in Huntington's Disease. Brain Pathology *21*, 419–427.

van Wamelen, D.J., Aziz, N.A., Anink, J.J., van Steenhoven, R., Angeloni, D., Fraschini, F., Jockers, R., Roos, R.A.C., and Swaab, D.F. (2013). Suprachiasmatic Nucleus Neuropeptide Expression in Patients with Huntington's Disease. Sleep *36*, 117–125.

van Wamelen, D.J., Roos, R.A., and Aziz, N.A. (2015). Therapeutic strategies for circadian rhythm and sleep disturbances in Huntington disease. Neurodegener Dis Manag *5*, 549–559.

van Wamelen, D.J. van, Aziz, N.A., Roos, R. a. C., and Swaab, D.F. (2014). Hypothalamic Alterations in Huntington's Disease Patients: Comparison with Genetic Rodent Models. Journal of Neuroendocrinology *26*, 761–775.

Wang, H.-B., Whittaker, D.S., Truong, D., Mulji, A.K., Ghiani, C.A., Loh, D.H., and Colwell, C.S. (2017). Blue light therapy improves circadian dysfunction as well as motor symptoms in two mouse models of Huntington's disease. Neurobiology of Sleep and Circadian Rhythms *2*, 39–52.

Wang, H.-B., Loh, D.H., Whittaker, D.S., Cutler, T., Howland, D., and Colwell, C.S. (2018). Time-Restricted Feeding Improves Circadian Dysfunction as well as Motor Symptoms in the Q175 Mouse Model of Huntington's Disease. ENeuro *5*.

Wang, Y., Ghezzi, A., Yin, J.C.P., and Atkinson, N.S. (2009). CREB regulation of BK channel gene expression underlies rapid drug tolerance. Genes Brain Behav *8*, 369–376.

Watanabe, T., Taguchi, Y., Shiosaka, S., Tanaka, J., Kubota, H., Terano, Y., Tohyama, M., and Wada, H. (1984). Distribution of the histaminergic neuron system in the central nervous system of rats; a fluorescent immunohistochemical analysis with histidine decarboxylase as a marker. Brain Res. *295*, 13–25.

Webb, I.C., Baltazar, R.M., Lehman, M.N., and Coolen, L.M. (2009). Bidirectional interactions between the circadian and reward systems: is restricted food access a unique zeitgeber? European Journal of Neuroscience *30*, 1739–1748.

Welsh, D.K., Takahashi, J.S., and Kay, S.A. (2010). Suprachiasmatic Nucleus: Cell Autonomy and Network Properties. Annu Rev Physiol *72*, 551–577.

Wexler, N.S., Lorimer, J., Porter, J., Gomez, F., Moskowitz, C., Shackell, E., Marder, K., Penchaszadeh, G., Roberts, S.A., Gayán, J., et al. (2004). Venezuelan kindreds reveal that genetic and environmental factors modulate Huntington's disease age of onset. Proc. Natl. Acad. Sci. U.S.A. *101*, 3498–3503.

Whittaker, D.S., Wang, H.-B., Loh, D.H., Cachope, R., and Colwell, C.S. (2017). Possible use of a H3R antagonist for the management of nonmotor symptoms in the Q175 mouse model of Huntington's disease. Pharmacology Research & Perspectives *5*, e00344.

Whittaker, D.S., Loh, D.H., Wang, H.-B., Tahara, Y., Kuljis, D., Cutler, T., Ghiani, C.A., Shibata, S., Block, G.D., and Colwell, C.S. (2018). Circadian-based Treatment Strategy Effective in the BACHD Mouse Model of Huntington's Disease. J Biol Rhythms 0748730418790401.

Williams, R.H., Morton, A.J., and Burdakov, D. (2011). Paradoxical function of orexin/hypocretin circuits in a mouse model of Huntington's disease. Neurobiol. Dis. *42*, 438–445.

Wright, D.J., Renoir, T., Gray, L.J., and Hannan, A.J. (2017). Huntington's Disease: Pathogenic Mechanisms and Therapeutic Targets. In Neurodegenerative Diseases, (Springer, Cham), pp. 93–128.

Yeh, Y.Y., and Zee, P. (1976). Relation of ketosis to metabolic changes induced by acute medium-chain triglyceride feeding in rats. J. Nutr. *106*, 58–67.

Youm, Y.-H., Nguyen, K.Y., Grant, R.W., Goldberg, E.L., Bodogai, M., Kim, D., D'Agostino, D., Planavsky, N., Lupfer, C., Kanneganti, T.D., et al. (2015). Ketone body β-hydroxybutyrate blocks the NLRP3 inflammasome-mediated inflammatory disease. Nat Med *21*, 263–269.

Zhang, R., Lahens, N.F., Ballance, H.I., Hughes, M.E., and Hogenesch, J.B. (2014). A circadian gene expression atlas in mammals: Implications for biology and medicine. PNAS *111*, 16219–16224.

Zuccato, C., Valenza, M., and Cattaneo, E. (2010). Molecular Mechanisms and Potential Therapeutical Targets in Huntington's Disease. Physiological Reviews *90*, 905–981.